T

In Situ Analysis of the Biomass and Distribution of Microphytobenthos

Claire Honeywill

A thesis submitted in partial fulfilment of the requirements for the degree of Doctor of Philosophy, at the University of St Andrews

School of Biology

University of St Andrews

August 2001

The University of St Andrews

Declarations

I, Claire Honeywill, hereby certify that this thesis which is approximately 48 000 words in length, has been written by m, that it is the record of work carried out by me and that it has not been submitted in any previous application for a higher degree.

I was admitted as a research student in September 1998 and as a candidate for the degree of Doctor of Philosophy in September 1999; the higher study for which this is a record, was carried out in the University of St Andrews between 1996 and 2001.

I hereby certify that the candidate has fulfilled the conditions of the Resolution and Regulations appropriate for the degree of Doctor of Philosophy in the University of St Andrews and that the candidate is qualified to submit this thesis in application for that degree.

In submitting this thesis to the University of St Andrews I understand that I am giving permission for it to be made available for use in accordance with the regulations of the University Library for the time being in force, subject to any copyright vested in the work not being affected thereby. I also understand that the title and abstract will be published and that a copy of the work may be made and supplied to any bona fide library or research worker.

Acknowledgements

I would like to thank all the members of SERG, past and present, for their friendship, encouragement and help. I would especially like to thank Mireille Consalvey, Scot Hagerthey and Rupert Perkins for their productive discussions and Irvine Davidson for his continued enthusiasm and always being there to listen. I am also grateful to James Blackburn and Karen Wiltshire for their help and advice with the HPLC and their friendship at the beginning of this study. A huge thanks to Mireille for all the collaborative work and for her cheerful enthusiasm and inspiration.

I would like to acknowledge all the members of the BIOPTIS team for providing data, and making the field campaigns such fun. I would like to extend my gratitude to Jacco Kromkamp and Rod Forster for their collaboration, advice, especially on fluorometry and their fruitful discussions, they were also great hosts during my visits to The Netherlands.

I am grateful to my supervisor, Dave Paterson, for his positive, enthusiastic support and advice throughout this study, and for believing in me.

Thanks to the Toll House family, Gen, Nick, Gordon, Mark, Rich, Dave, and honorary members, Les and Stew, for all their support and fabulous distractions. I especially appreciate all the support and encouragement from Mum, Dad and sister Paula, especially Dad for all that proof reading!

Lastly, I would like to say a huge thank you to Rich, without whose encouragement, support and calming influence, I would not have come so far.

... the diatoms were so abundant on the surface, that their photosynthetic activity was distinctly audible as a gentle sizzling... and the sand was frothy with bubbles of gas, presumably oxygen given off by them.

Herdman, 1924

CONTENTS

ABSTRACT

This thesis investigates the use of fluorescence techniques for the remote sensing of microphytobenthic biomass and distribution. Firstly, hardware was developed to facilitate the use of fluorometry for measuring microphytobenthos *in situ*. Comparisons between minimum fluorescence (Fo^{15}) and chlorophyll *a*, as proxies for microalgal biomass, were made over varied seasonal and spatial scales. The relationship between Fo^{15} and Chl *a* was strongest for diatom dominated samples where micro-sections (0.2 mm) of sediment were sampled. No spatial patterns were found in diatom patch size or dispersion. The coefficient of variation between patches (using the proxy Fo^{15}) made at scales from 2.5 - 500 cm, ranged from 5 to 150 %.

The first non-destructive quantitative temporal study of microphytobenthos at the sediment surface (Fo^{15}) was conducted. A proportion of the microphytobenthic community was found at the surface of the sediment during daylight tidal ebb and cells did not migrate from the surface at the end of tidal exposure. This has implications for re-suspension of cells during daylight immersion.

Algal stress measurements (*Fv/Fm*) were unreliable at low biomass. The calculation of photosynthetic parameters from relative electron transport rate on undisturbed cores was found to be unrepresentative of those made *in situ*.

The use of different units of expression for Chl *a* (both content and concentration) were investigated over temporal and vertical scales. Chl *a* content (μg Chl *a* g^{-1} dry sediment) decreased over an emersion period. In contrast Chl *a* concentration (mg Chl *a* m^{-2}) increased over this period. In this situation, contrasting Chl *a* determination could be wholly explained by the decrease in sediment water content over the period. These findings have implications for the estimation of biomass specific primary productivity.

ABBREVIATIONS AND TERMS

α	light utilisation efficiency
a*	specific absorption coefficient
Concentration	mass per volume
Content	mass per mass
Chl	chlorophyll
ΔF	quenched fluorescence ($Fm' - Fs$)
$\Delta F/Fm'$	the effective (or operating) efficiency of PSII photochemistry
DMF	Dimethylformamide
E	irradiance
E_k	light saturation intensity
ETR	electron transport rate
ETR_{max}	maximum electron transport rate
Fm	maximum fluorescence (PSII centres closed; Q_A reduced)
Fm'	maximum fluorescence in the light adapted state
Fm^{15}	maximum fluorescence after 15 minutes of dark adaption
FMS2	Fluorescence monitoring System 2
Fo	minimum fluorescence (PSII centres open; Q_A oxidised)
Fo^{15}	minimum fluorescence after 15 minutes of dark adaption
Fs	steady state fluorescence (minimum fluorescence in the light adapted state)
Fv	variable fluorescence ($Fm - Fo$)
Fv/Fm	the maximum efficiency of PSII photochemistry
HPLC	high precision liquid chromatography
NPQ	non-photochemical quenching
PAR	photosynthetically active radiation (350 – 700 nm)
P-E curve	photosynthesis versus irradiance curve
PSII	photosystem II
PPFD	photosynthetic photon flux density ($\mu mol\ m^{-2}\ s^{-1}$)
Q_A	the primary electron acceptor
rETR	relative electron transport rate (i.e. no correction for a*)
RT	retention time (of pigments on column in HPLC analysis)

Chapter 1

1. INTRODUCTION

1.1. General

Estuaries are important habitats and feeding grounds for a variety of organisms, e.g., birds, shellfish, demersal fish, invertebrates, algae, plants and bacteria (Crooks and Turner, 1999). Intertidal sediments are one of the most biologically productive natural ecosystems on earth, despite the extreme conditions of periodic exposure to the elements, dynamic tidal immersion and exposure to high levels of nutrients and toxins. Estuaries are generally areas of sediment deposition and many substances are known to adsorb to suspended particles (Admiraal, 1984). Waste products thus accumulate in the estuarine environment (Mathieson and Atkins, 1995). One of the major primary producing groups in this habitat are microscopic algae (Pinckney and Zingmark, 1991; Yallop *et al.*, 1994; MacIntyre and Cullen, 1996), even though their photosynthetic activity is restricted to the narrow illuminated layer of surface sediment. Microphytobenthos provide an important energy source for the estuarine food web (Sullivan and Moncreiff, 1990, Pinckney *et al.,* 1994) supplying up to 45% of the organic budget of an estuary (Asmus *et al.*, 1998) and have a central role in moderating carbon flow in coastal sediments (Middleburg *et al.*, 2000). Estuarine microphytobenthic biomass often exceeds that of phytoplankton biomass in the overlying tidal waters (MacIntyre *et al.,* 1996).

In cohesive sediments, microphytobenthos are generally represented by three types of algae: blue green algae (Cyanophyta), euglenids (Euglenales), and diatoms (Bacillariophyta), the latter being the most dominant (Admiraal, 1984). Benthic diatoms can also influence the microstructure and properties of the sediment, due to the secretion of extracellular polymeric substances (EPS, Decho, 1990, Underwood *et al.*, 1995), which may increase sediment stability (Paterson, *et al.*, 1994; Paterson, 1997; Amos *et al.*, 1998) and enhance coastal defence (King and Lester, 1995). EPS is thought to be extruded from the raphe; a slit on the diatom frustule, as a means of motility (Edgar and Pickett-Heaps, 1984; Decho, 1990). EPS can also form a protection against desiccation (Daniel *et al.,* 1987) and toxicity (Pistocchi *et al.,* 1997).

Most of the photosynthetic organisms found in the intertidal estuarine habitat are motile and are able to migrate to the surface during daylight and into the sediment

when the mudflat is immersed by the tide, which could potentially scour the surface. Migration of diatoms in and out of the surface layer of sediment (micro-cycling) may occur during tidal emersion when conditions become stressful, this may be why diatom dominated microphytobenthos show few signs of light stress or nutrient limitation (Kromkamp *et al.*, 1998).

The measurement of microphytobenthic biomass and physiology are an essential aspect of the ecological study of these estuarine systems. Biomass (estimated from chlorophyll *a*) can often be a good indication of photosynthetic activity and thus productivity of the organisms (Pinckney and Zingmark, 1993c). The intertidal estuarine environment is by nature dynamic, exposed to the weather and tidal inundation, which can affect the biomass and physiology of the microphytobenthos. Biotic interactions such as grazing and infections by parasites can also play a part in the ecophysiology and may, intermittently, cause a rapid decline of a whole algal populations (Round, 1981). These physical and biological effects are introduced in the following sections. The following sections also introduce the concepts and methods for measuring biomass and photosynthesis.

1.2. Biomarkers

To assess biomass in a habitat, ecologists generally measure the wet/dry weight of the organisms or count the number of species and multiply by an average species biovolume. Microphytobenthic biomass is most commonly estimated from the proxy chlorophyll *a* (Chl *a*), which is extracted from a known unit of the sediment. EPS concentration is known to correlate highly with Chl *a* in diatom rich samples (Yallop and Paterson, 1994; Underwood *et al.*, 1995 Kelly *et al.*, 2001) and thus may also be a useful biomarker for diatoms. EPS can be easily extracted and measured from sediments, as it is largely made up of carbohydrates. Microalgal biomass has also been calculated by the product of cell numbers and biovolume (Hillebrand *et al.*, 1999), but this is a time consuming method as diatoms can vary greatly in size (from 5 – 300 μm in length) and shape. Taxonomic information on species composition can however be extremely valuable ecological tool. Species richness, diversity, evenness and similarity can all be calculated from counting and identifying species. Chl *a* determination, as a proxy for biomass, is undertaken after extracting and separating the photosynthetic pigments from known quantities of sediment. The identification of minor pigments (and their ratio to the major pigment Chl *a*) has been used for

categorising different groups of sediment inhabiting algae present, as different groups contain different pigments (Barranguet *et al.,* 1997; Brotas and Plante-Cuny, 1998). Diatoms have several pigments, two of which; fucoxanthin and chlorophyll *c* (Chl *c*), are generally not present in other algae found in estuarine sediment habitats (Millie *et al.,* 1993). Blue green algae contain the marker pigment zeaxanthin and euglenids have chlorophyll *b* (Chl *b*), lutein and diadinoxanthin. However zeaxanthin, Chl *b* and lutein are also present in green algae (e.g, *Enteromorpha*) or higher plant detritus which may also be present on estuaries. Therefore a combination of certain pigments and lack of others has been the recommended procedure for algal group identification (Barranguet *et al.*, 1997; Brotas and Plante-Cuny, 1998).

Pigments quantification from photosynthetic organisms can give an indication of the physiology of the light harvesting and photoprotection processes. In diatoms, Chl c and fucoxanthin are the main light harvesting pigments other than Chl a, and their increase in the pigments may indicate a decrease in available light. Diadinoxanthin, diatoxanthin and β - carotene are the main photoprotective pigments in diatoms. Diadinoxanthin de-epoxidates and is converted to diatoxanthin in the light, and diatoxanthin is converted to diadinoxanthin in low light or darkness (Olaizola and Yamomoto, 1994). This interconversion of pigments is known as the diadinoxanthin cycle and is similar to the xanthophyll cycle in green algae and higher plants. As a protective mechanism diatoxanthin may transfer absorbed energy to Chl *a* with lower efficiency than diadinoxanthin (Robinson *et al.*, 1997). Two pools of diadinoxanthin have been observed, one which of which does not undergo de-epoxidation (Willemoes and Monas, 1991; Arsalanne *et al.*, 1994; Olaizola and Yamomoto, 1994). β - carotene is also known to dissipate excess energy away from the reaction centres, to avoid damage. Therefore an increase in these photoprotective pigments may indicate that cells are under excessive irradiance. Any changes in the quantity of minor pigments can be measured absolutely as a concentration, normalised to cell count or by calculating the ratio of minor pigments to Chl *a*. There is evidence that *Phaeodactylum tricornutum*, an algae displaying the diadinoxanthin cycle also possesses the violaxanthin cycle (Lohr and Wilhelm 1999). Their data strongly suggests a biosynthesis from violaxanthin via diadinoxanthin to fucoxanthin. This supports the hypothesis that violaxanthin is a common intermediate in the biosynthesis of this type of carotenoid (Bjørnland and Liaaen-Jensen, 1989) and that

another important function for xanthophyll cycling maybe to optimise the biosynthesis of light harvesting xanthophylls under fluctuating light conditions.

Light harvesting pigment concentrations (the main one being Chl *a*) per cell can change in response to light levels. Decreased light levels will induce an increase of certain pigment quantities, in order to capture more energy and vice versa (Falkowski and LaRoche, 1991; Falkowski and Raven, 1997). Whilst this may confound biomass analysis, Chl *a* gives a good representation of the photosynthetic potential of the population (MacIntyre *et al.*, 1996) and can be a useful physiological measurement, especially in conjunction with cell counts. Weight or volume of cells would be a more accurate measure of diatom biomass, however it is extremely difficult, if not impossible, to separate the sediment from the cells for community weight or volume calculations. Furthermore individual cell volume calculations are intrinsically difficult, as diatoms are complex shapes and a single species decreases in size throughout their vegetative life cycle. It is therefore generally thought that Chl *a* concentration is a more representative measure, and most widely used method of quantifying biomass (MacIntyre *et al.*, 1996). Both Chl *a* content (mass per unit mass) and concentration (mass per unit volume; or area to a set depth) are widespread units of expression for measurements of microphytobenthic biomass, but these terms have been frequently confused in the literature (Flemming and Delafontaine, 2000). These authors advocate a stricter adherence to the correct use of these defined terms as their inter-comparison may be spurious (Flemming and Delafontaine, 2000).

1.3. Ecological dynamics

The physical and biological factors, which can influence the ecology of microphytobenthos in intertidal sediments, are described in the following section.

1.3.1. Irradiance

Day length and light intensity constitute two important factors for algae growth (Falkowski and LaRoche, 1991). For isolated cultures of benthic marine diatom species, Admiraal (1977a) documented that the minimum daily irradiance dose needed to attain light-saturated growth ranged from 2.5 to 5.0 mol m^{-2} day^{-1}

(above which no increase in growth rate was seen). He also found that some species had higher growth rates under an 8 h daily photoperiod, whilst other species had higher growth rates under a 16 h daily photoperiod. When an algal culture (*Dunaliella tertiolecta*) was moved from photosynthetically saturating light to sub-saturating irradiances, cells harvested more light (Sukenik *et al.,* 1990, cited in Falkowski and LaRoche, 1991). This was implemented by cells initially diverting biosynthesis from lipid and carbohydrate production to protein synthesis (namely: light harvesting chlorophyll protein).

1.3.1.1. Photic zone

Measurement of the photic depth with sediments is an important part of microphytobenthos research, as photosynthesis can only occur when light can be harvested by these organisms. In cohesive sediments the photic zone is generally thought to be less than 1 mm and has been reported as 0.27 mm and 0.6 mm deep in different studies (Serôdio *et al.*, 1997; Kromkamp *et al.*, 1998, respectively). These photic depths were obtained by either resettling various known amounts of sediment into identical chambers and measuring the light attenuation through the layer of sediment (Serôdio *et al.*, 1997) or resettling sediment and calculating attenuation coefficients assuming an exponential relationship between light and depth (Kromkamp *et al.*, 1998). A deeper photic zone (to 1% of the surface light) of 1.8 mm has actually been measured *in situ* in cohesive sediments (Paterson *et al.,* 1998). These measurements were measured using fibre optic light microsensors (Lassen *et al.,* 1992) which were lowered into sediments mechanically at steps of 0.1 mm.

1.3.2. Temperature

Temperature is a major controlling factor of photosynthesis in all plants. Estuarine sediments are subject to large temperature changes due to a combination of seasons, tidal cycle and weather conditions (Harrison and Phizacklea, 1985), and may vary more than 10°C within a few hours (Blanchard and Guarini, 1996). There are many studies of the effect of temperature on algal growth rate (e.g. Admiraal, 1977a, Davidson, 1991) and photosynthesis (e.g. Blanchard *et al.*, 1996). A progressive increase in photosynthetic capacity (maximum photosynthesis; P_{max}) of microphytobenthos, up to an optimum temperature (T_{opt}) of 25°C has been found, beyond which P_{max} declined (Blanchard *et al.*, 1996). T_{opt} did not differ in April,

September or December but the maximum P_{max} (at the T_{opt}) was twice as high in April as in September, which was twice the value as December (Blanchard *et al.*, 1996, 1997). Regardless of season, the thermal threshold, above which no photosynthesis occurs was always 38°C.

1.3.3. Salinity

The patterns of diatom species distributions in the intertidal zone have generally been attributed to the salinity gradient (Underwood, 1994). However, it is difficult in the field to separate the effects of salinity from nutrients, as nutrients increase seawards on some estuaries (Underwood *et al.,* 1998). Culture experiments have shown that many species of diatom remain photosynthetically active when subjected to salinity changes between 4 and 60 (Admiraal, 1984). This has also been found in the field, where many diatom species in the Wadden sea estuaries were found to be living over a wide range of salinities (Admiraal, 1984).

1.3.4. Heavy metals, nutrients and herbicides

In freshwater habitats, diatoms are used extensively as environmental indicators. A trophic index for freshwater diatoms was developed by Kelly and Whitton (1995) which uses easily identifiable taxa as indicators of the nutrient/trophic status of rivers. Also in 1995, Stewart published a study of algae as indicators of pollution, but again these used freshwater taxa. Recently, Underwood *et al.* (1998) assessed the distribution of estuarine diatoms along a nutrient gradient and found populations differed with distance from a sewage outfall. This was supported by laboratory experiments where increased ammonium was added to sediment cores and different populations increased or declined depending on the trophic status. Previous studies have shown similar results; where diatom populations were different over periods of decreasing organic waste conditions (Peletier, 1996). During a high organic waste period, an alternating dominance of diatom species (*Navicula salinarum* and *N. pygmaea*) was found. In a reduced organic waste period, that pattern had disappeared and species (*N. phyllepta* and *N. flanatica*), which have a lower tolerance to high ammonium and sulphide concentrations, became the dominant species (Peletier, 1996). Admiraal investigated many nutrient affects on estuarine benthic diatoms, e.g. their tolerance to high concentrations of nutrients (Admiraal, 1977c) or to conditions of high organic decomposition (Admiraal, 1977b). Also, some species of pennate

diatoms are tolerant to oil and heavy metals (Admiraal, 1984; Miles, 1994). Secretion of EPS is thought to be a form of protection against both desiccation (Daniel *et al.*, 1987) and toxicity, e.g., Pistocchi *et al.* (1997) found that copper increased the amount of polysaccharide exudate in diatoms.

Nutrient deficiency is rarely reported for microphytobenthos in cohesive sediment estuarine environments, as there is generally thought to be sufficient (or excessive) nutrient loading in these systems (Underwood and Kromkamp, 1999). Nutrient deficiency and more specifically, nitrogen and iron limitation in phytoplankton has shown to decrease the efficiency of photosynthesis.

1.3.5. Faunal influences

Diatoms are the main primary producers in estuarine mudflat systems and are thus the main food source for herbivors. Sediment inhabiting micro-, meio- and macro-fauna commonly feed on benthic diatoms, some feed selectively by species or cell size, whilst others may feed more generally on mixed benthos (Admiraal, 1984). Investigations have shown removal of grazing species can increase the densities of diatoms in the sediment (Underwood and Paterson, 1993; Smith *et al.*, 1996). The summer decrease in diatom abundance maybe due to the grazing of herbivores as isolated cultures grown in discrete chambers on a mudflat, grew well during the summer period (Admiraal and Peletier, 1980). Macrofauna can also alter the biomass at the surface by bioengineering and bioturbation, that is the formation of burrows, around which they feed, excretion of faecal pellet over the surface and mixing of surface layers into deeper layers and vice versa (Ford pers com.).

1.3.6. Infection

It is not known to what extent microphytobenthic diatoms can be infected by parasites, although several studies observe parasitism in planktonic communities. Various types of newly identified parasites; ameobic, nanoflagellate and polymorphic (of uncertain taxonomic position), have been discovered infecting species of planktonic marine diatoms over the past few years (see Kuhn and workers, 1997-1999; Schweikert and Schnepf, 1996, 1997). Parasitic fungi have also been seen to infect planktonic diatoms (Taylor, 1976 and Round, 1971 in Admiraal, 1984). Unidentified fungi were observed infecting particular species of estuarine diatoms, leaving other species in the same habitat unaffected (Admiraal, unpublished in

Admiraal, 1984). Host specificity of fungal (Cytrid) parasites has also been documented in freshwater diatoms (Doggert and Porter, 1995; Holfeld, 1998). Extensive parasitism of 2 closely related planktonic diatoms species by a nanoflagellate was observed in natural populations of the Wadden Sea (Tillman, 1999). Recently, it was hypothesised that parasites of phytoplankton may at times be successful competitors to zooplankton in controlling energy flow and food web dynamics and that they may play a regulating role in phytoplankton succession due to their pronounced selectivity (Tillman, 1999). It has also been hypothesised that background extinctions are caused by host-specific viral action (Emiliani, 1993). Observations of community wide pathogenic infections are rare, with the exception of a probable pathogenic bacterium causing death of all diatom species in benthic community of a desert stream (Peterson *et al.*, 1993).

1.4. Spatial variability

Spatial variability in microphytobenthos biomass, physiology and community assemblage has been documented from the estuarine habitat. Spatial distribution can vary on a horizontal scale both within tidal zone and longshore (Paterson *et al.*, 1994). Spatial variations are present on a both a horizontal scale, indicated by microspatial patchiness of surface biomass (Pinckney and Sandulli, 1990) and on a vertical scale within the surface sediment layers (Wiltshire, 2000; Kelly *et al.*, 2001). Temporal distribution is also an important variable, as microphytobenthos are known to migrate to the surface during tidal exposure and, as in many biological systems, seasonal changes also occur.

1.4.1. Horizontal distribution

Microphytobenthos are renowned for having patchy distributions, on both a small and large scale, in muddy estuaries and numerous repetitions are needed to get representative values (MacIntyre *et al.*, 1996). These authors suggest a minimum of 5 replicates (12.6 cm^2 each) is needed to reduce the coefficient of determination (CV) to 45% in a 2500 cm^2 area (MacIntyre *et al.*, 1996). The horizontal distribution of microphytobenthos has been statistically investigated with patches ranging from < 4 to 113 cm^2 (of 0.64 cm^2 core areas; Blanchard, 1990). Yallop and Paterson (1994) studied the distribution patterns of diatom assemblages on a larger scale in the Severn estuary, U.K. They studied a number of different sites on a longshore direction and

found high biomass (Chl *a*) on the sites with finer cohesive grains, compared with the sites with sandier sediments. They also found that after a storm, when finer grains were deposited onto a normally sandy site, diatom biomass increased.

1.4.2. Vertical distribution

It is well known that intertidal microphytobenthos inhabit the sediment surface, to a depth of 1.5 mm (Kühl *et al.*1994) or 3 mm (Pinckney *et al.*, 1994), but often most of the diatom biomass is present in the top 0.2 - 0.4 mm during daylight tidal exposure (Taylor, 1998; Wiltshire, 2000; Kelly *et al.*, 2001). Therefore, the resolution of sediment sampling is an important aspect in the study of microphytobenthos. Because of the migratory behaviour of the community, the vertical distribution of biomass will change with the time of sampling within the tidal period (see following section). The depth of sampling will also affect how much photosynthetically inactive biomass (PIB), present below the photic zone, as well as photosynthetically active biomass (PAB) is being measured (Kelly *et al.*, 2001). Recently the Chl *a* concentration in the upper 1 mm have been used (Barranguet *et al.*, 1998; Kromkamp *et al.*, 1998), however, the standard approach has been to measure Chl *a* quantity in the upper 5 mm (Brotas and Plante-Cuny, 1998), although intervals as large as 10 mm have been used (MacIntyre *et al.*, 1996). Deeper coring techniques will include PIB from detrital material (both algal and higher plant) which has been incorporated into the sediment bed through the processes of bioturbation, sediment deposition and from spores and resting stages of various algal groups. The separation of these two pools of Chl *a* (PAB and PIB) is important for the accurate determination of the distribution and activity of microphytobenthos. The development of the Cryolander, which samples the surface sediment with no distortion, followed by micro-sectioning is a major advance in the sampling of active microphytobenthos in intertidal cohesive sediments (Wiltshire *et al.*, 1997b; Wiltshire, 2000; Kelly *et al.*, 2001, also see Methods section). Kelly *et al.* (2001) compared depth profiles from Cryolanders with coarse cores and concluded that coarse cores did not give sensitive enough measurements of biomass because results incorporated PIB.

1.4.3. Temporal distribution and migratory behaviour

The tidal rhythm affects many marine biological processes. The movement of, often dynamic, tides over a microphytobenthic mat could potentially scour the organisms from the surface. Many studies have shown that diatoms migrate to the

surface when the tide is low and back down into the sediment when the tide returns (Perkins, 1960; Palmer and Round, 1965 and 1967; Round and Palmer, 1966; Brown *et al.*, 1972; Happey-Wood and Jones, 1988; Pinckney and Zingmark, 1991; Hay *et al.*, 1993; Garcia-Pichel *et al.*, 1994; Serôdio *et al.*, 1997; Kromkamp *et al.*, 1998). These studies use various methods to demonstrate this migratory behaviour. Perkins (1960) visually assessed the brown coloration of diatoms on the surface of the Eden Estuary with an increased colour during tidal exposure periods. Some authors used periodic collection of lens tissues that were subsequently analysed for species composition or Chl *a* concentration (e.g. Palmer and Round, 1965; Hay *et al.*, 1993). It has been documented that there is a species-specific emergence from a mixed diatom assemblage (Round and Palmer, 1966; Paterson, 1986; Hay *et al.*, 1993) in intertidal sediments. Other more recent methods used the optical properties of Chl *a* to trace migration at the surface of the sediment (Serôdio *et al.*, 1997; Kromkamp *et al.* (1998); Paterson *et al.* (1998); Serôdio and Catarino, 2000). These experiments resulted in increasing fluorescence when the tide was low during the day and decreasing when the tide was in or during the night. Kromkamp *et al.* (1998) also demonstrated an increase in fluorescence alongside an increasing spectral reflectance (in the algal absorption spectrum) on a mudflat during initial tidal emersion. Paterson *et al.* (1998) confirmed the optical influence of diatom migration on sediments.

Vertically, *Gyrosigma spencerii*, a typical estuarine diatom, moved through natural sediments at a rate of approximately 0.19 $\mu m\ s^{-1}$ (Hay *et al.*, 1993). These authors also found that on the surface of artificial sediment the same species moved at a rate of 4.7 $\mu m\ s^{-1}$, some 25 times faster than vertically through the sediment. Happey-Wood and Jones (1988) also showed that the speed and distance travelled (on glass under microscope) of *P. angulatum* also followed a tidal rhythm, both increasing during emersion periods.

Both tidal and diurnal rhythms have also been found to affect the photosynthetic rhythms of microphytobenthic algae. Blanchard and Guarini (1996) found that maximum photosynthesis was higher when the low tide was at midday, but this is not always clear.

1.4.3.1. Seasonality

Seasonal trends are seen in terms of microphytobenthic biomass, composition and productivity. Annual biomass variation and annual changes in primary

productivity of microphytobenthos in the estuarine habitat is widely documented, over 30 intertidal studies are reviewed by MacIntryre *et al.* (1996), with more recent studies in annual biomass undertaken by Yallop and Paterson (1994); George (1995); Cariou-Le Gall and Blanchard (1995); Brotas *et al.* (1995), and primary productivity by Underwood and Kromkamp (1999). Few studies show annual variability of cell densities (MacIntryre *et al.*, 1996 documents 8 studies in their review) and even fewer survey the species assemblages over different seasons (e.g. Coljn and Dijkema, 1981; Admiraal *et al.*, 1984; Oppenheim, 1991; Underwood, 1994).

In the spring, diatoms bloom in many habitats, including the intertidal estuary. Spring blooms start earlier at top shore as there are longer periods of irradiance. Blooms appearing where there is more light has also be seen in phytoplankton, which bloom earlier in clearer offshore water than more turbid near-shore waters (Gieskes and Kraay, 1975 cited in Admiraal and Peletier, 1980). Thus Admiraal and Peletier (1980) proposed increasing irradiance not temperature as a trigger for the spring bloom.

Microphytobenthos decrease in density during the summer under natural conditions (Admiraal & Peletier, 1980; Colijn, 1978 (cited in Admiraal & Peletier, 1980)). This could be due to a combination of grazing, nutrient depletion, sediment stability and desiccation, since isolated cultures grown in discrete chambers on a mudflat grew well during the summer period (Admiraal & Peletier, 1980).

In the winter months diatom biomass is generally lower than in spring and autumn (Admiraal and Peletier, 1980), as light becomes a limiting feature for microphytobenthic photosynthesis. However diatom blooms are still observed on the top shore during winter, and only thin blooms on the low shore (Colijn and Dijkema, 1981; Dijkema (1975, cited in Admiraal and Peletier, 1980). There are particular species that only grow during the winter e.g. *Navicula salinarum* (Admiraal, 1984); Underwood (1994) also records a change in species composition with seasons.

Maximum photosynthesis was found to have seasonal trends; it was twice as high in April as in September, which was twice the value as December (Blanchard *et al.*, 1996, 1997).

1.5. Photosynthesis

Physiological monitoring of microalgae often measures the responses of photosynthesis. Photosynthetic measurements can be used for the assessment of stress

response (Govindjee, 1995), to both natural (e.g., temperature, irradiance) and unnatural effects (heavy metal, nutrients and certain herbicides). These can include the efficiency of photosynthesis, whether any effects are limiting or damaging and how acclimated the organisms are to their surroundings.

In its most simple form oxygenic photosynthesis is the process that drives the reduction of carbon dioxide to carbohydrates, using light energy which has been absorbed by Chl *a*, and can be expressed in the equation:

$$2H_2O + CO_2 + \text{light} \xrightarrow{\text{Chl } a} (CH_2O) + H_2O + O_2 \qquad \text{Equation 1.1}$$

Light energy is absorbed by a suite of pigments in the antennae system, this energy is then channelled to the reaction centres. The reaction centres contain Chl *a* molecules which use the energy transferred from the antennae to participate directly in photosynthesis. These reaction centre reactions are known as the light reactions and describe the oxidation of water and can be expressed in the equation:

$$2H_2O + \text{light} \xrightarrow{\text{Chl } a} 4H^+ + 4e^- + O_2 \qquad \text{Equation 1.2}$$

The light reaction is followed by a dark reaction which takes place in the chloroplast stroma, and describes the reduction of carbon dioxide and can be expressed in the equation:

$$CO_2 + 4H^+ + 4e^- \longrightarrow CH_2O + H_2O \qquad \text{Equation 1.3}$$

Thus measurement of photosynthesis can be made by monitoring the oxygen evolution or the carbon uptake (see below).

The majority of microphytobenthic diatoms have autotropic metabolism and have pigments to harvest light and use CO_2, water and nutrients for growth, although some species of diatoms have heterotrophic metabolism (see Admiraal, 1984 and references there in).

The rate of photosynthesis of microphytobenthos has often been treated as synonymous with microphytobenthic productivity, although there are discrepancies between them. Photosynthesis is generally measured as oxygen evolution or carbon uptake, which maybe different from the amount of energy/biomass generated (i.e.

productivity). Primary productivity of intertidal microphytobenthos has been studied extensively (see McIntyre, 1996; also see Underwood and Kromkamp, 1999 for a review on the methodology and factors influencing, microphytobenthic productivity).

Photosynthesis is primarily dependent on irradiance, followed by temperature and nutrient status. Photosynthetic rate has a non-linear relationship with irradiance known as the photosynthesis-irradiance (*P-E*) curve (Fig. 1.1). There are several photosynthetic parameters that can be measured or calculated: photosynthetic rate, light utilisation efficiency (α), light saturation intensity (E_k) and maximum photosynthetic rate (P_{max}). The latter three parameters are calculated from plotted *P-E* curves (Sakshaug *et al.*, 1997) and are characterised by 3 distinct regions of the curve (Fig. 1.1). The first is the initial linear slope of the *P-E* curves (at lower irradiance), where the photosynthetic rate is limited by irradiance and is thus linearly proportional to irradiance (the slope is a measure of α). The next region is the plateau or peak, which is a measure of the maximum potential photosynthetic rate (P_{max}). In the third region of the curve the rate declines, giving a measure of photoinhibition (ß) and can be due to permanent damage of photosystems or temporary shutting down of the systems. The irradiance at which photosynthesis is no longer limited by light absorption (and photochemical energy conversion) is known as the light saturation parameter (I_k or E_k). E_k can be calculated using the equation (Sakshaug *et al.*, 1997 and Kromkamp *et al.*, 1998, also see Fig. 1.1):

$$E_k = P_{max}/\alpha \qquad \text{(units are } \mu\text{mol m}^{-2}\text{ s}^{-1}\text{)} \qquad \text{Equation 1.4}$$

1.6. Methods of measuring photosynthesis

There are several methods for measuring photosynthesis, and ultimately production, of photosynthetic organisms. The two main methods are measurements of rates of oxygen evolution and rates of carbon uptake. Fluorescence, a relatively new method has been developed for measurements of photosynthesis in microalgae cultures (Hofstraat *et al.*, 1994; Geel *et al.*, 1997) and phytoplankton (Falkowski and Kolber, 1995). This technique has recently been applied to benthic diatoms, using both suspensions of natural assemblages (Hartig *et al.*, 1998) and undisturbed cores (Kromkamp *et al.*, 1998). The methods used for measuring photosynthesis are explained in more detail below and are reviewed in Underwood and Kromkamp (1999). Both oxygen evolution and fluorescence are products of the light reactions,

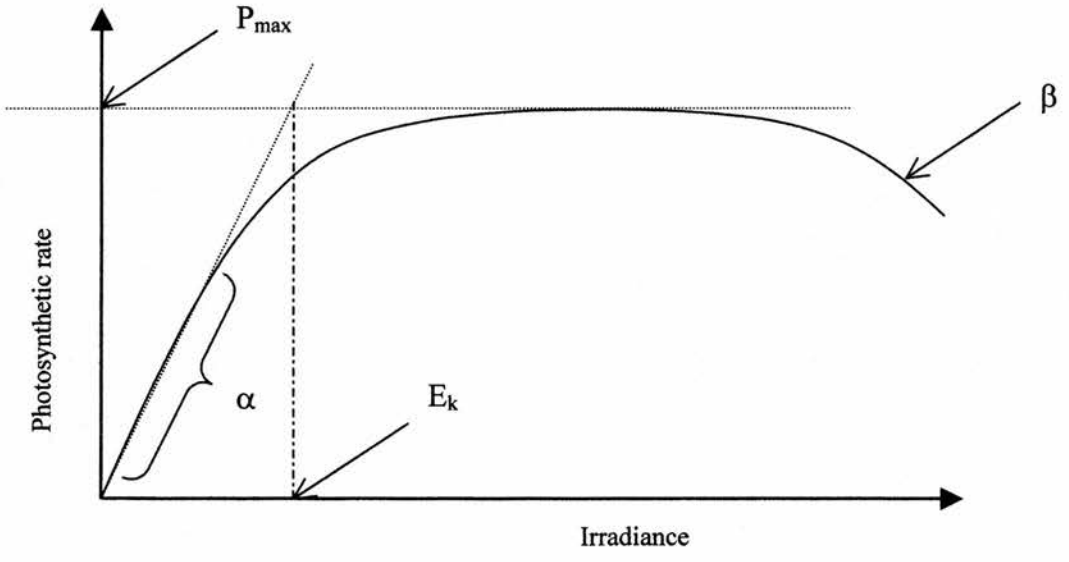

Figure 1.1. The photosynthesis versus irradiance curve (*P-E* curve), showing the light utilisation efficiency (α), light saturation intensity (E_k), maximum photosynthetic rate (P_{max}) and photoinhibition (ß)

fluorescence measures the electron flow at the (PSII) reaction centre. Labelled carbon uptake is a product of the dark reactions.

1.6.1. Fluorescence

It is well known that Chl *a* emits fluorescence in the red band upon excitation by light energy (Kautsky & Hirsch, 1931; Govindjee, 1995), and an increase in Chl *a* gives a greater fluorescence yield. Fluorometry has been used extensively for the measurement of extracted Chl *a* concentration and also for the estimation of phytoplankton Chl *a* concentration *in vivo* (e.g. Lorenzen, 1966; Vyhnálek, 1993). *In vivo* fluorescence emanates from the antenna system, not simply from Chl *a*, and at room temperature fluorescence emanates mostly from PSII, with minor contributions from PSI (Krause & Weis, 1991). Electron transport rate can be derived from various fluorescence measurements and is described in more detail below.

1.6.1.1. Pulse Modulated Fluorescence

Modulated fluorometry has become an important method for the measurement of *in vivo* photochemical processes, as measurements can be made during photochemistry (under ambient or induced irradiance) for the determination of electron transport rate (Hartig *et al.,* 1998). The technique is non-intrusive and extremely fast, measuring rates over time scales of less than a second. A measure of stress response using the maximum efficiency of photochemistry at PSII can also be estimated (Genty *et al.,* 1989). Pulse modulated fluorescence has also been used for the estimation of Chl *a* quantity (Serôdio *et al.*, 1997; Chapter 4).

Modulated fluorometry exposes the sample to very short pulses of light, enough to induce a reliable fluorescence signal (which is monitored during this short period of excitation) but not enough to induce significant photochemistry (Schreiber *et al.*, 1986). The short pulses of light, made with a measuring light (ML) are set at a suitable excitation wavelength to induce fluorescence, and are most commonly available in blue (470 nm) or red (650 nm). These wavelengths are optimal for excitation of different groups of algae. The major groups of algae have different excitation spectra for Chl *a* fluorescence because of the varied accessory pigment complexes in the antennae systems. A blue ML will induce optimal fluorescence from diatoms and green algae. A red ML induces fluorescence from cyanobacteria, although diatoms and green algae will also fluoresce, but to a lesser extent than under

a blue ML (Yentsch & Yentsch, 1979). Fluorescence measurements (induced by the ML) made in the dark are from the pigment bed and is a measure of completely oxidised (relaxed) primary electron acceptors in PSII (Q_A). This level of fluorescence of dark adapted cells under the ML is known as minimum fluorescence (*Fo*). This parameter has been used for the estimation of Chl *a* quantity in sediments (Serôdio *et al.*, 1997; Barranguet and Kromkamp, 2000).

Pulse Modulated Fluorescence techniques (developed by Schreiber *et al.*, 1986) have recently been successfully adapted for the study of microphytobenthic photosynthesis (Hartig *et al.*, 1998; Kromkamp *et al.*, 1998). These techniques measure the activity of photosystem II (PSII) reaction centres present in the cells. Hence the measurements made are of the rate of production of electrons by the water splitting system of PSII. As a measure of stress response, the maximum efficiency of photochemistry at PSII is determined from the variable fluorescence (*Fv*, see below). Variable fluorescence is calculated from the difference between minimum and maximum fluorescence (*Fo* and *Fm*, respectively) and are made from dark adapted organisms. *Fm* is measured during a short pulse of saturating light, where the electron acceptor becomes reduced, and the photochemical energy conversion of PSII becomes saturated. From these two parameters, variable fluorescence (*Fv*) and the maximum efficiency of photochemistry at PSII can be estimated (Genty *et al.*, 1989) using the equation

$$\Phi m = (Fm - Fo) / Fm = Fv/Fm \qquad \text{Equation 1.5}$$

Where Φm or *Fv/Fm* is the maximum efficiency of photochemistry at PSII.

In ambient (or other constant) light the fluorescence of photosynthetic organisms will rise to a level, steady state fluorescence (*Fs* or *F*). When a saturating pulse of light is applied, light adapted maximum fluorescence (*Fm'*) is induced. *Fm'* is lower than *Fm* because some of the electron acceptors are already reduced during photosynthesis. The effective efficiency of photochemistry at PSII can then be calculated (Genty *et al.*, 1989) as follows

$$\Delta\Phi = (Fm' - Fs) / Fm' = \Delta F / Fm' \qquad \text{Equation 1.6}$$

Where $\Delta\Phi$ or $\Delta F/Fm'$ is the effective efficiency of photochemistry at PSII.

When algae are adapted to ambient light the photosynthetic electron transport rate (ETR) can also be calculated (Genty *et al.*, 1989; Hofstraat *et al.*, 1994) as follows:

$$ETR = E \times \Delta\Phi \times \sigma_{PSII} \qquad \text{Equation 1.7}$$

E is the irradiance and σ_{PSII} is the functional absorption cross section of PSII (i.e. the light absorbed by PSII to drive photochemistry). Hartig *et al.* (1998) uses the specific absorption coefficient (a*) which is the absorption cross section of the algae (as opposed that of PSII). The specific absorption coefficient is easily measured spectrophotometrically when cells are in suspension, and has the units: m^2 g Chl a^{-1}. The absolute value for ETR is equivalent to primary productivity rate (Hartig *et al.*, 1998). a* or σ_{PSII} are difficult parameters to measure in diatoms on a sediment surface, however, relative ETR (rETR) can still be approximated by the product of irradiance and effective efficiency, which have been used in the determination of photosynthetic activity (Kromkamp *et al.*, 1998).

The ETR calculated is the ETR per PSII unit. To measure the ETR per unit of Chl *a* (Je), the number of PSII per mg of Chl *a* must be measured and is thus:

$$Je = ETR \times n_{PSII} \qquad \text{Equation 1.8}$$

If the conversion of ETR to oxygen evolution (or to carbon) is required, the number of electrons needed to produce an oxygen molecule (or to fix one carbon molecule) (θ) must be obtained and is calculated as follows:

$$Je^{O2} = \Delta\Phi \times E \times \sigma_{PSII} \times n_{PSII} \times \theta^{O2} \qquad \text{Equation 1.9}$$

or $$Je^{C} = \Delta\Phi \times E \times \sigma_{PSII} \times n_{PSII} \times \theta^{C} \qquad \text{Equation 1.10}$$

Where Je^{O2} and Je^{C} is the oxygen evolution or carbon uptake and θ^{O2} and θ^{C} are the number of electrons needed to produce an oxygen molecule or to fix one carbon molecule, respectively.

A good correlation ($r = 0.88$) was documented between ^{14}C based primary production measurements (mg C mg^{-1} Chl *a* h^{-1}) and fluorescence based

measurements for microphytobenthos suspensions (Hartig *et al.*, 1998). Other photosynthetic parameters (i.e., light saturation index; light intensity at which maximum production is reached; and effective efficiency) did not correlate as well between the 2 methods (Hartig *et al.*, 1998).

A linear relationship was found at limiting light intensities between O_2 based primary production measurements (mg O_2 mg^{-1} Chl *a* h^{-1}) and fluorescence-based measurements on marine algae suspensions (Geel *et al.,* 1997). The relationship became non-linear at saturating intensities and is probably due to the Mehler reaction or pseudocyclic electron transport, which affects linear electron transport or consumption of oxygen (Geel *et al.,* 1997; Flameling and Kromkamp, 1998).

1.6.1.2. Other fluorescence techniques

Systems other than pulse modulated fluorometers can measure photosynthesis, but make slightly different measurements. They include pump and probe (P&P) fluorometry, and fast repetition rate (FRR) fluorometry. These two latter techniques can be used in the study of fluorescence kinetics, but also allows the derivation of functional cross-section from a sequence of subsaturating excitation pulses (Kolber *et al.*, 1998).

1.6.2. Carbon uptake

Diatoms use both carbon dioxide (CO_2) and bicarbonate (HCO_3^-) in photosynthesis, this is shown by the active uptake of both of these carbon sources in a benthic fresh water species (Rotatore and Colman, 1992). Planktonic diatoms have also been shown to avoid CO_2 limitation by the use of HCO_3^- (Korb *et al.*, 1997). Photosynthesis and primary productivity can be measured using radio-labelled carbon, in the form of $^{14}CO_2$ or H $^{14}CO_3$. This process measures the uptake of ^{14}C by the organisms over a given period of time (Revsbech and Jørgensen, 1981; Blanchard *et al.*, 1997). Lewis and Smith (1983) developed a device called a photosynthetron, which measures the uptake of $H^{14}CO_3$ by suspensions of microalgae in a controlled environment.

1.6.2.1. Infra-Red Gas Analysis (IRGA)

Photosynthesis of higher plants is often measured using IRGA methods. This process monitors the absorption of CO_2 of the organism over time. CO_2 depletion, in a closed chamber is measured spectroscopically (CO_2 absorbs at a particular

wavelength; in the infra-red region). This technique cannot be used for organisms living in wet habitats (e.g. microphytobenthos) as they utilise CO_2 from surrounding water, not solely from the air. This method was however, recently assessed by colleagues at the University of Essex (Underwood pers. com.) with dense mats of diatoms, and was found to be unsuitable.

1.6.3. Oxygen evolution

There are two main methods of measuring oxygen evolution, one which measures oxygen exchange using Bell jars (Barranguet, 1997) and the other uses oxygen microprobes or microsensors. The Bell jars method measures oxygen evolved from the biofilm, which has diffused into the overlying water or air contained in the jar. The oxygen microprobes method lowers a measuring probe into the biofilm and sediment. Oxygen microprobes have become a useful tool in measuring the depth distribution of oxygen in undisturbed biofilms within the surface layers of sediment/biofilm (Revsbech and Jørgensen, 1983).

1.7. Aims

This thesis investigates the use of florescence techniques for the remote sensing of microphytobenthos biomass and distribution. The objectives of this study were:

- To ascertain the relationship between Fo^{15} and diatom biomass, under natural field conditions (Chapter 4 and 5).
- To develop hardware for the use of fluorometry in the field for measuring microphytobenthos *in situ* (Chapter 3). The development of this hardware was in conjunction with R. Forster and J. Kromkamp from the Netherlands Institute for Ecology (NIOO).
- To compare Fo^{15} and algal biomass over a seasonal scale (Chapter 4) and on a large spatial scale, to include an inter-estuary study (Chapter 5).
- To compare the different units of expression of Chl *a* (both content and concentration), to ascertain their comparability across temporal and vertical spatial scales (Chapter 6).
- To statistically examine the migratory behaviour of microphytobenthos *in situ*, on a short-term temporal scale, over hours and days (Chapter 7).

Chapter 2

2. MATERIALS AND METHODS

2.1. Sites

Several sites at three locations across Europe were studied (Fig. 2.1). The main sampling location was the Eden Estuary, Scotland. The other sampling locations were the Sylt Rømø Basin in Germany and the Westershelde and Oostershelde, near Yerseke in the Netherlands (Fig. 2.1). Scientists from the University of St Andrews, ASU, Ireland; NIOO, the Netherlands; GKSS and RuG, Germany surveyed these three locations during 3 large field campaigns (BIOPTIS EU MAS3-CT97-0158). The surveying included ground truthing numerous parameters with simultaneous remote sensing measurements in order to determine algorithms. My role in the each campaign was primarily to assess the sediment surface using fluorometry as part of the ground-remote sensing team.

The intertidal areas sampled during this study were diverse in size, sediment properties and biota (BIOPTIS Final Report). The Eden Estuary was particularly heterogeneous in algal groups, whereas Sylt and Yerseke sites had diatoms with some *Zostra* sp. presence (this will be checked by pigment fingerprinting; BIOPTIS Final Report). The Sylt sites were dominated by sandy sediments, except grid C which was finer grained (BIOPTIS Final Report). The Eden Estuary and Yerseke sites were all finer grained sediments (BIOPTIS Final Report). The Eden Estuary also had macroalgae present on grid B, mainly *Enteromorpha*, but some *Porphyra* was also present.

2.1.1. Eden Estuary

The Eden Estuary is situated on the east coast of Scotland (56°22'N, 2°50'W), with a mean tidal range of 3.7 m. It is a bar built, mesotidal estuary according to the geomorphological classification scheme and has a total area of 10.41 km^2, 9.37 km^2 of which are intertidal (Davidson and Buck, 1997). The Eden Estuary is a National and local Nature Reserve, with 2 SSSI areas (Mathieson and Atkins, 1995). Approx. 76% of the catchment of the Eden Estuary is prime agricultural land and the total oxidised nitrogen from 1990 to 1994 upstream of the estuary ranged between 6.92-8.57 mg/l (Clelland 1994). These nitrogen concentrations input into the estuary were one of the

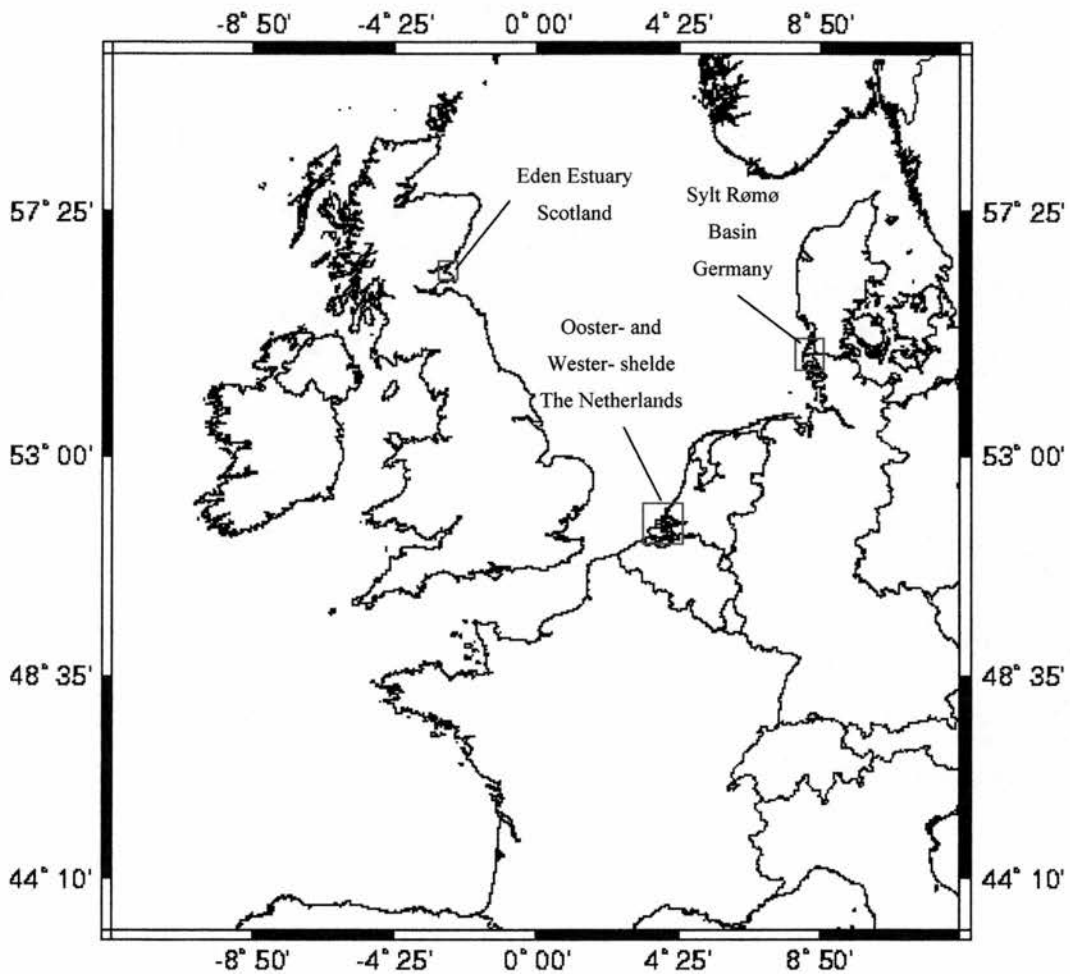

Figure 2.1. The locations of the intertidal areas studied in Europe

highest in comparison to other Scottish river/estuarine systems (Mathieson and Atkins, 1995).

A transect on the Eden Estuary situated near a Paper Mill was the site frequently used in this study (Fig. 2.2); dates were specified for each experiment under each section. Three grids on the Eden Estuary were also surveyed for a BIOPTIS campaign in August-September 1999. Grid EA was towards the mouth of the estuary on the southern shore, Grid EB spanned the channel near the Paper Mill and Grid EC was a sandy site at the mouth of the estuary on the southern shore (Fig. 2.3). Each grid node was numbered with the prefix E or E1, for Eden and the 1st Eden study (Figs 2.4, 2.5, 2.6), although this study did not include further studies on the Eden.

2.1.2. Sylt-Rømø Basin

The Sylt-Rømø Basin is situated on the west coast of the German/Netherlands border (54°97'N, 8°35'W). It is a 100 km^2 sheltered sandy tidal flat situated between the two islands of Sylt and Romo, which both extend around the basin. During May-June 1999, three grids, situated along the inner east side of the island of Sylt, were surveyed during the BIOPTIS campaign. Grid SA was the most northerly, Grid SC the most southerly and Grid SB between SA and SC (Fig. 2.7).

2.1.3. Westershelde and Oostershelde

The Westershelde and Oostershelde are situated in the south west of the Netherlands near the town of Yerseke. Three grids in this area were surveyed in June 2000 for the third BIOPTIS campaign (Fig. 2.8). Grid YA was on Bezlingsche-Ham (51°26'N, 3°55'W), a muddy site on the northern shores of the Westershelde (Fig. 2.9). Grid YB was on Zandkreek (51°32'N, 3°53'W), a sandy/muddy site on the southern shore of the Oostershelde (Fig. 2.10). Grid YC was on the Molenplaat (51°26'N, 3°57'W), a tidal sandflat in the middle of the Westershelde, only accessible by boat (Fig. 2.11).

2.2. Sediment sampling

Pigments and water content were analysed from surface sediments, obtained using various *in situ* freezing techniques. Freezing of the sediment *in situ* was undertaken so minimum alteration of pigments due to transport and storage took

Figure 2.2. A) The location of the Eden Estuary in the UK. B) The Location of the Paper Mill transect on the north shore of the Eden Estuary

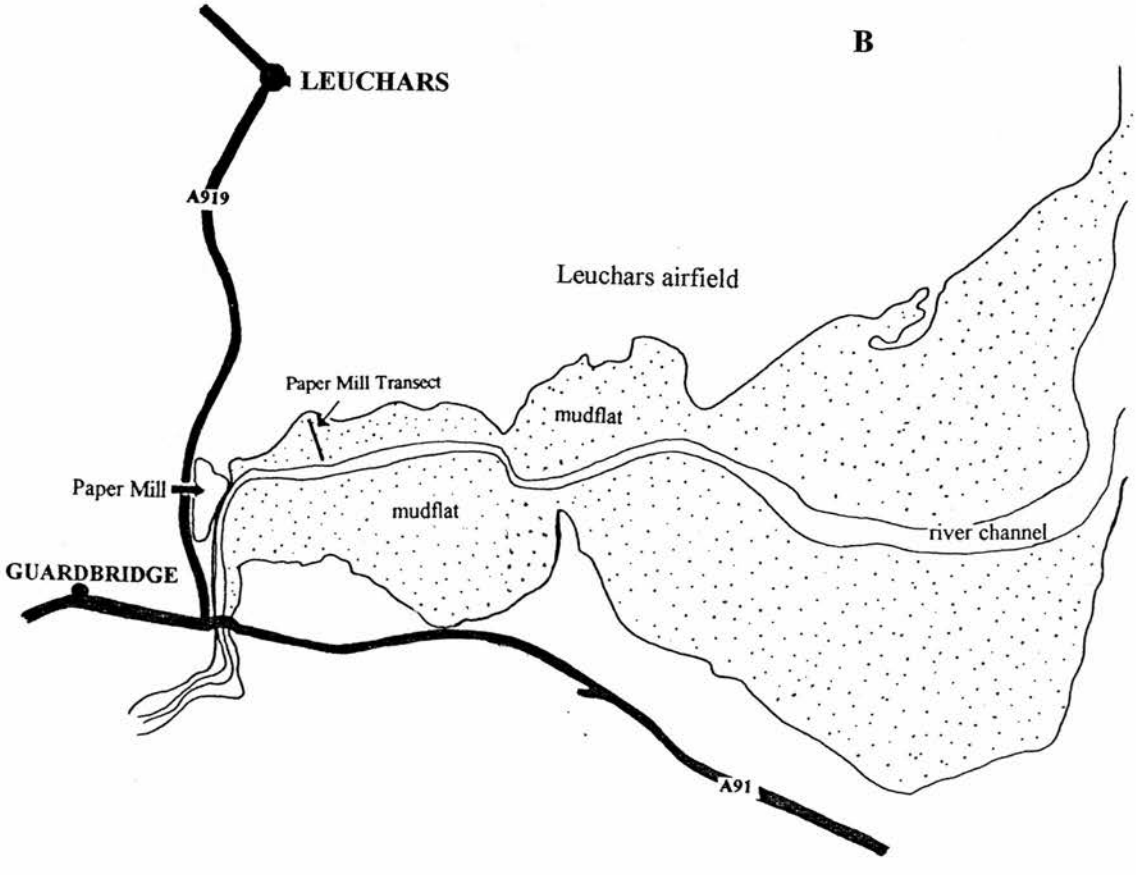

Figure 2.3. The Eden Estuary showing the BIOPTIS grid locations

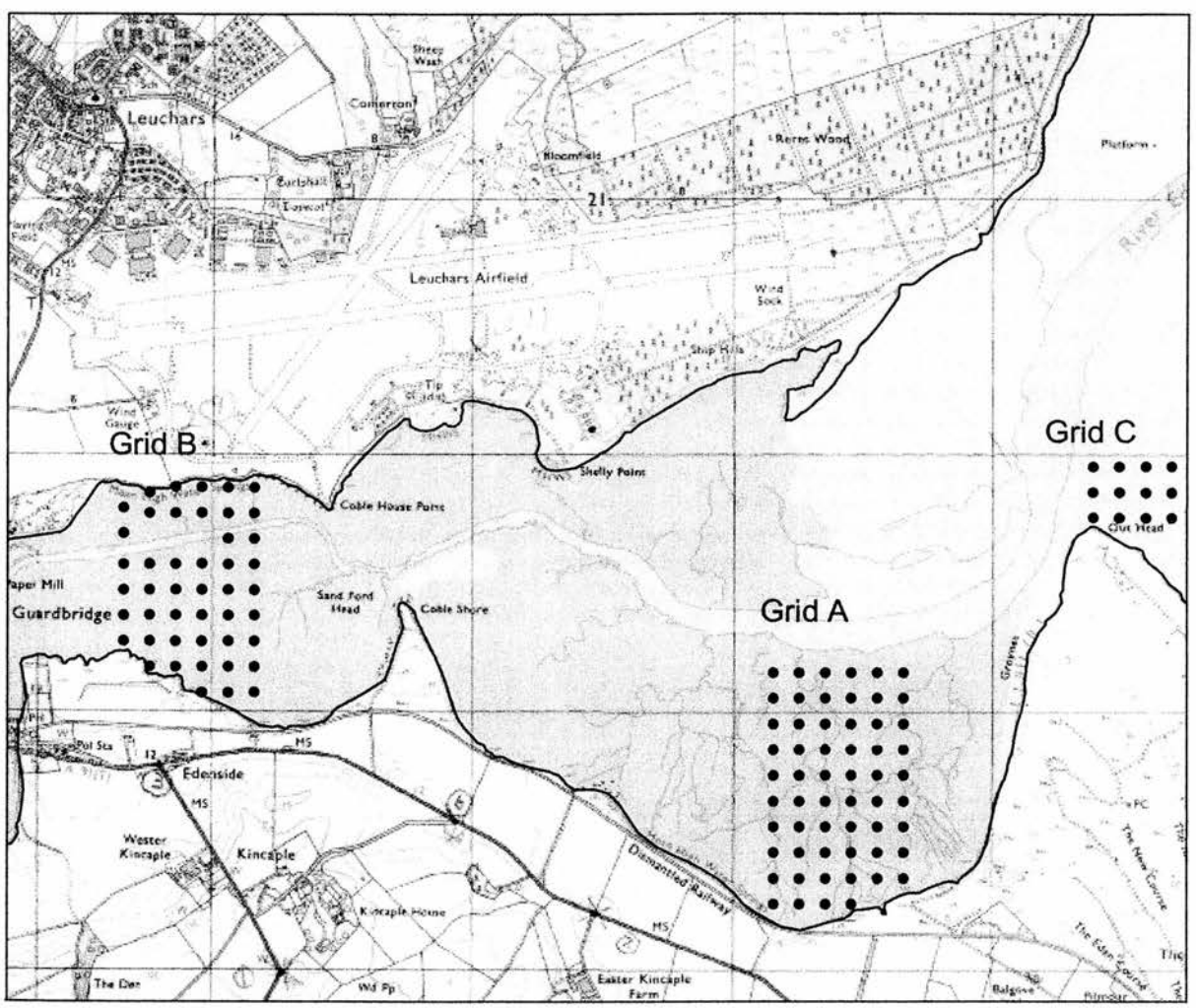

Site EDEN
Grid A

Gridpoint Names

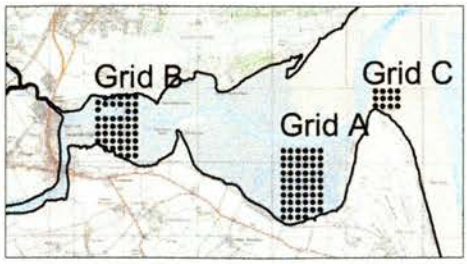

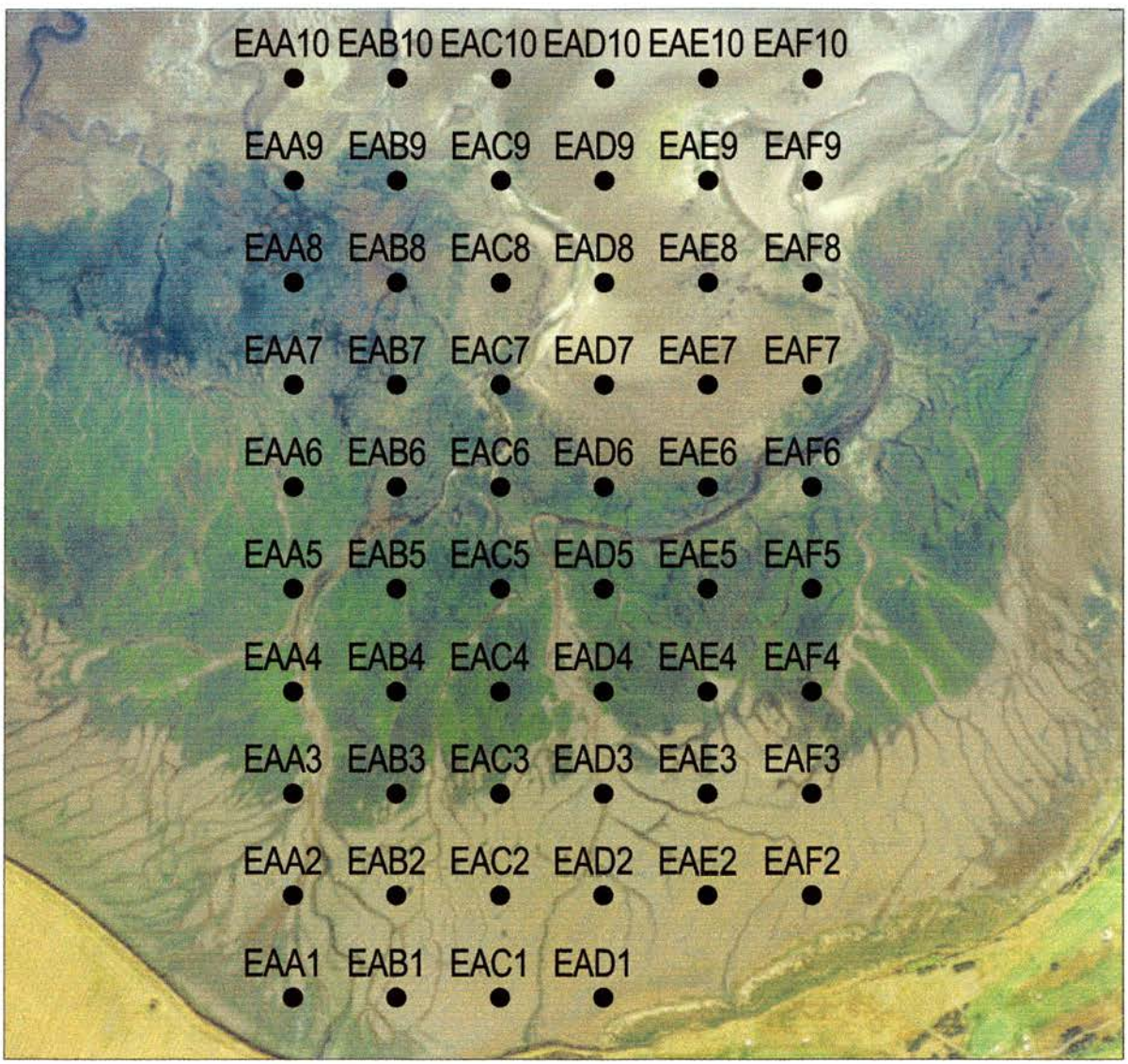

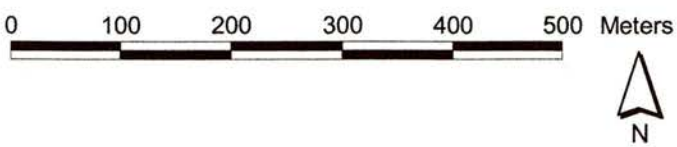

Background Image:
NERC aerial photograph
Date: 03-09-99

Data origin: University College Cork (ASU)

Figure 2.4. The Eden Estuary grid A showing node locations superimposed over an aerial photograph (taken with permission from BIOPTIS Atlas, with thanks to Kerstin Stelzer, thanks also to ASU for GPS node positioning and NERC for aerial photograph)

Site EDEN
Grid B

Gridpoint Names

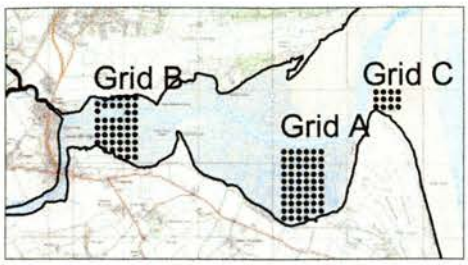

0 100 200 300 400 500 Meters

N

Background Image:
NERC aerial photograph
Date: 03-09-99

Data origin: University College Cork (ASU)

Figure 2.5. The Eden Estuary grid B showing node locations superimposed over an aerial photograph (taken with permission from BIOPTIS Atlas, with thanks to Kerstin Stelzer, thanks also to ASU for GPS node positioning and NERC for aerial photograph)

Site EDEN
Grid C

Gridpoint Names

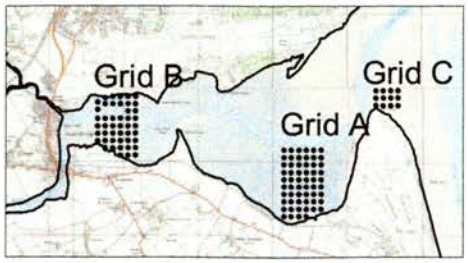

0 100 200 300 400 500 Meters

N

Background Image:
NERC aerial photograph
Date: 03-09-99

Data origin: University College Cork (ASU)

Figure 2.6. The Eden Estuary grid C showing node locations superimposed over an aerial photograph (taken with permission from BIOPTIS Atlas, with thanks to Kerstin Stelzer, thanks also to ASU for GPS node positioning and NERC for aerial photograph)

Site YERSEKE
Grid A

Gridpoint Names

0 100 200 300 400 500 Meters

N

Background Image:
NERC aerial photograph, ATM
Date: 27-06-00

Data origin: University College Cork (ASU)

Figure 2.9. Grid YA on the Westershelde showing node locations superimposed over an aerial photograph (taken with permission from BIOPTIS Atlas, with thanks to Kerstin Stelzer, thanks also to ASU for GPS node positioning and NERC for aerial photograph)

Figure 2.7. The Sylt Rømø Basin and position of the Sylt grids SA, SB and SC. Numbers in the top frame are Northings (vertical) and Eastings (horizontal).

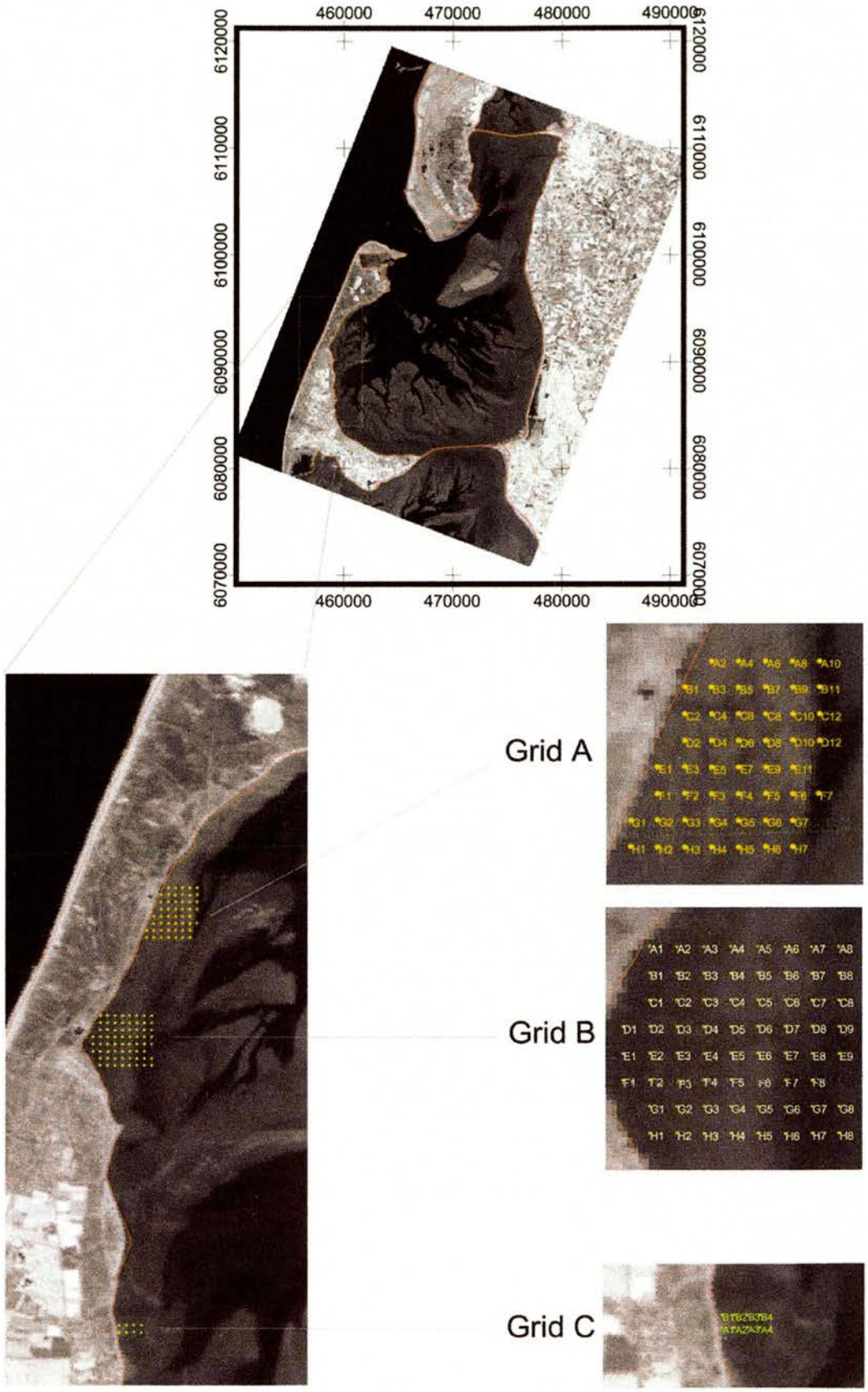

Figure 2.8. The BIOPTIS grid locations on the Westershelde (Grids A and C) and the Oostershelde (Grid B) near the town of Yerseke

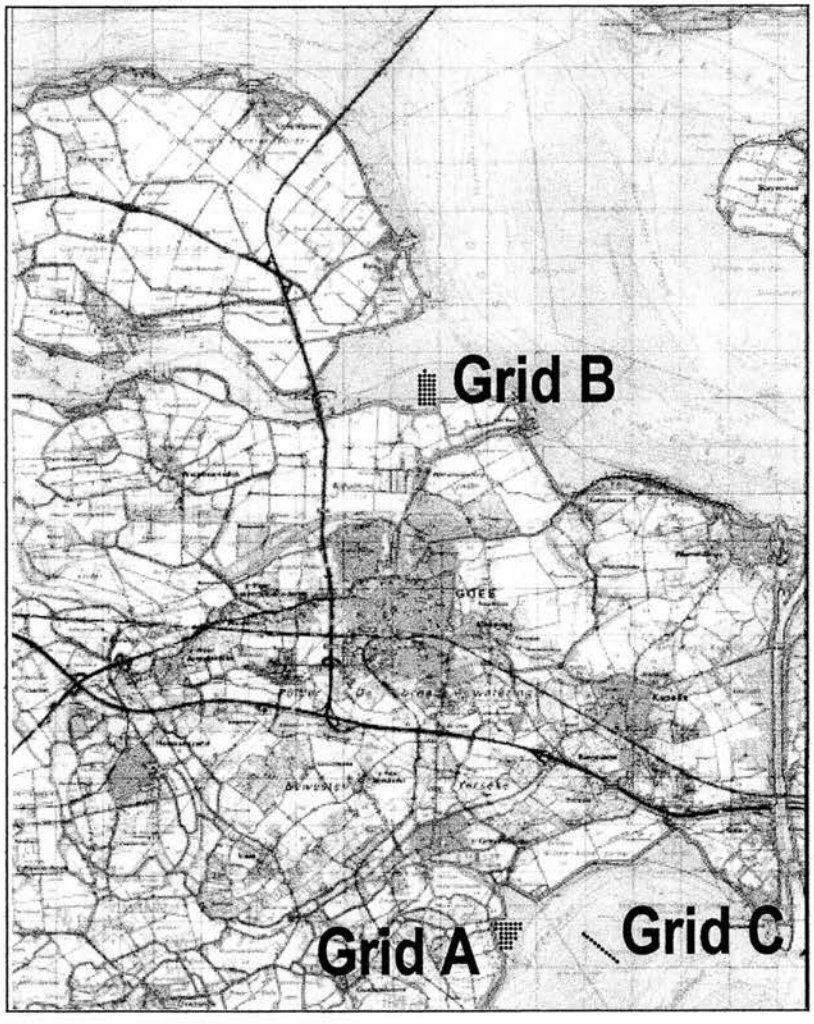

Site YERSEKE
Grid B

Gridpoint Names

0 90 180 270 360 450 Meters

N

Background Image:
NERC aerial photograph (ATM)
Date: 27-06-00

Data origin: University College Cork (ASU)

Figure 2.10. Grid YB on the Oostershelde showing node locations superimposed over an aerial photograph (taken with permission from BIOPTIS Atlas, with thanks to Kerstin Stelzer, thanks also to ASU for GPS node positioning and NERC for aerial photograph)

Site YERSEKE
Grid C

Gridpoint Names

0 100 200 300 400 500 Meters

N

Background Image:
NERC aerial photograph (ATM)
Date: 27-06-00

Data origin: University College Cork (ASU)

Figure 2.11. Grid YC on the Molenplaat on the Westershelde showing node locations superimposed over an aerial photograph (taken with permission from BIOPTIS Atlas, with thanks to Kerstin Stelzer, thanks also to ASU for GPS node positioning and NERC for aerial photograph)

place. The techniques used were contact coring and the Cryolander. The contact core method was developed as a faster method (~2 min) than Cryolanding, however it was less accurate and disturbed the surface sediment matrix as pressure is exerted on deployment. The Cryolander, used for examining depth micro-distribution of sediment properties but was a more time consuming method. Cryolanders take approximately 5-10 min to collect and further slicing in the laboratory could take 15-30 min to cut into blocks and slice (see below). Each sample has 6 sections for analysis (although in some cases pooling of deeper layers reduced depth sections to 4). Contact cores were therefore used for large studies encompassing numerous samples, where Cryolanding was impracticable.

Once samples were frozen using either technique, they were stored frozen and in darkness under liquid nitrogen (LN_2) for transportation to the laboratory, where they were stored at –80°C until further analysis.

2.2.1. Contact Core

The contact coring technique freezes a surface disc of sediment (2-3 mm deep) with a diameter of 56 mm, giving an area of 2463 mm^2. The equipment needed for this procedure was an aluminium dish, plastic collar, liquid Nitrogen (LN_2), slicer (artists palette knife), labelled aluminium foil. The aluminium dish, with the plastic collar in place, was placed onto the sediment surface and gently pushed down to the depth of the collar (2mm), so the base of the dish makes contact with the sediment surface (Fig. 2.12). LN_2 was then poured into the dish. After 30 s the dish with collar still attached was removed. Freezing times were assessed for each site, as water content and ambient temperature affect the time needed to freeze 2mm of sediment. Typically times ranged between 10 and 30 s. Any sediment not flush with the collar was quickly removed by scraping the artists palette knife across the base of the corer, level with the edge of the plastic collar. The collar was then removed and the frozen disc of sediment was wrapped in pre-labelled foil and stored under LN_2.

For certain studies where smaller areas of sediment were needed for analysis (e.g. surface location from which fluorescence measurements were made), frozen contact cores were re-cored, with a sharp metal corer, to a diameter of 314 mm^2. Other studies incorporated the whole core (i.e. campaigns in Sylt, Eden and Yerseke). The core was then lyophilised, homogenised and stored in the dark at –80°C until being sub-sampled for pigment analysis.

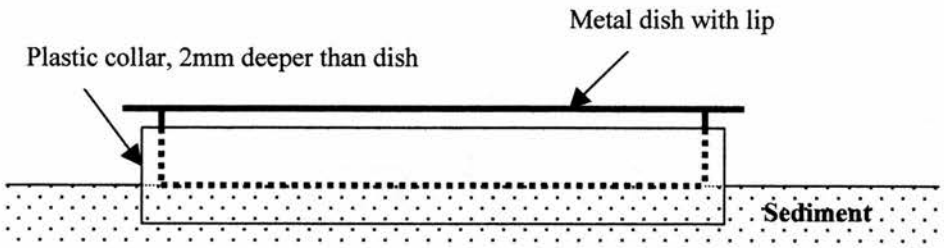

Figure 2.12. The contact corer in place on the sediment surface

2.2.2. Cryolander

The sediment surface is frozen slowly using the Cryolander technique (Wiltshire *et al.*, 1997), producing a frozen "plate" of sediment over 10 mm in depth and 50 mm diameter. The sediment was frozen by slowly dripping liquid nitrogen (LN_2) onto cotton wool suspended in a brass tube above the sediment. Once the sediment surface began to freeze (this needed to happen gradually to prevent surface distortion), more LN_2 was poured into the tube and onto the sediment, until the required depth was frozen. The brass tube was then lifted from the sediment surface with frozen sediment attached, this was removed and wrapped in pre-labelled foil whilst still frozen and stored under LN_2. In the laboratory, a 10 mm^2 block was cut from the frozen sediment using a lapidary saw (if necessary in the exact location of a fluorescence measurement). The blocks were then sectioned at 0.2 mm intervals from the surface to 0.6 mm, then at 0.4 mm to a depth of 1mm, followed by 0.5 mm sections to 2 mm depth (Fig. 2.13). Some studies only show 0.4 mm, 1 mm and 2 mm depth sections and were calculated by summing the respective sections (Fig. 2.13). The rest of the blocks were sectioned directly to 0.2 mm, 0.4 mm, 1 mm and 2 mm. The surface of the sediment collected with the Cryolander was often not completely flat. Thus 'zero depth' was determined at the point at which 90-95% of the area was visibly level. Any undulations above this point were included in the 0-0.2 mm slice. Sectioning was carried out using a freezing microtome (Leitz Wetzlar Kryomat 1703) and sections were removed from the knife using a fine paintbrush and suspended in distilled water in an Eppendorf tube (1 ml). Once each section had been transferred, they were re-frozen immediately and lyophilised in preparation for pigment analysis.

2.3. Water content

The sediment water content was determined as the percentage water of wet sediment using the formula:

$$\% \text{ water content} = (Wt_{wet} - Wt_{dry}) / Wt_{wet} * 100 \qquad \text{Equation 2.1}$$

Where Wt_{wet} is the wet sediment mass and Wt_{dry} is the dry sediment mass.

The usual method for water content determination is to dry the sediment in an oven at 110°C until a constant weight is obtained, which can take up to 5 days for ~5g (BIOPTIS protocols). In this study all samples were analysed for pigment analysis

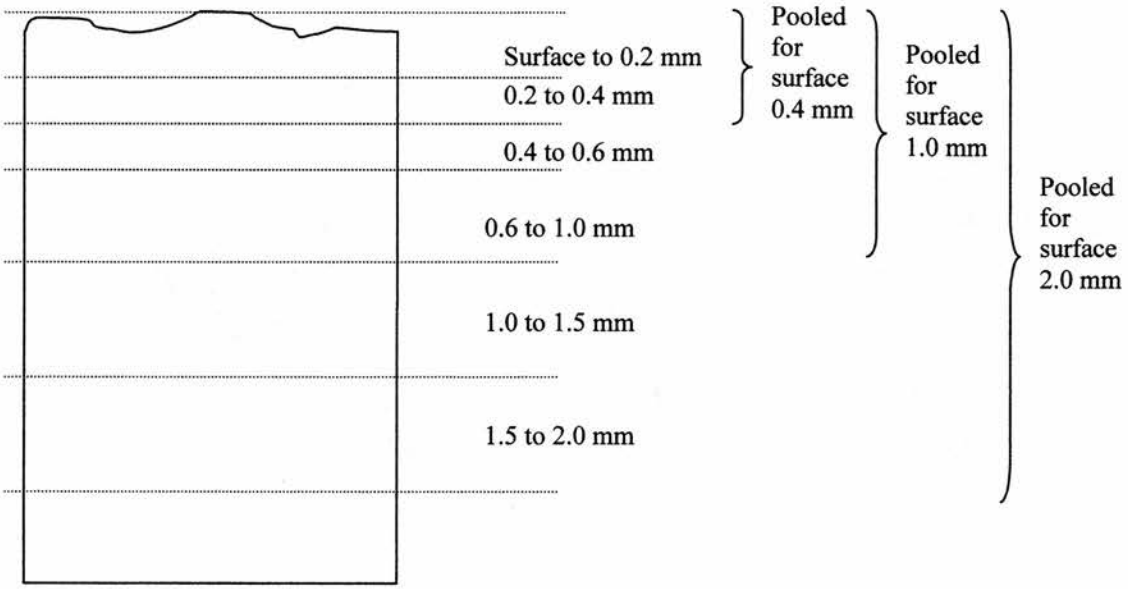

Figure 2.13. Cross section through a Cryolander sediment core with dotted lines marking the position of the cuts. Undulated surface is included in the top slice

and were thus freeze dried (lyophilisation) to avoid pigment breakdown. Therefore a comparison of water content determination was made between the oven drying method and lyophilisation.

Surface sediment samples were collected from the low shore at the Paper Mill site on the Eden Estuary in February 1999. The sediment was homogenised and divided into 10 sub-samples of approximately 5 g each. Five sub-samples were placed on foil dishes and dried in an oven at 110°C until a constant weight was obtained. The remaining 5 sub-samples were placed into plastic bags, frozen and lyophilised until a constant weight was obtained. Samples were weighed before and after drying to ascertain the water as percentage per mass of wet sediment (Equation 2.1). Lyophilised samples were also weighed before and after freeze drying.

Wet fresh sediment and wet frozen sediment did not differ in weight (data not shown). The average water content was 40.2 g +/-0.2 of the oven dried sediment, and 40.6 g +/-0.4 of the lyophilised sediment. There was no significant difference between these two methods ($t = -1.90$, $df = 5$, $P = 0.12$). Therefore lyophilised sediment determination was used throughout this study to determine water content of sediment.

2.4. Pigment analysis

Pigments were analysed using high precision liquid chromatography (HPLC) after solvent extraction from lyophilised sediments. Frozen samples were lyophilised (freeze-dried) in the dark, until dry (~24-48 hrs) in an Edwards Modulyo Freeze Dryer, in which samples remain frozen at –60°C under vacuum. Samples were freeze dried until completely dry (approx. 24 hr). As soon as the samples were removed from the freeze dryer they were sealed and stored in the dark at –80°C.

2.4.1. Pigment Extraction

Pigment extraction involved adding either 1 ml of 100% acetone or 90% dimethylforamide (DMF) to the lyophilised sediment sample (~0.04 g for cohesive sediments or ~0.1 g for sandy sediments) and pigments were extracted for a minimum of 24 hours at -70 ^{0}C (acetone) or 4^{0}C in the dark (DMF). Extractant and sediment were separated by filtration through a 0.2 μm pore syringe filter (Whatman^{TM}). Acetone was used until March 2000, then DMF was used after that date (see Chapter 3).

2.4.2. Pigment separation and detection (HPLC)

A range of pigments was identified by reverse phase HPLC. The HPLC system consisted of a quaternary Perkin Elmer 410 high pressure pump, a Waters WISP 417 autosampler , a Waters column oven and a Waters 910 diode-array detector (Figure 2.14). These HPLC instruments; pump, autosampler and detector were co-ordinated from a computer using Millenium software, which also integrated and stored the results of the separation and detection. The column was a reversed phase Nucleosil C18 (Capital HPLC Ltd) and was kept in a column oven at 25 °C. The autosampler was cooled to 4-6°C and set to inject a quanitity of distilled water prior to injection of the sample, at a ratio of 2.33 (30 µl) to the sample injection volume. The water helped to sharpen chromatogram peaks (Wiltshire, 2000). Extractions were injected (70 µl) onto a binary gradient, which ran for 45 min. The flow rate was 1 ml min^{-1} and the two solvents used were: eluant A:- 80% methanol, 10% water, 10% buffer (1.5 g acetate, 7.7 g ammonium acetate in 100 ml of distilled water), eluant B:- 90% methanol, 10% acetone (gradient 1, Table 2.1; Wiltshire & Schroeder, 1994). All solvents were HPLC grade and degassed prior to running by gently bubbling helium through them for 5-10 min. Chl *a* eluted at 25 min, and analysis of peak area was used to quantify the pigment. After June 1999 this protocol was altered to include a third solvent mixture (C) to aid the separation and speed of carotene elution (Wiltshire, BIOPTIS protocols). Eluant C was 56.5% Methanol and 43.5% Propanol. The running time was extended by 5 min to ensure elution of all pigments, giving a total running time to 40 min (gradient 2, Table 2.2).

Three concentrations of Chl *a* standards (see below) were analysed with every sample batch to obtain a standard curve, from which accurate Chl *a* concentrations of sample extracts were calculated using regression analysis.

The columns were cleaned or changed as soon as the peaks become diffuse and began to merge with neighbouring peaks, approximately every 300-600 samples. The column was cleaned by flushing through with a gradient consisting of solvents of different polarities. Hexane and water were used and as these solvents are immiscible, acetone was used as an intermediary solvent (Table 2.3). A test sample was processed before and after a cleaning gradient, and if peaks did not sharpen then a new column was used.

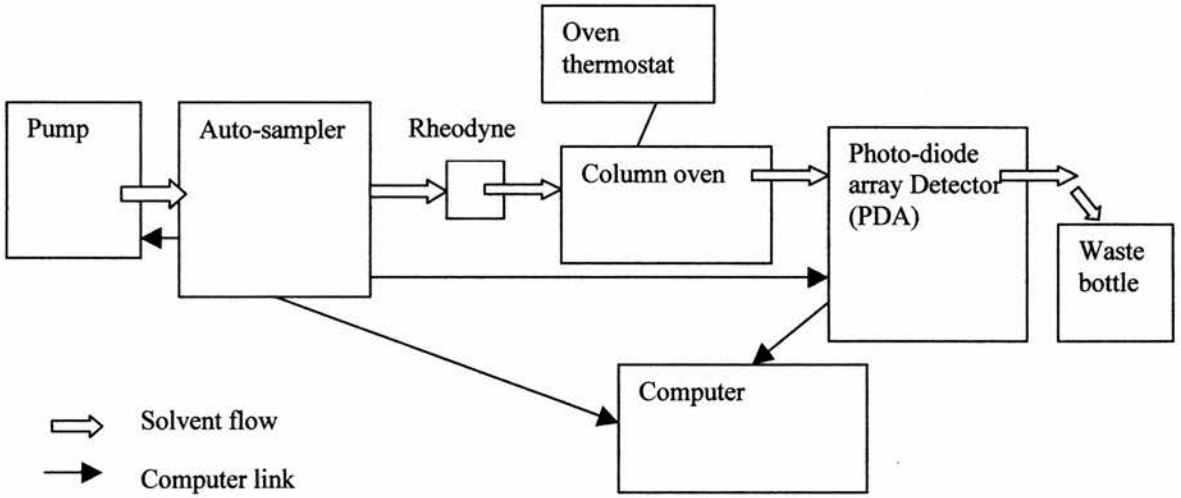

Figure 2.14. Waters HPLC System with Perkin Elmer Pump

Table 2.1. HPLC gradient 1

Step	Flow rate (ml/min)	Step Time (min)	Total Time (min)	Solvents		Curve
				%A	%B	
0	1	0	0	100	0	
1	1	5	5	50	50	linear
2	1	5	10	50	50	
3	1	5	15	0	100	linear
4	1	22	37	0	100	
5	1	8	45	100	0	linear

Table 2.2. HPLC gradient 2

Step	Flow rate (ml/min)	Step Time (min)	Total Time (min)	Solvents			Curve
				%A	%B	%C	
0	1	0	0	100	0	0	
1	1	5	5	50	50	0	linear
2	1	5	10	50	50	0	
3	1	5	15	0	100	0	linear
4	1	10	25	0	100	0	
5	1	2	27	100	0	0	linear
6	1	2	29	0	0	100	linear
7	1	3	32	0	0	100	
8	1	3	35	100	0	0	linear
9	1	5	40	100	0	0	

Table 2.3. HPLC column cleaning gradient

Step	Flow rate (ml/min)	Step Time (min)	Total Time (min)	Solvents			Curve
				%A water	%B acetone	%C hexane	
0	1	0	0	0	100	0	
1	1	5	5	100	0	0	linear
2	1	10	15	100	0	0	
3	1	30	45	0	100	0	linear
4	1	10	55	0	100	0	
5	1	30	85	0	0	100	linear
6	1	10	95	0	0	100	
7	1	30	125	0	100	0	linear
8	1	20	145	0	100	0	

2.4.3. Pigment Identification

Identification of pigments was made using spectral signatures, retention time (RT) and, in some cases, band ratios (see below), following Jeffrey *et al.* (1997 part IV) and Wiltshire and Schroeder (1994). Each sample produced a chromatogram, at a wavelength of 430 nm with the RT of each pigment (an example is shown in Fig. 2.15). Each peak was then integrated by area, which was used for the quantification of the pigments. A spectrum of each peak, from 350 –700 nm, was also processed, which was matched against a set of known pigment spectra. The known pigment spectra (shown in Figs 2.16) were previously stored in a database (Millennium library). The database of pigment spectra was compiled from standards and from extracts from seaweed or sediment, and each spectrum identified against published spectra (Jeffrey *et al.*, 1997). Chl *a* was the only pigment standard run with every batch of samples. Minor pigment standards run at intervals were; Fucoxanthin, Diadinoxanthin, Diatoxanthin, Myxoxanthin, and chlorophylls *c1* and *c2* (obtained from VKI); chlorophyll *b* (Sigma) and Zeaxanthin from an unknown source. Various macroalgae; *Enteromorpha* sp, *Laminaria* sp., *Fucus* sp., *Ceramium* sp., *Porphyra* sp, which have easily identifiable pigments, were collected from the rocky shore on East Sands in St Andrews. These algae were analysed after freezing under liquid nitrogen and crushing with a mortar and pestle. A pigment classification table was produced for the frequent identity of pigments (Table 2.4).

Peak (or band) absorbance maxima (shown on each spectrum) were used as classification characters for pigments. Band ratios were also used for the identification of many pigments which have multiple peak maxima, as RT and wavelength maxima can be similar between some of the carotenoids (Jeffrey *et al.*, 1997). Band ratios (expressed as percentage) compare the absorbance maxima of the II and III band from the between band baseline (Fig. 2.17). For example, the RT and wavelength maxima of lutein and diatoxanthin are very similar but lutein has a III:II bands ratio of 60% and diatoxanthin of 30% (Table 2.4).

2.4.3.1. Standard pigments

Chl *a* standard curves, derived from *Anacystis nidulans*, Sigma™, were made by dissolving 1 mg in 100% acetone in a 250 ml volumetric flask. The concentration was then corrected after absorbance measurement using spectrophotometery (as 1 mg cannot always be transferred accurately). This was obtained by measuring the

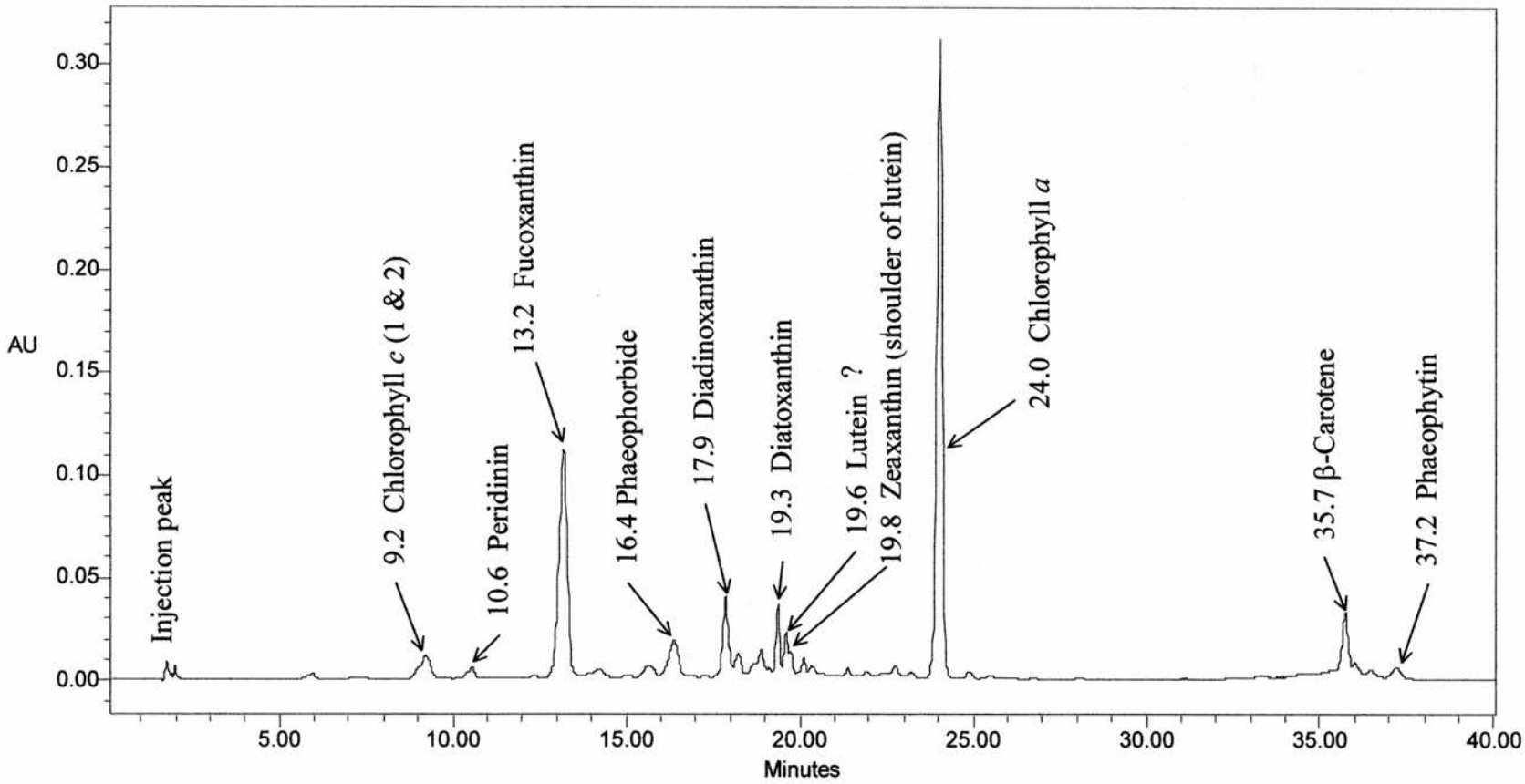

Figure 2.15. Chromatogram of a typical sediment extraction. AU = absorbance units. Arrows indicate identified peak and numbers indicate retention time (min) followed by pigment type

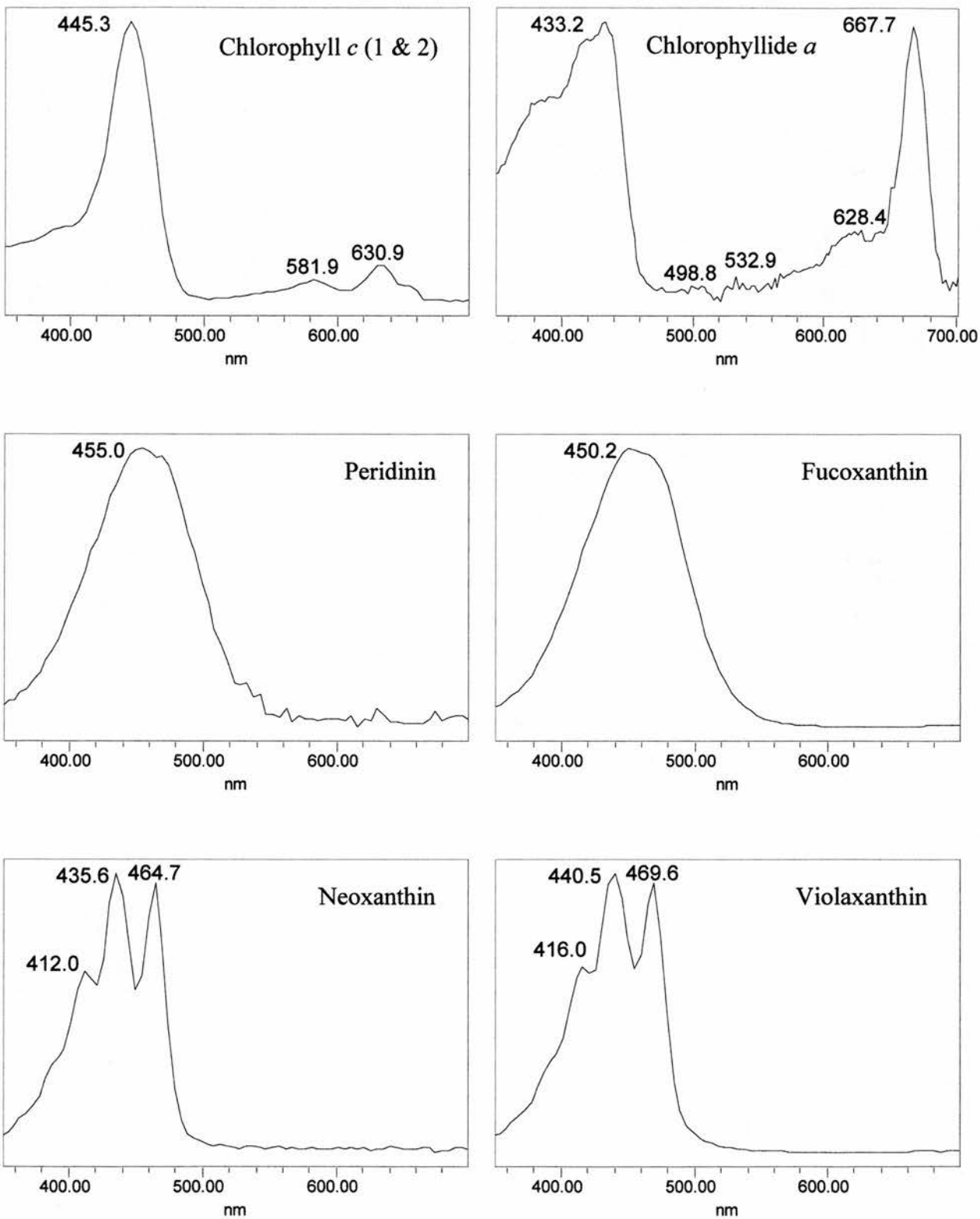

Figure 2.16. Pigment spectra in order of elution (page 1 of 4). Numbers denote wavelength of peak maxima

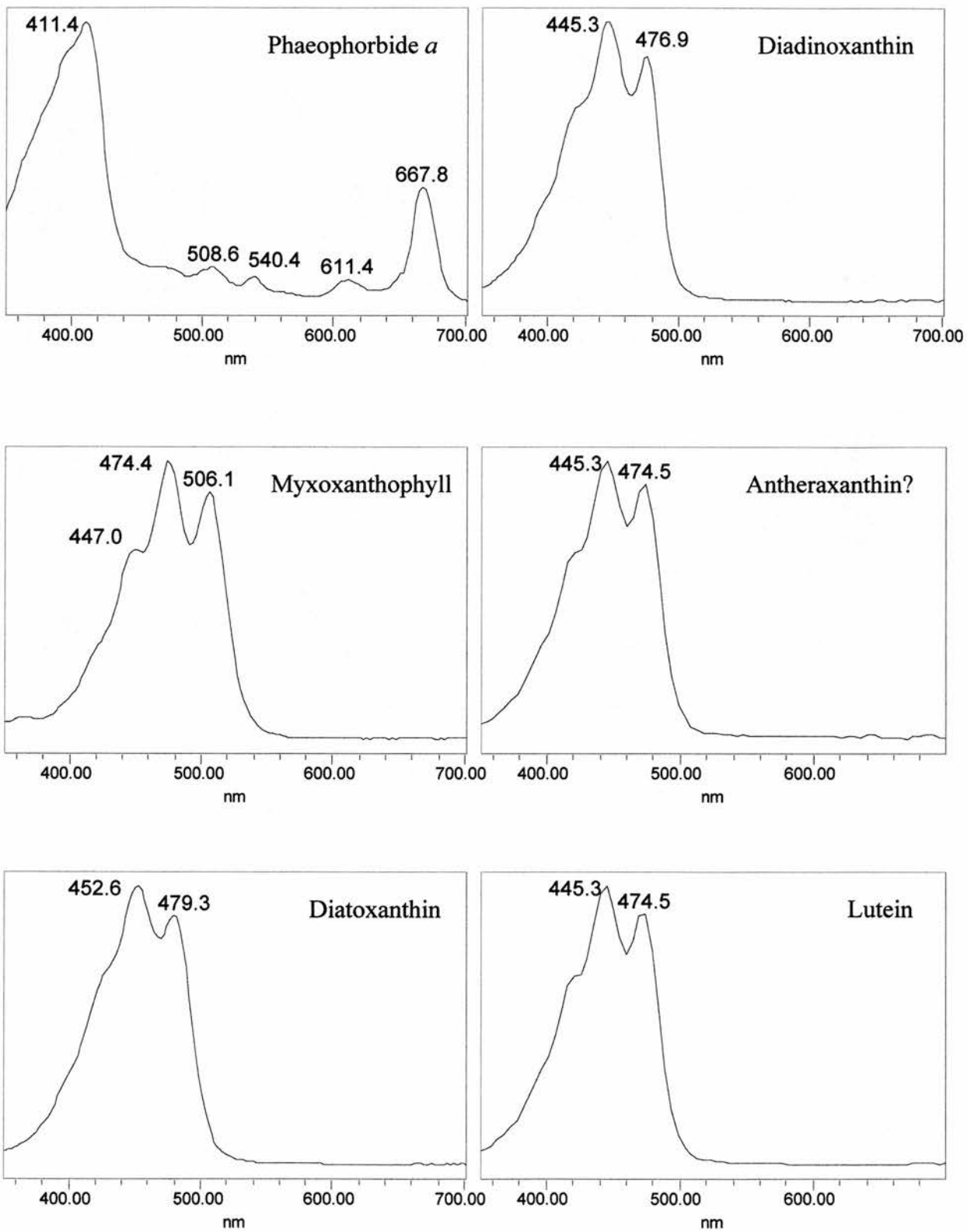

Figure 2.16. Pigment spectra in order of elution (page 2 of 4). Numbers denote wavelength of peak maxima. Where identification is uncertain, a ? follows the proposed name

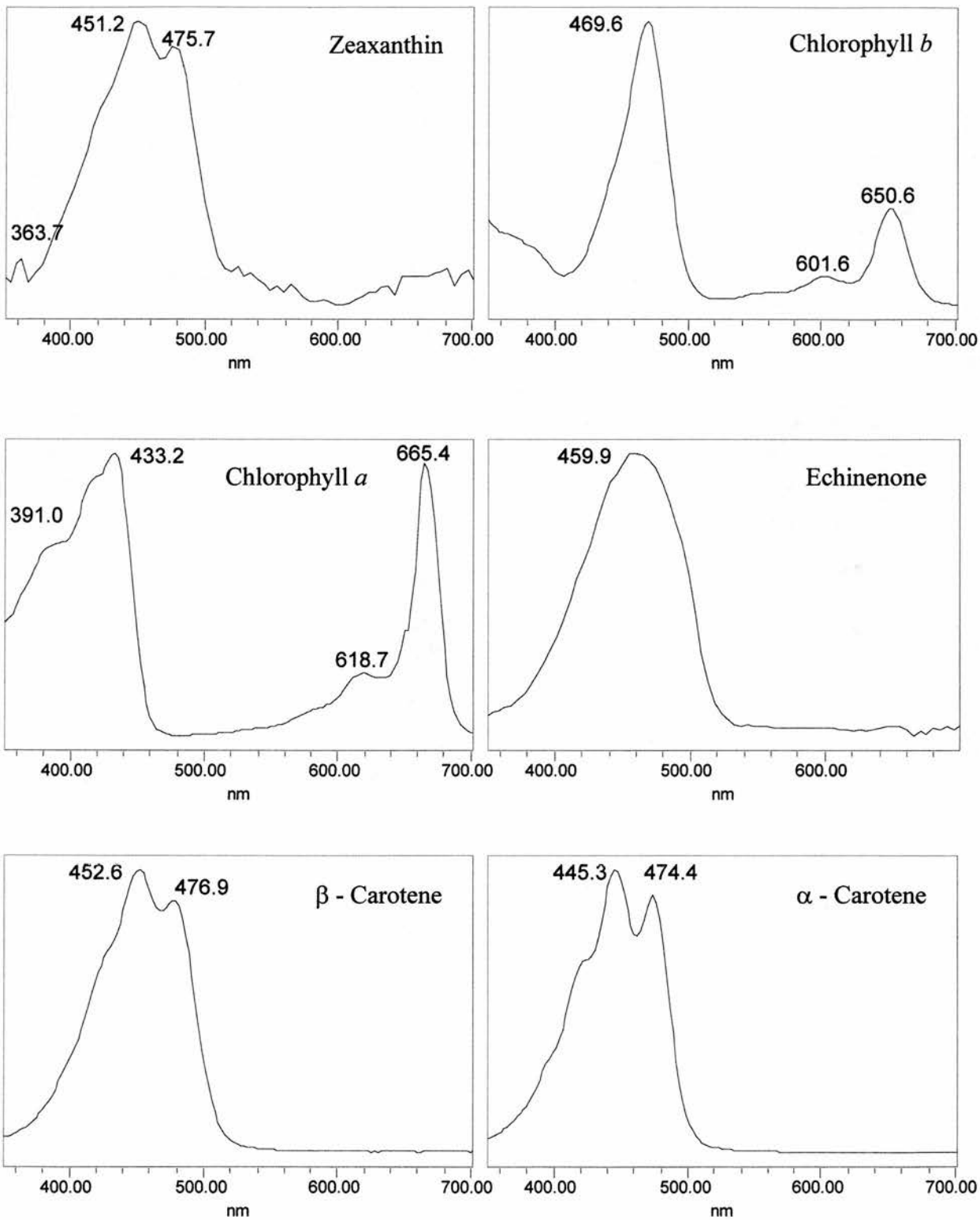

Figure 2.16. Pigment spectra in order of elution (page 3 of 4). Numbers denote wavelength of peak maxima

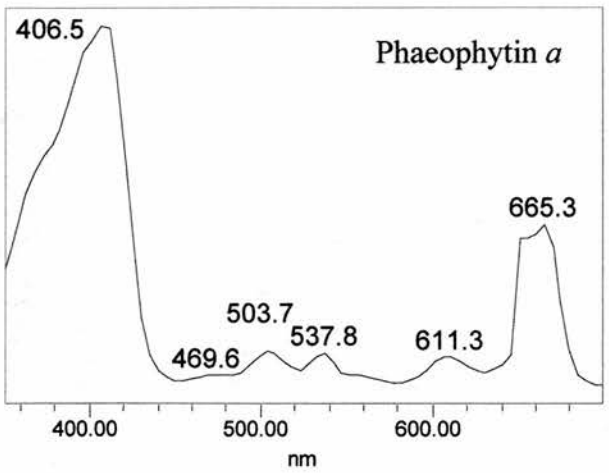

Figure 2.16. Pigment spectra in order of elution (page 4 of 4). Numbers denote wavelength of peak maxima

Table 2.4. Identification details of pigment elution and spectra stored in Millennium library database

RT	Pigment	Wavelength of peaks (λ) Major peak (λmax)	2nd peak (minor)	3rd peak (minor)	approx. Band ratio % III:II	Source used in library	From literature (Jeffrey *et al*., 1997) Present in algae (minor or *trace*)	Notes
9.2	Chlorophyll *c*	445	630	581		*L.saccharina*	B D P	
9.9	Chlorophyllide *a*	433	667			Sediment (Apr 96)		Breakdown product of Chl *a*
10.5	Peridinin	450 to 470	none			Old dry sediment	Df	Wide peak
13.2	Fucoxanthin	450	none			*L.saccharina*	D P B	
14.1	Neoxanthin	435	464	411	80-90	*Enteromorpha*	G H B (*Eg*)	
16.1	Violaxanthin	440	469		93	*L.saccharina*	G B H	Xan-cycle. Greens (low light)
16.4	Phaeophorbide *a*	410	665			Old dry sediment		Breakdown product of Chl *a*
17.9	Diadinoxanthin	445	474		65	VKI standard	D P Df Eg	Diadino-cycle. Major diatom pigment (low light)
17.9	Unknown Lm440	440		462		*L.saccharina*		Comes off in seaweeds, which don't have diadino
18.2	Myxoxanthophyll	474	506	447		VKI standard	C	Not seen in samples
18.3	Antheraxanthin	445	474		55	*Ulva*	(G H *C*)	Xan-cycle. Greens (mid light)
19.3	Diatoxanthin	450	479	427	30	VKI standard	(*D P Df Eg*)	Diadino-cycle. Diatom (high light)
19.6	Lutein	445	469		60	*Enteromorpha*	R* G H	
19.8	Zeaxanthin	455	483	428	28	Sediment (E1BB47e)	C (R G H)	Xan-cycle. Greens (high light)
21.9	Chlorophyll *b*	469	665			Sigma standard	G Eg	
24.0	Chlorophyll *a*	430	665			Sediment	All groups	
35.1	Echinenone	459				*Enteromorpha*	(C G Eg)	
35.7	β-Carotene	450	479	*433*		*Ceramium* (July 99)	(G H R* C *Df Eg P*)	
35.9	α-Carotene	445	474	*423*		*Ceramium* (July 99)	(G C)	
37.2	Phaeophytin *a*	406	665			Old dry sediment		Breakdown product of Chl *a*

Key

D	Diatoms	Diadino	Diadinoxanthin
R	Red algae (e.g. Ceramium)	Xan	Xanthophyll
B	Brown algae (e.g. Laminaria/Fucoids)	*	From own observations
P	Prymnysiophytes		
Df	Dinoflagellates		
G	Green algae (e.g. Enteromorpha/Ulva)		
H	Higher plants		
Eg	Euglenophytes		
C	Cyanophytes		

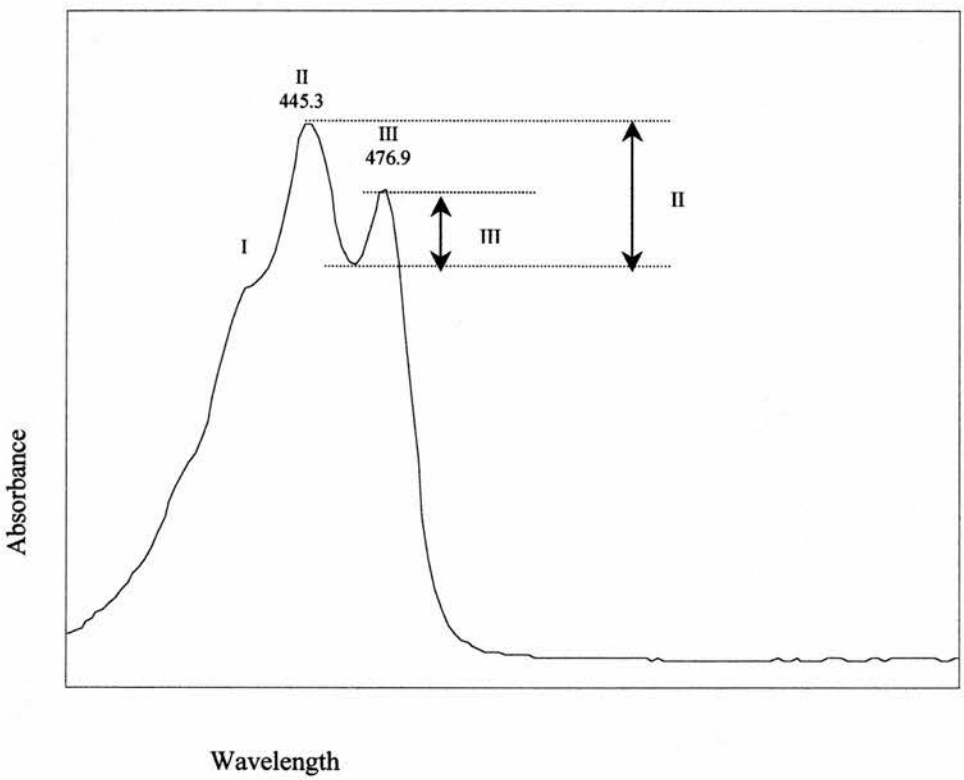

Figure 2.17. The diadinoxanthin spectra, showing bands I, II and III; band I is only visible as a shoulder. Bands II and III baseline and maxima are shown by dotted lines, arrows indicate absorbance height used in band ratios

absorbance of Chl *a* at the corrected peak maxima (λ max), along with a published extinction coefficient in the equation;

$$C = ([abs\ 662] - [abs\ 750] / E) \times 1000 \qquad \text{Equation 2.1}$$

Where C is the concentration of Chl *a* in mg l^{-1}, abs 662 and abs 750 are the absorbance at 662 nm; the λ max of Chl *a,* and 750 nm; the wavelength used for turbidity correction. E is 88.15, the extinction coefficient for Chl *a* in acetone (Jeffrey *et al.*, 1997).

The stock solution (~5 mg/l) was then diluted to give a range of concentrations; the lowest concentration being ~0.5 mg/l. Sample extracts were always within these standard concentrations. Higher extract concentrations were diluted to within this range, as the column can become overloaded, neither were lower concentrations used, as pigments become inaccurately quantified and repeatability lost.

Chl *a* standards were expensive, therefore half of the stock solution was stored frozen at –80°C until further use. The remaining stock and diluted solutions were kept at 4°C for regular use. Chl *a* in acetone was stored at 4°C and used until breakdown started to occur (usually up to 3 months), this was indicated by isomers or epimers Chl *a* apparent on chromatograms close to the RT of Chl *a*.

2.4.3.2. Pigments

Pigments concentrations, other than Chl *a*, were not quantified by concentration, as the majority of pigment standards were extremely expensive or unavailable (with the exception of Chl *b* which can be obtained from Sigma). A selection of pigment standards was run at intervals to check on RT and spectra. Minor pigments were therefore expressed as a ratio to Chl *a*, using chromatogram peak areas at a wavelength of 430 nm. Using ratio to Chl *a*, as an expression of pigment quantity is an accepted method of expressing pigments (Wiltshire and Schroeder, 1994; Cariou-Le Gall and Blanchard, 1995; Barranguet *et al.*, 1997; Wiltshire *et al.*, 1998; Wiltshire, 2000). These authors, however, express pigment ratios in mass:mass or mole:mole, which give a different ratio than each other and a different ratio than peak area:peak area. Thus a direct comparison between the peak area ratios in this thesis and other workers cannot be made.

2.4.3.3. Algal group identification

Identification of broad algal groups, can be made using the presence of a suite of pigments, as the presence of individual pigments is insufficient for identification (Barranguet *et al.*, 1997; Brotas and Plante-Cuny, 1998). Chl *c*, fucoxanthin and diadinoxanthin are present in diatoms; Chl *b* with lutein, zeaxanthin and violaxanthin are present in chlorophytes; zeaxanthin, with no Chl *b*, lutein or violaxanthin indicate a presence of cyanophytes; and Chl *b* and diadinoxanthin with no fucoxanthin indicates the presence of euglenophytes.

2.5. Fluorometry

In this study, chlorophyll *a* fluorescence was used as a technique as an indicator of phyto-biomass on the sediment surface (Chapter 4, 5 and 7) and for the measurement of several photosynthetic parameters of this biomass. Most of the studies were performed on microphytobenthos *in situ* or on undisturbed cores in the laboratory. The pulse-modulated fluorescence technique was used in this study (Schrieber *et al.*, 1986). The fluorometer used throughout this study was a portable Hansatech FMS2 with a blue measuring light. Instrument settings and probe height above the sediment (4 mm) were kept constant for comparative purposes. A probe height of 4 mm was used throughout and is discussed in Chapter 3 and 4. FMS2 settings used were gain: 99; modulation frequency level 3; minimum fluorescence measurement duration: 2.8 sec; The FMS2 monitors fluorescence in units called 'bits' using a pulse amplitude modulation measuring beam. The FMS2 also has an actinic light source, which was set to saturate photochemistry (reduce all primary electron acceptors) the saturation intensity level used was 60, which gave a photosynthetic photon flux density (PPFD) of over 3000 μmol m^{-2} s^{-1}, and a saturation intensity pulse width of 1.0 s. Settings were tested on fresh undisturbed microphytobenthos for optimisation. The actinic light source was programmed to produce a gradient of light levels necessary for the determination of *P-E* curves.

In this study two fluorescence parameters were routinely obtained after a set period of dark adaption as a measure photosynthetic. The first measurement was after 15 min in the dark, and was termed minimum fluorescence (Fo^{15}), the second measurement was then made immediately during a saturating pulse of light, and was termed maximum fluorescence (Fm^{15}). These terms were based on *Fo* and *Fm* values (Schreiber *et al.*, 1986) but may vary from intrinsic values of *Fo* and *Fm*, which can

be difficult to establish. Minimum fluorescence is a measurement of the fluorescence emanated from the pigment bed, when the primary electron acceptors in the absence of light are fully oxidised, i.e. in a relaxed state with no photochemistry occurring. Maximum fluorescence is a measure of the fluorescence emanated from the pigment bed, when the primary electron acceptors are fully reduced, under saturating light levels. These two parameters (Fo^{15} and Fm^{15}) are then used in the calculation for a measure of the maximum efficiency at PSII (*Fv/Fm*; Chapter 1). A period of 15 min dark adaption was selected as optimal to reduce variation in *Fo* due to previous light conditions and has been used by previous authors (Kromkamp *et al.,* 1998). Longer dark adaption was rejected to avoid changes in the Chl *a* at the surface possibly induced by diatom migration. Fo^{15} and *Fv/Fm* measurements, made on dark-adapted cells were obtained as an indicator of biomass at the surface (see Chapter 4) and stress response (respectively).

Dark adaption measurements were made at 4 mm from the surface it was placed upon (sediment). This was facilitated by fitting an inverted black funnel over the probe tip, which protruded 4 mm from the tip of the probe (Fig. 2.18). Small inverted black dishes were placed on the sediment 15 min prior to measurements and were quickly replaced by the funnel and probe tip. The funnel and probe tip were held steady whilst the fluorescence measurement was being made. This technique was deployable with 1 person but arduous during large studies (e.g. BIOPTIS field campaigns) as it was difficult to hold the probe steady and depress the measuring button simultaneously. Thus dark adaption chambers were developed for measurements in the field (see Chapter 3).

Light dependant fluorescence measurements (*Fs, Fm'*) were also used for a measurement of photophysiological processes (Q_A reduction, Serôdio *et al.* 1997 and refs therein). $\Delta F/Fm'$ measurements were made on light adapted cells as a measure of the effective efficiency of photochemistry at PSII. The product of $\Delta F/Fm'$ and a simultaneous measurement of the photosynthetically active radiation in PPFD gave a measure of relative photosynthetic electron transport rate (ETR), and is useful in the determination of photosynthetic activity (Kromkamp *et al.*, 1998). The probe was held at an angle to the sediment surface during these measurements so the cells were not shaded. This was again difficult to deploy alone and an angled probe holder was developed to make measurements in the light (see Chapter 3).

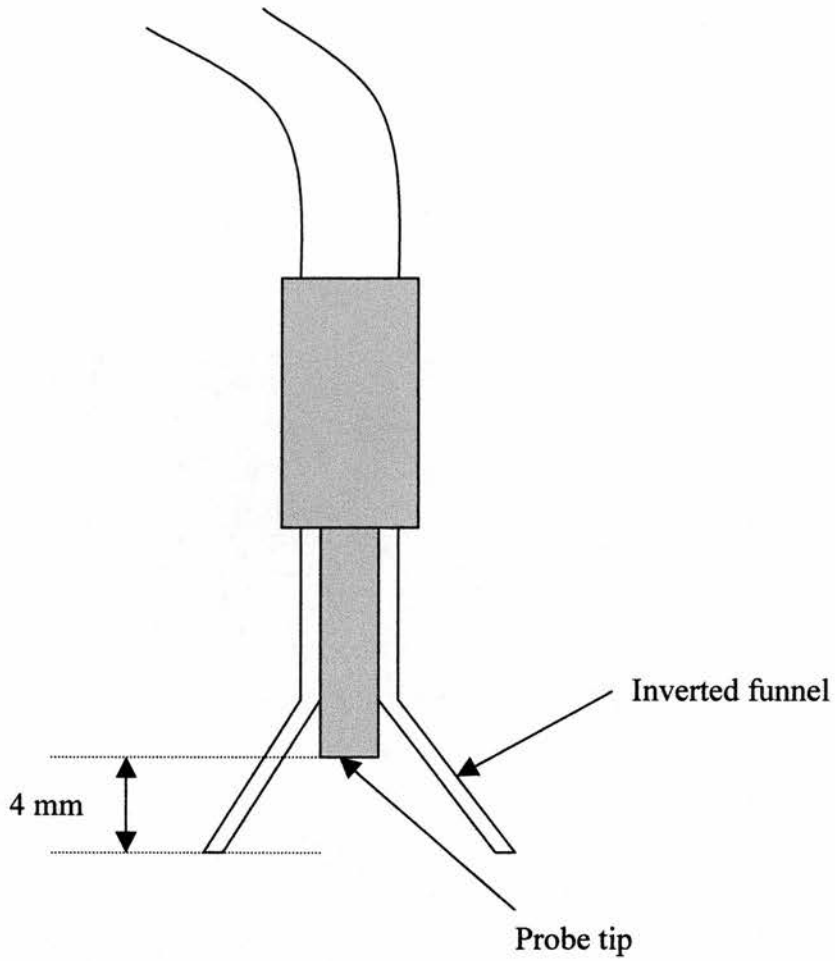

Figure 2.18. Cross section of the fluorometer probe tip with inverted funnel attached. The funnel facilitates fluorescence measurements to be made at 4 mm from the sample. The shaft of the funnel was made from silicone tubing and thus did not slip once in place

To make ETR measurements under stepped irradiance in the laboratory, the probe was held perpendicular to the sediment at a height of 4 mm using a screw-type adjustable clamp stand. The stepped irradiance was then applied using the FMS2 actinic light source. The irradiance from this source was previously calibrated at each step by placing a PAR sensor under the probe at 4 mm (Table 2.5).

2.6. Statistical analysis

Standard deviations were used for all +/- values. Product moment correlations were performed on normally distributed data, while non-normally distributed data was either log transformed, or ranked (if logging did not normalise data) prior to analysis. Model 2 regression analysis (reduced major axis regression) were performed when both axis (e.g. fluorescence and Chl *a*) had indeterminate variables (Fowler & Cohen, 1990). Two sample data, with less than 30 replicates were analysed for differences using the *t*-test, after checking for normal distribution. More than two samples were analysed for differences using ANOVA, data were checked for normal distribution and homoscedacity. If data was unbalanced or post hoc analysis was needed of 2 (or more) factor comparison, then a General Linear Model (GLM) was used. Assessment of the normal distribution of data sets was determined using a correlation based test on the probabilities of occurrence (Ryan-Joiner). In this test a high P value indicates data was drawn from a normally distributed population.

Table 2.5. The incident PPFD (μmol m^{-2} s^{-1}) at a probe height of 4 mm when the FMS2 actinic light source was used (calibrated using a LI-COR PAR sensor). These PPFD measurements were replicated on each date to check the repeatability of the instrument. Further replication was made at a later date.The FMS2 light source varied very little with an average CV of 3%. PPFD were used for the calculation of ETR-*E* curves.

	28-Aug-98						23-Feb-00					Both days	
	replicate						replicate						
FMS2 actinic setting	1	2	3	4	**mean**	**SD**	1	2	3	**mean**	**SD**	**mean**	**SD**
0	0.2	0.2	0.2	0.2	**0.2**	***0.0***	0.2	0.2	0.2	**0.2**	***0.0***	**0.2**	***0.0***
1	7.9	7.4	6.5	6.3	**7**	***0.8***	8.1	8.2	7.8	**8**	***0.2***	**7.5**	***0.8***
3	16.1	15.6	13.9	13.5	**15**	***1.3***						**14.8**	***1.3***
5	29.2	29	26.5	25.7	**28**	***1.8***	30.2	30.3	30.5	**30**	***0.2***	**28.8**	***1.9***
8	62.6	62.7	58	56.9	**60**	***3.0***						**60.1**	***3.0***
9	76.7	77	73.4	71.7	**75**	***2.6***	81.8	81.5	81.1	**81**	***0.4***	**77.6**	***4.1***
11	114	115.3	110	108	**112**	***3.4***	121	121	120	**121**	***0.3***	**116**	***5***
14	190	192	186	182	**188**	***4.4***	200	200	199	**200**	***0.4***	**193**	***7***
16	255	258	251	246	**253**	***5.2***	267	267	267	**267**	***0.2***	**259**	***9***
18	333	337	330	324	**331**	***5.5***	351	350	350	**350**	***0.6***	**339**	***11***
21	477	483	473	465	**475**	***7.5***	501	500	498	**500**	***1.4***	**485**	***14***
25	720	729	715	703	**717**	***10.8***						**717**	***11***
28	943	954	935	922	**939**	***13.5***	989	983	980	**984**	***5.0***	**958**	***26***
32	1299	1313	1291	1271	**1294**	***17.5***	1335	1342	1333	**1337**	***4.7***	**1312**	***26***
36	1719	1742	1715	1734	**1728**	***12.7***						**1728**	***13***
39		2100	2069	2081	**2083**	***15.6***						**2083**	***16***
42		2504	2466	2478	**2483**	***19.4***						**2483**	***19***
46		3109	3062	3077	**3083**	***24.0***						**3083**	***24***
50		3800	3737	3750	**3762**	***33.3***						**3762**	***33***

Chapter 3

3. DEVELOPMENT OF METHODS

The following chapter describes the procedures considerably developed during this work. The first was improving a protocol for algal pigment extraction. Improvement of pigment extraction was necessary as chlorophyll *c* (Chl *c*) was not being extracted from microalgae using, a well used extractant, acetone. Also acetone incompletely extracted chlorophyll a (Chl *a*) from *Enteromorpha.* The second technique was to develop pulse modulated fluorometric techniques for use on sediment inhabiting microalgae *in situ.* The section on the development of pulse modulated fluorometric techniques includes some preliminary studies made in the field, comparisons with laboratory data and a discussion of the advantages and limitations of fluorometric measurements.

3.1. Pigment extraction

3.1.1. Introduction

At the beginning of this study, pigment extraction was carried out with acetone as described in many previous publications (Wiltshire & Schroeder, 1994; Cariou-Le Gall and Blanchard, 1995; Wiltshire *et al.*, 1998). However it became clear this was not effectively extracting Chl *a* from macroalgae (present at many sites). The extraction of Chl *a* from samples containing *Enteromorpha* was gauged as incomplete because sequential extractions gave erratic concentrations, even after sonication before each extraction step. Acetone extraction efficiency is known to be poor, however sonication and subsequent extractions have been used to overcome this inefficiency to ascertain total pigment concentration of sediment sample (Wright *et al.*, 1997; Wiltshire BIOPTIS protocols). Therefore a quicker and more efficient extractant was desirable.

Dimethylformamide (DMF) is known to extract most of the Chl *a* from macroalgae (Porra *et al.*, 1989). In this method, pigments were extracted from wet material, in comparison to the acetone method, which extracts from lyophilised material.

Extraction efficiency of these 2 solvents of both sediment, *Enteromorpha* and a mix of the two were tested. Rehydration, prior to acetone or DMF extraction was also tested. However, rehydration is time consuming and may initiate enzymatic breakdown of pigments, namely Chl *a* to chlorophyllide *a*, especially in

Enteromorpha. Therefore comparisons were made between prior rehydration of lyophilised samples followed by 100% DMF and simply adding 90% DMF to the dried material. Further studies were also made of the extraction efficiency of minor pigments by these different solvents, as Chl *c*, a major pigment in microphytobenthos (Jeffrey *et al.*, 1997) was not being extracted in acetone.

3.1.2. Material and methods

3.1.2.1. Trial A; Solvent Comparison

A comparison of the effectiveness of acetone and DMF solvents on the extraction of pigment from various samples was made. Samples were sediment, *Enteromorpha* or a mix of both, collected from the Eden Estuary during the BIOPTIS campaign or on other dates (see Table 3.1). These solvents (2 mls) were used on both lyophilised material and rehydrated (for 10 min with 0.2 mls water) lyophilised material. Acetone was added to the samples (with sand for pure *Enteromorpha* samples) for 48 hr at –80°C, followed by sonication in a bath with salt ice for 90 min (BIOPTIS protocols). DMF was added to samples for 12 hr at 4°C.

Sequential extractions (2 or 3) were made on selected (2 of each type of sample) acetone and wet DMF samples to calculate 100 % extractable pigment. Extraction coefficients were then applied to all samples (where necessary).

Table 3.1. Details of samples used in solvent extraction tests (with sample location and date of collection) Samples were lyophilised (unless otherwise stated) and stored at –80°C in the dark prior to analysis.

Sample code	Sample description and location and date of collection
Ent 1	*Enteromorpha* from South shore Eden Estuary, November 1999
Ent 2	*Enteromorpha* from top shore rocks, East Sands, July 1999
Ent 3	*Enteromorpha* from top shore rocks, East Sands, July 1999
Ent 4	*Enteromorpha* from South shore Eden Estuary, November 1999
Ent 5	Fresh *Enteromorpha* from top shore rocks, East Sands, April 2000
Sed 1	Core surface (collected on previous day, kept in tidal conditions), February 2000
Sed 2	Core surface (collected on previous day, kept in tidal conditions), February 2000
Sed 3	Core surface (collected on previous day, kept in tidal conditions), February 2000
Sed 4	Homogenised sediment surface, top shore, July 1999
Sed 5	Core surface (collected on previous day, kept in tidal conditions), April 99
Sed 8	Fresh surface sediment, top shore, April 2000

3.1.2.2. Trial B; Comparison of 100% versus 90% DMF

Comparisons were made of extraction effectiveness of 100% DMF on rehydrated lyophilised samples and 90% DMF on lyophilised samples. Samples were sediment, *Enteromorpha* or a mix of both, collected from the Eden Estuary during the BIOPTIS campaign or on other dates (see Table 3.1). These samples included a fresh sediment and an *Enteromorpha* sample which were also analysed to ascertain whether chlorophyllide *a* occurs naturally, under ambient conditions. These 'fresh' samples were stored frozen at -80°C before extraction in DMF.

3.1.3. Results

3.1.3.1. Trial A; Solvent Comparison

The spectra of Chl *a* from extracts in DMF and acetone were found to be identical using spectrophotometry (not shown). Chl *a* extraction efficiency from *Enteromorpha* samples using acetone was poor, even from rehydrated samples (Fig. 3.1A). DMF alone was a poor extractant and prior rehydration of sample was needed. DMF, on average, extracted more than twice the amount of Chl *a* than acetone from rehydrated samples containing *Enteromorpha*.

Chl *a* extraction from sediments was comparable between the two solvents, and rehydration made little difference (Fig. 3.1B). Acetone extracted, on average, slightly more (102%) Chl *a* than DMF from rehydrated sediment samples.

Retention time and spectra of pigments, using HPLC, was exactly the same with each solvent extract (not shown). Lower chlorophyll *b* (Chl *b*) to Chl *a* ratios were found in acetone (ratios of 0.1 to 0.2) compared to rehydrated DMF extraction (ratios of 0.2 to 0.25) (Fig. 3.2A). Only DMF extracted Chl *c* from diatom samples (Fig. 3.2B). There were slightly higher fucoxanthin to Chl *a* ratios using purely acetone than in rehyrated samples and DMF (Fig. 3.2C). The higher ratio found with acetone was similar for most other pigments; lutein, diadinoxanthin, neoxanthin, violaxanthin, β-carotene, α-carotene (data not shown).

3.1.3.2. Trial B; Comparison of 100% versus 90% DMF

Rehydration plus 100% DMF versus 90% DMF, showed no differences in Chl *a* extraction (Fig. 3.3). Rehydrating *Enteromorpha* samples prior to extraction yielded a ratio up to 0.1 of chlorophyllide to Chl *a* with DMF and up to 0.2 with acetone.

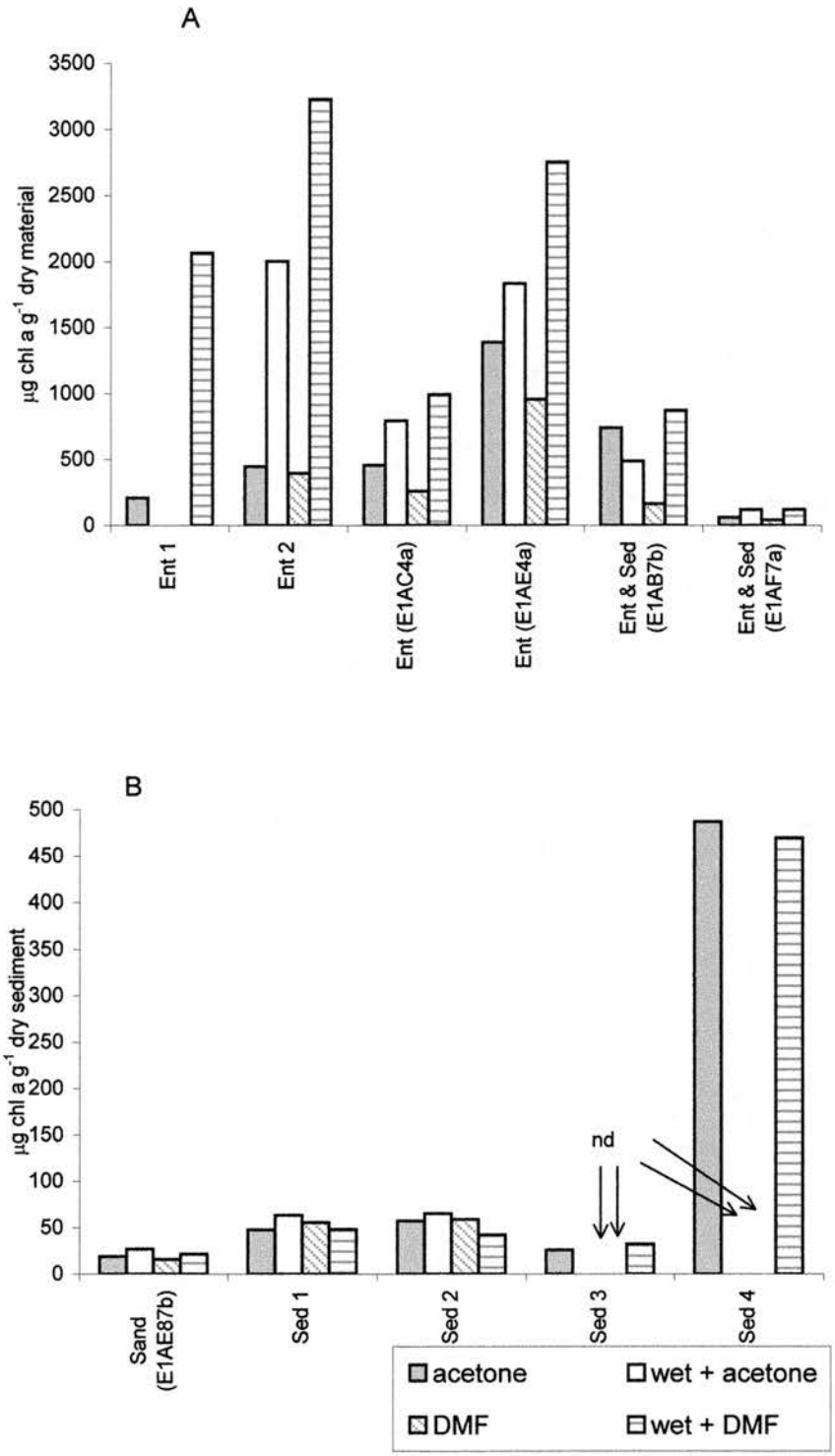

Figure 3.1. Trial A; A comparison of Chl *a* content using different extraction solvents, with or without prior rehyration (wet = rehydration; Ent = *Enteromorpha* ; Sed = muddy sediment; see text for sample number reference; nd = no data). A) The Chl *a* content of *Enteromorpha* samples.B) The Chl *a* content of sediment samples

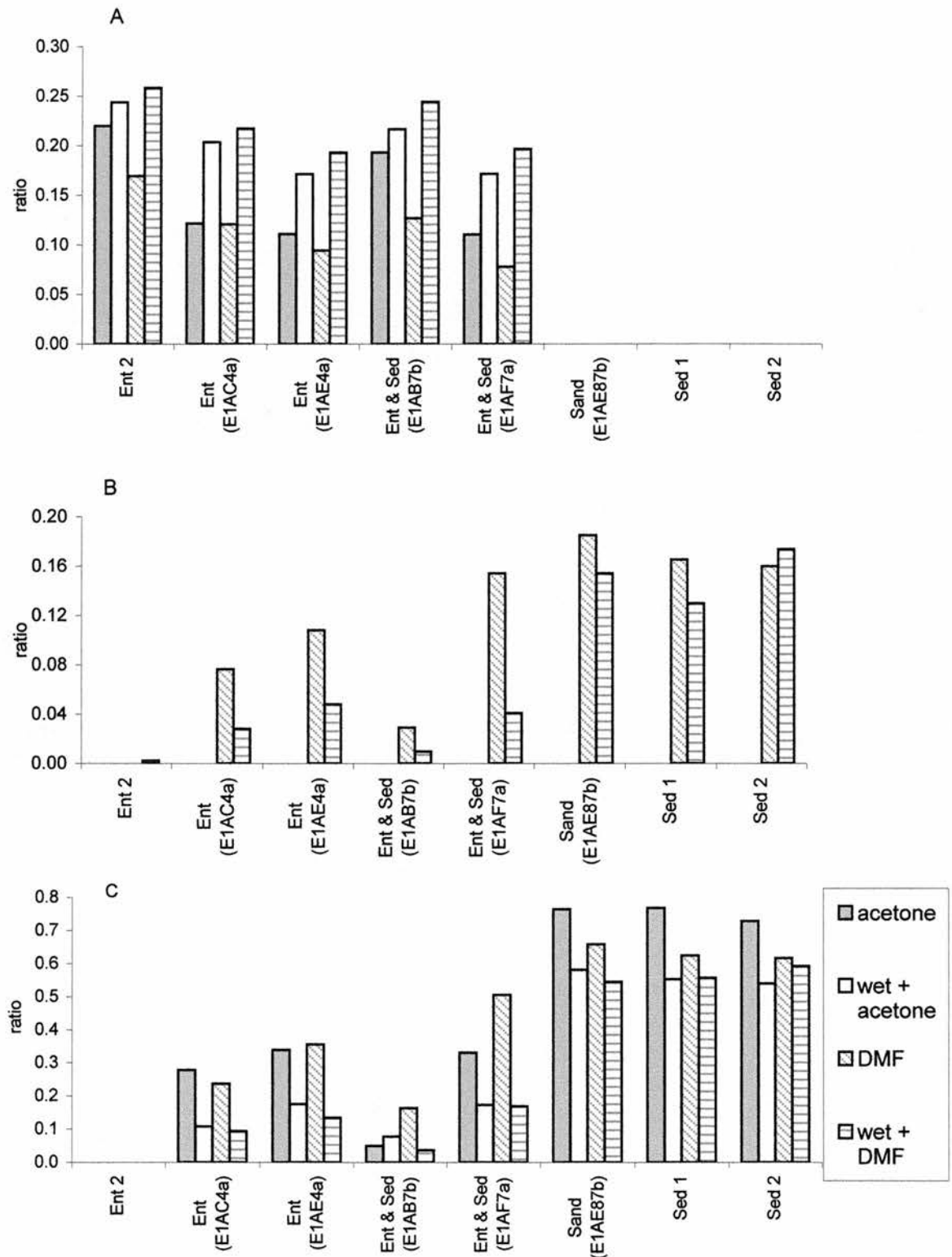

Figure 3.2. A comparison of three major accessory pigments (pigment ratio to Chl *a*) using different extraction solvents, with or without prior rehyration (wet = rehydration; Ent = *Enteromorpha*; Sed = muddy sediment; see text for sample number reference). A) Chl *b*:Chl *a* ratios. B) Chl *c*:Chl *a* ratios. C) Fucoxanthin:Chl *a* ratios

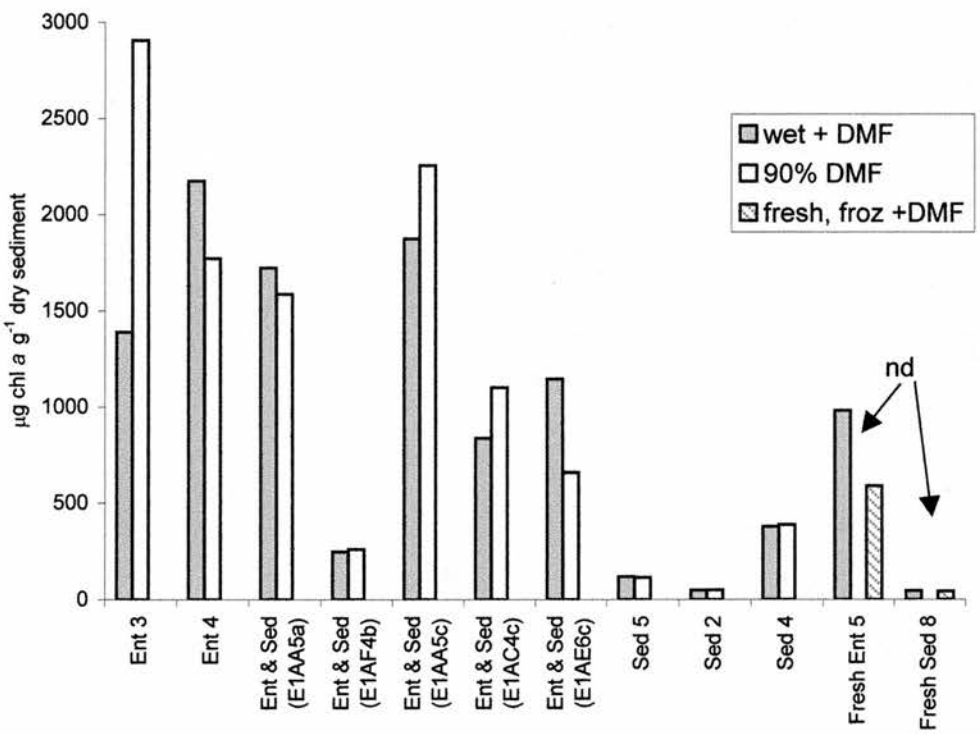

Figure 3.3. Trial B. A comparison of Chl *a* content after different rehydration processes; water added prior to solvent extraction or water added with solvent. Fresh samples were also compared (Ent = *Enteromorpha*; Sed = muddy sediment; see text for sample number reference; nd = no data)

Extraction of fresh *Enteromorpha* samples, however, yielded no chlorophyllide. Using 90% DMF decreased the ratio of chlorophyllide to Chl *a* to 0.6 (Fig 3.4B). Mud samples yielded no chlorophyllide under any treatment (Figs 3.4A and B).

3.1.4. Conclusions

90% DMF should be used for extraction of samples containing *Enteromorpha*, as acetone does not extract all Chl *a* or *b* from this algae. 90% DMF was also the only solvent preparation tested that extracted Chl *c* from sediment samples. Rehydrating *Enteromorpha* samples should thus be avoided, as it causes Chl *a* to breakdown to chlorophyllide *a*.

Microphytobenthic samples showed no difference in Chl *a* extraction between solvents, therefore results from either extraction method were comparable. During the study period for this thesis acetone was used until March 2000, then DMF was used after that date.

Buffered methanol (95%) has also been used to extract Chl *c* (Brotas and Plante-Cuny 1996; 1998). In this study, tests were not carried out using methanol, however it has been compared to other solvents elsewhere for the extraction of phytoplanktonic algae (Jeffrey *et al.,* 1997). These authors concluded that DMF was the best extractant (especially for resistant algae, such as cyanobacteria), although for general use, sonication in methanol may be preferable as an extraction solvent due to the higher toxicity of DMF.

3.2. The development of fluorometry for use on mudflats

3.2.1. Introduction

The estuaries of Europe are areas of great ecological and commercial significance, which for centuries have been exploited by man. An understanding of the dynamics and ecology of these estuarine systems is fundamental to understanding human impacts. Estuarine mudflats are also one of the most productive natural ecosystems on earth, despite the extreme conditions of periodic exposure to the elements, and dynamic tidal immersion. Microphytobenthos are the major primary producers in these systems (Yallop *et al.*, 1994, MacIntyre & Cullen, 1996). Therefore measuring the *in situ* photosynthetic properties of algae, from which productivity or stress can be calculated, is highly desirable.

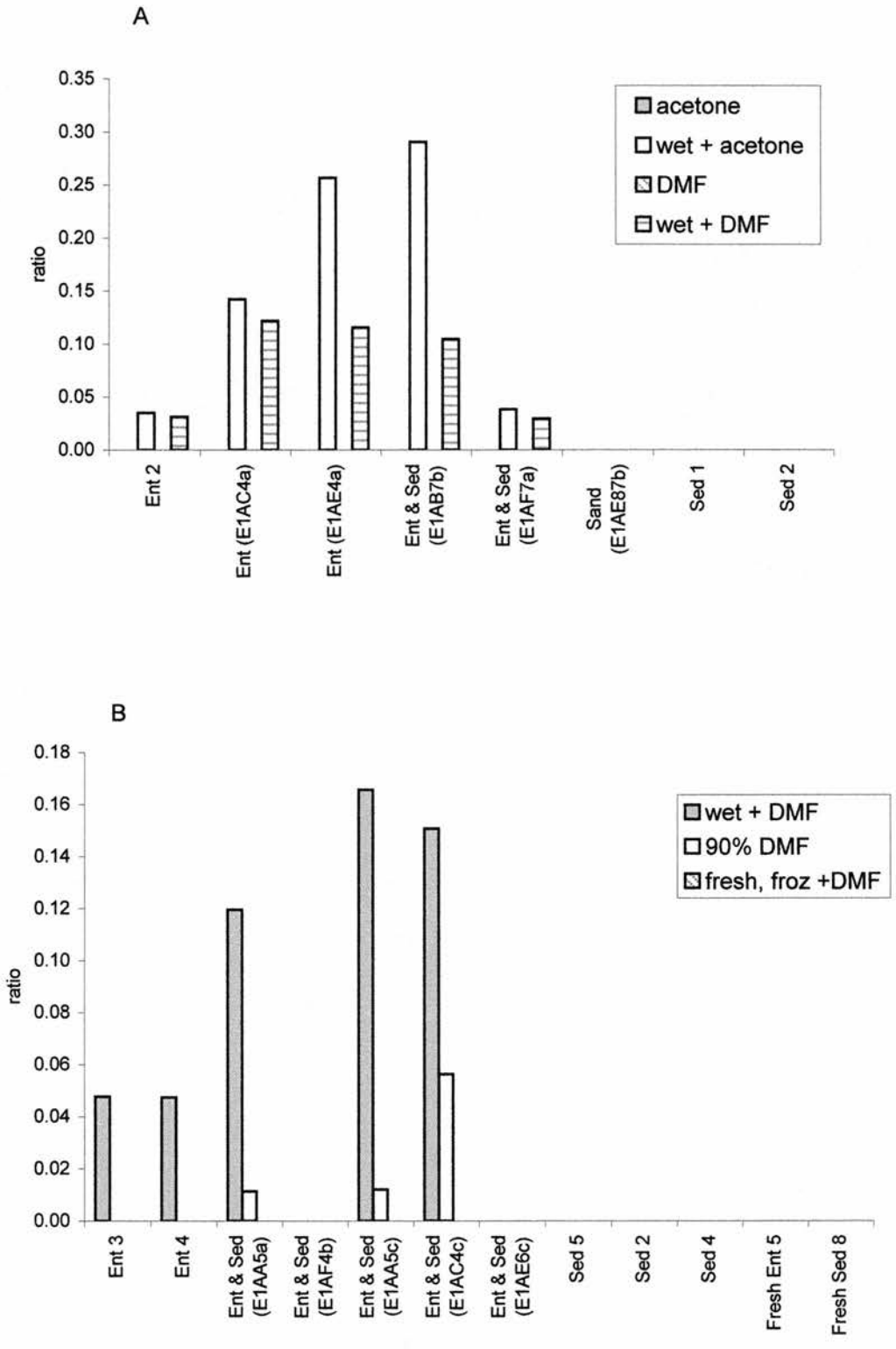

Figure 3.4. A comparison of chlorophyllide *a* determination using different extraction solvents and different rehydration processes (Ent = *Enteromorpha*; Sed = muddy sediment; see text for sample number reference). A) Trial A. A comparison of extraction solvents; Chlorophyllide *a*:Chl *a* ratios. B) Trial B. A comparison of water addition before or during extraction; Chlorophyllide *a*:Chl *a* ratios.

Pulse modulated fluorometry has been used extensively for the measurement of photosynthesis in higher plants and phytoplankton, but only recently has it been used for the study of microphytobenthos *in situ*. Much of the hardware associated with the fluorometer is thus designed for the study of leaves (the leaf clip) or liquid samples (cuvettes). Workers using *in situ* fluorometry for the study of microphytobenthos in the literature have placed the fluorometer probe in a micromanipulator, which is then held above the biofilm and can thus measure at various heights from the sample (Serôdio *et al.,* 1997; Kromkamp *et al.,* 1998; Barranguet and Kromkamp, 2000; Serôdio and Catarino, 2000). The height (and the accuracy of measuring the height) of the probe from the microphytobenthos sample can have implications on the basic parameter measurements, a high signal to noise ratio is preferred. Increasing the height of the probe from the sample decreases fluorescence signal (i.e. minimum and maximum fluorescence; *Fo* and *Fm*). An optimum height above the sample is chosen to give signals within the measuring range of the instrument. Probe height is required to be constant between the minimum and maximum fluorescence measurements. However, probe height is not an important factor for the resulting ratio data i.e. measures of photosynthetic efficiency at PSII; *Fv/Fm* or *ΔF/Fm'* (see Chapter 2). Higher values *Fo* and *Fm* will facilitate less error. However, if minimum fluorescence after 15 minutes of dark adaption (Fo^{15}) is to be used as a measure of biomass (Chapter 4) then probe height is of great importance. Probe height accuracy in the field can be problematic as the surface of the sediment is neither flat nor hard, and probe height inaccuracies up to a millimetre or two will result in different fluorescence signals.

Recently fluorometry has been used to measure photosynthetic properties of algae in sediments (Hartig *et al.,* 1998, Kromkamp *et al.,* 1998, Barranguet and Kromkamp, 2000). These authors made measurements in the laboratory on cores or slurries taken from the field. Kromkamp *et al.* (1998) showed that pulse modulated fluorescence techniques can be used to follow changes in photosynthetic activity of microphytobenthos. Further studies have revealed that relative electron transport rate (rETR) calculated from PAM fluorescence measurements can be converted to carbon fixation (Barranguet and Kromkamp, 2000) with the use of a conversion factor (EE). Their study showed a good correlation ($r^2 = 0.79$) between these 2 methods (rETR and carbon fixation using the ^{14}C bicarbonate uptake in a Photosynthetron). However

outliers in their study warrant further investigations. The discrepancies found were in either sandy sites with differing optical properties than muddy sites or on samples out of the main growing season (Barranguet and Kromkamp, 2000). They also found no correlation between photosynthetic parameters; maximum photosynthesis (ETR_{max}), light utilisation efficiency and (α) and the light saturation parameter (E_k). Scatter in photosynthetic rate and differences in the other photosynthetic parameters could be due to differences in assemblage response of the two methods, as fluorescence measures undisturbed cells on the surface of sediment and ^{14}C measures the response of the cells and surface sediment in a homogeneous slurry. The irradiance used for rETR measurements was calculated from a surface measurement and assumes an exponential decrease with depth (MacIntyre and Cullen, 1996). Whereas irradiance used for the photosynthetron was averaged for the vial.

Alternative methods for the measurement of microphytobenthic photosynthesis are the tracing of carbon fixation or measurement of oxygen evolution. Oxygen evolution is generally measured in the laboratory due to the bulk and sensitivity of the amplifying instruments and delicacy of the probes. Oxygen microprobes have become a useful tool in measuring the depth distribution of oxygen in undisturbed biofilms within the surface layers of sediment/biofilm cores (Revsbech and Jørgensen, 1983). Carbon fixation measurements are made on homogenous slurries of surface sediment in the laboratory as controlled condition are required, this destroys the sediment matrix and microgradients present in natural systems. Carbon fixation is a measurement of the dark reaction, however measurements of O_2 evolution may have a closer relationship to ETR, as oxygen evolution and fluorescence are measurements during the light reactions of photosynthesis (Kromkamp *et al.*, 1998). ETR measurements calibrated against O_2 evolution are not yet available in the literature.

The use of fluorescence as a tool for measuring photosynthesis *in situ* has many advantages. To ascertain the real photosynthetic properties of benthic algae it would be highly preferable to make measurements *in situ*, as yet neither O_2 evolution or C fixation techniques are usually measured in the field. Disturbance of microalgae can occur during transportation. The ambient light and temperature climate is difficult to mimic in the laboratory. Not being confined to a transportable sample number is also advantageous.

This study showed data collected during a survey of the Eden Estuary, where fluorescence was used to estimate biomass and photosynthetic measurements (stress response and rETR) of microphytobenthos *in situ*. Fluorescence measurements made during this campaign were shown and compared to laboratory measurements. The limitations of the technique are discussed. Hardware designed for fluorescence measurements in the field are also presented.

3.2.2. Materials and methods

During a field campaign, *in situ* measurements using fluorometry were made on three grids on the Eden Estuary, Scotland. Two large (A and B) and one small grid (C) were surveyed in different areas of the estuary. The nodes within the grids were 100 m apart and a total of 312 separate measurements were included in this study. Macroalgal measurements were excluded.

Fluorescence measurements made during these field campaigns were;

- minimum fluorescence after 15 min of dark adaption (Fo^{15})
- the maximum efficiency of photochemistry at PSII (*Fv/Fm*) after 15 min of dark adaption
- the effective efficiency of photochemistry at PSII ($\Delta F/Fm'$) in ambient light

Fo^{15} was used as a measure of biomass (Chapter 4). The maximum efficiency of photochemistry at PSII is a good measure of stress (Genty *et al.*, 1989) and the effective efficiency of photochemistry at PSII when multiplied by the photosynthetic photon flux density (PPFD) can give a good measure of relative photosynthetic ETR (Kromkamp *et al.*, 1998).

Measurements were made in the laboratory to attempt to minimise problems associated with field studies. These measurements were made on undisturbed cores or on *Ulva* sp. collected on the previous day from the Eden Estuary. These samples were kept in fresh seawater in low light conditions, to decrease stress, so it was assumed that *Fv/Fm* values would be constantly maximal. Background measurements of *Fo* and *Fm* were made on pigment-free sediment and *Ulva* sp.. The sediment was cleaned in hydrogen peroxide (30 %) for several days, until effervescence stopped. The *Ulva* sp.was bleached in 1 % sodium hypochlorite (diluted domestic bleach) overnight, after which no pigmentation was evident. Two fluorometers were used; a Walz PAM 2000 and a Hansatech FMS2. In the laboratory the probe was suspended above the sediment or *Ulva* sp. with the use of a micromanipulator. Rapid repeated

measurements at a probe height of 4 mm were carried out using an inverted funnel, which was attached to the probe tip (Chapter 2; Fig. 2.18).

3.2.2.1. Probe height

To study the effect that probe height variation may have on the variability of the Fo^{15} signal (as a measure of biomass), measurements were made at various probe heights from the sediment surface of undisturbed cores. Six undisturbed cores (numbered B1–B6) were brought back from the field and kept under laboratory conditions (no tide and irradiance levels of 300 μmol m^{-2} s^{-1}). The six cores had varying biomass coloration on the surface and were diatom dominated (checked using pigment fingerprinting). Fluorescence measurements (Fo^{15}) were made with the FMS2, around the time of low tide. Seven sets of measurements on each core were made at a 4 mm probe height from the sediment, interspersed (randomly) with 3 measurements at 10 mm and one measurement each at 2, 6, 8 and 16 mm probe height. Ten minutes of dark adaption was carried out between each measurement.

3.2.2.2. Equipment developed

Holders were developed for portable fluorometer probe tips to facilitate steady fluorescence measurements of the sediment surface in the field. The probe tip end of both the fluorometers were of similar diameter, therefore holders designed in this study were adaptable. However, the probe tip lengths were different, but this was easily overcome with the use of spacers (made from plastic tubing). This work was in conjunction with R. M. Forster and J. Kromkamp from the NIOO institute, Yerseke, The Netherlands.

3.2.2.2.a. Dark-adapted measurements

A closed chamber was designed to hold the probe remotely at set heights from the sediment for measurement of dark-adapted parameters (Fig. 3.5A). The base of the chamber was flat and wide to aid stability (long nails can be added to the base for further stability if sediment is not firm). The chamber lid was 2 cm deep and had a hole for the probe, the depth and close fit of the hole facilitates perpendicular support of the probe. The use of different size spacers allowed different probe heights to be set. The lid (with a hole off centre) fitted loosely over the chamber which gave it the ability to swivel, therefore four measurements were made within one chamber by

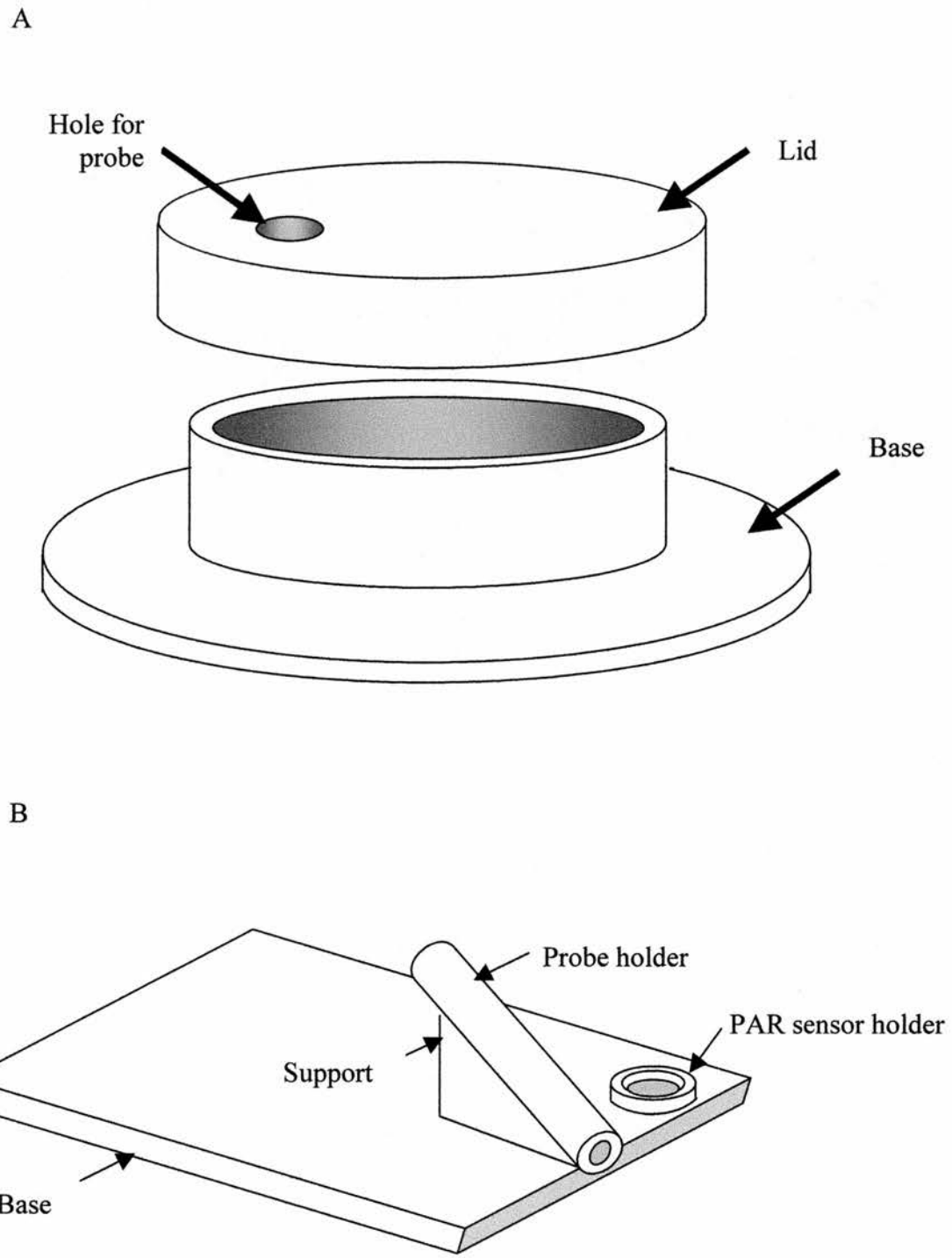

Figure 3.5. Hardware developed for the use of fluorescence in the field. A) Dark adaptation chamber (65 mm internal diameter; 140 mm external base diameter). B) Angled probe holder (230 x 120 mm base; 12.5 mm internal diameter of probe holder with support at 30°; 24 mm internal diameter of PAR sensor holder)

swivelling the lid by 90°. Several chambers were placed on the sediment surface at one time to facilitate further replication.

3.2.2.2.b. Light measurements

Equipment was also designed for holding the fluorometer probe remotely from the sediment at an angle to avoid light shading (Fig. 3.5B). The base was flat and wide for stability. The probe holder, a hollow tube, was supported at an angled of 30° and had an internal rim at the base to stop the probe from sliding through. The PAR sensor holder was made to fit a standard LICOR PAR sensor (Fig. 3.5B), but any size can be made depending on the PAR sensor specifications.

Measurements to determine the effective efficiency of photochemistry at PSII ($\Delta F/Fm'$) and PPFD were made under natural light for measurement of *in situ* rETR, using the equation (Kromkamp *et al.*, 1998);

$$rETR = \Delta F/Fm' \times PPFD \qquad \text{Equation 3.1}$$

Measurements under decreasing steps of diluted natural light were also made. These were facilitated by placing different density filters over the sediment surface for 3 to 5 minutes, leaving enough space for the angled probe holder to be placed underneath. The fluorescence ($\Delta F/Fm'$) and PPFD measurements under different irradiances were then used in the calculation of ETR-*E* curves. The filter system (for decreasing natural light) for use in conjunction with the angled probe holder was constructed from clear Perspex sheet. The filters were slotted between 2 pieces of Perspex sheet, which was supported by short legs, high enough for the Perspex sheet to clear the bottom half of the angled probe holder. Different density filters can be interchanged by slotting between the Perspex sheets, thus shading and making measurements *in situ* on the same patch of sediment. However in this study, 6 filters were placed adjacent to each other on the sediment surface, allowing the rapid determination of 7 irradiance levels (including ambient).

3.2.2.3. ETR-E curves

Photosynthetic activity was studied after construction of rETR versus irradiance (ETR-*E*) curves from data collected in the field using natural and filtered irradiance levels and also from measurements made in the laboratory under artificial

irradiance levels. Measurements in the laboratory were made using the actinic light source of the FMS, set at increasing intensities for ETR-*E* curve irradiance steps. The probe was suspended 4 mm perpendicular to the sediment. As measurements in the field were made at an angle, a comparison was made between rETR measurements under filtered irradiance at a probe angle and rETR measurements using the FMS2 light source with the probe suspended perpendicular above the sediment surface.

Curve fitting was applied to data using an exponential relationship taking account of photoinhibition (Walsby, 1997) and substituting rETR for photosynthetic rate;

$$rETR = [ETR_{max}] * (1 - \exp(\alpha * E / [ETR_{max}])) * R * \beta \qquad \text{Equation 3.2}$$

Where rETR is the relative rate of electron transport, ETR_{max} is the maximum rETR, α is the initial linear slope (calculated using linear regression of data under 100 $\mu mol\ m^{-2}\ s^{-1}$), E is the irradiance in $\mu mol\ m^{-2}\ s^{-1}$, R is the intercept of the initial linear slope and β is the slope of the decrease after the peak. Equation parameters are first approximated, followed by computer iteration to decrease the overall error for optimum fit of the line to the data. Iteration was performed using a Generalized Reduced Gradient (GRG2) nonlinear optimization code in Excel solver (Walsby, 1997). ETR_{max} and α were then calculated from predicted values, following the optimum curve and E_k (the light saturation parameter) was derived using the equation;

$$E_k = ETR_{max} / \alpha \qquad \text{Equation 3.3}$$

3.2.3. Results

3.2.3.1. Probe height

A study was carried out to assess the error which may be encountered in Fo^{15} values as a result of probe height inaccuracies in the field, which may be a problem because of sediment surface topography.

Minimum fluorescence had a strong significant exponential decay relationship with increasing probe height for the determination of Fo^{15} ($r^2 \geq 0.98$, $P < 0.001$, Fig. 3.6A). Previous studies used a probe height of 4 mm (Chapter 4), therefore this was

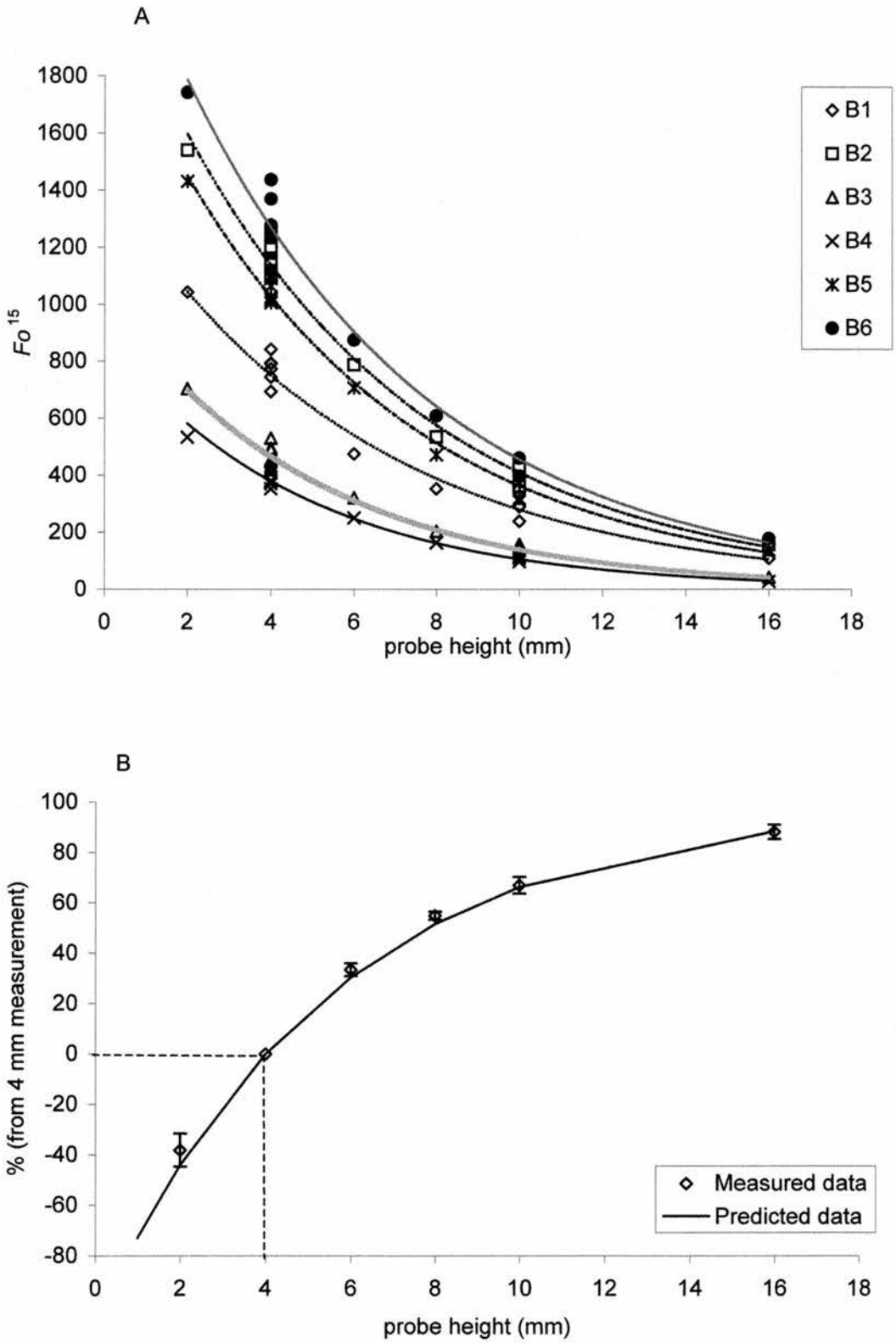

Figure 3.6. A) Fo^{15} values at different probe heights on six different cores (B1-B6) and exponential curve fits. B) Percentage difference in Fo^{15} values at different probe heights, and predicted line through data. Solid line indicates the standard 4 mm probe height used

used as the standard measurement. The increases or decreases in Fo^{15} values with probe height, from 4 mm, were calculated as a percentage of the standard measurement (Fig. 3.6B). Using exponential decay regression, Fo^{15} measurements made within 0.5, 1 or 2 mm of the base measurement decreased or increased the standard value by 9%, 18% or 37% (respectively). The variation found with increasing or decreasing sample distance was compared to the variation found in replicate measurements at specific accurate heights. The variation (in percentage difference from first reading) between 7 replicates at 4 mm was +/- 8.5 %, whilst the variation between 3 replicates at 10 mm was 8.2 %.

3.2.3.2. Stress response measurements (Fv/Fm)

Paired Fo^{15} and *Fv/Fm* measurements were made in the field and on undisturbed cores in the laboratory. During field campaigns, samples with low biomass (indicated by low Fo^{15} measurements) showed a tendency towards high *Fv/Fm* values (Fig. 3.7A). The point at which *Fv/Fm* became dependent on Fo^{15} was determined by regression analysis. All *Fv/Fm* data was regressed against each Fo^{15} value, then low Fo^{15} data were removed until the regression had a non significant slope. A non-significant slope occurred when with an Fo^{15} data values below 150 were removed. Paired Fo^{15} and *Fv/Fm* measurements were made in the laboratory to enabled probe height to be manipulated to facilitate lower Fo^{15} values on exactly the same sample. Samples included both undisturbed cores with microphytobenthic biofilms and flat thalli of *Ulva*. It was assumed that undisturbed cores and *Ulva* thalli were not stressed and was supported by the fact that they gave high *Fv/Fm* values at sufficient Fo^{15} levels. Similar results, of increased *Fv/Fm* with low Fo^{15}, were found in the laboratory with undisturbed cores and *Ulva* (Fig. 3.7B).

Preliminary observations using the Walz PAM 2000 were made on *Ulva*, and on sediments (Forster and Kromkamp, unpublished results) This indicated that this instrument showed an opposite relationship to the FMS2. That is, the Walz PAM 2000 showed decreased *Fv/Fm* at low Fo^{15} values.

3.2.3.2.a. Corrections of Fv/Fm

During this study Fo^{15} *and* Fm^{15} measurements of pigment-free sediment and *Ulva* were made, in order to determine if any background fluorescence signals were significant. Background Fo^{15} values were always zero or 1, but Fm^{15} values ranged

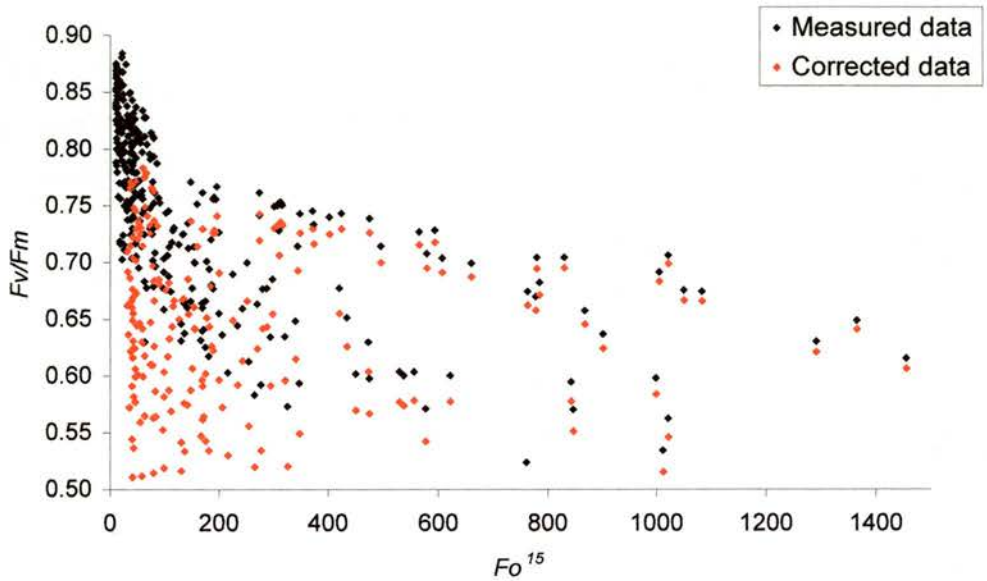

Figure 3.8. Data from the Eden BIOPTIS field campaign (the same data as Fig 3.7A). The relationship between *Fv/Fm* and Fo^{15}. The instrument *Fv/Fm* values and the *Fv/Fm* values after a correction factor was applied (see text)

from 15 (air/bleached thalli) to 22 (sediment). When the background Fm^{15} values were applied to the equation *Fv/Fm*, it made little difference in the relationship, therefore alternative corrections were explored. Medium to high biomass field samples with high *Fv/Fm* values (~0.75) indicating healthy unstressed organisms were selected. Medium to high biomass samples were selected as having Fo^{15} values between 400 to 700. From these selected samples the Fo^{15} and *Fv/Fm* values were regressed to ascertain the intercept for use as a correction factor for the whole set of data. These intercepts were then applied as a correction of the Fm^{15} values and *Fv/Fm* were recalculated (Fig. 3.8, Eden field data; Fig. 3.9A, laboratory cores; Fig. 3.9B, *Ulva*).

Walz PAM 2000 results on *Ulva* thalli show a decrease in *Fv/Fm* at low very low Fo^{15} values (Fig. 3.9C). Therefore a negative background value was calculated from regression intercept of Fo^{15} and Fm^{15}.

3.2.3.3. ETR-E curves

Comparisons of rETR between the actinic light source from the FMS2 (with the probe perpendicular to the sediment) and using filtered irradiance (with the probe at an angle) were very good (Fig. 3.10A).

No corrections were made for background in $\Delta F/Fm'$, as no relationship between $\Delta F/Fm'$ and lower biomass samples was apparent (data not shown). Data from laboratory cores which had an Fo^{15} (first measurement of the irradiance steps) of under 150 were not used, and field data with a steady state minimum fluorescence (*Fs*) value below 50 were not used. This lower value was selected, after examination of the field data, as a cut off point, below which $\Delta F/Fm'$ values show large variablity.

Relative ETR versus irradiance (ETR-*E*) curves were plotted from data collected in the field and gave an ETR_{max} values of 487, an α of 0.756 and an E_k of 644 μmol m^{-2} s^{-1}. Measurements made in the laboratory under artificial irradiance levels gave an ETR_{max} of 249, an α of 0.708 and an E_k of 352 μmol m^{-2} s^{-1}. Laboratory cores show no photoinhibition, even in excess of natural irradiances (Fig. 3.10A). There is insubstantial replication above 1000 μmol m^{-2} s^{-1} to derive photoinhibition in the field data, although the curve showed a decrease at higher PPFD values due to 2 high irradiance data points (Fig. 3.10B).

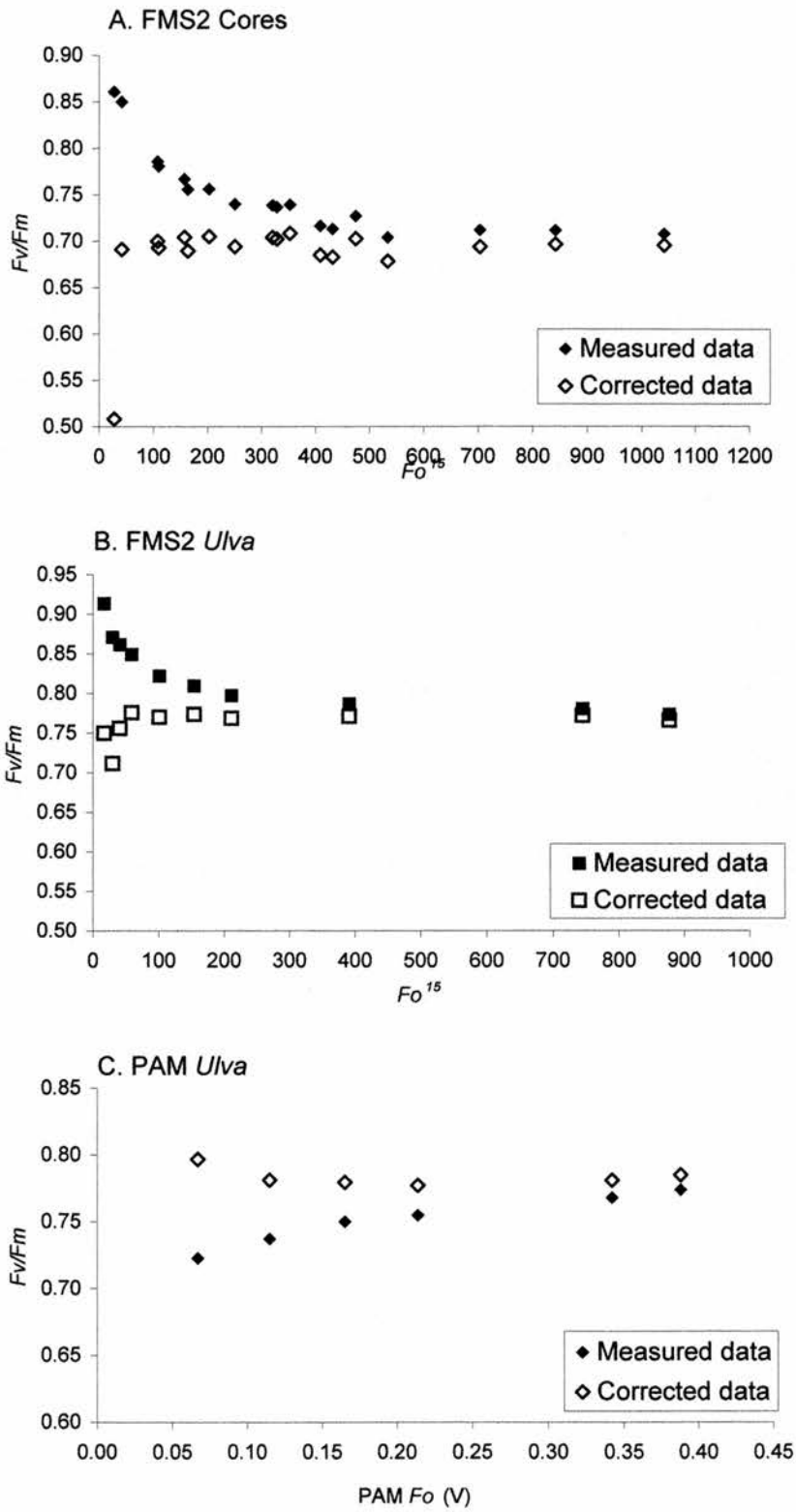

Figure 3.9. The relationship between Fo^{15} and both instrument and corrected *Fv/Fm* values from data collected in the laboratory. Corrected *Fv/Fm* values were calculated from an *Fm* intercept coefficient (see text). A) FMS2 measurements of sediment cores; an intercept coefficient of 144 was used for corrected data. B) FMS2 measurements of *Ulva;* an intercept coefficient of 128 was used for corrected data. C) Walz PAM measurements of *Ulva,* an intercept coefficient of -0.0881 was used for corrected data

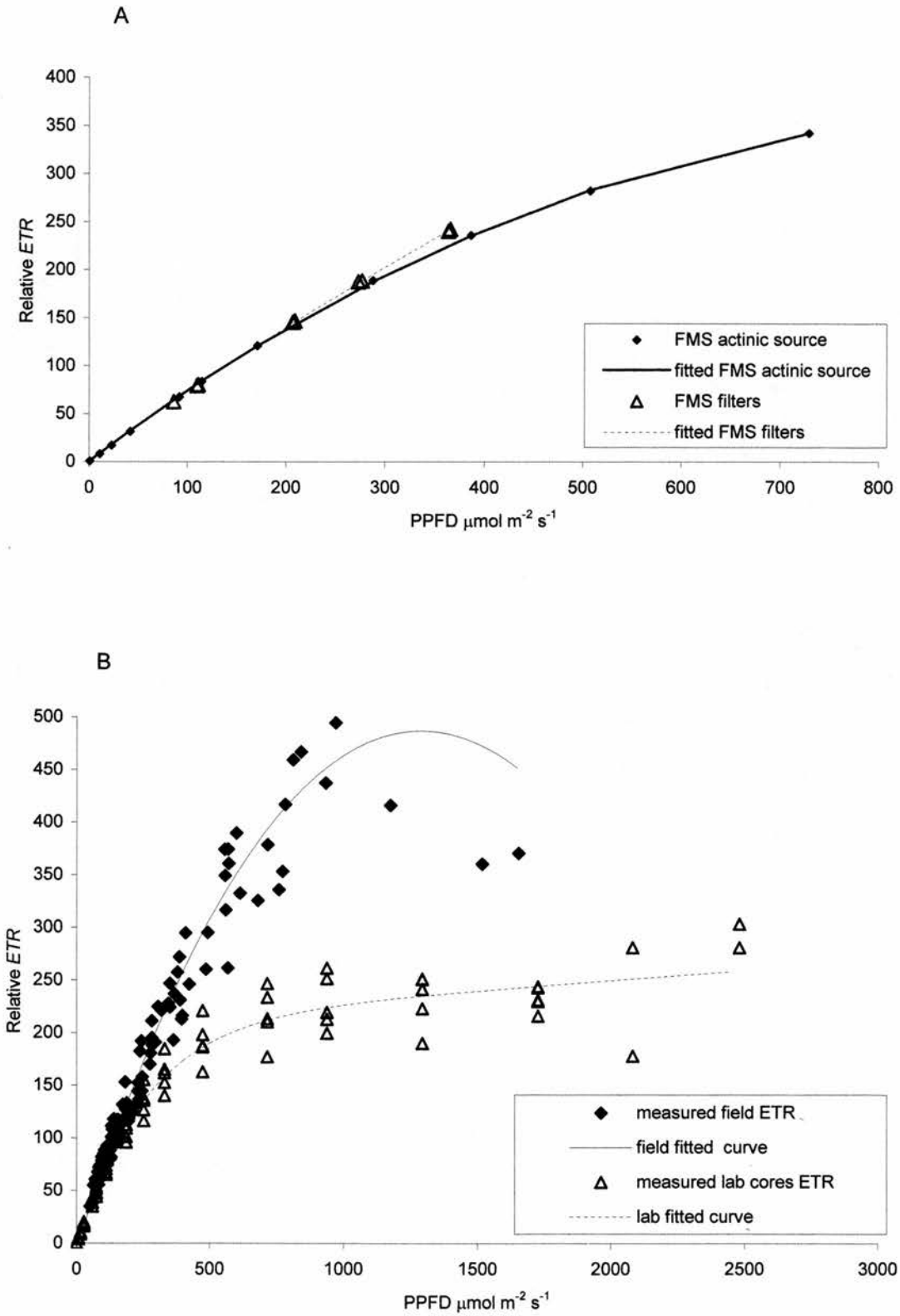

Figure 3.10. Relative electron transport rates versus irradiance (ETR-*E*) curves comparing data from either the FMS2 light source or a filtered light source. A) Sediment core in the laboratory; the filtered light was a halogen source. B) Eden Grid A field data; the filtered light was filtered ambient irradiance

3.2.4. Discussion

3.2.4.1. Probe height

In the field, the accuracy of probe height from the sediment surface is difficult to set accuratly due to the nature of the sediment surface topography. In the laboratory, Fo^{15} measurements were made at various probe heights to ascertain the variation which may be expected due to surface topography. There was a decreasing signal in fluorescence with increasing probe height from the sediment. This relationship would be expected as light exponentially decreases with distance.

Measurements with an error more than 2 mm distance from a probe height of 4 mm are unlikely, the error is more likely to be nearer 1 mm. Therefore a +/-1 mm probe height error would give up to 18 % decrease or increase in fluorescence signal. This error was acceptable, and was just over twice the difference that was found in natural variation between replicates (8 %). Careful placement of both the dark adaption chamber and the probe will of course keep the error to a minimum.

3.2.4.2. Efficiency measurements

The dependence of *Fv/Fm* ratio on low Fo^{15} values may be a natural phenomenon, i.e. that very low biomass microphytobenthic biofilms were less stressed, due to lack of competition for nutrients and light. However, this theory was rejected due to the fact that *Fv/Fm* ratios obtained were extremely high (> 0.85) and unlikely in microalgae (Büchel and Wilhelm, 1993). Also, the slope in Fo^{15} values below 150 was extremely steep compared with values over 150 (Fig 3.7A). An Fo^{15} of 150 was equivalent to about 60 mg m^{-2} in a 2 mm deep core (Chapter 4) which was not particularly low in terms of biomass (Guarini *et al.*, 1998; Barranguet and Kromkamp 2000).

Using the FMS, the corrections made for Fm^{15} values, calculated from regression intercepts, ranged from 84 to 144. This indicated that Fm^{15} was being over estimated or Fo^{15} was being under estimated. At lower biomass readings the error was accentuated as the background value became a larger proportion of the measured value. These calculated Fm^{15} correction factors were much higher than the measured background Fm^{15} values, which ranged between 14 and 22. Background values calculated from regression intercepts (using the PAM 2000), showed an under estimation of Fm^{15} values (the opposite to the FMS2). This led us to conclude that the

instruments were limited to higher biomass measurements. Studies of higher plants rarely deal with low biomass. However, pulse modulated fluorescence has been used for the study of phytoplankton and microalgal culture studies (Ting and Owens, 1992; 1993; 1994; Büchel and Wilhelm, 1993; Hartig *et al.*, 1998; Flameling and Kromkamp, 1998). It has been previously documented that cells in suspension should be studied at low concentrations, a maximum of 8 μg Chl *a* ml^{-1}, for reproducible results (Ting and Owens, 1992) or at around 20 mg Chl *a* l^{-1} (Büchel and Wilhelm, 1993). These authors show that the *Fm/Fo* ratios decrease with increasing Chl *a* concentration. Ting and Owens (1992) document an *Fm/Fo* value of 4 at low Chl *a* concentrations to 1.6 at high Chl *a* concentrations, an *Fm/Fo* ratio of about 4 is the value found in healthy unstressed cells (giving an *Fv/Fm* of about 0.75). These authors hypothesised that using dilute cell concentrations decreased the reabsorbtion, scattering and reflection processes which may effect excitation and saturating lights as well as the fluorescence signal (Büchel and Wilhelm, 1993). A biofilm is a dense mat of cells and may act more like a leaf than a suspension of cells in regards to reabsorbtion, scattering and reflection processes.

The correction of Fm^{15} using the intercept from Fo^{15} against Fm^{15} is, of course, dependent upon measurements being made on unstressed cells at high biomass, which may not always be possible. It is therefore concluded from this investigation that a correction factor could be applied, but only under certain circumstances. Correction factors may be confidently applied to low biomass samples if studies under the same treatment could include unstressed *Fv/Fm* measurements including a reasonably high biomass range. However, under many conditions these assumptions will not be met and therefore *Fv/Fm* should only be determined from samples which have an Fo^{15} value which is higher than 150 (using the FMS2 and the settings described).

3.2.4.3. ETR-E curves

This study showed that the response of algae under laboratory conditions was not representative of the response of microphytobenthos *in situ*. The shift in E_k of microphytobenthos from 644 to 352 μmol m^{-2} s^{-1} (*in situ* to laboratory) showed photoacclimation to lower light levels over a period of hours. Comparative measures of rETR between algae which have been acclimated to natural light levels (field measurements) to those which have been exposed to short periods of high light

(laboratory measurements), after acclimating to low light for a few hours levels, is problematic. The ideal scenario is that the *P-E* (analogous to ETR-*E*) response should reflect the photoacclimational state of the organism at the time of sampling (Sakshaug *et al.*, 1997). Unless incubation time is only a few minutes, some acclimation to the incubation treatment will occur. Therefore, the measurement of *P-E* parameters *in situ* are favoured. However, natural conditions are highly variable and therefore different responses are going to be found depending on prior conditions e.g. measurements made in full sunlight may be acclimation to previous constant full sun, acclimation to previous cloudy conditions, or acclimated to fluctuating conditions. Continuous recording of ambient irradiance prior to light acclimated measurements would be necessary to draw any conclusions regarding the acclimated state of the algae.

Several studies of the photoacclimation of phytoplankton exist (see review by Falkowski and LaRoche, 1991; Anning *et al.*, 2000), macrophytes (Falkowski and Raven, 1997 and refs therein) and ice algae (Robinson *et al.*, 1997). However, very few photoacclimation studies of microphytobenthos (Blanchard and Cariou LeGall 1994; Barranguet *et al.*, 1998; Kromkamp *et al.*, 1998) exist. Blanchard and Cariou-Le Gall (1994) studied the seasonal and hourly patterns in *P-E* parameters. It was unclear how soon after collection Blanchard and Cariou LeGall (1994) and Barranguet *et al.* (1998) made their measurements, although measurements were made on slurries, which destroys the possibility of algae microcycling within the sediments as a photoprotective response (Kromkamp *et al.*, 1998). Kromkamp *et al.* (1998) however, made measurements on intact cores kept under natural conditions and therefore a more representative measurement of *in situ* responses as algae were made as they were able to microcycle. Microcycling describes the movement in and out of the surface layer of sediment as a means to optimising their position to ambient conditions (e.g. light climate or nutrient availability). Blanchard and Cariou-Le Gall (1994) showed a different photosynthetic response of microphytobenthos in slurries between incubations of short (20 min) or long (3 hr) irradiance steps for *P-E* curves. These authors concluded that longer incubations artificially induce photoinhibitory effects, because the algae are in slurries and are unable to migrate into the sediment.

3.2.5. Conclusions

This study showed that careful interpretation of fluorescence measurements must be made and that signal values should be optimised by careful probe

manipulation. When low biomass samples ($Fo^{15} < 150$, equivalent to approximately < 57 mg/m^{-2}) are being studied in may be necessary to make one measurement at 4 mm for biomass estimation followed by a decrease in probe height for maximum efficiency estimation. This can be easily facilitated with the use of spacers attached to the probe tip.

It is clear that the photoacclimative response of microphytobenthos has not yet been fully explored and that much information remains to be obtained by making *in situ* fluorometry measurements.

Chapter 4

4. DETERMINATION OF MICROPHYTOBENTHIC BIOMASS USING PULSE MODULATED MINIMUM FLUORESCENCE

4.1. Introduction

Estuarine mudflats are one of the most productive natural ecosystems on earth, despite extreme variation in physical conditions. The major primary producers in these systems are the microphytobenthos (Yallop *et al.*, 1994; MacIntyre & Cullen, 1996) comprising of euglenids, cyanobacteria, flagellates and diatoms, the latter group tend to be dominant in temperate estuarine mudflats. Microphytobenthos can supply up to 45% of the organic budget of an estuary (Asmus *et al.*, 1998).

The accurate measurement of the active phyto-biomass in sediments is essential for many ecophysiological studies in estuaries. Microphytobenthic biomass is commonly estimated by determining the quantity Chl *a* per unit of sediment using destructive techniques. Chl *a* is generally quantified after extraction by solvents from the sediment, followed by separation from other pigments using HPLC techniques, an accurate but lengthy and expensive method. A less costly technique is the quantification of Chl *a* spectrophotometrically (after extraction), however this technique is generally less accurate than HPLC methods (Pinckney *et al.*, 1994).

Microphytobenthos can only photosynthesise within the surface photic zone, which in cohesive sediment is less than 1 mm (Paterson *et al.*, 1998) and has been reported as 0.27 mm and 0.6mm in different studies (Serôdio *et al.*, 1997; Kromkamp *et al.*, 1998, respectively). Thus, the measurement of Chl *a* restricted to the photic zone will give a better indication of the photosynthetically active microphytobenthos present (Kelly *et al.* 2001).

It is well known that Chl *a* emits fluorescence in the red band upon excitation by light energy (Kautsky & Hirsch, 1931; Govindjee, 1995), and an increase in Chl *a* gives a greater fluorescence yield. Fluorometry has been used extensively for the measurement of extracted Chl *a* concentration and also for the estimation of phytoplankton Chl *a* concentration *in vivo* (e.g. Lorenzen, 1966; Vyhnálek, 1993). *In vivo* fluorescence emanates from the antenna system, not simply from Chl *a*, and at room temperature fluorescence emanates mostly from photosystem II, with minor contributions from photosystem I (Krause & Weis, 1991). Phytoplankton has generally been measured *in vivo* using Impulse fluorometers. This type of fluorometer

measures the fluorescent intensity of dark-adapted cells during saturating flashes of actinic light or after the addition of DCMU (Büchel & Wilhelm, 1993). These measurements could be comparable to the maximal fluorescence (*Fm*) readings made using a modulated fluorescence technique (see below).

Modulated fluorometry has become an important method for the measurement of *in vivo* photochemical processes, as measurements can be made during photochemistry (under ambient or induced irradiance) for the determination of electron transport rate.

Modulated fluorometry exposes the sample to very short pulses of light, enough to induce a reliable fluorescence signal (which is monitored during this short period of excitation) but not enough to induce significant photochemistry (Schreiber *et al.*, 1986). The short pulses of light, made with a measuring light (ML) are set at a suitable excitation wavelength to induce fluorescence, and are available in blue (470 nm) or red (650 nm). These wavelengths are optimal for excitation of different groups of algae. The major groups of algae have different excitation spectra for Chl *a* fluorescence because of the varied accessory pigments complexes in the antennae systems. A blue ML will induce optimal fluorescence from the diatoms and green algae. A red ML induces fluorescence from the cyanobacteria, although diatoms and green algae will also fluoresce, but to a lesser extent than under a blue ML (Yentsch & Yentsch, 1979). The level of fluorescence of dark adapted cells under the ML is known as minimum fluorescence (*Fo*).

Fluorescence of living cells can be affected by many environmental variables (Falkowski & Kiefer, 1985) such as the past and current status of irradiance, temperature, nutrients and herbicides as well as pigment composition and the presence of other fluorescing material. The influences that may affect the determination of *Fo* are also fully discussed in a review by Büchel & Wilhelm (1993). During photosynthesis energy from photons gets used in both photochemical and non-photochemical processes. Both of these processes affect fluorescence quenching. In the absence of light the primary electron acceptor in photosystem II (Q_A) is oxidised and fluorescence is at the minimum level (*Fo*). Light energy reduces Q_A and fluorescence is increased. Thus dark adaption ensures that Q_A is completely oxidised, this results in all reaction centres being 'open' producing a stable *Fo*. Irradiance also increases non-photochemical quenching (NPQ), where excess energy, which could be

potential damaging, is dissipated as heat or via the xanthophyll cycle (Demmig-Adams & Adams III, 1992; Ruban & Horton 1995). Thus if dark adaptation is incomplete then Q_A may not be fully oxidised and reversal of NPQ may not be complete which will result in either increased or decreased *Fo* per Chl *a* unit respectively. Excessive photons can cause two types of photoinhibition. Dynamic photoinhibition, which is readily reversed after a short period of dark, where Q_A is re-oxidised and NPQ reversed, thus *Fo* recovers. However, chronic photoinhibition occurs after extended periods of excessive photons and can decrease efficiency in energy transfer from the antennae system to the reaction centre or damage the PSII (Ruban & Horton 1995). This damage or decreased efficiency may give a stable, but altered, *Fo*.

A reduction to Q_A or decreased efficiency in energy transfer will be reflected in the variable fluorescence shown by a decreased maximum efficiency of photochemistry at PSII (*Fv/Fm*). This parameter (*Fv/Fm*) can be determined by measuring the *Fm* value directly after the *Fo* determination and used in the calculation of $Fv/Fm = (Fm - Fo) / Fm$. Thus *Fv/Fm* is a good indicator of any change to the fully dark adapted value of *Fo*.

Serôdio *et al.* (1997) found complete recovery of *Fo* after 10 minutes of dark adaptation of cultured algae pre-treated (for short periods) at 200-2000 μmol m^{-2} s^{-1}. The dark recovery period for chronic inhibition, after which *Fo* and *Fm* become stable, may however take hours in higher plants (Xu & Wu, 1996). Several studies have shown microphytobenthos *in situ* show no signs of chronic photoinhibition due to their ability to avoid excess light by migrating into the sediment (Barranguet *et al.*, 1998; Kromkamp *et al.*, 1998; Blanchard & Cariou-le Gall, 1994).

Nutrient deficiency of phytoplankton has been shown to increase the fluorescence to Chl *a* ratio (Kiefer, 1973a). Also in phytoplankton, nitrogen and iron limitation has been shown to cause less efficient energy transfer from the antennae to the PSII centre, which results in increased *Fo* and decreased *Fv/Fm* (Greene *et al.*, 1994). Chlororespiration may also cause an increase in *Fo*, due to plastoquinone reduction (Ting and Owens, 1993).

Fluorescence may come from several sources other than active biomass; Chl *a* not bound to proteins, fluoresces much more intensely (Büchel & Wilhelm, 1993);

phaeopigments and other dissolved organic material may fluoresce, as do some inorganic substances.

The properties of light within microphytobenthic biofilms will also affect the excitation and detection of fluorescence. Re-absorption of fluorescence by neighbouring cells will decrease the fluorescence detected (as cell concentration increases then re-absorption increases). Light scattering and attenuation of both excitation beam and fluorescence emitted, through the sediment, biofilm and air, will also reduce the fluorescence detected (Büchel & Wilhelm, 1993; Serôdio *et al.*, 1997).

Despite these sources of variation, Lorenzen (1966), Vyhnálek (1993) and Serôdio *et al.* (1997) all suggest a strong relationship between Chl *a* concentration and fluorescence.

Fluorescence measurements can be made quickly and remotely and are an invaluable tool for non-destructive temporal studies of microphytobenthos (Underwood & Kromkamp, 1999). Serôdio *et al.* (1997), using a modulated fluorometer, showed a strong relationship between *Fo* measurements from microphytobenthos and Chl *a* content in sediments. Their study was laboratory based and used only thin homogeneous layers of algae and sediment (Serôdio *et al.*, 1997). Since the present study was undertaken, Barranguet & Kromkamp (2000) showed the relationship between Chl *a* concentration and *Fo* in undisturbed sediment cores, and found a significant correlation, but scattered data. The variation Barranguet & Kromkamp (2000) found could be due to several factors affecting fluorescence (see above), but could also be due to the depth sampled for Chl *a* analysis. It has been shown that in microphytobenthic rich sediments Chl *a* is concentrated at the very surface; in 0.2 – 0.4 mm (Taylor, 1998; Wiltshire, 2000, Kelly *et al.*, in press). Serôdio *et al.* (1997) sampled Chl *a* per unit sediment weight (which can be highly affected by water content, affecting any areal measurements) and Barranguet & Kromkamp (2000) sampled Chl *a* in 1 mm of sediment (per unit area). The aim of this study was to verify or reject the relationship found between minimum fluorescence and Chl *a* quantity in different depths of sediment under natural field conditions.

4.2. Materials and Methods

Natural sediments were measured both *in situ* and from undisturbed cores collected from the Eden Estuary, Scotland (56° 22' N, 02° 51' W), dates and details of *in situ* measurements are shown in Table 4.1 (n = 24). Undisturbed cores were

Table 4.1. Environmental data collected at the time of *in-situ* Cryolander samples. n/d = no data, S.D. = standard deviations

Date	Sediment temp	Weather	PPFD ($\mu mol\ m^{-2}\ s^{-1}$)	Time of low tide GMT	Time of measurement GMT	Average Fv/Fm ±S.D.	Sediment type	Site	Tidal zone
20 Oct 1998	5°C	cloudy	200	09:35	10:00	0.747 ±0.022	cohesive mud	Eden North shore	low-mid shore
14 Aug 1999	19°C	rainy cloudy	300	10:50	11:30	0.714 ±0.025	cohesive mud	Eden North shore	top shore
14 Jan 2000	n/d	n/d	n/d	13:10	13:00	0.748 ±0.045	cohesive mud	Eden North shore	top shore
4 Apr 2000	6°C	sunny spells	600 variable	08:35	09:00	0.530 ±0.077	cohesive mud	Eden North shore	top shore
4 Apr 2000	8°C	sunny spells	1000 variable	08:35	11:00	0.408 ±0.066	muddy sand	Eden South shore	mid shore

collected from all tidal zones of the Eden Estuary in April 1999 (n = 11) and from the low shore February 2000 (n = 18) and also from the top shore of the Tay estuary in June 1999 (n = 15).

4.2.1. Environmental variables measured

A range of variables was also measured for the *in situ* part of this study during four different seasons; sediment type, tidal zone, temperature (ranged between 5 and 19 °C) and ambient photon flux density (PPFD) which varied between 200 and 1000 μmol m^{-2} s^{-1} (see Table 4.1).

4.2.2. Sediment sampling

Laboratory measurements were made on undisturbed cores, collected using plastic corers (8 cm diameter and 11 cm deep). Cores were kept intact, at room temperature and at an irradiance of 300 μmol m^{-2} s^{-1} during daylight hours. Measurements took place on the day after collection.

Chl *a* was extracted from either Cryolander (*in situ* samples) or contact cores (laboratory data). Fine scale resolution of depths within 2 mm was obtained from Cryolander samples to give a more accurate measurement of the active biomass.

The contact coring technique produces a surface disc of frozen sediment (2-3 mm deep) with a diameter of 56 mm. The technique is based on a method described by Anderson & Black (1980) to analyse the texture and composition of intertidal sediments. A removable plastic collar is attached to the rim of an aluminium dish (surface area 2100 mm^2) such that the collar extends 2 mm beyond the bottom of the dish. A core is collected by pushing the dish and collar into the sediments until the bottom of the dish makes contact with the sediment. Approximately 30 ml of liquid nitrogen (LN_2) is poured into the dish. The time needed to freeze 2 to 3 mm of sediment is dependent on the sediment type (mud, muddy-sand, sand), water content, and environmental conditions (temperature and wind). In general, 45-60 seconds is sufficient for mud and mud-sand sediments. The core and frozen sediment is then removed and excess sediment removed by scraping until the sediment is flush with the lip of the collar. The frozen disc is then removed from the dish and collar, placed in aluminium foil, and stored under LN_2.

Contact coring was developed in preference to other coarse coring techniques (Kelly *et al.*, 2001) for several reasons. Firstly, the sample is frozen immediately,

decreasing any transportation effects (e.g. darkness) that may affect the pigments, also contact cores are comparable to Cryolander samples, which are likewise frozen *in situ*. Secondly, the method is simple and many samples can be collected over a short period of time. Thirdly, only the surface sediments (2 - 3 mm) are collected, closer to the photic zone than some coarse coring methods, which samples the surface 5 mm.

For the analysis in this study, the centres of the frozen contact cores were re-cored (with a sharp metal corer) to a diameter of 20 mm (314 mm^2 area), which included the exact surface location from which fluorescence measurements were made. This smaller core was then lyophilised, homogenised and sub-sampled for pigment analysis.

The Cryolander technique involves the freezing of the sediment surface using LN_2, producing a frozen "plate" of sediment over 10 mm in depth and 50 mm diameter (Wiltshire *et al.*, 1997, Kelly *et al.*, in press). These samples were kept frozen in darkness under LN_2 and transported to the laboratory where they were kept at –80°C for further analysis. In the laboratory a 10 mm block was cut from the frozen sediment in the exact location of the fluorescence measurement. The blocks were then sectioned at intervals from the surface (zero to 0.2 mm, 0.2 mm to 0.4 mm, 0.4 mm to 1 mm and 1 mm to 2 mm). The surface of the sediment collected with the Cryolander is rarely flat. Thus 'zero depth' is determined at the point at which 90-95% of the area is visibly level. Any undulations above this point are included in the 0 - 0.2 mm slice. Once each section had been sliced and transferred to an eppendorf, the sediments were re-frozen and lyophilised in preparation for pigment analysis.

4.2.3. Fluorometry

A portable Hansatech Fluorescence monitoring System (FMS2), which employs the pulse-modulated fluorescence technique (Schreiber *et al.*, 1986) with a blue measuring light was used in this study. Instrument settings and probe height above the sediment (4 mm) were kept constant. At 4 mm height, the fluorometer measures approximately 120 mm^2 of sediment surface (probe tip 31 mm^2). FMS2 settings used were gain: 99; modulation frequency level 3; *Fo* duration: 2.8 sec; saturation intensity level 60 and pulse width 1.0 sec. To minimise the affects that photochemical processes have on fluorescence yield, measurements were made on dark-adapted cells. Light dependant fluorescence measurements (*Fs, Fm'*) were not used as they are the parameters used in the measurement of photophysiological

processes (Q_A reduction), which intrinsically vary with the natural variation in ambient light (Serôdio *et al.* 1997 and references therein). In this study two fluorescence parameters were routinely obtained after a set period of dark adaption, one before and one during a saturation pulse of actinic light. The first measurement was made in the dark, after 15 minutes and termed minimum fluorescence (Fo^{15}), within seconds the second measurement was made during a saturating pulse of light, termed maximum fluorescence (Fm^{15}). These terms are based on *Fo* and *Fm* values (Schreiber *et al.*, 1986) but may vary from intrinsic values of *Fo* and *Fm*, which are difficult to establish. The period of 15 minutes dark adaption was selected as optimal to reduce variation in *Fo* due to previous light conditions and has been used by previous authors (Kromkamp *et al.,* 1998). Longer dark adaption was rejected to avoid changes in the Chl *a* at the surface possibly induced by diatom migration.

Fv/Fm was also measured as an indicator of stress response (Büchel & Wilhelm, 1993), and may be a good indicator of any change in *Fo* due to physiological or environmental variables.

4.2.4. Measuring protocol

Measurements were made at the time of low tide or soon after to decrease any interference from migratory effects (Serôdio *et al.*, 1997; Kromkamp *et al.*, 1998; Paterson *et al.*, 1998). It was assumed that most of the biomass would be at the very surface at low tide (see fig. 5 Serôdio *et al.*, 1997 which shows a peak in *Fo* at the time of low tide). The active Chl *a* present would thus be within the measurement depth of the fluorometer and would consequently decrease variability due to active biomass in deeper layers of sediment.

In the field or laboratory, fluorescence measurements were made after 15 minutes of dark adaption using an inverted black dish. This was followed by Cryolander coring or contact coring within 30 minutes.

4.2.5. HPLC (high performance liquid chromatography)

Chl *a* was identified by reverse phase HPLC. For the full methodology see Wiltshire & Schroeder (1994). Extraction involved adding either 1 ml of 100% acetone or 90% DMF to the sediment sample (0.04-0.1 g) and pigments were extracted for a minimum of 24 hours at -70 °C or 4°C in the dark. Extractant and sediment were separated by filtration through a 0.2 µm pore syringe filter

(Whatman™). Chl *a* standards (derived from *Anacystis nidulans*, Sigma™) were analysed with every sample batch to obtain a standard curve.

The HPLC system consisted of a quaternary high pressure pump (Perkin Elmer 410), an autosampler (Waters WISP 417) and a diode-array detector (Waters 910). The column was a Nucleosil C18 (Capital HPLC Ltd) kept in a column oven at 25 °C. Extractions were injected onto a binary gradient. The flow rate was 0.8 ml min^{-1} and the two solvents used were: eluant A:- 80% methanol, 10% water, 10% buffer (1.5 g acetate, 7.7 g ammonium acetate in 100 ml of distilled water), eluant B:- 90% methanol, 10% acetone. Chl *a* eluted at 25 minutes, and analysis of peak area was used to quantify the pigment (Wiltshire & Schroeder, 1994).

In this study Chl *a* quantity will be expressed in two ways for wider applicability and comparability of the results; Chl *a* concentration (per unit area of sediment surface) and Chl *a* content (per unit dry weight of sediment).

4.2.6. Statistical analysis

Product moment correlations were performed on *in situ* (Chl *a* per m^{-2}) raw data (normally distributed), while the remainder of the data (*in situ* Chl *a* per kg^{-1} and combined lab and *in situ* data sets) were transformed (natural logarithm). Model 2 regression analysis (reduced major axis regression) were performed as both axis (fluorescence and Chl *a* quantity) were indeterminate variables (Fowler & Cohen, 1990).

4.3. Results

Results from both *in situ* and laboratory cores were combined (n = 68) for initial examination. Both Fo^{15} and Fm^{15} were correlated against Chl *a* concentration (per m^2) in approximately the top 2 mm of sediment (Fig. 4.1), and both had highly significant positive relationships (both $P < 0.001$) (Table 4.2). However Fo^{15} had a stronger relationship with Chl *a* concentration than Fm^{15}. Only 25% ($r^2 = 0.246$) of the variation in Fm^{15} was explained by the variation in Chl *a* concentration whereas 56% ($r^2 = 0.557$) of the variation in Fo^{15} was explained by the variation in Chl *a* concentration (see coefficients of determination in Table 4.2).

A sub-sample (all *in situ* field measurements, n = 24) from data shown in Fig. 4.1 was also analysed on a finer scale (four sub sections within 2 mm). As the sample depth became shallower, the correlation between Chl *a* in that section and Fo^{15}

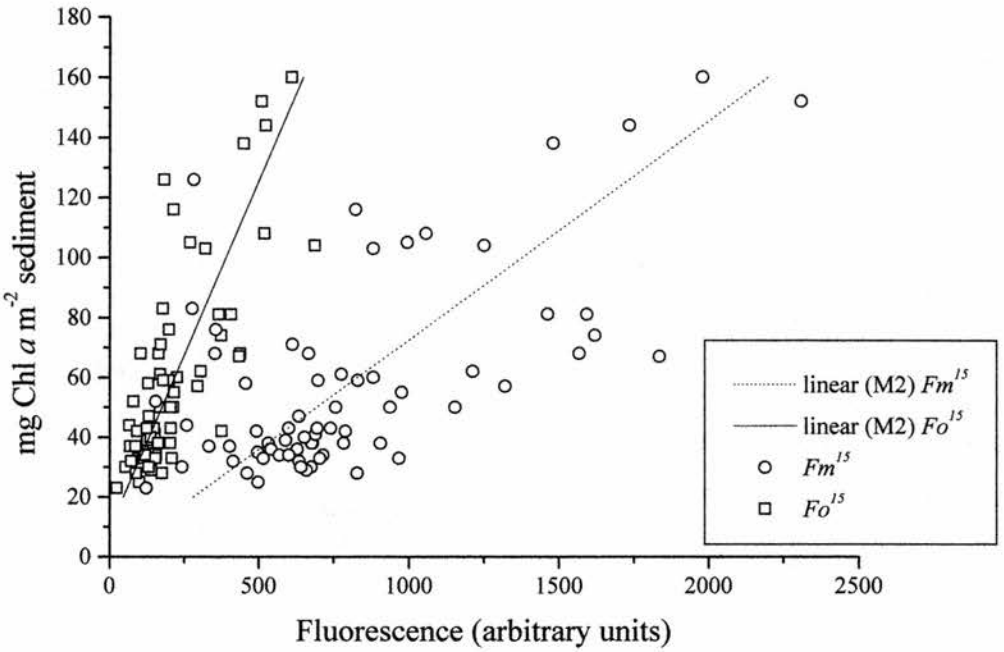

Figure 4.1. The relationship between Chl *a* in approximately the top 2 mm of sediment and both Fo^{15} and Fm^{15}. Model 2 linear regression lines are plotted for Fo^{15} and Fm^{15}. The data includes both contact core laboratory data and the 0 to 2 mm section of the Cryolander core. Chl *a* is depicted on the dependant axis because it is the predicted variable

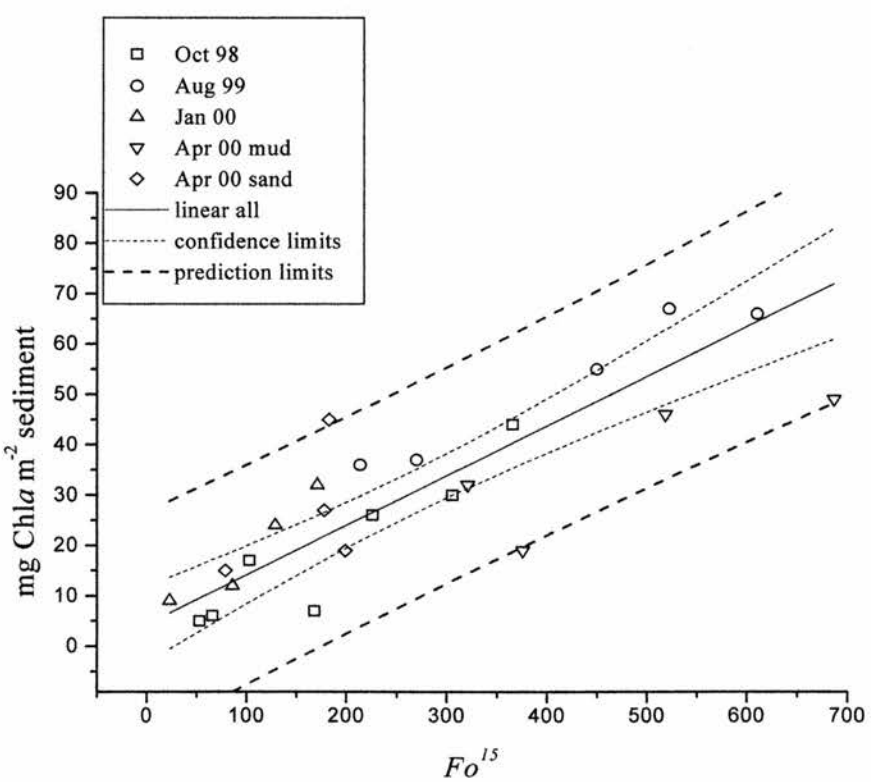

Figure 4.2. The relationship between Fo^{15} and Chl *a* (per area of sediment) in surface 0.2 mm of sediment. These are field *in situ* data and different seasons are depicted by different markers (see legend). Model 2 linear regression line is plotted for all data. Inner and outer dotted lines indicate confidence and prediction zones, respectively

Table 4.2. Product moment correlation coefficients (r) and coefficient of determination (r^2) of Fo^{15} and Fm^{15} with chlorophyll *a* content per area of sediment in different depths of sediment

	mg chl *a* m^{-2} Sample depth	n	Fo^{15}		Fm^{15}		P value (for r)
			r	r^2	r	r^2	
In situ data	0 - 0.2 mm	24	0.840	0.705	0.838	0.702	Both < 0.001
	0 - 0.4 mm	24	0.835	0.697	0.825	0.681	Both < 0.001
	0 - 1.0 mm	24	0.782	0.611	0.788	0.621	Both < 0.001
	0 - 2.0 mm	24	0.713	0.508	0.718	0.516	Both < 0.001
Lab and *in situ* data	0 - ~3mm	68	0.746	0.557	0.496	0.246	Both < 0.001

Table 4.3. Product moment correlation coefficients (r) and coefficient of determination (r^2) of Fo^{15} and Fm^{15} with chlorophyll *a* content per mass of sediment in different depths of sediment

	mg chl *a* kg^{-1} Sample depth	n	Fo^{15}		Fm^{15}		P value (for r)
			r	r^2	r	r^2	
In situ data	0 - 0.2 mm	24	0.831	0.705	0.846	0.716	Both < 0.001
	0 - 0.4 mm	24	0.806	0.650	0.825	0.681	Both < 0.001
	0 - 1.0 mm	24	0.795	0.632	0.798	0.637	Both < 0.001
	0 - 2.0 mm	24	0.790	0.624	0.780	0.608	Both < 0.001
Lab and *in situ* data	0 - ~3mm	68	0.667	0.445	0.453	0.205	Both < 0.001

became stronger (Table 4.2 and 4.3). The Chl *a* concentration (per area) in the top 0.2 mm of these samples showed the strongest relationship with Fo^{15} (r = 0.84) (Table 4.2; Fig. 4.2). Therefore over 70% ($r^2 = 0.705$) of the variation in Fo^{15} was explained by the variation in Chl *a* concentration. The prediction limits of the relationship between Fo^{15} and mg Chl *a* m^{-2} show a large variation if a single measurement of Fo^{15} were to be made (Fig. 4.2 outer dotted lines). For example if a single measurement of an Fo^{15} of 400 was made then we can be 95% confident that it will give a Chl *a* concentration of 43.7 ± 21.7 mg m^{-2}. However, if replicates were taken this error will decrease. If a variety of samples were taken, reflecting a normal distribution of biomass then we could be 95% confident an Fo^{15} of 400 will give a Chl *a* concentration of 43.7 ± 5.4 mg m^{-2} (Fig. 4.2 inner dotted lines).

The coefficient of determination decreased with sample depth (Table 4.2). Regression analysis was performed on *in situ* data and as the sample depth became smaller the intercept of the regression became smaller, approaching zero (see Table 4.4). The slope of the regression between Fo^{15} and Chl *a* also became shallower with decreasing sample depth (Fig. 4.3). The samples that deviated most from the regression line were examined for any environmental differences (e.g. signs of stress (*Fv/Fm*); temperature; season; see Table 4.1 and Fig. 4.2), and no obvious relationships were apparent. The samples with decreased *Fv/Fm*, in April 2000, were found under higher PPFD (Table 4.1). However it was unclear whether high light affected Fo^{15}, as removing the low *Fv/Fm* did not strengthen the relationship between Fo^{15} and Chl *a*. The regression coefficient of each data point was calculated ([Chl *a* – intercept]/ Fo^{15}) and correlated against each set of variables i.e. temperature, PPFD and *Fv/Fm*, and no relationships were found (not shown).

Correlations were also performed on Fo^{15} and Chl *a* per mass of sediment (Fig. 4.4 and Table 4.3). Similar relationships to Chl *a* concentration are apparent between fluorescence and Chl *a* content (Compare Tables 4.2 and 4.3). That is, weaker relationships between Fo^{15} and Chl *a* with increasing sample depth. This relationship (Fo^{15} and Chl *a* in sediment mass) gives an exceptionally low intercept (zero Fo^{15} = -72 mg Chl *a* kg^{-1}, Table 4.4) implying less sensitivity at lower biomass than Chl *a* per area.

Table 4.4. Model 2 regression coefficients (reduced major axis regression) of Fo^{15} and with chlorophyll *a* content per area or mass of sediment and in different sample depths

Expression of chlorophyll *a* content	Sample depth	Fo^{15}	
		slope	intercept
Per mass mg chl *a* kg^{-1}	0 - 0.2 mm	1.300	-72.13
Per area mg chl *a* m^{-2}	0 - 0.2 mm	0.099	4.28
	0 - 0.4 mm	0.132	7.37
	0 - 1.0 mm	0.188	12.78
	0 - 2.0 mm	0.225	23.26
	0 - ~3mm	0.232	9.55

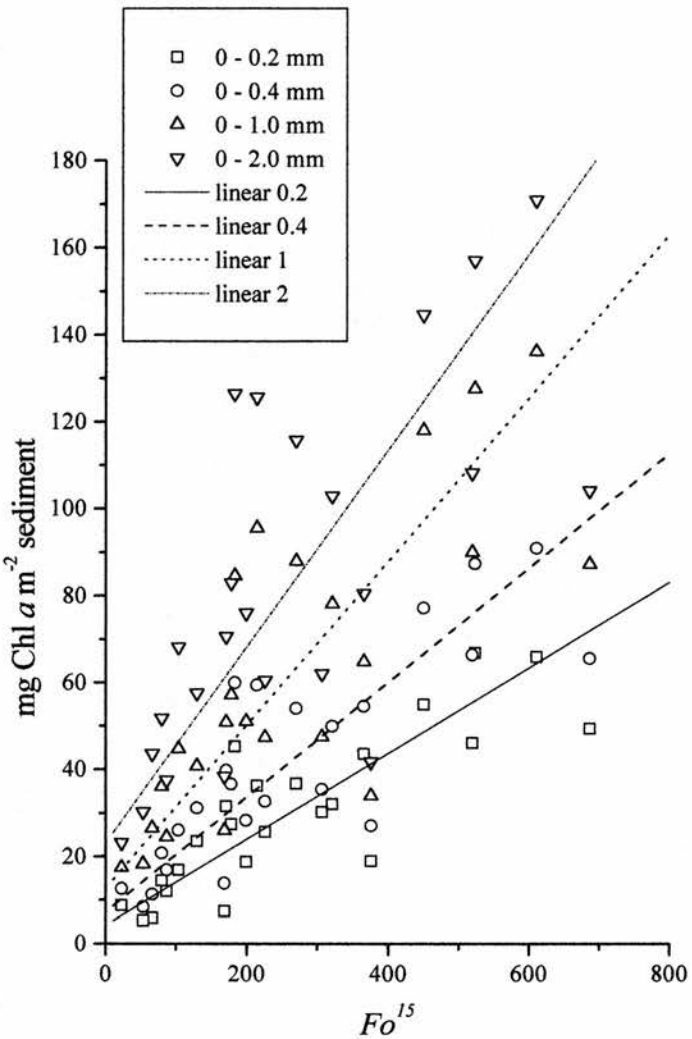

Figure 4.3. The relationship between Fo^{15} and Chl *a* in different sample depths of sediment. Model 2 linear regression lines are plotted separately for each sampling depth

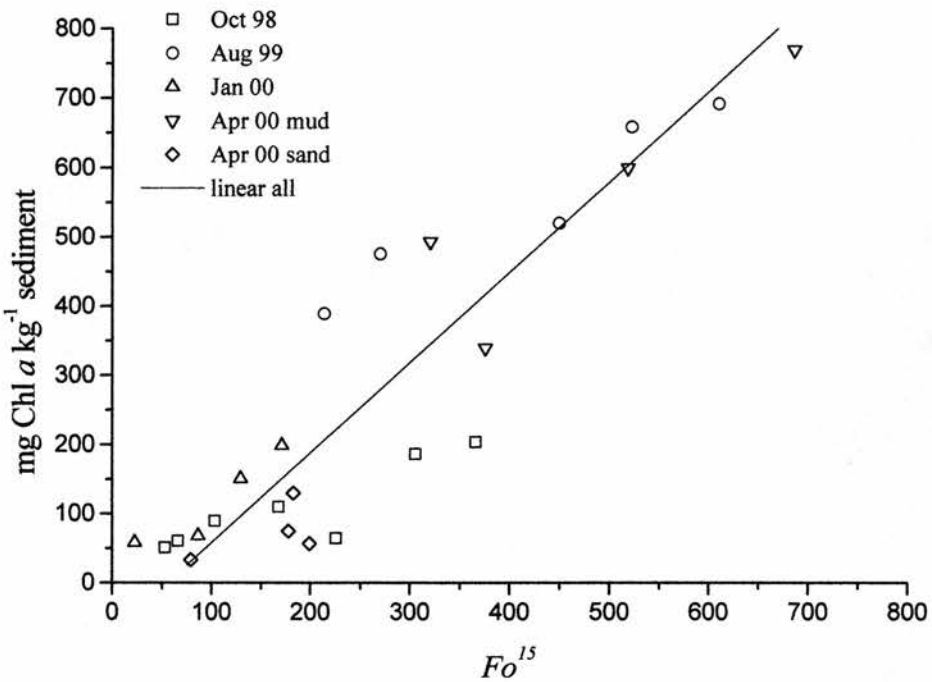

Figure 4.4. The relationship between Fo^{15} and Chl *a* (per mass of sediment) in surface 0.2 mm of sediment. These are field *in situ* data and different seasons are depicted by different markers (see legend). A model 2 linear regression line is plotted for all data

4.4. Discussion

There was a stronger correlation between Fo^{15} and Chl *a* in samples comprising the surface 0.2 mm than in samples including deeper layers. This is likely to be due to fluorescence response only being measured within the depth of light penetration, which in cohesive sediments is closer to 0.2 mm than 2 mm (Serôdio *et al.*, 1997). This supports work by Paterson *et al.* (1998), showing a stronger correlation of spectral reflection with Chl *a* in the surface 0.2 mm than with Chl *a* in 5 mm surface scrapes.

The measuring depth of fluorometry will be less than that of the photic depth due to attenuation of both fluorescence signal and the measuring beam, as blue light is attenuated within sediments more quickly than photosynthetically active radiation (Lassen *et al.*, 1992; Kromkamp *et al.* 1998). It has been reported that most of the fluorescence (detectable by a PAM fluorometer) emanates from a sediment depth of 0.15 mm (Kromkamp *et al.* 1998). This depth may be even smaller in our study, as a blue measuring light will be attenuated more quickly than the red measuring light used by Kromkamp *et al.* (1998). Another important factor is that upwelling fluorescence will be attenuated through the sediment and the air (Serôdio *et al.*, 1997).

An error in probe height will increase the variation found in the relationship between Fo^{15} and Chl *a*. The topography of the sediment surface is uneven and thus it is impossible to know the exact height of the probe. Further studies are being undertaken to assess to what extent probe height may have on the fluorescence signal.

A shallower slope exists between Fo^{15} and Chl *a* in the surface 0.2 mm than between Fo^{15} and Chl *a* in the surface 2 mm, which means there is a faster rate of Fo^{15} increase, per unit of Chl *a*, as the sampling depth became smaller (Fig. 4.3). This shows that although there is Chl *a* at depths greater than 0.2 mm, it is not necessarily all photo-active. This also indicates that as Chl *a* on the surface increases, so does Chl *a* at depth (below the fluorometer detection).

A positive intercept of Fo^{15} at zero Chl *a* concentration was found, supporting other studies (Serôdio *et al.* 1997; Barranguet & Kromkamp, 2000), showing a background signal was present. We tested for a background signal and found zero measurements of Fo^{15} on organic free sediments (cleaned in hydrogen peroxide). This indicates that the background signal may come from non-chlorophyll *a* organic matter. Photosynthetic efficiency (*Fv/Fm*) within the window of our measurements

(see Table 4.1) did not appear to affect Fo^{15} deviation from the regression line. The intercept of Chl *a* concentration increases with increasing sampling depth. This could be explained by increasing background signal, although, as previously stated, detection is unlikely to go below the finest depth sampled here. The more likely explanation is therefore Chl *a* is present in the sediment at levels below the fluorometer detection.

Samples with decreased *Fv/Fm* were found under higher PPFD indicating that samples were affected by photoinhibition or nutrient limitation (as 15 minutes was not long enough for complete recovery). However it was unclear whether high light affected Fo^{15}, as removing the low *Fv/Fm* values did not strengthen the relationship between Fo^{15} and Chl *a*. The regression coefficients of the data did not correlate against any of the variables; temperature, PPFD or *Fv/Fm*.

Further studies could encompass higher temperatures and irradiances to ascertain their affects on Fo^{15}, the highest temperature and PPFD in this study was 19 °C and 1000 μmol m^{-2} s^{-1} respectively, both about half of the level which could be expected on sunny summer days. Serôdio *et al.* (1997) however found no affect of temperature on *Fo* up to 43°C in a diatom culture and Kiefer (1973b) found temperature had no effect on the fluorescence of *in vivo* Chl *a* of phytoplankton. Several days of high light might have an affect on the photosystem, causing photoinhibition and altered *Fo* values. However, several studies have shown microphytobenthos *in situ* do not show signs of excess light inhibition (photoinhibition) due to their ability to avoid excess light by migrating into the sediment (Barranguet *et al.*, 1998; Kromkamp *et al.*, 1998; Blanchard & Cariou-le Gall, 1994). It is however unclear how *Fo* is affected after dark recovery following long-term high irradiances.

Further studies should also examine higher algal biomass to ascertain whether the relationship between Fo^{15} and Chl *a* becomes asymptotic. The Eden Estuary rarely has Chl *a* concentration (from microphytobenthos) higher than 160 mg m^{-2} (in 2 mm depth) or 350 mg Chl *a* kg^{-1} (in 2 mm depth). Although other estuaries have comparable maximum values (Marennes Oleron Bay, France; Molenplaat, The Netherlands: Cariou le Gall & Blanchard, 1995; Colijn & Dijkema, 1981), some intertidal flats have Chl *a* concentrations up to 400 mg m^{-2} (Ems Dollard; Colijn & de Jonge, 1984) or 800 mg m^{-2} (Texel, The Netherlands; Paterson *et al.*, 1994).

It is important to identify the microalgae present, as microphytobenthic groups (i.e. euglenids, flagellates and cyanobacteria) have different accessory pigments and thus different fluorescence properties. Different pigments have different optimal excitation wavelengths for fluorescence (Schreiber *et al.*, 1993; Büchel & Wilhelm, 1993), and thus it would be impossible to differentiate biomass of each group with a single colour measuring light. Cyanobacteria would seriously alter the relationship between Chl *a* and Fo^{15}, as these organisms have a different pigment system (PSII antennae) than that of eucaryotes and exhibit only weak fluorescence from Chl *a* (Bryant, 1986; Sepälä & Balode, 1998).

Testing the generic validity of the relationship is important, as most of the data included in this study are from the Eden Estuary. A further study incorporating different estuaries with a wider variety of sediment types would be valuable to extend the application of these findings.

Possible artefacts from breakdown products are unlikely to affect fluorescence as they are rarely found in the surface 0.2 mm. However, if microphytobenthos are scarce, then settling of detrital material (such as senescent plankton) could be a major source of error. This could be detected with few samples collected for pigment fingerprinting.

4.5. Conclusions

The biomass of *in situ* diatom assemblages can be estimated using Fo^{15}. Measurements should however be taken carefully, as many factors can introduce errors. Measurements should be made close to low-tide to decrease migratory effects at surface. To decrease variation and other errors in the relationship between Chl *a* and Fo^{15}, sub-samples (incorporating a range of values) should be taken and analysed for Chl *a* concentration and the groups of algae present identified. Measurements made on algae that are able to dark-adapt within 15 minutes are preferable (this should occur with healthy cells on a cloudy day), this can be checked by simultaneously measuring *Fv/Fm*. If dark-adaptation of algae does not occur within 15 minutes then care should be taken in the interpretation of results. However, no difference was found between the value of Fo^{15} in ambient light (1000-1600 μmol m^{-2} s^{-1}) than the Fo^{15} recorded in 50% shaded conditions (Perkins *et al.*, in press). Fluorescence measurements show that fine depth resolution (close to the scale of light

penetration) is important in measuring photosynthetically active Chl *a* concentration in sediments.

Once established, the advantages of fluorescence detection of biomass are considerable. Non-destructive analysis of surface biomass allows time-series and spatial analysis to be conducted on natural sediments. This technique will therefore considerably advance our knowledge of the temporal and spatial distribution of microphytobenthos.

Chapter 5

5. CAN FLUORESCENCE BE USED TO MEASURE MICROPHYTOBENTHIC BIOMASS DISTRIBUTION ON A LARGE SCALE?

5.1. Introduction

One of the major primary producers in depositional estuarine habitats are microscopic algae (Pinckney and Zingmark, 1991; Yallop *et al.*, 1994; MacIntyre and Cullen, 1996). Microphytobenthos provide an important energy source for the estuarine food web (Sullivan and Moncreiff, 1990, Pinckney *et al.*, 1994) supplying up to 45% of the organic budget of an estuary (Asmus *et al.*, 1998) and have a central role in moderating carbon flow in coastal sediments (Middleburg *et al.*, 2000). Estuarine microphytobenthic biomass often exceeds that of phytoplankton biomass in the overlying tidal waters (MacIntyre *et al.*, 1996). The measurement of microphytobenthic biomass and physiology are an essential aspect of the ecological study of these estuarine systems.

Biomass (estimated from Chl *a*) can often be a good indication of photosynthetic activity and thus productivity of the organisms (Pinckney and Zingmark, 1993c). The intertidal estuarine environment is, by nature, dynamic, exposed to the weather and tidal inundation, which can affect the biomass and physiology of the microphytobenthos. Biotic interactions such as grazing and infections by parasites can also play a part in the ecophysiology and may, intermittently, cause a rapid decline of whole algal populations (Round, 1981).

In cohesive sediments, microphytobenthos are generally represented by three types of algae: cyanobacteria (blue green algae; Cyanophyta), euglenids (Euglenales), and diatoms (Bacillariophyta), the latter being the most dominant (Admiraal, 1984). Most of the microphytobenthos found in the intertidal estuarine habitat are motile and are able to migrate to the surface during daylight and into the sediment when the mudflat is immersed by the tide, which could potentially scour the surface. Migration of diatoms in and out of the surface layer of sediment (micro-cycling) may also occur on a smaller temporal scale during tidal emersion when conditions become stressful. This may be why microphytobenthos, dominated by diatoms, showed no signs of light stress or nutrient limitation *in situ*, after hours of exposure to high ambient light conditions (Kromkamp *et al.*, 1998).

In general, ecologists assess biomass in a habitat using the mass of organisms per unit area. The quantity of chlorophyll *a* (Chl *a*) per sediment unit has more commonly been measured as an estimate of the microphytobenthic biomass in estuarine systems (e.g. Pinkney *et al.*, 1994; MacIntyre *et al.*, 1996; Barranguet and Kromkamp, 2000; Paterson *et al.*, 2000). EPS concentration was found to be highly correlated with Chl *a* in diatom rich samples (Yallop and Paterson, 1994; Underwood *et al.,* 1995 Kelly *et al.,* 2001) and thus may also be a useful biomarker for diatoms. EPS can be easily extracted and measured from sediments, as it is mainly made up of colloidal carbohydrates, which are water soluble. Counting cell numbers, and calculating biovolume, as a measure of biomass, is time consuming and problematic, as diatoms can vary greatly in size (5 – 300 μm in length) and shape. Taxonomic information on species composition can however be an extremely valuable ecological tool, as species richness, diversity, evenness and similarity are all affected by environmental factors (Sullivan, 1978; Snoejis, 1994). Chl *a*, as a proxy for biomass of any photosynthetic material is quantified after extraction from known quantities of sediment. Pigment extracts from sediments are either measured spectrophotometrically (Lalli *et al.,* 1984) or the pigments are separated and quantified using HPLC (Wiltshire and Schroeder, 1994). The identification of pigments (and the ratio of some pigments to Chl *a*) has been used for categorising different groups of sediment-inhabiting algae present, as different groups contain different pigments (Barranguet *et al.,* 1997; Brotas and Plante-Cuny, 1998). Diatoms have several pigments, two of which; fucoxanthin and chlorophyll *c*, are generally not present in other algae found in estuarine sediment habitats (Millie *et al.,* 1993). Blue green algae contain the marker pigment zeaxanthin and euglenids have chlorophyll *b*, lutein and diadinoxanthin. However zeaxanthin, chlorophyll *b* and lutein are also present in green algae (e.g, *Enteromorpha*) or higher plant detritus which may also be present on estuaries. Therefore a combination of certain pigments and lack of others has been the recommended procedure for algal group identification (Barranguet *et al.*, 1997; Brotas and Plante-Cuny, 1998).

Pigment concentrations can change in response to light levels; decreased light levels induce increased quantities of light harvesting pigments to capture more energy and vice versa (Falkowski and LaRoche, 1991; Falkowski and Raven, 1997). Thus, Chl *a* quantity per cell, can be a useful determinant of photoacclimation. Whilst an

increase in Chl *a* per cell may confound biomass analysis, Chl *a* can give a good representation of the photosynthetic potential of the population (MacIntyre *et al.*, 1996). Weight or volume of cells would be a more accurate measure of diatom biomass, however it is extremely difficult, if not impossible, to separate the sediment from the cells for community weight or volume calculations. Furthermore individual cell volume calculations are intrinsically difficult, as diatom shapes can be complex and some species decrease in size throughout their vegetative life cycle. It is therefore generally thought that quantifying Chl *a* is a more representative measure, and is the most widely used method, of biomass estimation (MacIntyre *et al.*, 1996). Recently Chl *a* content and concentration of sediment has been shown to have a strong relationship with the minimum fluorescence parameter (Fo^{15}) (Serôdio *et al.*, 1997; Barranguet *et al.*, 1998; Chapter 4). Fluorescence measurement is rapid and a non-invasive technique and is thus an invaluable tool for temporal and spatial studies of microphytobenthos (Underwood and Kromkamp, 1999).

This Chapter analyses studies made during survey campaigns of three intertidal areas in Northern Europe. Measurements of both Fo^{15} and Chl *a* concentration of the surface sediment were made on a large spatial scale for comparison (within and between intertidal areas). This investigation took place under the BIOPTIS project (EU MAS3-CT97-0158), which was to assess the biological and physical dynamics of intertidal sediment ecosystems, by remote sensing and ground truthing measurements. Paired Fo^{15} and Chl *a* concentration measurements were made to encompass a variety of intertidal sediments, and extend the range of sample types for the examination of the relationship previously found between these parameters (Serôdio *et al.*, 1997; Barranguet and Kromkamp, 2000; Chapter 4). Fluorescence was measured using two different models of fluorometer and a comparison between these instruments was made.

5.2. Materials and Methods

This section is a general material and method description for the 3 following studies (sections 5.3, 5.4 and 5.5).

Three intertidal areas in Northern Europe were surveyed during the BIOPTIS campaigns (see Chapter 2). Paired measurements of Chl *a* concentration of the surface sediment and the minimum fluorescence level after 15 minutes of dark adaption (Fo^{15}) were made. Chl *a* concentration was determined from samples collected using

the contact corer, which collects the surface 2-3 mm of sediment (Chapter 2). Fo^{15} was determined from both the Hansatech FMS2 and the Walz PAM2000. These two fluorometers have different wavelength excitation beams (also termed measuring lights (ML)) and different integration methods. Therefore a calibration between these instruments was made from selected sites, during mesoscale measurements.

The chamber used for fluorescence measurements (Chapter 3) was placed over the exact area later contact cored for Chl *a* concentration. The scale of fluorescence measurements was much smaller than that of the contact corer; Fo^{15} measures an area of approximately 120 mm^2 and the contact core measures an area of approximately 2550 mm^2. The dark adaption chamber was of similar diameter to that of the contact corer, thus replication of fluorescence measurements (spatially within the chamber) should give a more representative value of the area sampled for Chl *a*. On the Sylt sites only one Fo^{15} measurement was made at each node replicate, i.e. one per contact core. On the Eden sites, three Fo^{15} measurements were made at each node replicate (four for the mesoscale studies) and on the Yerseke sites five Fo^{15} measurements were made at each node replicate. This increase in replication of fluorescence measurements within the chamber occurred because of an improvement of the dark adaption chamber design (Chapter 3).

5.2.1. Mesoscale measurements

Specific nodes (within the synoptic grids) were selected to study on a smaller scale (Mesoscale studies). On Sylt, mesoscale studies were carried out on grids A and B, in the location of nodes SAC1, SBB4 and SBD1 (Fig. 2.7). On the Eden Estuary sites on grids A and B were chosen, around nodes E1AE8 and E1BB4 (Fig. 2.4 and 2.5). The node E1AE8, under visual assessment, had different types of macroalgae as well as sediment and/or microalgae. The other node for a mesoscale study, E1BB4, on visual assessment, had an area of diatoms and an area of cyanobacteria. The protocol for mesoscale measurements was to place 5 replicate dark adaption chambers randomly, 20 cm apart (Fig. 5.1). This was then repeated, placing the chambers at 100 cm and 500 cm apart. FMS2 fluorescence measurements (Fo^{15}) were then taken, followed, within 5 minutes by PAM2000 measurements (Fo^{15}) within each chamber. Chambers were then removed and contact cores taken from the sediment covered by the chambers. Thus FMS2 measurements, PAM2000 measurements and Chl *a* concentration of the sediment were all coupled. One fluorescence measurement was

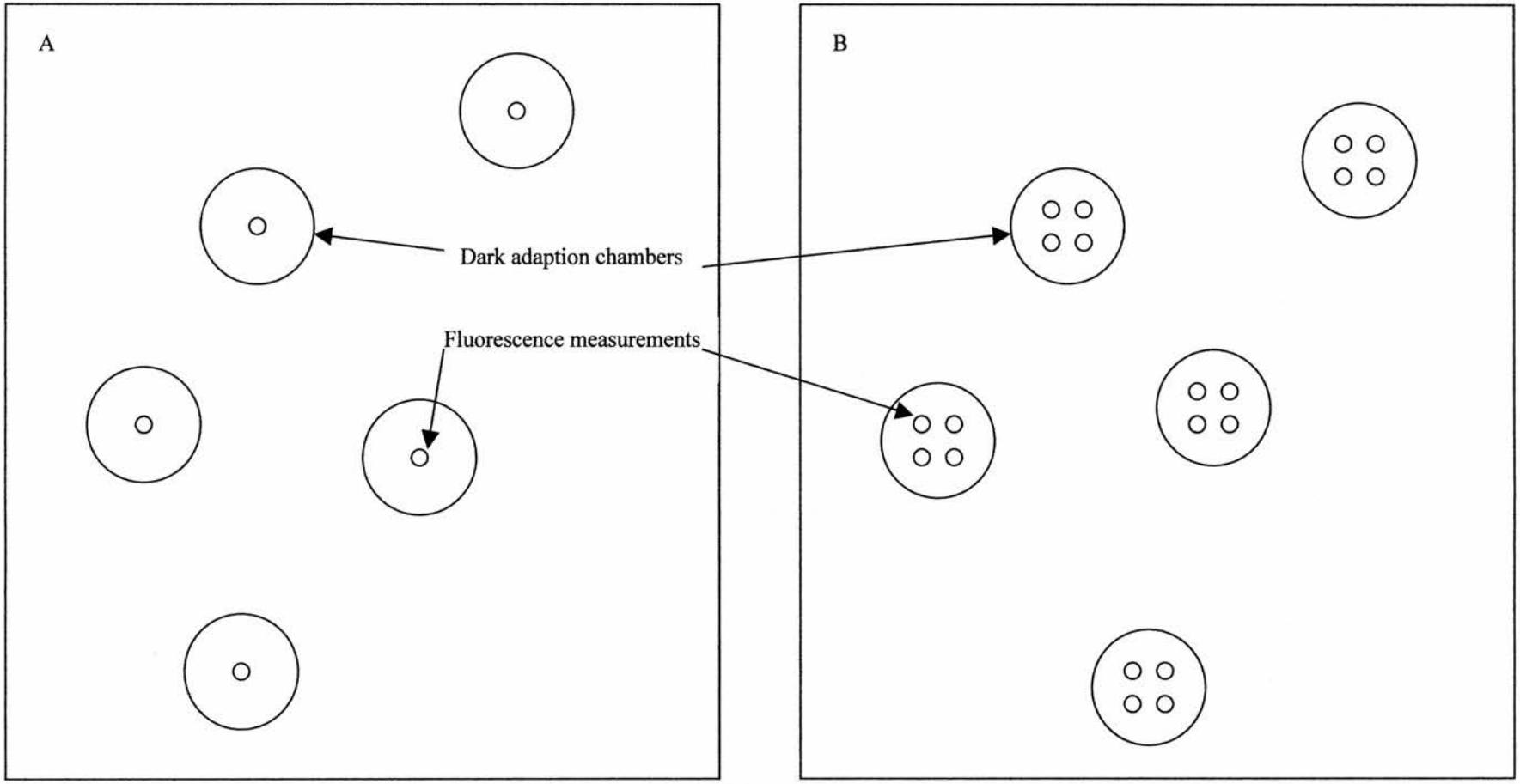

Figure 5.1. Sampling scheme for mesoscale study. Five replicate chambers were placed at specific distances apart (20 cm, 100 cm and 500 cm). Figures A and B show the sampling scheme on Sylt and The Eden respectively. Eden fluorescence replication within a dark adaption chamber (equivalent to the contact core area) was increased to four (only three fluorescence replicates were made per chamber for Eden synoptic measurements)

made per chamber on Sylt. The fluorometer only measured a small area (~1.2 cm^2), which was deemed as unrepresentative of a contact core sampling area. Therefore further replication within the chamber was made during the Eden campaign. Four evenly spaced fluorescence measurements (2.5 cm apart) were made within each chamber to provide a more representative measure of the Chl *a*. Each replicate within a chamber was measured with both instruments. Eden mesoscale studies were therefore able to include a comparison between Fo^{15} measurements at a scale of 2.5 cm. No mesoscale measurements were made in Yerseke, but measurements were made at most synoptic grid nodes with both instruments, bar several nodes on Grid B, which had only PAM2000 measurements. On the Yerseke sites, five fluorescence measurements were made within each chamber with both instruments. These fluorescence measurements were not paired, thus averages of the 5 fluorescence measurements per chamber were used for instrument comparisons. Extra measurements for inter-instrument calibration were made on Sylt cores from nodes SAE and SAC and on the Eden Estuary around nodes E1AB1 and E1AC1. 75% of the nodes on Grid C on the Eden Estuary were also measured with both instruments.

Mesoscale fluorescence measurements were thus used for inter-instrument comparisons and calibrations, and for the study of diatom biomass distribution at varied horizontal scales.

5.2.2. Synoptic studies

During the synoptic survey, 3 randomly placed replicate samples were taken at each grid node using the contact corer to determine Chl *a* (see Chapter 2). On the Sylt, Eden and Yerseke sites, Fo^{15} measurements were made on each replicate prior to contact coring. Fluorescence measurements were made within a dark adaption chamber (same area as the contact corer), which was placed on the sediment surface for a period of 15 minutes dark adaption. On the Eden and Yerseke sites, sub-replicates of fluorescence measurements were made within each dark adaption chamber. Thus comparisons of Chl *a* concentration and Fo^{15} measurements were made on a large spatial scale. During the synoptic measurements on the Sylt and Eden locations, FMS2 measurements were made on every other transect, the remaining transects were measured using the PAM2000. Therefore complete coverage of the synoptic grids using Fo^{15} could be made after intercalibration (from mesoscale measurements) of the PAM2000 into FMS2 values (BIOPTIS final report).

5.3. The comparison and calibration of two fluorometers

5.3.1. Introduction

A comparison between 2 pulse amplitude modulated fluorometers (Hansatech FMS2 and Walz PAM2000) was made on various types of algae *in situ*, from three locations across Europe. This study was a continuation of a comparison of laboratory microalgal monocultures (Forster *et al.*, in prep). An excellent, though varying (with different taxonomic groups of algae) relationship was found between Fo^{15} of the different fluorometers in this previous study. This present fluorometer comparison of microphytobenthos *in situ* was made to test the applicability of the previous laboratory findings to field measurements.

5.3.2. Results

5.3.2.1. The comparison of instruments

Values of Fo^{15} from the FMS2 and the PAM2000 fluorometers from all the sites and locations were compared and had a strong positive relationship (Spearmans Rank correlation, r_s = 0.876, n= 1308, P <0.001; Fig. 5.2A). However, data was heavily skewed towards the low values, and there was much uneven scatter (Fig. 5.2A and B). Data was grouped into type of algae/sites for further analysis. Grouping by different algae was only relevant for Eden sites, the Sylt data were from sandy sediments with very little visible algae and was thus pooled (Fig. 5.3A; Table 5.1). Data from the 3 Yerseke grids were quite similar, although grid B had a slightly different relationship between instruments than A and C (Fig. 5.3B; Table 5.1). Eden data included several types of algae and a sandier site, which were kept separate as each situation gave a slightly different calibration relationships (Fig. 5.4A and B). Correlations between instruments of different groups of algae or sites were made and were all strongly significant (Table 5.1), further details of the gradients of the relationship between instruments, with each set of data are discussed in the following sections.

5.3.2.2. The calibration of PAM2000 to FMS2 Fo^{15} values

During the extensive synoptic mapping, only half of the Fo^{15} measurements were made with each instrument, therefore a conversion factor was calculated to determine FMS2 Fo^{15} values from the PAM2000 Fo^{15} measurements to provide

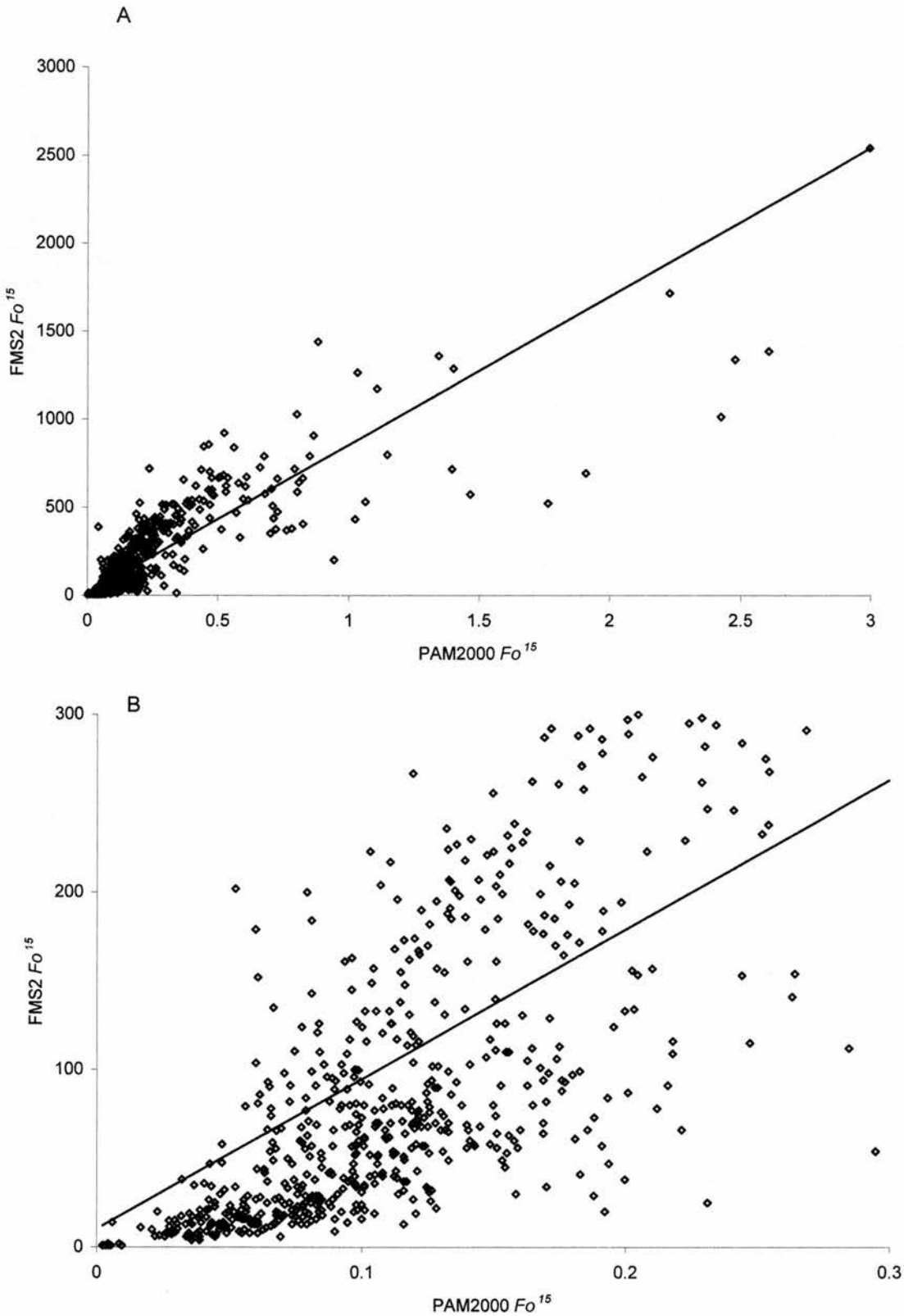

Figure 5.2. The relationship of Fo^{15} values between the FMS2 and the PAM2000. Data from all three campaigns in the Sylt Rømø Basin, the Eden Estuary and Yerseke sites. A) All data. B) Low value data. Regression lines are also plotted on both figures for all data

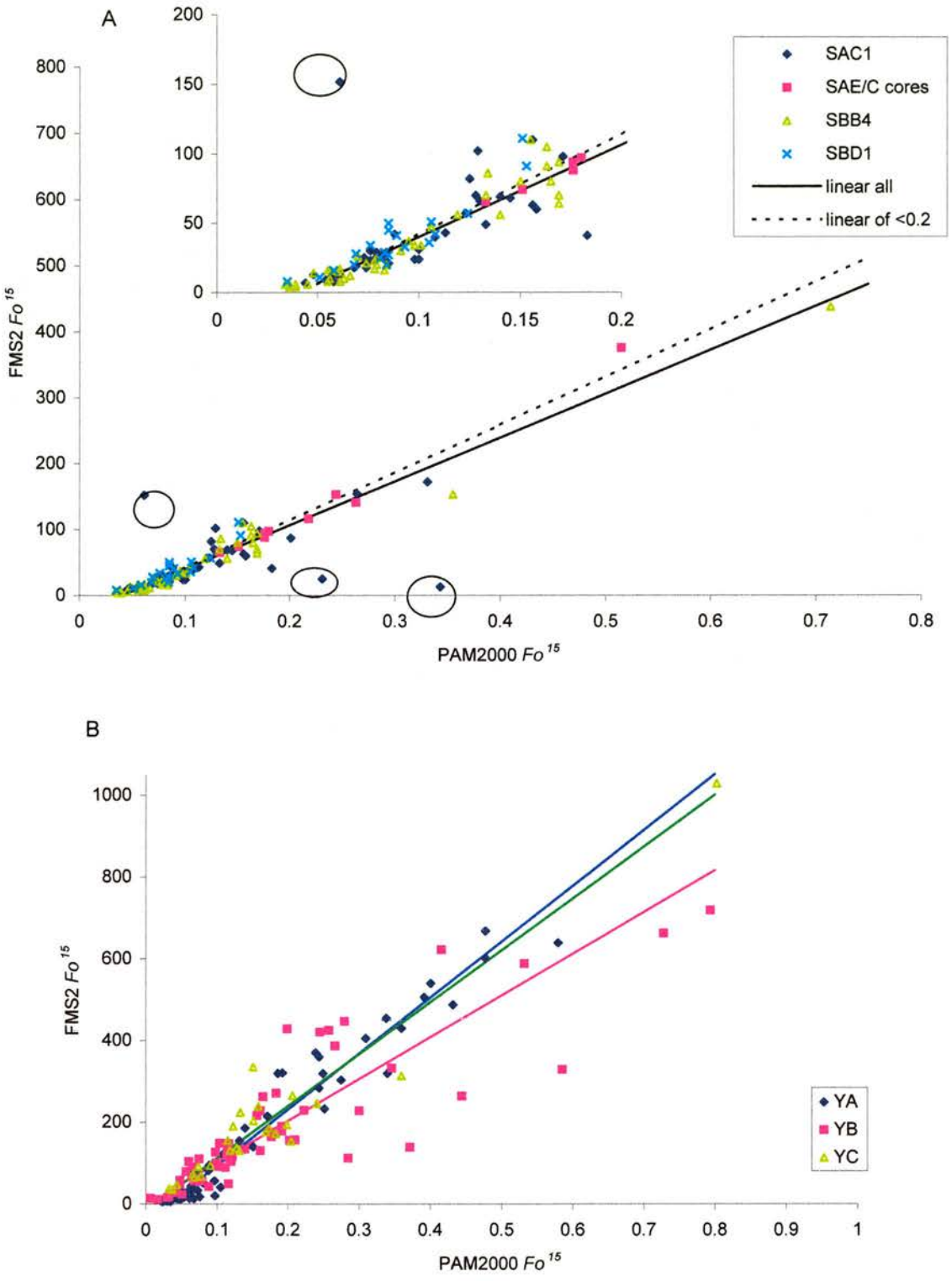

Figure 5.3. The relationship of Fo^{15} values between the FMS2 and the PAM2000. A) All Sylt Rømø Basin data; inset = low value data detail. Regression lines are also plotted on both figures for all data (solid) and for low value data below PAM200 Fo^{15} values of 0.2 (dotted), circled data points were classed as outliers. B) All Yerseke sites with respective regression lines for each grid

Table 5.1. Correlation and regression statistics of the relationship between PAM2000 and FMS2 Fo^{15} values for all the BIOPTIS campaign sites; all correlations and regressions are very highly significant ($p < 0.001$). * = data used for instrument calibration; N/A = not applicable

Data set	Site/samples (values are PAM2000 Fo^{15})	Range (PAM2000 Fo^{15})	n	Spearmans rank correlation coefficient	Model 2 regression coefficients	
					Slope	Intercept
All	Data from all three campaigns pooled	0.002 to 2.997	764	0.858	843.0	10.2
* All Sylt (no out.)	All Sylt data from grids SA and SB without outliers	0.03 to 0.714	116	0.955	677.8	-26.7
Sylt (low no out.)	SA and SB values below 0.2 data without outliers	0.03 to 0.183	107	0.945	722.2	-30.3
All Yerseke	All following YA, YB and YC data sets pooled	0.006 to 0.8	152	0.907	1197.3	-22.0
YA and YC	Yerseke grids YA and YC pooled	0.02 to 0.8	95	0.941	1341.8	-35.3
YA	Grids YA	0.02 to 0.6	69	0.908	1366.1	-41.9
YB	Grids YB	0.006 to 0.8	57	0.872	1020.5	-0.4
* YB low	Grids YB values lower than 0.15	0.006 to 0.16	31	0.799	1297.8	-23.1
YC	Grids YC	0.03 to 0.8	26	0.862	1269.6	-14.6
All Eden	All following Eden data sets pooled	0.002 to 2.997	493	0.838	803.7	25.9
* E1AE8 (Ent.)	Node E1AE8 samples just containing *Enteromorpha*	0.06 to 2.997	55	0.933	815.0	91.9
E1AE8 (Ent. low)	Node E1AE8 samples < 1.0 containing *Enteromorpha*	0.06 to 0.85	49	0.906	844.6	83.2
E1AE8 (Por.)	Node E1AE8 samples just containing *Porphyra*	0.218 to 2.6	15	0.925	513.3	-93.8
E1AE8 (n.m.)	Node E1AE8 samples containing no macroalgae	0.039 to 0.598	155	0.878	1341.1	5.8
E1BB4 (diat.)	Node E1BB4 samples just containing diatoms	0.026 to 1.033	40	0.852	1333.2	-53.1
* E1 AE8 + BB4 (sed+diat.)	Nodes E1AE8 samples containing no macroalgae and E1BB4 just samples containing diatoms pooled	0.026 to 1.03	195	0.903	1263.3	10.7
E1 AE8 + BB4 (sed+diat.) low and rec.	Values below 0.7 from above data set, but randomly reconstructed (see text)	0.026 to 0.667	78	0.904	1351.5	-21.4
E1BB4 (b.g. +diat. –1 out.)	Node E1BB4 samples containing a mixture of cyanobacteria and diatoms with one outlier removed	0.026 to 0.221	59	0.823	454.3	-12.1
E1BB4 (b.g. –1 out)	Node E1BB4 samples containing cyanobacteria with one outlier removed	0.038 to 0.295	55	0.821	511.0	-22.6
E1 AB1 and AC1	Nodes E1 AB1 and AC1	0.065 to 0.2	80	0.729	756.1	-13.0
* E1C	Grid E1C	0.002 to 0.101	32	0.927	498.3	-2.1

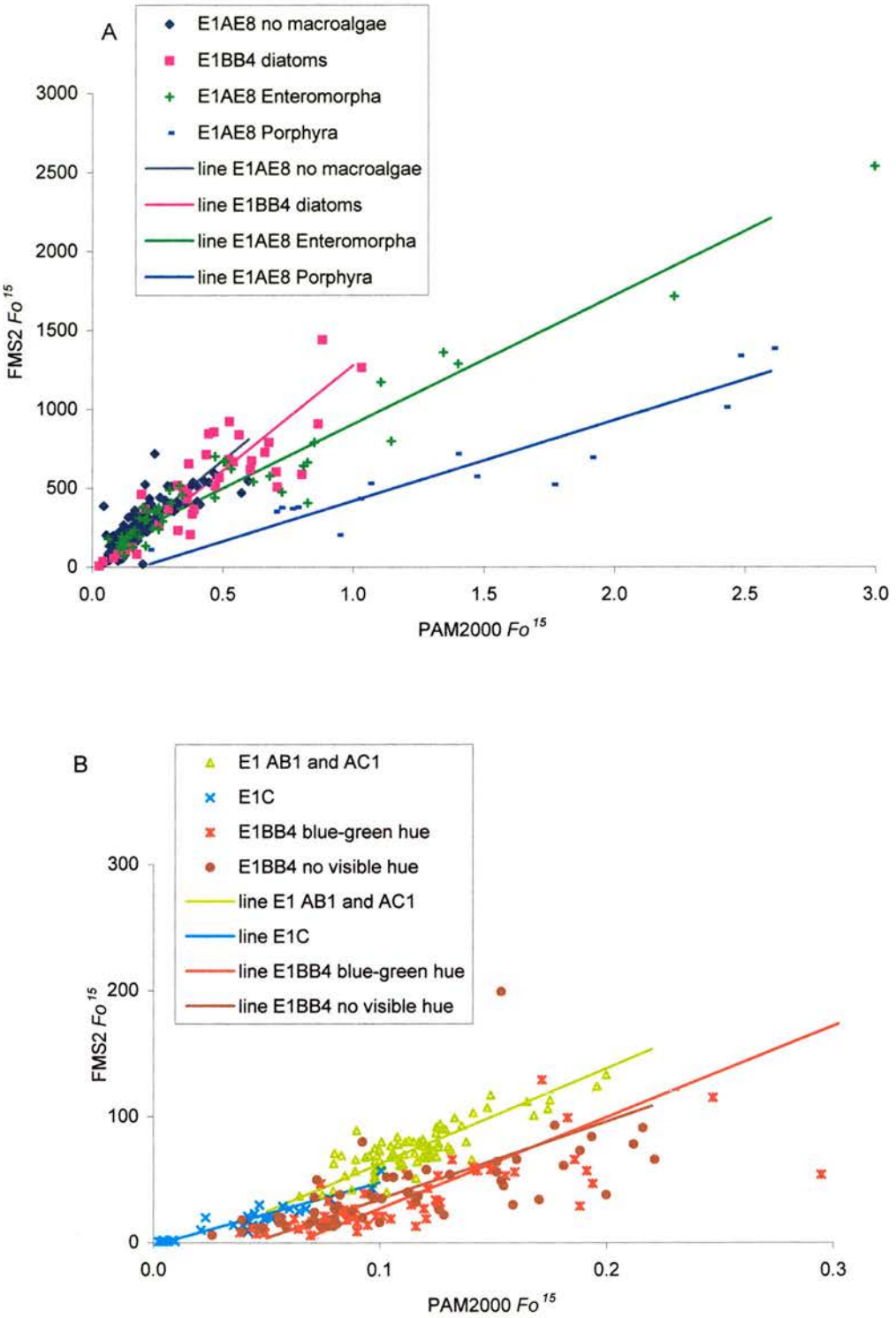

Figure 5.4. The relationship of Fo^{15} values between the FMS2 and the PAM2000. Data from the Eden Estuary sites. A) Data from samples which had Fo^{15} values ranging > 0.5. B) Data from samples which had Fo^{15} values < 0.3. Regression lines are also plotted for each set of data

complete coverage of grids. Once it had been determined that there was a good correlation of Fo^{15} measurements between the 2 instruments, a conversion factor was resolved for each data set using coefficients from linear regression analysis (see above and Table 5.1). Model 2 regression analysis (reduced major axis regression; Fowler and Cohen 1990) was used to convert PAM2000 Fo^{15} readings into FMS2 Fo^{15} values, as both were independent variables.

5.3.2.2.a. Sylt

There was a similar relationship between fluorometer Fo^{15} measurements on all the Sylt mesoscale sites (Fig. 5.3A), therefore data was pooled for inter-instrument comparisons. The Sylt data set had a few outliers (3 circled data points; Fig.5.3A). These outliers were identified as having residuals above 100, when the rest of the data had an even spread of residuals below 60. These outliers were re-measured the following day by collecting cores from the same sites. These re-measured sites followed the same slope as the majority of data. Thus these outliers were removed before further analysis. One of the assumptions of regression analysis is that data is evenly spread along the range measured. This assumption was not met because there were only a few data points at high Fo^{15} values (above PAM2000 Fo^{15} values over 0.2). Data was thus analysed before (all Sylt data set) and after removal of high data points (Sylt, no low data set). This latter data set had readings below PAM2000 Fo^{15} values of 0.2 removed (Table 5.1, Fig. 5.3A inset). Both these data sets had similar regression coefficients (slope and intercept) whether high data points were included or not. Therefore the calibration was reliable up to PAM2000 Fo^{15} values of 0.2. PAM2000 Fo^{15} values between 0.2 and 0.5 must be used with caution, although the relation appeared robust. There were however, only a few synoptic readings above 0.2 (PAM2000 Fo^{15}) which needed calibrating to FMS2 values. The regression equation used for the calibration of Sylt PAM2000 Fo^{15} measurements to FMS2 values (Fig. 5.5A) included high values but excluded outliers;

$$\text{FMS2 } Fo^{15} = (677.8 * [\text{PAM } Fo^{15}]) - 26.7 \qquad \text{Equation 5.1}$$

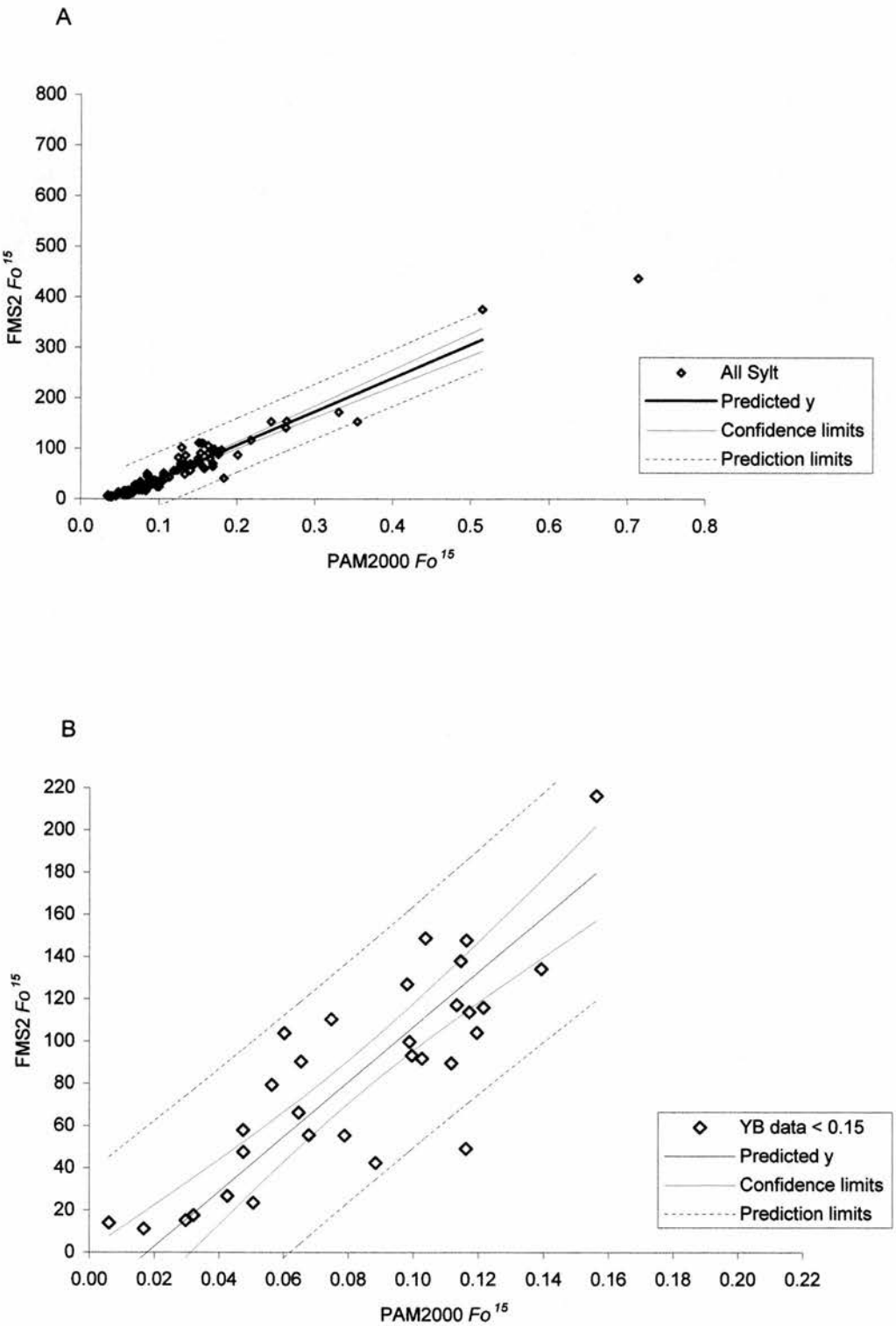

Figure 5.5. The relationship of Fo^{15} values between the FMS2 and the PAM2000. Prediction and confidence limits are also shown. A) Sylt Rømø Basin data with 3 outliers removed. B) Yerseke grid B data below PAM2000 Fo^{15} values of 0.15

5.3.2.2.b. Yerseke

The Fo^{15} measurements made on the Yerseke grid A and grid C sites had similar regression slopes between instruments, grid B however had a shallower slope (Fig. 5.3B; Table 5.1). Conversion of PAM2000 Fo^{15} measurements to FMS2 values was only necessary on grid B, as full coverage of grids A and C were made with the FMS2. Paired instrument measurements from grid YB was heavily skewed towards the low values (Fig. 5.3B). However, only PAM2000 Fo^{15} values below 0.15 needed correcting to FMS2. Paired instrument measurements below this value were normally distributed (PAM data R = 0.978, FMS data R = 0.98; both $P > 0.1$), therefore regression analysis could be confidently applied to PAM2000 data under 0.15. The regression equation used for the calibration of Yerseke grid B PAM2000 Fo^{15} values below 0.15 was (Fig.5.5B):

$$\text{FMS2 } Fo^{15} = (1297.8 * [\text{PAM } Fo^{15}]) - 23.1 \qquad \text{Equation 5.2}$$

5.3.2.2.c. Eden

Samples from the Eden were grouped by type of alga or site as they each produced a different calibration relationship between these instruments (Fig.5.4A and B). Samples which contained *Porphyra* clearly showed shallower slopes than samples containing diatoms (Fig.5.4A) as did samples containing cyanobacteria (visually indicated by blue-green hue, Fig. 5.4B; Table 5.1). Regression lines and coefficients for *Porphyra* or cyanobacteria are shown for interest, but conversion was not necessary, as synoptic samples which were visually identified as containing these algae were measured with the FMS2. PAM2000 measurements which needed calibration with FMS2 values were those containing *Enteromorpha*; sediment and diatoms; or grid C sand.

There were insufficient samples containing *Enteromorpha* for reliable instrument calibration, as correction of PAM2000 Fo^{15} values below 2 were necessary (Fig. 5.6A). Regression analysis was performed as a tentative indication of the relationship between the two instruments for this alga (Fig. 5.6B). The equation used for tentative prediction of FMS2 values from PAM2000 *Enteromorpha* Fo^{15} measurements was;

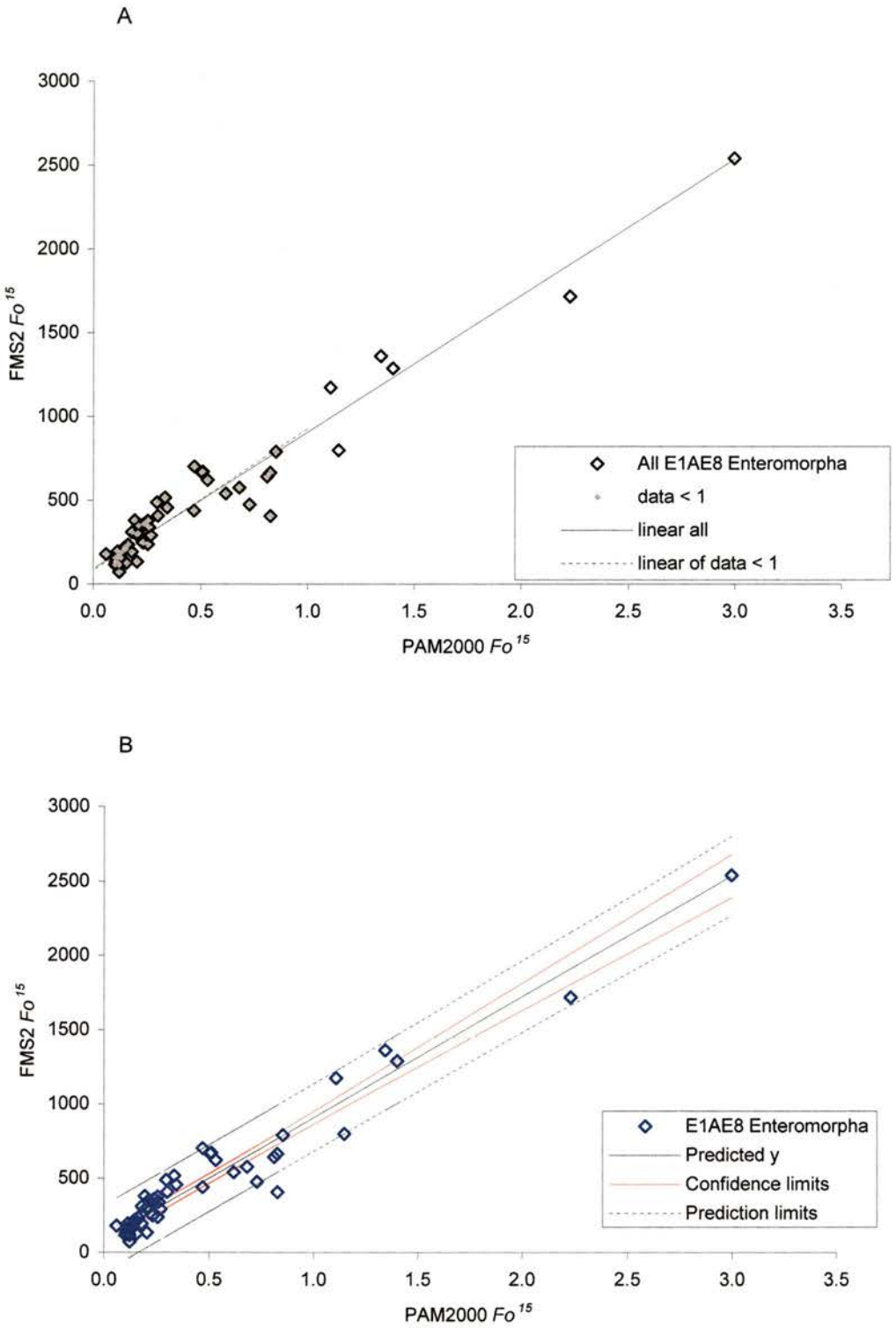

Figure 5.6. The relationship of Fo^{15} values between the FMS2 and the PAM2000. *Enteromorpha* data from the Eden Estuary. A) Regression lines through all data (solid line) and through data < 1 (PAM2000 Fo^{15} value). B) Prediction and confidence limits around the regression of all *Enteromorpha* data

$$\text{FMS2 } Fo^{15} = (815.0 * [\text{PAM } Fo^{15}]) + 91.9 \qquad \text{Equation 5.3}$$

There was a very strong correlation of Fo^{15} between instruments on Eden Grid C data (Fig. 5.7). These samples were all sandy sediment of low biomass and all PAM2000 Fo^{15} values to be corrected were within the range of the calibration data. The calibration data also showed a nearly normal distribution of PAM data ($R = 0.954$, $P < 0.02$) and normal distribution of FMS2 data ($R = 0.979$, $P > 0.1$). Thus regression analysis could be confidently used for prediction (Fig. 5.7). The equation used for the correction of PAM2000 Fo^{15} measurements to FMS2 values for grid C data was;

$$\text{FMS2 } Fo^{15} = (498.3 * [\text{PAM } Fo^{15}]) - 2.1 \qquad \text{Equation 5.4}$$

The remaining sites were from fine sediments with varying amounts of microphytobenthos (mainly diatoms) and were again heavily skewed towards the low values. Regression relationships between the instruments from Eden mesoscale grids E1AE8 and E1BB4 (diatoms) had a similar slope (Fig. 5.4A; Table 5.1) and were thus pooled to give a larger range of Fo^{15} values. Only PAM2000 values below 0.7 needed correction. Therefore higher values from the instrument calibration were removed. This left data which was still heavily skewed to the lower values (Fig. 5.8A). To gain a normal distribution of the remaining data, and thus reliable predictive capacity, low values were randomly reconstructed. Data were reconstructed (every other point of ranked data removed) until near normal distribution was obtained (PAM $R = 0.979$, $P < 0.05$; FMS $R = 0.984$, $P > 0.05$). Regression analysis was then performed on both the complete set of data and the reconstructed set of data. There was very little difference (in slope and intercept) between both sets of data (Table 5.1). Thus indicating the prediction was robust when all calibration data was used. The regression statistics for the whole set of data (below 0.7) were used for prediction of PAM2000 Fo^{15} measurements to FMS2 values of fine sediment and diatoms (Fig. 5.8B), and was;

$$\text{FMS2 } Fo^{15} = (1263.3 * [\text{PAM } Fo^{15}]) + 10.7 \qquad \text{Equation 5.5}$$

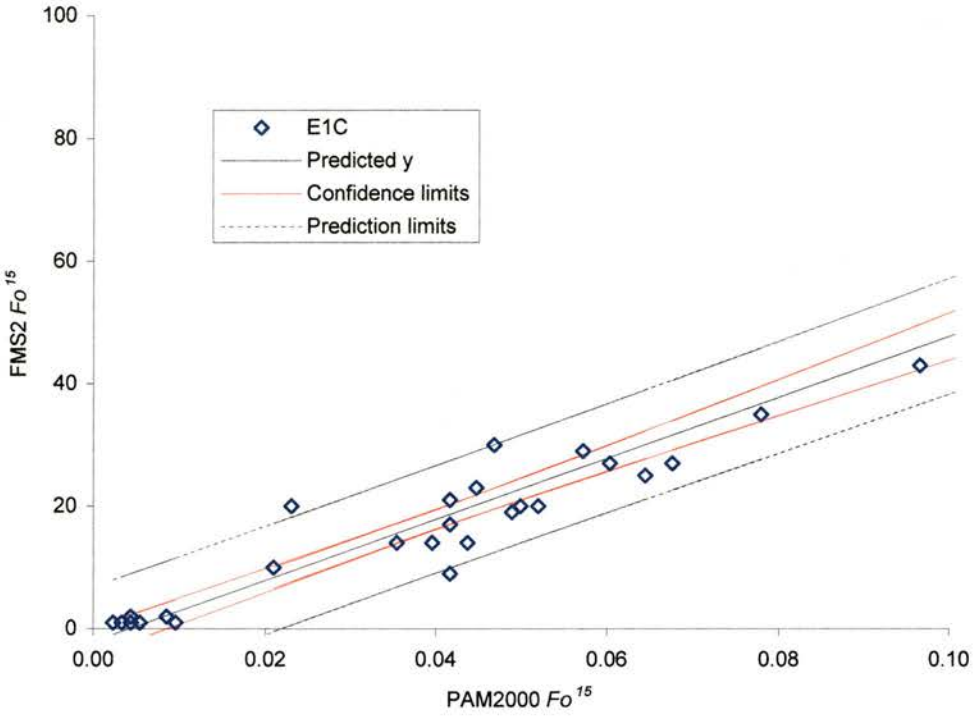

Figure 5.7. The relationship of Fo^{15} values between the FMS2 and the PAM2000. Data from grid C, the Eden Estuary. Regression line with prediction and confidence limits are shown

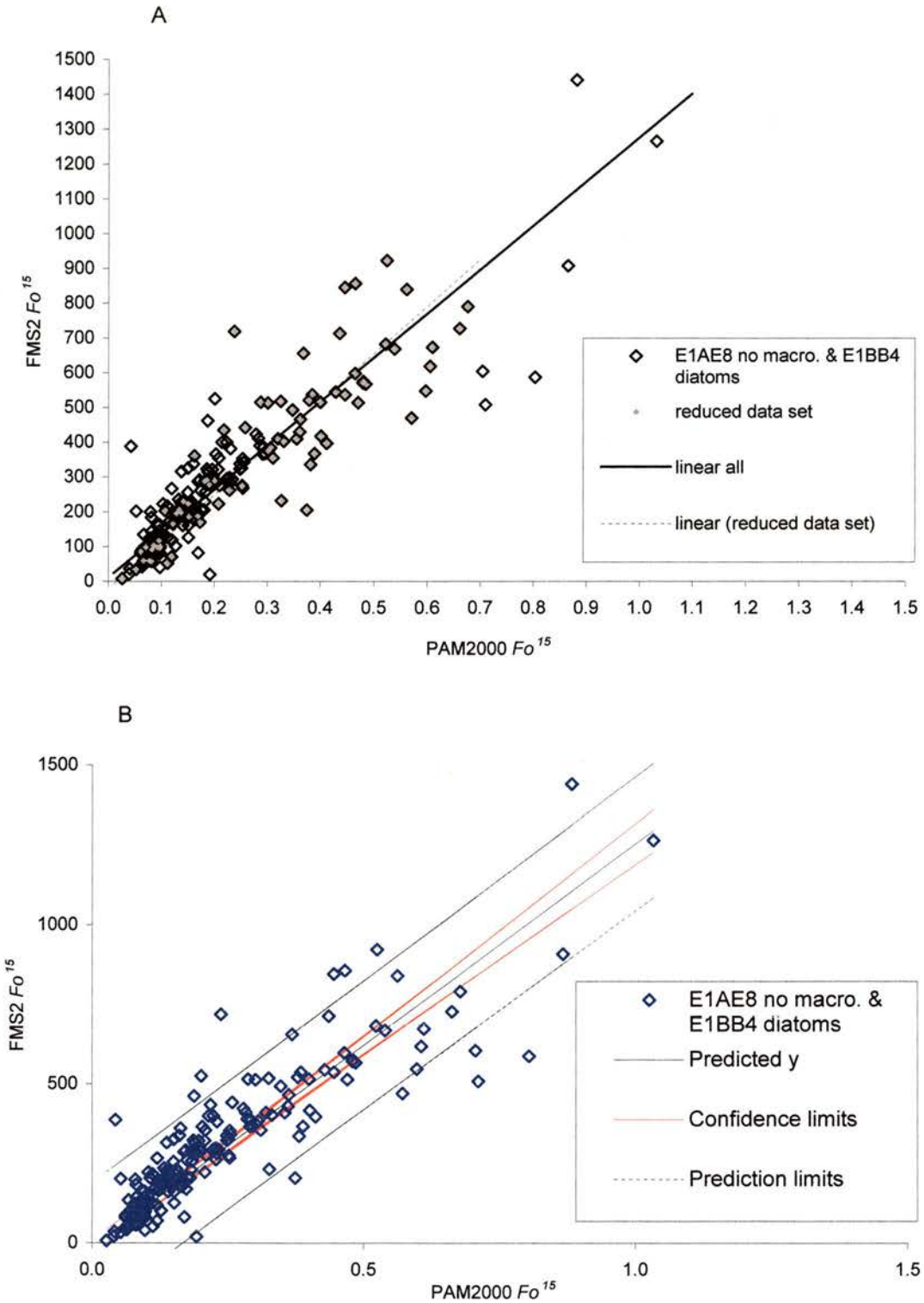

Figure 5.8. The relationship of Fo^{15} values between the FMS2 and the PAM2000. Data from the Eden Estuary, samples with no macroalgae (macro.) and no visible cyanobacteria (E1AE8 no macroalgae and E1BB4 diatoms data sets). A) Regression lines through all data (solid line) and reconstructed data set of values data below PAM2000 Fo^{15} values of 0.7; there was very little difference in regression slopes between the two. B) Prediction and confidence limits around the linear regression

5.3.2.2.d. Comparison of all sites

It was not possible to statistically compare regression slopes for different algae or samples, as Fo^{15} values were not always within the same range for each set of data (Table 5.1) neither did they all meet the assumptions for reliable regression analysis. However the general linear trends (Figures 5.9A and B) showed that fine sediment and diatoms (E1AE8 no macroalgae, E1BB4 diatoms and Yerseke samples) had steeper slopes between instruments than *Porphyra,* cyanobacteria (Eden) and sandy sediments (E1C and Sylt). The *Enteromorpha* slope between instruments was similar to the diatom slope, but was a little shallower.

5.3.3. Discussion

This study established that measurements in the field using Fo^{15} values obtained from different kinds of algae, or different habitats can give contrasting results from different instruments. Each instrument varies in its sensitivity of response to different algae. The reason for this was the different wavelength of the respective excitation beam (also termed measuring lights; ML). Excitation beams of different wavelengths are optimal for excitation of different groups of algae (Schreiber *et al.*, 1993; Büchel & Wilhelm, 1993). The FMS2 has a blue (470 nm) measuring light and the PAM2000 has a red (650 nm) measuring light. The major groups of algae have different excitation spectra for Chl *a* fluorescence because of the varied accessory pigments complexes in the antennae systems. A blue ML will induce optimal fluorescence from the diatoms and green algae. A red ML induces optimal fluorescence from the cyanobacteria, although diatoms and green algae will also fluoresce, but to a lesser extent than under a blue ML (Yentsch & Yentsch, 1979).

Previous studies also showed a wider range of Fo^{15} measurement from cyanobacteria when using a red ML (PAM2000) than with a blue ML (FMS2) (Forster *et al.*, in prep.). This was highlighted by a shallower regression slope when the FMS2 Fo^{15} data is plotted against the PAM2000 data. The opposite was found when samples were dominated by diatoms. The selective measurement of different algae with different colour ML confounds the Chl *a* to Fo^{15} relationship. However using a combination of different colour ML could lead to useful identification, in a mixed sample, of the source of Chl *a* biomass in terms of algae type. Indeed an instrument has recently been developed to selectively measure the response of a single type of algae in a mixed sample (Schreiber, 2000). These instruments are at present

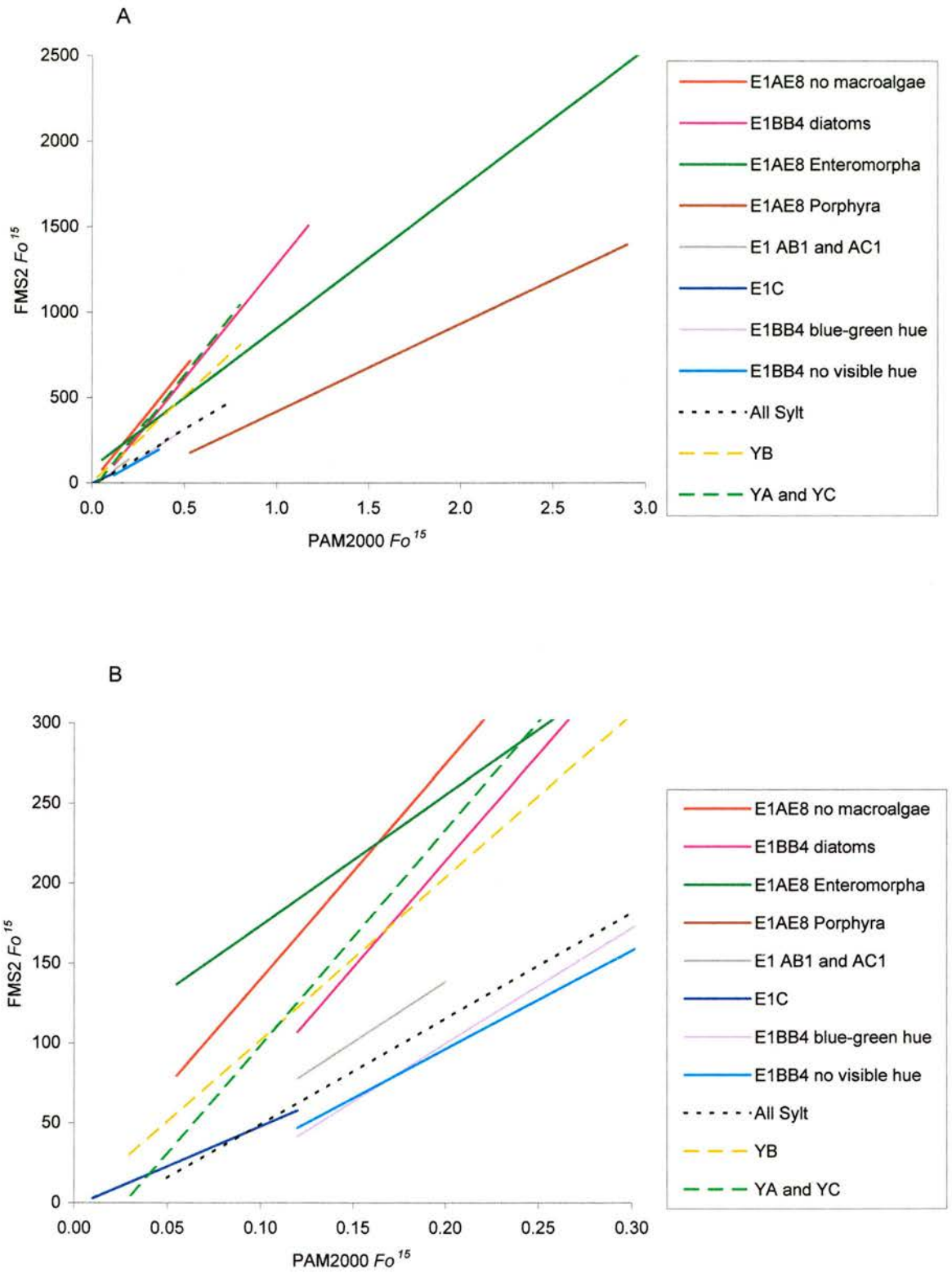

Figure 5.9. The relationship of Fo^{15} values between the FMS2 and the PAM2000. Regression lines of data from all field campaigns in The Sylt Rømø Basin (Sylt), Eden Estuary (samples number prefixed with E1) and from the Yerseke sites (prefixed with Y). A) All regression lines. B) Portion of figure A to show lower value detail

designed for phytoplankton samples in a cuvette and, although data is as yet unpublished, have shown promising results (Schreiber, 2000).

5.4. The relationship between Chl *a* and Fo^{15} on a large scale

5.4.1. Introduction

Previous studies have shown a correlation between Chl *a* content or concentration of the surface sediment and the fluorescence parameter *Fo* or Fo^{15} (Serôdio *et al.*, 1997; Barranguet *et al.*, 1998; Chapter 4). During campaigns surveying three intertidal areas in Northern Europe, Fo^{15} and Chl *a* concentration of the surface sediment were measured. This was to assess the spatial distribution of the surface microphytobenthos biomass, and to ground truth airborne remote sensing data (BIOPTIS final report). Paired Fo^{15} and Chl *a* concentration measurements were made on a large spatial scale (within and between intertidal areas) to encompass a variety of intertidal sediments, to extend the range of sample types of the relationship found in Chapter 4.

Previous comparisons between Chl *a* and Fo^{15} revealed a stronger relationship with decreasing Chl *a* sampling depth, which was due to the depth (0.2 mm) of sediment sampled for Chl *a* measurements becoming closer to the depth of Fo^{15} detection (Chapter 4). It has also been determined that Fo^{15} did not change significantly during 4 hours prior to tidal emersion in comparison to its peak value for the period (see Chapter 7).

The previous relationship found between Chl *a* and Fo^{15} (Chapter 4) was used as an indication of diatom biomass and was compared to the Chl *a* and Fo^{15} data measured during this study.

5.4.2. Materials and Methods

See above for general materials and methods of sampling (Section 5.2).

Paired Chl *a* and Fo^{15} measurements were made during the synoptic and mesoscale BIOPTIS field campaign surveys. Chl *a* was measured in the surface sediment as a proxy for phyto-biomass. Samples for Chl *a* analysis were collected using the contact corer which sampled approximately the surface 2 mm of sediment. FMS2 Fo^{15} data was used for comparison with Chl *a*, to decrease any variation and error, which may have been incorporated during PAM2000 to FMS2 calibration.

The previous comparisons between Chl *a* and Fo^{15} (Chapter 4) were made on samples of similar size. This study however compares Chl *a* and Fo^{15} in deeper samples (contact cores), which were sampled during the whole emersion period and of different measurement areas (Chl *a* concentration was determined from contact cores of sample area 2550 mm^2 whereas Fo^{15} was determined from 120 mm^2 measurement area). During the Sylt campaign only one Fo^{15} measurement per contact core was made, thus the comparative area for the two measurements was very different. An improvement of the relative measurement areas was made in the subsequent campaigns by increasing the Fo^{15} measurements within the contact core area. Thus during the Eden campaign, 3 (synoptic) and 4 (mesoscale) Fo^{15} measurements per contact core were made which was further increased to 5 during the Yerseke campaign.

5.4.3. Results

5.4.3.1. Sylt

All Sylt samples grouped together, showed no significant relationship between Chl *a* concentration and Fo^{15} measurements ($P > 0.05$; Table 5.2; Fig. 5.10). Grid SB was the only grid which showed a significant relationship between Chl *a* concentration and Fo^{15} measurements ($P < 0.001$; see Table 5.2). At the low shore on grid SB, there were diatom biofilms, specifically on nodes SBA8 and SBC8, these fell on a previously predicted line between biomass and Fo^{15} (Chapter 4 model) and are circled on the graph (Fig. 5.10). Most of the Sylt data points were above the previously predicted line, indicating high Chl *a* concentration with low Fo^{15} measurements. Measurements from Grid SA tended to fall below the predicted line especially SAG1 and SAE1 which were sites very high in the tidal zone.

5.4.3.2. Eden

Overall, Eden samples showed a strong significant relationship between Chl *a* concentration and Fo^{15} measurements ($P < 0.001$, Table 5.2) but also showed a great amount of scatter (Fig. 5.11). However, this included samples visually identified as containing cyanobacteria. Samples containing cyanobacteria were mostly from the mesoscale study at E1BB4, where obvious patches of blue-green hue were sampled and compared to nearby patches with a golden brown hue and an area with no

Table 5.2. Correlation between Fo^{15} and chlorophyll a over a large scale, both between and within intertidal sediment areas

Location and Grid	n	r_s value (Spearmans rank)	P value	Regression coefficients		
				Slope	Intercept	R^2
Previous relationship (Chapter 4)				*0.232*	*9.55*	
All Sylt grids	159	0.212	> 0.05		No analysis	
Sylt A	36	0.165	> 0.1		No analysis	
Sylt B	66	0.539	< 0.001		No analysis	
Sylt C	14	0.488	> 0.05		No analysis	
All Eden	227	0.378	< 0.001		No analysis	
All Eden grids with no Cyanobacteria with low Fo	115	0.822	< 0.001	0.269	13.84	0.604
All Yerseke grids	147	0.761	< 0.001	0.287	7.79	0.577
Yerseke A	78	0.698	< 0.001	0.227	8.00	0.715
Yerseke B	40	0.664	< 0.001	0.324	22.10	0.645
Yerseke C	29	0.603	= 0.001	0.416	-18.80	0.267

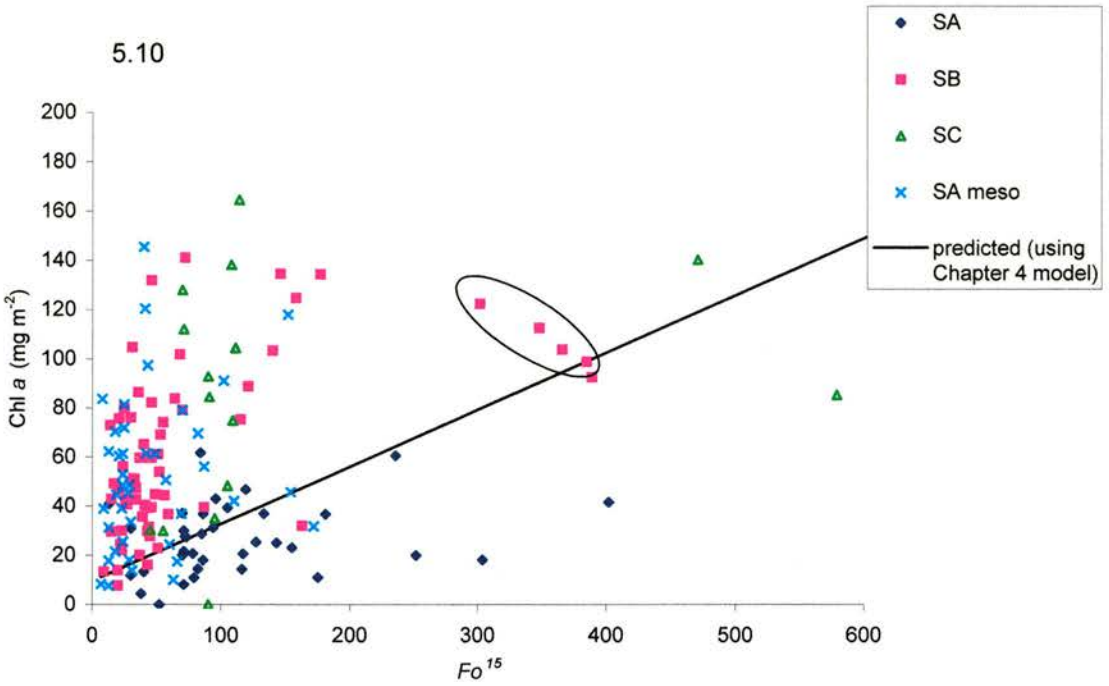

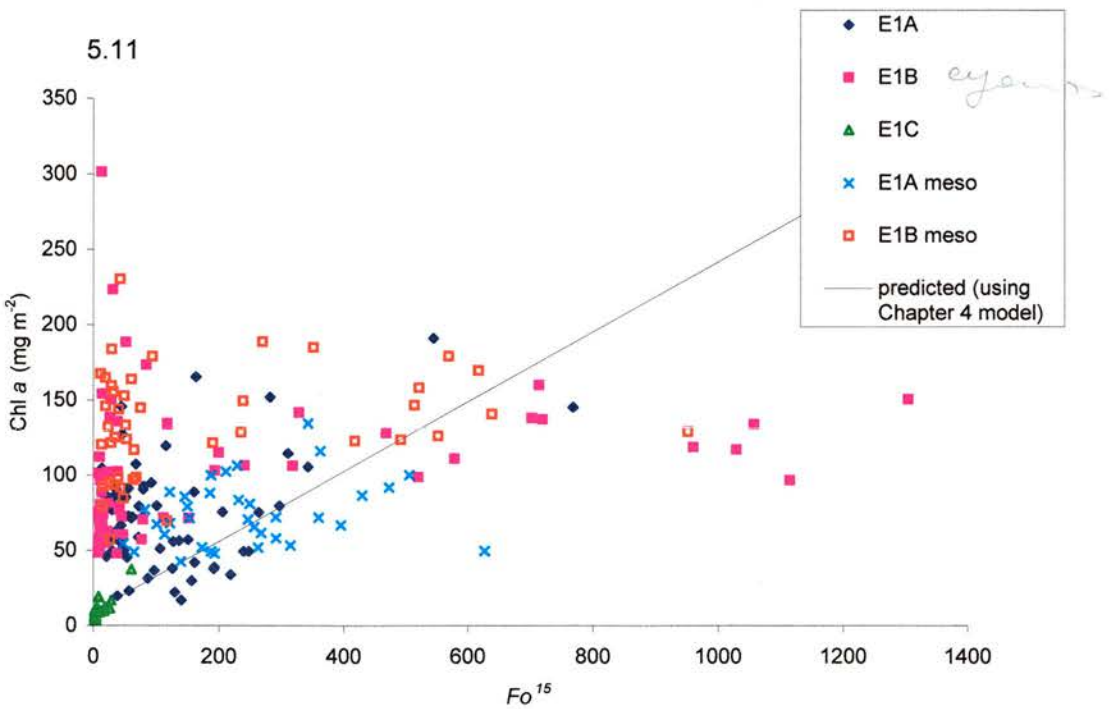

Figures 5.10 and **5.11**. The relationship between FMS2 Fo^{15} and Chl *a* concentration in approximately the surface 2 mm of sediment. **5.10**. Data from all Sylt Rømø basin grids, May-June 1999. The 4 circled data points indicate the only samples with visibly high diatom biofilms. **5.11**. Data from all Eden Estuary grids, August-September 1999

apparent coloration. This small study at node E1BB4 was analysed in detail before going on to analyse all Eden data.

5.4.3.2.a. Diatom and cyanobacterial fluorescence (node EIBB4)

Samples E1BB3, E1BB46 and E1BB49 had a visible surface golden brown coloration, typical of diatoms. Samples E1BB41, E1BB44 and E1BB47 had a visible blue-green hue, typical of cyanobacteria. Samples E1BB42, E1BB45 and E1BB48 had a no visible surface coloration. Samples were numbered as such due to the replicate scale (n = 5); E1BB41 to 3 were sampled at 20 cm lag replicates, E1BB44 to 6 were sampled at 100 cm lag replicates and E1BB47 to 9 were sampled at 500 cm lag replicates. All samples (except one) from the sites with a blue-green coloration and the sites with no coloration had a range of Chl *a* concentrations but had relatively low fluorescence signals (Fig. 5.12), with Fo^{15} values all below 100 (apart from 1 outlier). These mesoscale samples were also analysed for pigments using the HPLC. The samples with a visible blue-green hue showed similar Chl *a* concentrations to the other E1BB4 sites (Fig.5.13A). The main diatom marker pigments, fucoxanthin and Chl *c*, were present in higher quantities on site with a brown hue (averages of 0.7 and 0.17 ratios to Chl *a*, respectively) than on site with a blue-green hue (averages of 0.47 and 0.11 ratios to Chl *a*, respectively) (Figs 5.13B and C). The secondary diatom marker pigments, diadinoxanthin and diatoxanthin were also present in higher quantities on site with a brown hue (averages of 0.21 and 0.025 ratios to Chl *a*, respectively) than the site with a blue-green hue (averages of 0.14 and 0.013 ratios to Chl *a*, respectively) (Figs 5.13D and E). Zeaxanthin, the marker pigments for cyanobacteria, was present in higher quantity (average of 0.1 ratio to Chl *a*) on the site with a blue-green hue than the site with a brown hue (average of 0.04 which included lutein ratio to Chl *a*) (Fig. 5.13F). The site with no visible coloration showed marker pigments (ratios of Chl *c*, fucoxanthin, diadinoxanthin and diatoxanthin to Chl *a*) similar to that of the blue-green site but with slightly less zeaxanthin (average of 0.07 ratio to Chl *a*) (Figs 5.13A to F).

The pigment fingerprints indicate the site with a blue-green hue had some diatoms present as well as cyanobacteria; the site with a brown hue had mainly diatoms present, with small amounts of cyanobacteria; and the site with no visible coloration had cyanobacteria and diatoms present. The Fo^{15} values for the blue-green and no visible coloration sites were quite similar and all below a value of 100 (apart

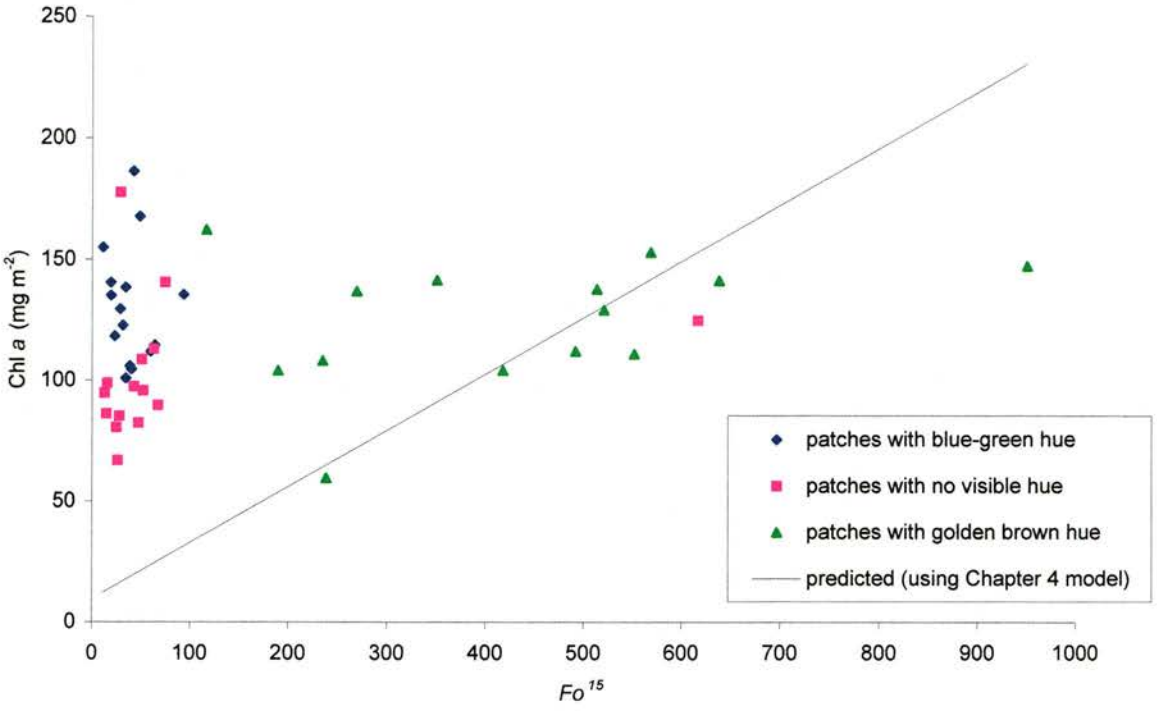

Figure 5.12. The relationship between FMS2 Fo^{15} and Chl *a* concentration in approximately the surface 2 mm of sediment. Data from the Eden Estuary node E1BB4, 1 September 1999. The colour of the patches were visually identified

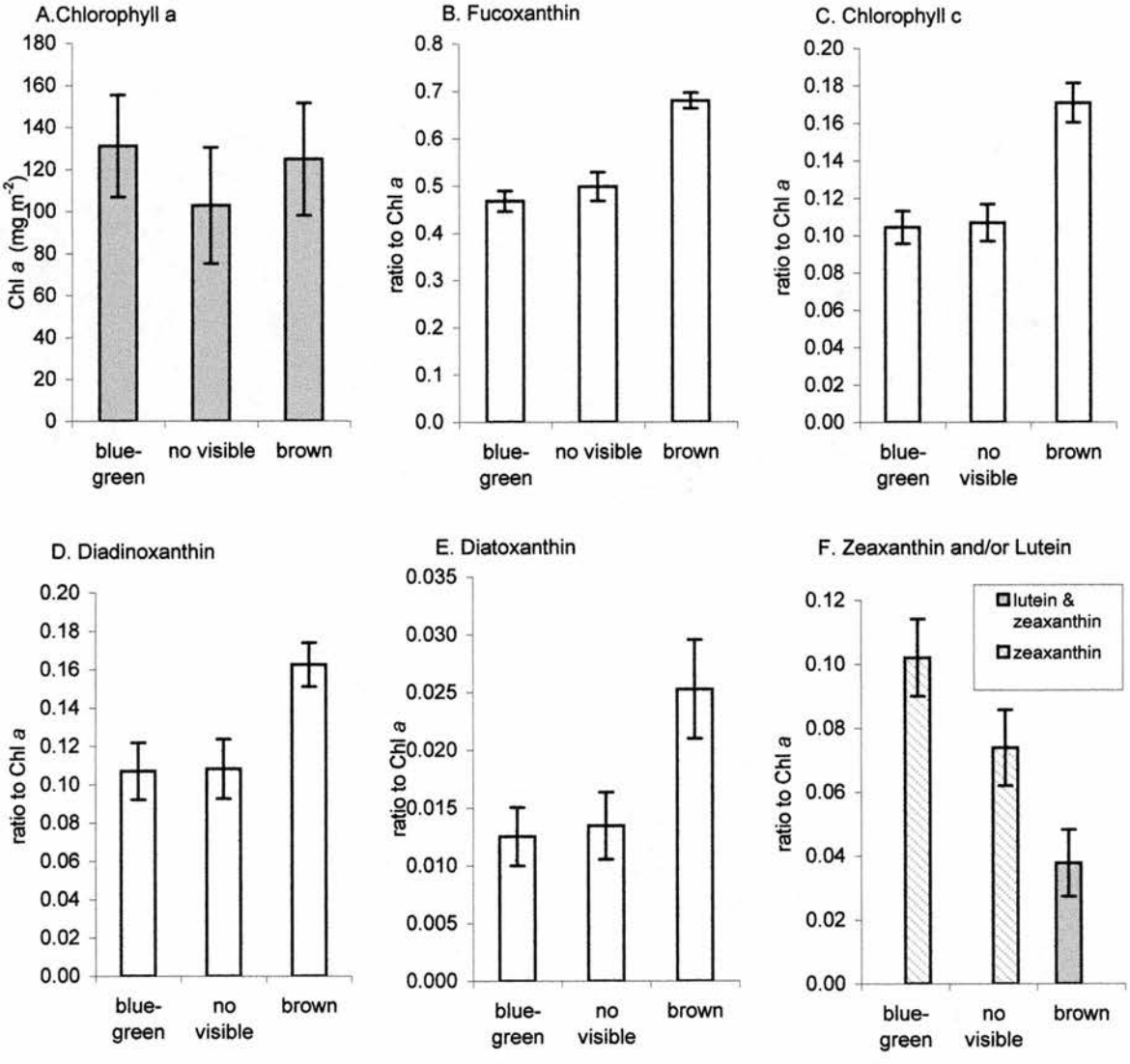

Figures 5.13. Pigments in approximately the surface 2 mm of sediment. Data from the Eden Estuary node E1BB4, 1 September 1999. Blue-green, no visible and brown indicate the visibly identified colour of the sediment surface. A) Chl *a* concentration. B) to F) Pigment ratios to Chl *a*. F) The filled bar indicates the sum of the lutein and zeaxanthin ratios to Chl *a*, as they were eluted next to each other and were not integrated separately. The hatch-filled bars indicate purely zeaxanthin ratios to Chl *a* (n = 3 to 5 +/-SD). Pigment ratios are in peak area of pigment:peak area of Chl *a* (at 430 nm)

from 1 outlier). Fo^{15} values on the brown site had higher values, ranging from 100 to over 600. This indicates that the relationship between Chl *a* and Fo^{15} was highly dependant on alga type. This implies that the samples from the Eden sites, which had a large range in Chl *a*, but very low Fo^{15} values may indicate a significant presence of cyanobacteria, even though a blue-green hue was not visible. From this E1BB4 study it was concluded that samples which had a high Chl concentration (> 40 mg m^{-2}) and low Fo^{15} values (< 100) were likely to be indicative of cyanobacteria.

5.4.3.2.b. All Eden sites

Eden data showed some samples with a large range in Chl *a*, but very low Fo^{15} values. The E1BB4 study concluded that these samples were likely to have has a significant presence of cyanobacteria. There were also 6 samples from the Eden Estuary which showed Fo^{15} values which were particularly high (above 900) for diatom biofilms and such levels had not been found in previous studies (Chapter 4 and 7). These samples also had relatively low Chl *a* concentration (~120 mg m^{-2}) when compared to a previous study (Chapter 4). These 6 samples were outliers from the remaining Eden samples (Fig. 5.11). For a comparison of Fo^{15} and Chl *a* concentration of diatom dominated microphytobenthos, samples which had a cyanobacteria presence or unusually high Fo^{15}, were removed from the data set (Fig. 5.14). The regression coefficients of the line was then calculated using Model 2 regression techniques (slope = 0.269, intercept = 13.8) and showed a statistically strong relationship ($P < 0.001$; Table 5.2). These coefficients were found to be similar to the regression coefficients from a previous study, which showed a good relationship between Fo^{15} and Chl *a* in 2 mm of sediment (Chapter 4, slope = 0.225 and intercept = 23.3). However, the gradient of the regression from the Eden was steeper than that of the previous study (Fig. 5.14).

5.4.3.3. Yerseke

Yerseke samples from all the grids showed a strong relationship between Chl *a* concentration and Fo^{15} measurements ($P < 0.001$, Table 5.2; Fig. 5.15). Grid YA was the only data which gave similar regression coefficients to the previous study, whilst grids YB and YC had steeper slopes (Chapter 4; Table 5.2; Fig. 5.15).

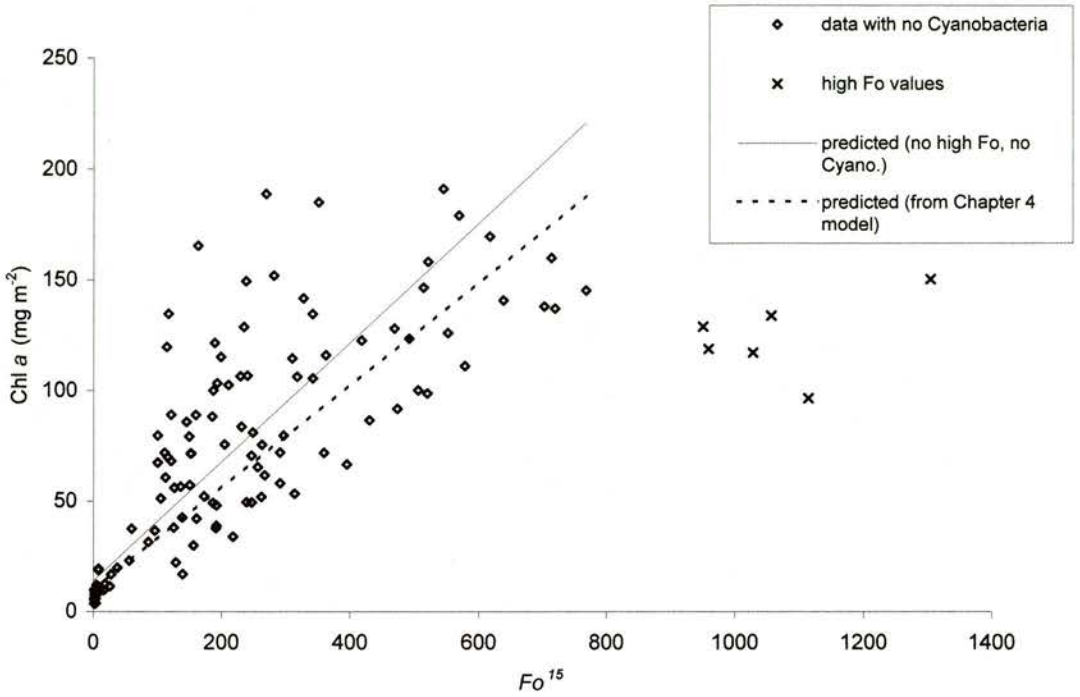

Figure 5.14. The relationship between FMS2 Fo^{15} and Chl *a* concentration in approximately the surface 2 mm of sediment. Data from all Eden Estuary grids with both high Fo^{15} values (crosses) and samples containing cyanobacteria (Cyano.) removed before regression analysed, August-September 1999

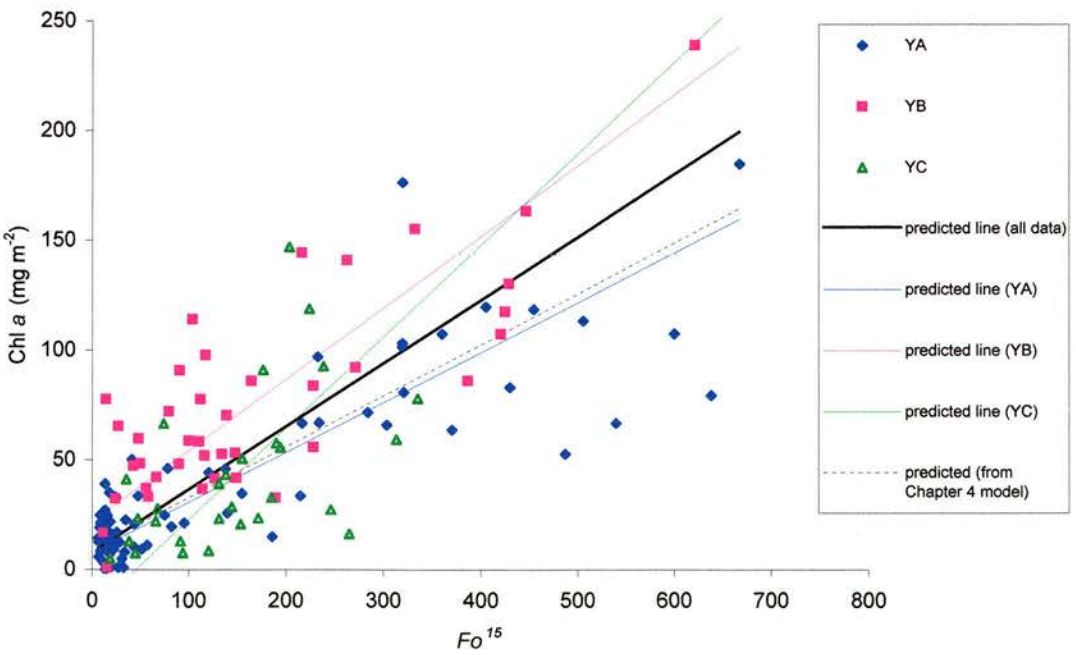

Figure 5.15. The relationship between FMS2 Fo^{15} and Chl *a* concentration in approximately the surface 2 mm of sediment. Data from all Yerseke grids (2 outliers removed), June 2000

5.4.3.4. All sites and locations

Some of the scatter around the line for predicting Chl *a* from Fo^{15} can be explained by the type of algae present in the sample. However, it was hypothesised that the increased variation around the prediction line may be further affected by the following factors:

- that samples measured in the last 4 hour of emersion would have a stronger relationship than those measured earlier in the exposure period, due to the migratory behaviour of the microphytobenthos (Chapter 7)
- a smaller sampling depth for Chl *a* (2 mm) would have a stronger relationship than deeper samples. (Contact core depth varied from 2 to 8 mm)
- greater replication of Fo^{15} measurements within a contact core would be more representative of the area sampled for Chl *a*

These hypotheses were tested by grouping samples by time after ebb, grouping by contact core depth or grouping by coefficients of variation of Fo^{15} within a contact core. Data hypothesised to increase variation were removed from data sets and re-correlated, i.e. samples taken within the first 3 hours after tidal ebb, cores deeper than 3 mm and cores with a highly variable internal coefficient of variation (CV) in Fo^{15} were removed. No stronger relationships were found after removal of these hypothesised variables.

5.4.4. Discussion

Cyanobacteria were found to have a weaker fluorescence signal than diatoms. Accordingly, cyanobacteria samples had a weaker Fo^{15} to Chl *a* relationship. The gradient of the relationship between Fo^{15} to Chl *a* from the Eden campaign was steeper than that of a previous study (Chapter 4), which might indicate a significant cyanobacterial presence in this study. Grids YB and YC had steeper gradients, which may also indicate cyanobacteria were present on these locations.

Generally, Chl *a* had a strong relationship with Fo^{15} on Eden and Yerseke sites, although there was a lot of scatter. Yerseke samples had scatter both above and below the predicted line from Chapter 4; i.e. both decreased and increased fluorescence to Chl *a* ratios. Eden scatter was mostly above the predicted line from Chapter 4; i.e. decreased fluorescence to Chl *a* ratios. Sylt samples had many samples

with decreased fluorescence to Chl *a* ratios, but also had and a few samples containing increased fluorescence to Chl *a* ratio.

5.4.4.1. Decreased fluorescence to Chl a ratios

The decrease in fluorescence to Chl *a* ratio can be partly explained by the presence of cyanobacteria, as the E1BB4 study showed (section 5.4.3.2.a). Cyanobacteria have a different pigment system (PSII antennae) than that of eucaryotes and exhibit only weak fluorescence from Chl *a* (Bryant, 1986; Sepälä & Balode, 1998). Thus the presence of cyanobacteria will decrease the fluorescence to Chl *a* ratio in a mixed sample. However, a decrease in fluorescence to Chl *a* ratio may also be due to non-photochemical quenching (NPQ). It is not known to what extent NPQ affects the fluorescence to Chl *a* ratio of microphytobenthos *in situ* (see Chapter 7 for further discussion of NPQ).

Sylt sites show, on the whole, a decreased fluorescence to Chl *a* ratio. These sites were dominated by sand, whereas cohesive sediments dominated all the Yerseke grids and Eden grids A and B. Sandy sites are likely to have different species composition than that of cohesive sediment habitats. Microalgae living in a sand habitat (epipsammon) may have a different fluorescence to Chl *a* ratio. Epipsammon are less motile (Round, 1981) and thus are unable to move away from damaging irradiances. Therefore they may have different photoprotective responses than species adapted to cohesive sediment habitats (epipelon).

Sylt sites pigments have not yet been analysed using HPLC, but results from spectrophotometry showed no Chl *b*, with some Chl *c* (BIOPTIS Database). The Chl *c* ratios to Chl *a* (weight ratio) of these samples were however approx. 0.2 and were no different than other SA samples, indicating diatom dominance.

5.4.4.2. Increased fluorescence to Chl a ratios

A few Eden samples had inexplicably high fluorescence to Chl *a* ratios, they were thus assumed to either contain non-organic fluorescing material or Chl *a* not bound to proteins. Some Sylt (grid A) and some Yerseke samples also showed increased fluorescence to Chl *a* ratios. High fluorescence to Chl *a* ratios may also indicate unhealthy biofilms, which may contain senescing algae, nutrient deficient algae (Kiefer, 1973a; Greene *et al*, 1994) or photo-damaged algae (Demers *et al.*, 1991). These factors were rejected, as *Fv/Fm* (a good indicator of stress or damage)

values for these samples were no lower than other samples, indicating a healthy assemblage.

5.4.5. Conclusions

Fluorescence was a reasonably good predictive tool of Chl *a* biomass from diatom dominated microalgae inhabiting cohesive sediments. However, the presence of cyanobacteria significantly altered the fluorescence to Chl *a* ratio relationship compared with diatoms. Therefore, pigment analysis or species identification is necessary to identify whether cyanobacteria are present. The use of single wavelength excitation beam fluorescence detection alone, as an indicator of biomass is therefore not viable on a large scale, without taxonomic safeguards.

5.5. The spatial distribution of Fo^{15}

5.5.1. Introduction

Microphytobenthos are renowned for having patchy distributions, on a variety of scales, in muddy estuaries numerous repetitions are needed to get representative values of biomass (MacIntyre *et al.,* 1996). MacIntyre *et al.* (1996) suggested that a minimum of 5 replicates was needed to reduce the CV of biomass to 45% in a 2500 cm^2 sampling area (25 x 12.6 cm^2 core area; MacIntyre *et al.,* 1996). The horizontal distribution of microphytobenthos has been statistically investigated with patch sizes ranging from <4 to 113 cm^2 (64 x 0.64 cm^2 core areas, total area (16 x16 cm) 256 cm^2; Blanchard, 1990).

Mesoscale distribution was studied using the FMS2 Fo^{15} data, and therefore describes the distribution of mainly diatoms. In the previous section (5.4) Fo^{15} showed a small increase with increasing Chl *a* from a cyanobacterial source, therefore this alga was effectively 'ignored' using the FMS2. Diatom biomass, estimated using Fo^{15}, was measured at different scales to ascertain whether scale had an effect on variability. Scales were chosen that were considered relevant to airborne remote sensing; using 20 to 500 cm lags.

5.5.2. Materials and Methods

See above for general materials and methods of sampling (Section 5.2).

Enteromorpha and *Porphyra* were present in some of the E1AE8 replicates, so these were removed, which left at least 3 replicates at each scale. Replication within

each scale was repeated, totalling 3 sets of replicate measurements at each scale. Therefore only the spatial distribution of diatoms was analysed.

5.5.3. *Results*

On the Eden grid A site (E1AE8), there were no significant differences between Fo^{15} replicated at 20 cm apart than Fo^{15} replicated at 500 cm apart, neither were there significant differences between 20 cm and 500 cm lags (Fig. 5.16A). However, there were significantly higher Fo^{15} values at 100 cm lags than at 500 cm lags. On the Eden grid B site (E1BB4), there were no significant differences in Fo^{15} measured at any scale (Fig. 5.16A). Neither were there significant differences in Fo^{15} at any scale from Sylt samples (Fig. 5.16B).

The variability between Fo^{15} measurements (surface diatom biomass) can vary extensively at any of the scales measured in this study. Variability ranged from 20 to 150% between 20, 100 and 500 cm replicate scale on both the Eden Estuary and the Sylt Rømø basin (Fig.5.17A and B). A smaller, within chamber scale comparison (2.5 cm) between replicates was also made on the Eden Estuary, which also showed a large range in variability (Fig.5.17A). All the CVs of replicates at 2.5 cm apart are not shown (45 sets of replicates), but the CV ranged from 5 to 150% (Fig.5.17A).

5.5.4. *Discussion*

Generally a similar mean Fo^{15} values were produced, regardless of the scale between replicates (comparing 20, 100 and 500 cm lags). Therefore any of these scales, for replication, will result in a representative value Fo^{15} to infer diatom Chl *a*. This also showed that 5 replicates were sufficient to get a representative average value.

The CV, of replicates measured at any of the scales in this study, ranged from 5 to just over 150%. There was no specific change (increase or decrease) in CV with decreased replicate scale. Even at a small scale of 2.5 cm apart, CV can vary up to 150%. This showed that diatom patch sizes vary at any scale of 2.5 cm or above. Because the CV was large at all scales measured, patch sizes may be below the area of measurement, which in this case was 1.2 cm (area measured by the probe at a height of 4 mm). Microscopic study of sediment surfaces (LTSEM) have shown diatoms can be isolated, clustered and cover whole areas (I. R. Davidson and M. Consalvey pers. comm.), therefore dispersion of cells may be random.

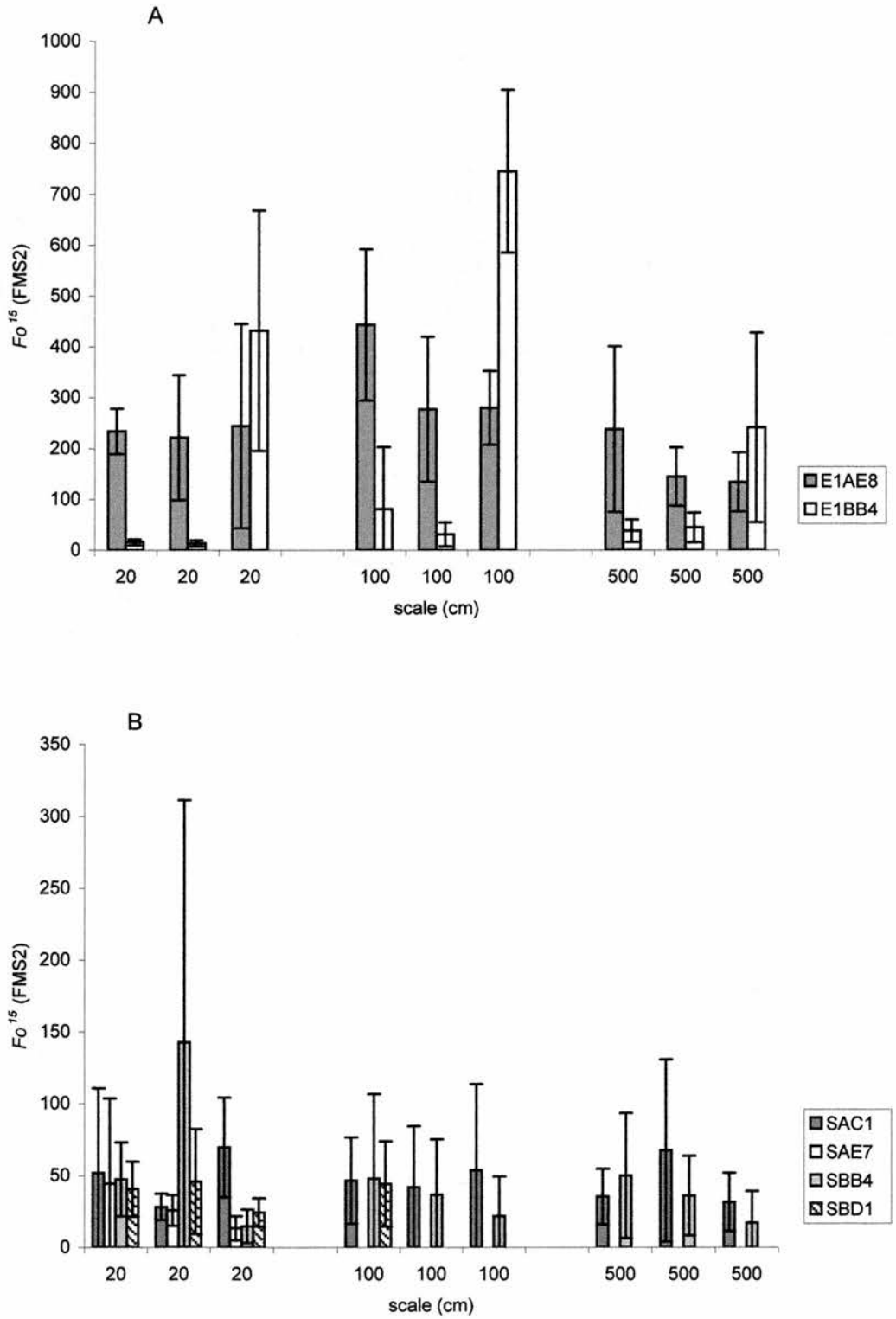

Figures 5.16. The mean Fo^{15} values of replicate measurements at three different scales. A) The Eden Estuary (n= 5 +/-SD for all samples except for E1AE8 first and last 100 cm scale which are n=4, and E1AE8 middle 100 cm and middle and last 500 cm scale which are n=3) . B) The Sylt Rømø Basin (n=5 +/-SD). No bars = no data

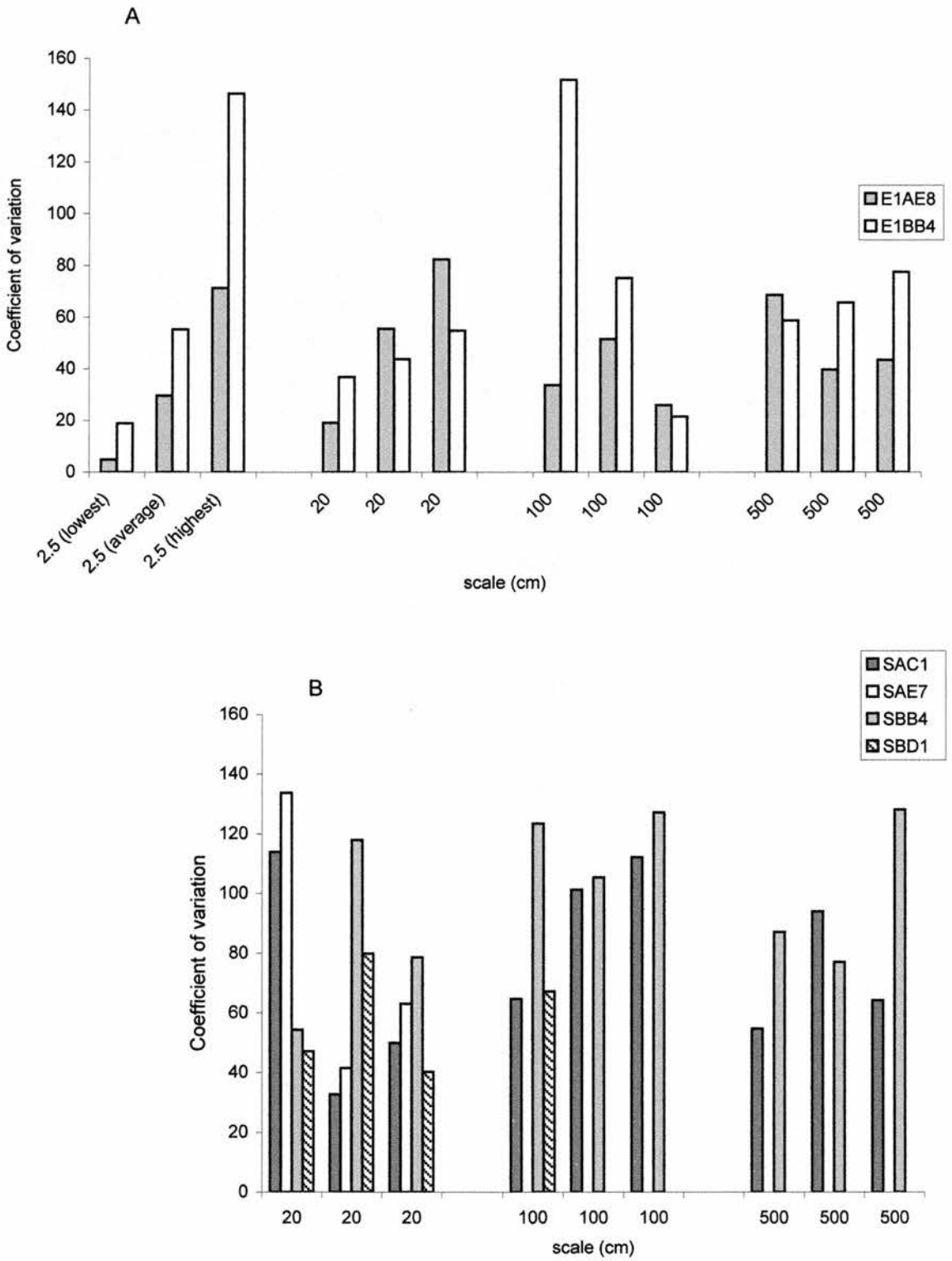

Figures 5. 17. The coefficient of variation of replicate measurements at three different scales. A) The Eden Estuary, only the the lowest highest and average CV for 2.5 cm data set are shown clarity (2.5 cm scale replicates n= 4). B) The Sylt Rømø Basin. No bars = no data. (See Fig. 5.16 for number of replicates)

Chapter 6

6. ANALYSIS OF CHLOROPHYLL *A* IN INTERTIDAL, COHESIVE SEDIMENTS: THE IMPLICATIONS OF SEDIMENT DENSITY

6.1. Introduction

Microphytobenthos inhabit the top few centimetres of intertidal cohesive sediments, but can only photosynthesise in the narrow photic zone at the very surface of the sediment. In cohesive sediments the photic zone has been measured as the top 0.27, 0.6 or 1.8 mm (Serôdio *et al.*, 1997; Kromkamp *et al.*, 1998; Paterson *et al.*, 1998, respectively). Microphytobenthos are the main primary producers in these systems (Pinckney and Zingmark, 1991; Yallop *et al.*, 1994; MacIntyre and Cullen, 1996). These algae provide an important energy source for the estuarine food web (Sullivan and Moncreiff, 1990, Pinckney *et al.*, 1994) supplying up to 45% of the organic budget of an estuary (Asmus *et al.*, 1998) and have a central role in moderating carbon flow in coastal sediments (Middleburg *et al.*, 2000). Given their significance in intertidal systems, the quantification of microphytobenthic biomass is of great importance (Kelly *et al.*, 2001), as is the quantification of other microphytobenthic biomarkers or processes. Pinckney & Zingmark (1991) recognised that biomass was concentrated at the sediment surface, and that sampling techniques at that time could not be resolved to match the active distribution of microphytobenthos. Recent studies, have solved this challenge, resolving the vertical distribution of biomarkers in surface sediments using a cryo-sectioning technique, which have shown that biomass is concentrated in the top 0.2 – 0.4 mm surface section (Taylor, 1998; Wiltshire, 2000; Kelly *et al.*, 2001). Even at high biomass (determined by micro-sectioning), coarse coring (top 5 mm) did not detect variations in Chl *a* content between samples, whereas fine scale sampling showed significant differences (Kelly *et al.*, 2001). Chl *a* found below the photic zone has been defined as photosynthetically inactive biomass (PIB) and a low concentration of Chl *a* was detectable down to a depth to 50 mm (Kelly *et al.*, 2001). The surface section, to a depth of 0.2 mm is only 4% of the volume of a 5 mm deep core. Therefore a 5 mm sample depth includes a relatively large proportion of PIB which may effectively masks any surface enrichment. It has also been found that microscale sectioning allows the distinction between the photosynthetically active biomass (PAB) and PIB,

allowing a more accurate determination of biomass-specific primary production (Kelly *et al.*, 2001).

Micro-sectioning surface sediments is a time consuming technique and for large surveys, with numerous samples, may not be practicable (Chapter 2). This study investigates the relationship between the quantity of Chl *a* in the photic zone (defined as 0.2 mm) with that of deeper core samples.

The chosen units of expression for Chl *a*, in the measurement of standing stock and the interpretation of patterns found spatially and temporally, were discussed briefly in a previous study (Kelly *et al.*, 2001). Chl *a* has often been expressed as a content in sediment (μg Chl *a* g^{-1} dry sediment weight (μg Chl *a* g^{-1} dw)), but has also been expressed as a concentration (mg Chl *a* m^{-2}). Content and concentration are very different units which are not comparable, and it has been suggested that volumetric units should be used in sediment ecology (Flemming and Delafontaine, 2000). When denser, deeper sediment and its associated PIB was incorporated into a sample, Chl *a* expressed as content or concentration can give contrasting results (Kelly *et al.*, 2001). This can have implications for the measurement of biomass-specific production (Kelly *et al.*, 2001). These authors stated that for the accurate calculation of biomass-specific primary production only PAB should be utilised. They showed that if chlorophyll *a* was expressed as mg m^{-2} from a core deeper than the photic zone, PAB could be potentially over-estimated (as it includes PIB) and primary production in the photic zone would be under-estimated. In contrast, if Chl *a* was expressed as μg g^{-1} dw from a core deeper than the photic zone, PAB could be potentially under-estimated (as PAB is diluted by sediment containing PIB). In this case, primary production in the photic zone would be overestimated. The opposing effects these differing units of expression have on Chl *a* determination were not investigated in their study (Kelly *et al.*, 2001) but are examined and discussed in this present investigation. It has been recognised that comparing biotic variables (expressed per concentration, i.e. volume or surface area) in different sediments (grain type) and relating them to other variables, expressed per content (i.e. per mass) was not permissible (Flemming and Delafontaine, 2000). This is because sediment with different grain size has varying densities. These authors also showed that a previous study (Taylor and Paterson, 1998) which showed an enrichment of colloidal carbohydrate content at the surface compared with deeper layers would actually have

a constant colloidal carbohydrate concentration with depth, because of increasing sediment bulk density with depth (Flemming and Delafontaine, 2000).

The implications that sediment density may have on expressing Chl *a* as a content or a concentration was investigated here. The term sediment dry density (kg m^{-3}) used in this study is synonymous with dry mass density, sediment concentration and dry bulk density.

6.2. Materials and Methods

6.2.1. Sampling sites

Samples for this study were collected from the Eden Estuary Paper Mill site (Chapter 2). Samples were collected using the contact corer (see below) in May 2000, during a study of temporal changes in microphytobenthos at the sediment surface (Chapter 7). Sediment collected using the Cryolander (Wiltshire *et al.*, 1997; see below) were sampled at different times of the year, and were a sub-sample of those examined in Chapter 4 (Table 6.1). Samples included in the comparison between Chl *a* in 0.2 mm and 2 mm were also collected from the Paper mill site on the Eden Estuary from mid and low shore during November 1998; July 1997 and September 1997.

6.2.2. Coring techniques

Samples were collected using 2 freezing sampling techniques to collect the surface of the sediment; the contact corer and the Cryolander (Wiltshire *et al.*, 1997; Chapter 2). The contact corer samples approximately the surface 2 mm of sediment and the Cryolander samples approximately the surface 20 mm of sediment. Sediment collected using the Cryolander was then sectioned to the required depths (see below).

Chl *a* was determined from lyophilised sediment from both these sampling techniques using High Performance Liquid Chromatography (Chapter 2 and 3).

6.2.3. Comparisons of Chl *a processing methods in different core depths*

Chl *a* was determined from micro-sections of sediment collected using the Cryolander (Wiltshire, 2000; Kelly *et al.*, 2001). To elucidate whether processing large volumes of sediment or summing numerous smaller volumes had an effect on Chl *a* determination, a comparison of different processing methods was made. Chl *a* was measured to depths of 2, 3 and 5 mm, using a 'mixed sections' and a 'summed

Table 6.1. Environmental data of samples collected from the Eden Estuary North shore *in situ*. Sample were collected using the Cryolander sampling technique. n/d = no data, S.D. = standard deviations (sub-sample of samples used in Chapter 4; Table 4.1)

Date	Tidal zone	Sediment type	Time of low tide GMT	Time of collection GMT	Sediment temp.	Weather	PPFD (μmol m^{-2} s^{-1})
20 Oct 1998	low-mid shore	cohesive mud	09:35	10:00	5°C	cloudy	200
14 Aug 1999	top shore	cohesive mud	10:50	11:30	19°C	rainy cloudy	300
14 Jan 2000	top shore	cohesive mud	13:10	13:00	n/d	n/d	n/d
4 Apr 2000	top shore	cohesive mud	08:35	09:00	6°C	sunny spells	600 variable

sections' processing method (Fig 6.1). Sediment cores were sectioned at subsequent depths of 0.2, 0.4, 0.6, 1.0, 2.0, 3.0 and 5.0 mm. Each core section was then divided into two sub-samples. The first set of sub-samples were analysed directly for Chl *a* in each section. The second set of sub-samples, down to a depth of 2 mm, were homogenised and again divided into two further sub-samples (= 1/4 of a sample). The first of these samples was analysed directly for Chl *a* in a 2 mm depth, for comparison with the sum of the values obtained for the individual core sections comprising the top 2 mm sediment depth. The second sub-sample (= 1/4 of a 2 mm deep sample) was then mixed with 1/4 of the 2.0 to 3.0 mm core section and again divided into two further sub-samples (= 1/8 of a 3 mm sample). This first sub-sample (= 1/8 of a 3 mm deep sample) was again analysed for Chl *a* directly, whilst the second was mixed with 1/8 of the 3-5 mm core section for direct analysis of Chl *a*. In this way Chl *a* content (μg Chl *a* g^{-1} dw) and concentration (mg Chl *a* m^{-2}) was determined for each individual core section. In addition, the sum of individual sections to depth 2, 3 or 5 mm could be compared to the direct analysis of the mixed sections of the same depths (the values from summed sections were compared to mixed sections) (Fig 6.1). Ten samples compared 2 and 3 mm core depth analysis with analogous sub sections, of which 5 samples were analysed and compared to core depths of 5 mm.

Chl *a* determined by mixed section processing (in 2, 3 or 5 mm deep cores) was also compared with the Chl *a* determined from the surface 0.2 mm of sediment.

6.2.4. Temporal changes

Chl *a* in the surface sediment (to approximately a 2 mm depth) was measured using the contact corer during a study of the temporal changes in microphytobenthic biomass (Chapter 7). Six daily exposure periods were sampled at three times during each day. 5 replicates were collected as soon as the tide left the site (Time 1), 5 at the time of low tide (Time 2) and 5 just prior to tidal flood at the end of the emersion period (Time 3).

6.2.5. Statistics

Data was normally distributed therefore ANOVA and GLM were used, with Tukeys pairwise comparisons for *post hoc* analysis. Model 2, reduced major axis regression analysis was completed on normally distributed data. Standard deviations were used for variations and error bars throughout.

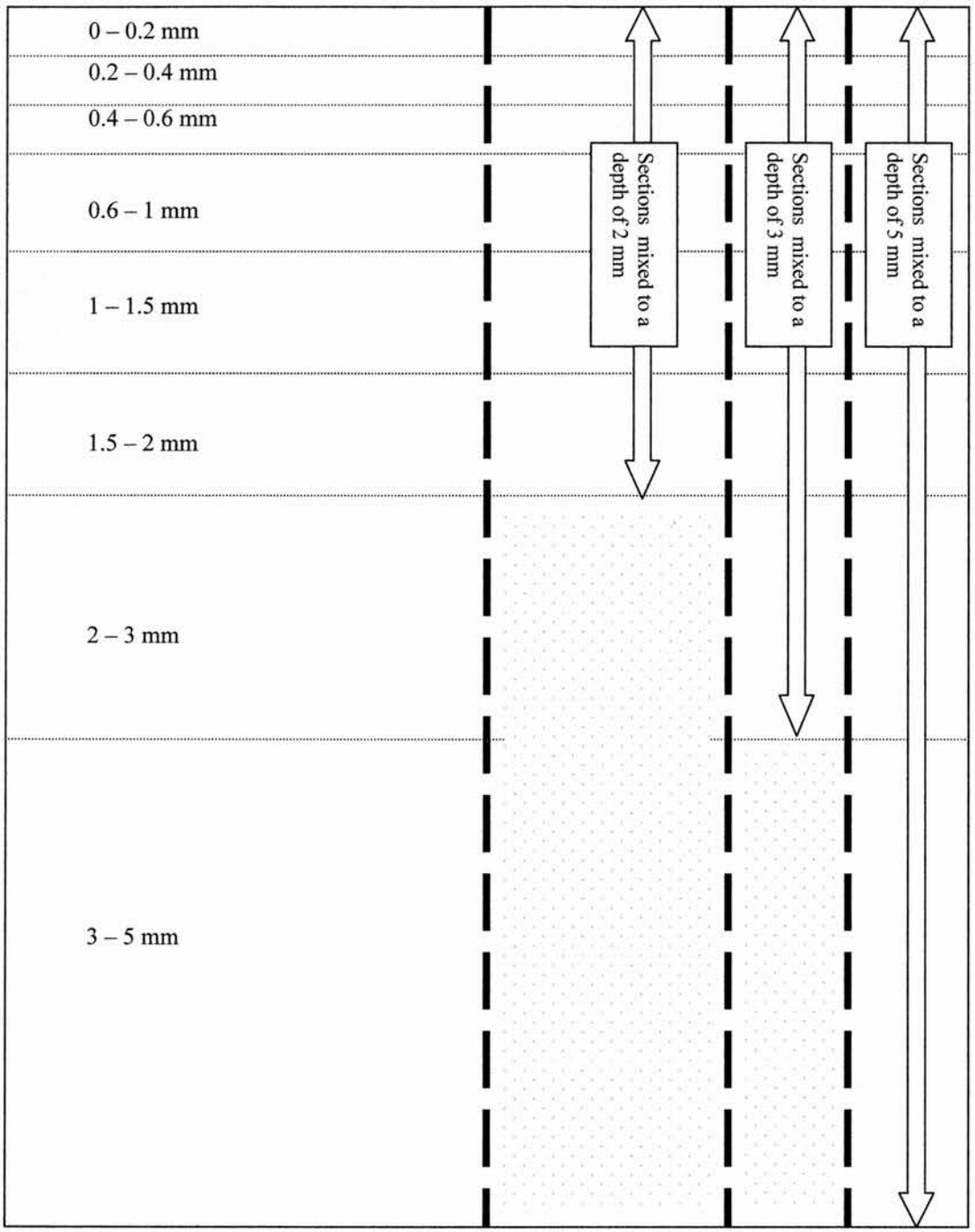

Figure 6.1. Processing method for the comparison of summed and mixed section sediment samples. The whole rectangle depicts a sediment core in cross section. The horizontal dotted lines indicate the depth at which the core was sectioned. The depth of each section is indicated on the left of the diagram. The vertical dashed lines indicate the proportions of the core used in each mixed sample. The dotted areas were discarded. Half of each section was analysed directly for Chl *a* (the left portion of the diagram). The sum of the Chl *a* in each individual section was determined (to the required depth). These summed Chl *a* determinations were then compared to the Chl *a* analysed from each of the mixed samples (shown by boxes and block arrows on the right of the diagram). Each section was homogenised before dividing into appropriate proportions

6.3. Results

6.3.1. Depth profiles

Chl *a* depth profiles showed an exponential decrease with increasing sediment depth, for both content (μg Chl *a* g^{-1} dw) and concentration (mg Chl *a* m^{-2} and g Chl *a* m^{-3} Figs 6.2A, B and C). Samples below 2 mm decreased in Chl *a* to a common value, which was independent of surface enrichment. The common background value of Chl *a* (of all depth profiles shown) between 2 and 5 mm depth in the sediments was, on average, 34 +/-17 μg Chl *a* g^{-1} dw, 3.3 +/-1.2 mg Chl *a* m^{-2} (of a 0.2 mm deep section) or 16 +/-6 g Chl *a* m^{-3}.

6.3.2. Comparison of Chl *a processing methods*

Comparisons of Chl *a* content/concentration between mixed section and summed section samples were made. Chl *a*, expressed as a content (per unit mass of dry sediment), showed significant differences between mixed sections and summed sections (Figs 6.3A, B, C; Table 6.2A). Summed sections showed significantly higher Chl *a* contents than the mixed sections (Table 6.2A). The Chl *a* content (from all months and all core depths) determined in 2 mm from mixed sections was on average 63 +/-17% of the summed sections. Although not significant, Chl *a* content from mixed sections as percentage of summed sections decreased with increasing core depth ($F_{1(2, 24)} = 3.1$, $P > 0.05$) (Fig 6.4A).

However, when Chl *a* was expressed as a concentration (per surface area), Chl *a* between mixed and summed sections were quite similar, and although not significant, summed sections generally had slightly higher Chl *a* concentrations (Figs 6.3A, B and C; Table 6.2B). The percentage of Chl *a* determined from mixed sections was on average 90% +/- 9% of the summed sections and there was no significant differences between core depths sampled ($F_{1(2, 24)} = 2.3$, $P > 0.1$) (Fig. 6.4B).

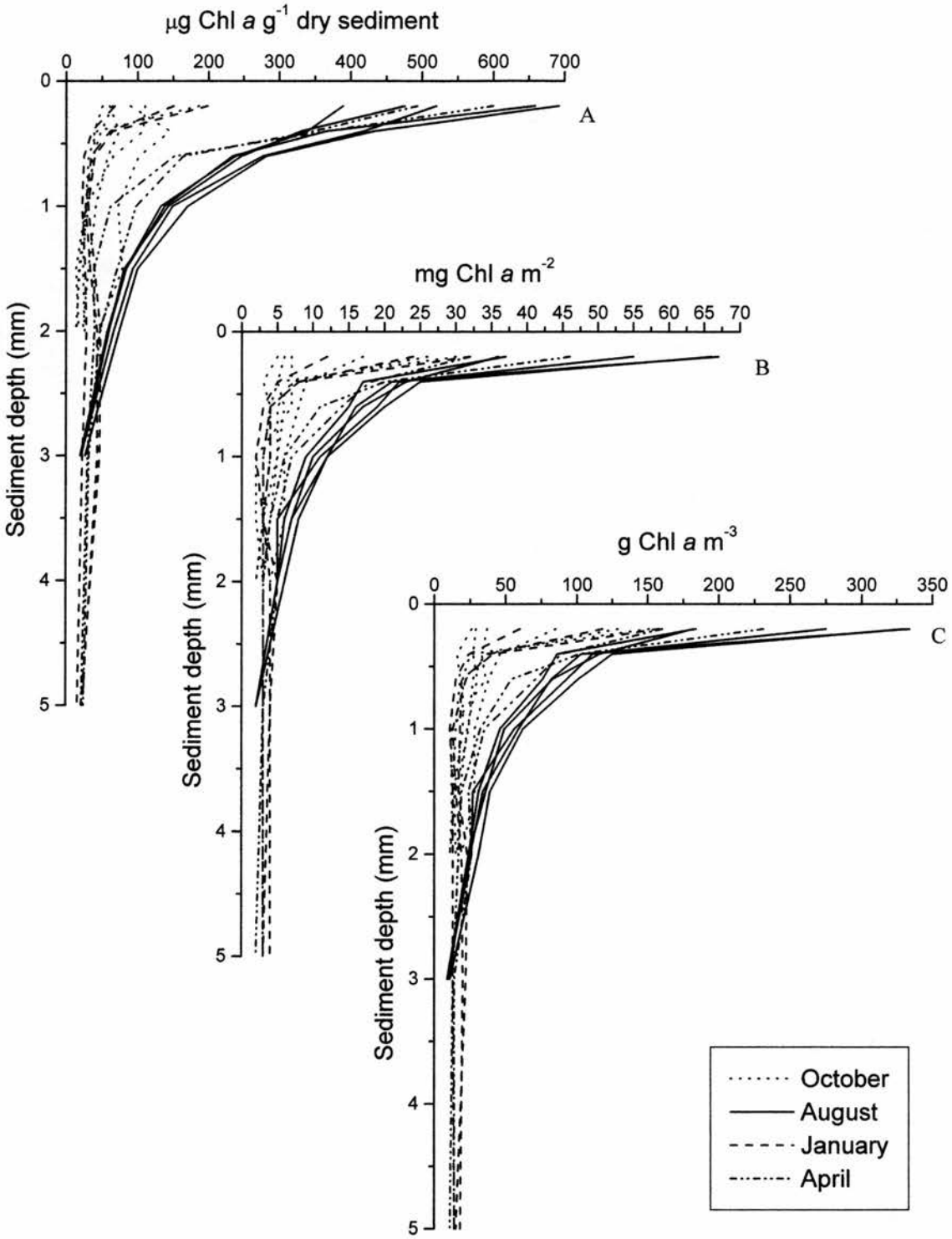

Figure 6.2. Microscale distribution of Chl *a* with sediment depth. Chl *a* is depicted in 3 alternative ways: A. Chl *a* content per mass of dry sediment. B. Chl *a* concentration per surface area. C. Chl *a* concentration per volume. The surface section values of g Chl *a* m^{-3} are approximations, as surface topography affects the accuracy of volume determination

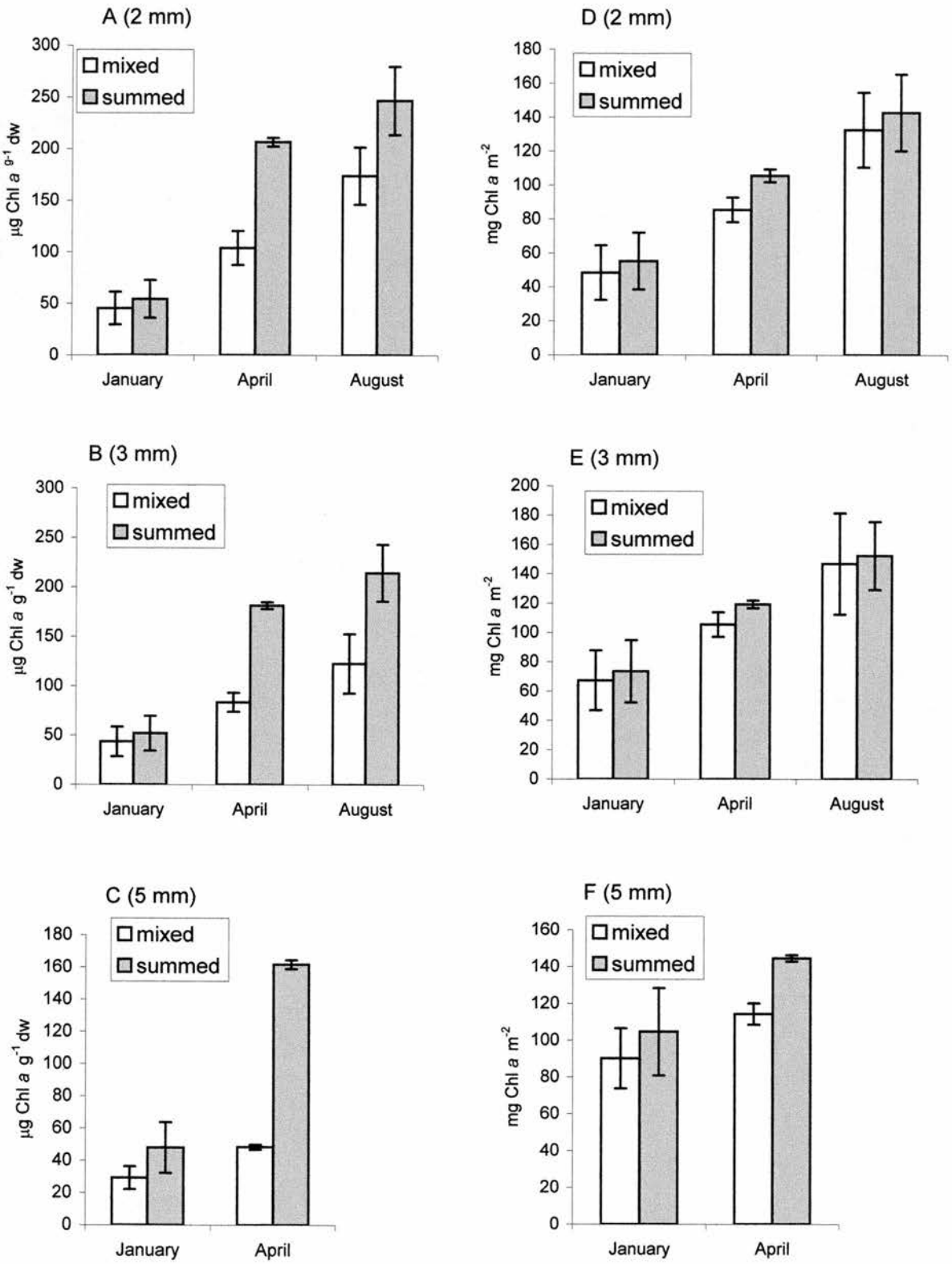

Figure 6.3. Chl *a* measured in different sediment core depths of sediment, using 2 different processing techniques over different times of the year (January, n = 3; Apri,l n = 2; August, n= 5; error bars are SD). A) - C) Chl *a* content in the sediment . D) - F) Chl *a* concentration in the sediment. A) and D) Chl *a* in the surface 2 mm. B) and E). Chl *a* in the surface 3 mm. C) and F) Chl *a* in the surface 5 mm

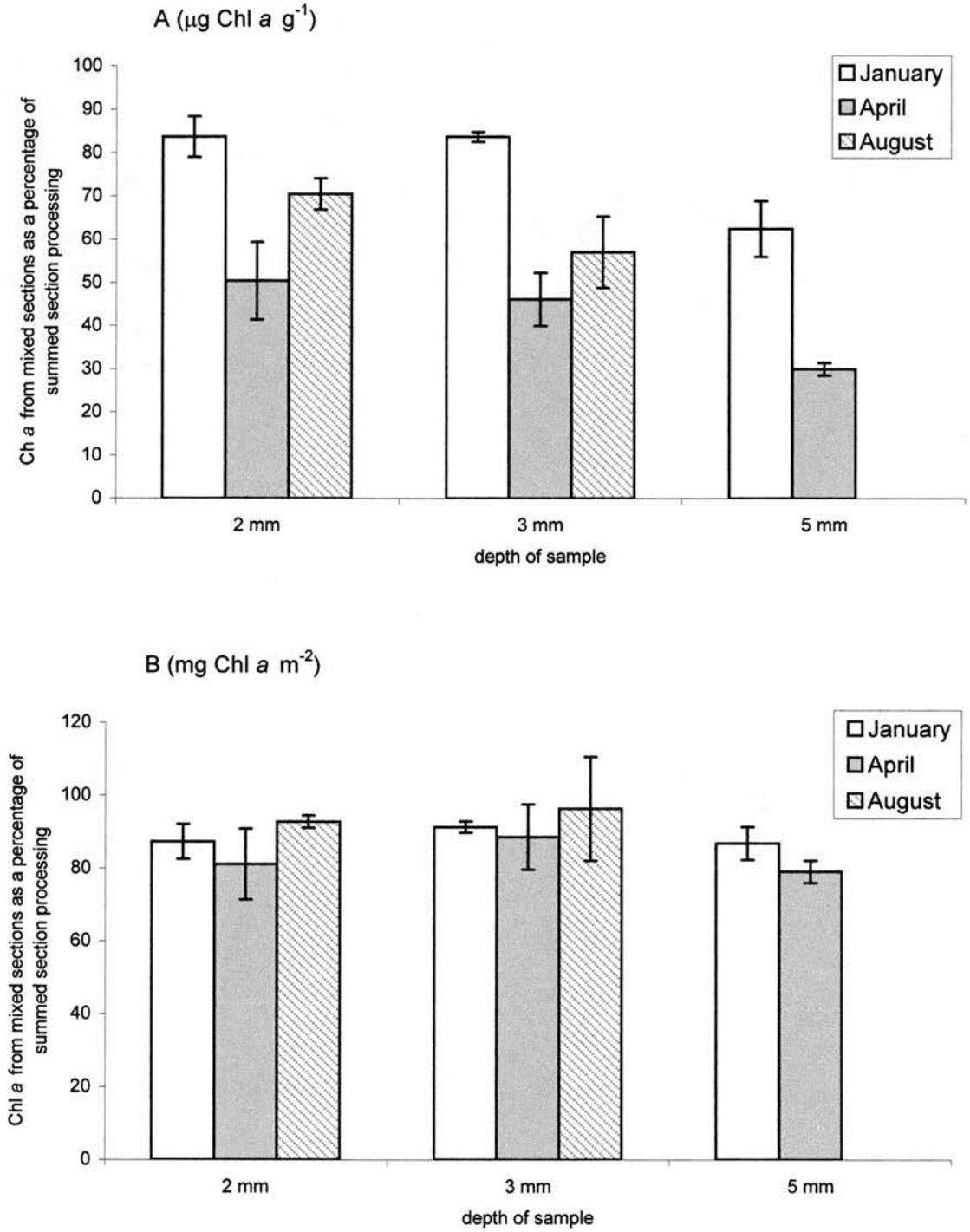

Figure 6.4. Chl *a* determined from mixed section processing as a percentage of summed section processing. Different sampling occasions on the Eden Estuary, in different core depths (n same as Fig. 6.3). A) Chl *a* content in the sediment. B) Chl *a* concentration in the sediment. There was no 5 mm data taken in August

Table 6.2. ANOVA of Chl *a* content (A) and concentration (B) between processing methods from Eden Estuary samples.

A

μg Chl *a* g^{-1}			
core depth	F	df	P
2 mm	25.9	1, 19	< 0.001
3 mm	33.2	1, 19	< 0.001
5 mm	109.4	1, 9	< 0.001

B

dw mg Chl *a* m^{-2}			
core depth	F	df	P
2 mm	1.9	1, 19	> 0.1
3 mm	0.5	1, 19	> 0.2
5 mm	4.3	1, 9	> 0.1

6.3.3. The relationship of Chl *a quantity in different core depths*

Chl *a* was determined from consecutive sections of sediment from 0.2 mm to 2 mm, 3 mm and, in some samples, 5 mm depths. The mixed sections method of processing was used to determine Chl *a* from deeper cores (i.e. 2, 3 and 5 mm). The quantity of Chl *a* in these different core depths were compared to ascertain how closely related Chl *a* determination was between different core depths, using the 2 different units of expression (Chl *a* g^{-1} dw and Chl *a* m^{-2}).

There were significantly higher Chl *a* contents in 0.2 mm core depths than Chl *a* in deeper cores (2, 3 and 5 mm) (Table 6.3A; Fig. 6.5A). Differences between coring depths were also found when Chl *a* was expressed as a concentration, but were opposite to those found in Chl *a* content. There were significantly lower Chl *a* concentrations in 0.2 mm core depths than Chl *a* in deeper cores (2, 3 and 5 mm) (Table 6.3B; Fig. 6.5B).

Table 6.3. ANOVA of Chl *a* content (A) and concentration (B) between cores of 0.2 mm and deeper core depths.

A

Chl *a* content (μg Chl *a* g^{-1} dw)			
core depth	F	df	P
2 mm	17.9	1, 19	< 0.001
3 mm	22.6	1, 19	< 0.001
5 mm	6.6	1, 9	< 0.05

B

Chl *a* concentration (mg Chl *a* m^{-2})			
core depth	F	df	P
2 mm	15.4	1, 19	< 0.001
3 mm	23.8	1, 19	< 0.001
5 mm	52.2	1, 9	< 0.001

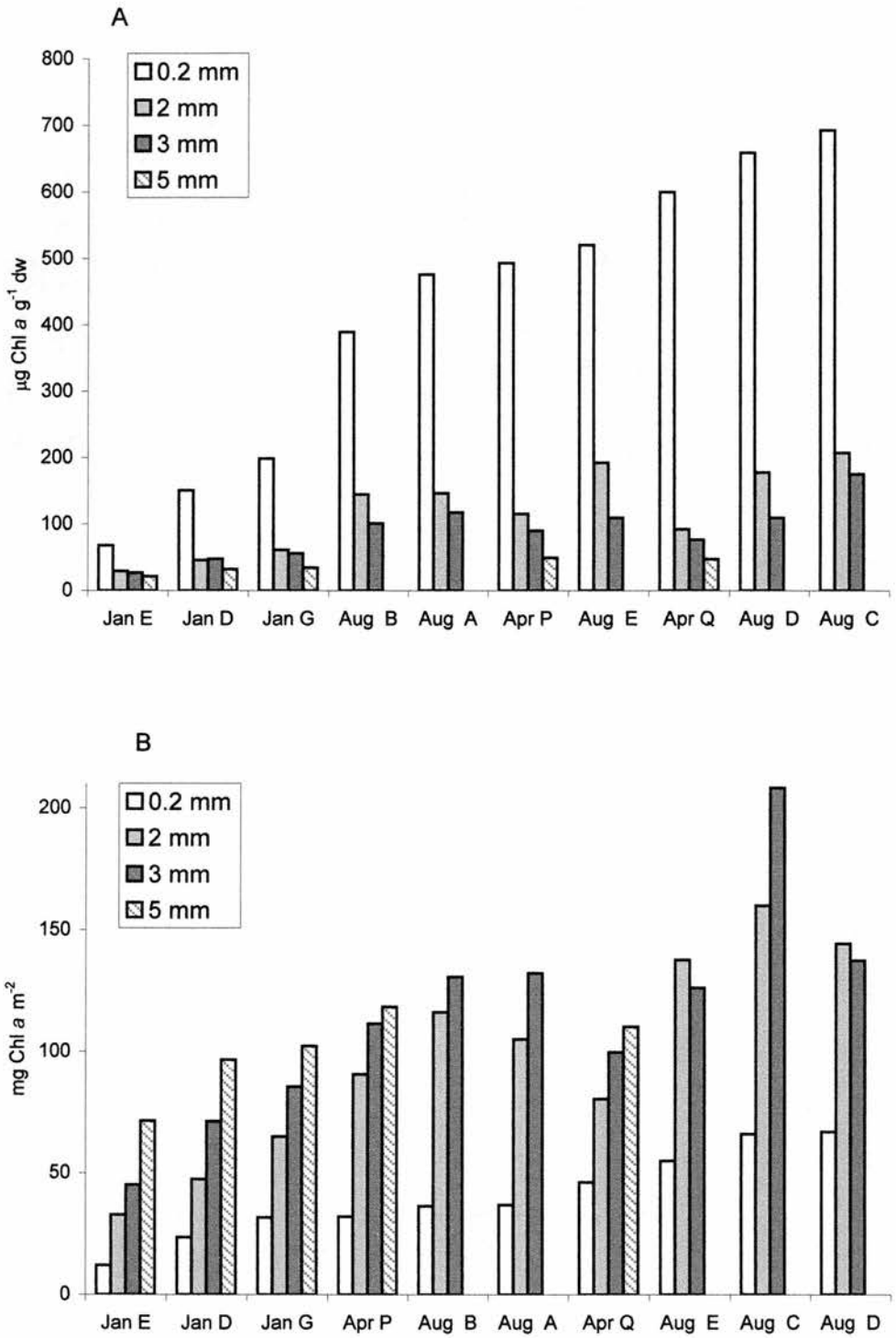

Figure 6.5. Chl *a* determination in varying core depths, using the mixed processing method for 2, 3 and 5 mm core depths. A) Chl *a* content per mass of dry sediment. B) Chl *a* concentration per surface area of sediment. Letters following month depict sample identification

There was a significant correlation between mg Chl *a* m^{-2} in 0.2 mm of surface sediment and mg Chl *a* m^{-2} in all deeper cores (2, 3 and 5 mm; Table 6.4; Fig. 6.6). Correlations were not performed on Chl *a* content between coring depths as this was addressed in a previous study (Kelly *et al.*, 2001).

The Chl *a* concentration in a 0.2 mm core depth as a percentage of Chl *a* in deeper cores increased with increasing biomass. Increasing biomass was inferred from increasing Chl *a* concentrations in the top 0.2 mm of sediment. More specifically, Chl *a* concentration in a 0.2 mm core depth as a percentage of Chl *a* in a 2mm cores showed a scattered logarithmic increase with increasing biomass ($R^2 = 0.433$, n = 29; Fig 6.6B). The correlation between the logged Chl *a* concentration in a 0.2 mm core depth as a percentage of Chl *a* in a 2mm cores and biomass (Chl *a* in 0.2 mm) was significant ($r = 0.662$; $P < 0.001$). Chl *a* concentration in a 0.2 mm core depth as a percentage of Chl *a* in both 3 and 5 mm cores showed a linear increase with increasing biomass ($R^2 = 0.690$ n = 10, $R^2 = 0.939$, n = 5, respectively; Fig 6.6B).

Table 6.4. Pearsons correlation of Chl *a* concentration between cores of 0.2 mm sediment depth and deeper core depths.

core depth	r	n	P
2 mm	0.924	29	< 0.001
3 mm	0.949	10	< 0.001
5 mm	0.895	5	< 0.05

6.3.4. *Temporal changes in Chl a*

Chl *a* in approximately the surface 2 mm of surface sediment (collected using contact coring) was measured during a study of the temporal changes in microphytobenthic biomass during tidal exposure (Chapter 7). Contact coring is not precise, and in this study the depth of cores ranged from 1.13 to 3.20 mm. The actual depth of each contact core was determined by measuring the frozen core with callipers. This variation in sample depths thus introduced an error of +/- 52 % in assuming a set volume from the surface area. A comparison of sample depths over time was made and the cores at Time 1 were significantly shallower than Time 2 and 3 ($F_{1(2, 89)} = 4.35$, $P < 0.02$, followed by Tukeys pairwise comparison at the $P < 0.05$

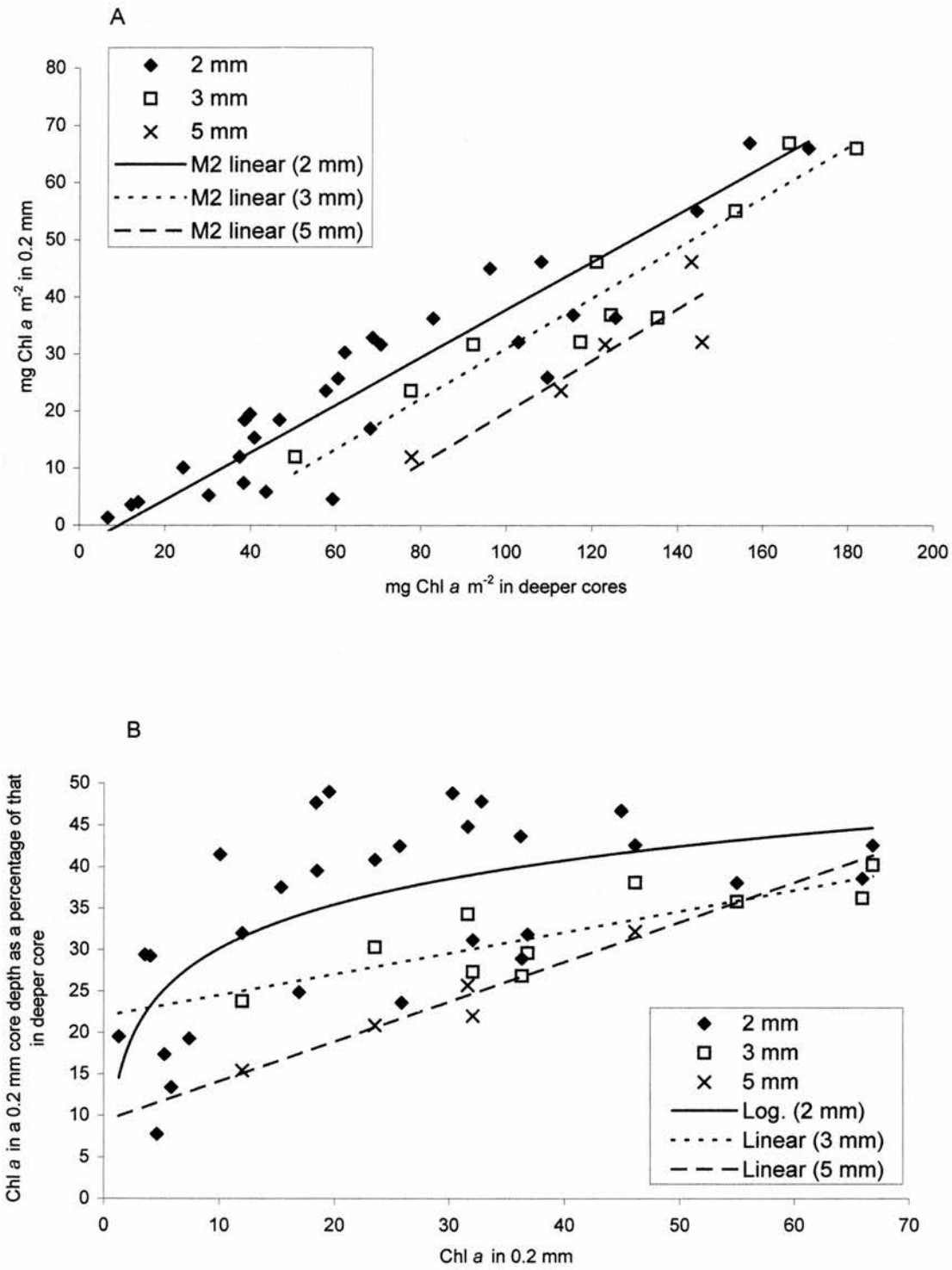

Figure 6.6. The relationship of Chl *a* concentration between the surface 0.2 mm and in deeper cores. A) Direct relationship showing Model 2 linear regression lines for each set of data. B) The percentage of Chl *a* in 0.2 mm as a percentage of that in deeper cores plotted against increasing Chl a in 0.2 mm deep cores

significance level). There was no significant different on core depth between Time 2 and 3 (see above for statistics).

Two sets of data were therefore selected for analysis, firstly all the data (n = 30), and secondly, reconstructed data of similar core depth. The reconstructed data were all the samples which were between a core depth of 1.90 and 2.10 mm; n = 5 for Time 1 and 2 and n = 6 for Time 3) (Fig. 6.7).

6.3.4.1. All data

Samples from 6 emersion periods were pooled and showed a significant decrease in Chl *a* content over time (Table 6.5; Fig. 6.8A). However, Chl *a* concentration increased over time, which were significant for both mg Chl *a* m^{-2} (Table 6.5; Fig. 6.8B) and g Chl *a* m^{-3} (Table 6.5; Fig. 6.8C).

Chl *a* content at Time 1 was significantly higher than at Times 2 and 3, but Times 2 and 3 were not significantly different (Table 6.6A). Chl *a* concentration (mg Chl *a* m^{-2}) at Time 1 was significantly lower than Times 2 and 3 , but Times 2 and 3 were not significantly different (Table 6.6B), Chl *a* concentration per volume (g Chl *a* m^{-3}) at Time 1 was significantly lower than Time 3 only, other times were not significantly different (Table 6.6C).

Table 6.5. ANOVA of Chl *a* content and concentration over an emersion period.

	F	df	P
μg Chl *a* g^{-1} dw	8.5	1, 89	< 0.001
mg Chl *a* m^{-2}	13.0	1, 89	< 0.001
g Chl *a* m^{-3}	3.3	1, 89	< 0.05

Table 6.6. P values of *post hoc* comparisons of Chl *a* content and concentration at times during an emersion period. Underlined values were significantly different

A

μg Chl *a* g^{-1} dw		
Time	1	2
2	<u>< 0.002</u>	
3	<u>< 0.005</u>	> 0.5

B

mg Chl *a* m^{-2}		
Time	1	2
2	<u>< 0.02</u>	
3	<u>< 0.001</u>	> 0.05

C

g Chl *a* m^{-3}		
Time	1	2
2	> 0.5	
3	<u>< 0.05</u>	> 0.1

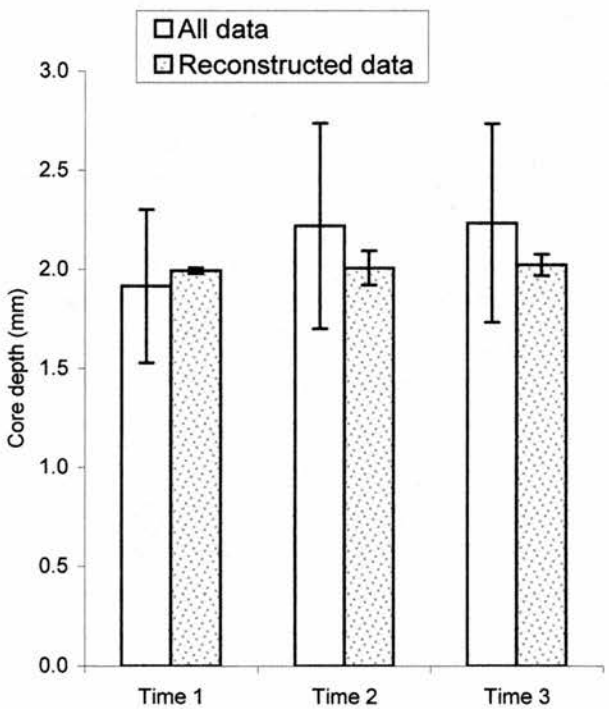

Figure 6.7. Sediment core depth of samples. Time 1 was just after tidal ebb, Time 2 was at low tide and Time 3 was just before tidal flood, during May 2000 (data from temporal study, Chapter 7). Samples were taken over 6 emersion periods and pooled for the 'all data' set (n = 30, error bars are SD). There were significantly shallower core depths at Time 1 when all the data was analysed. Samples for 'reconstructed data' set were thus samples of similar contact core depth (n = 5 or 6)

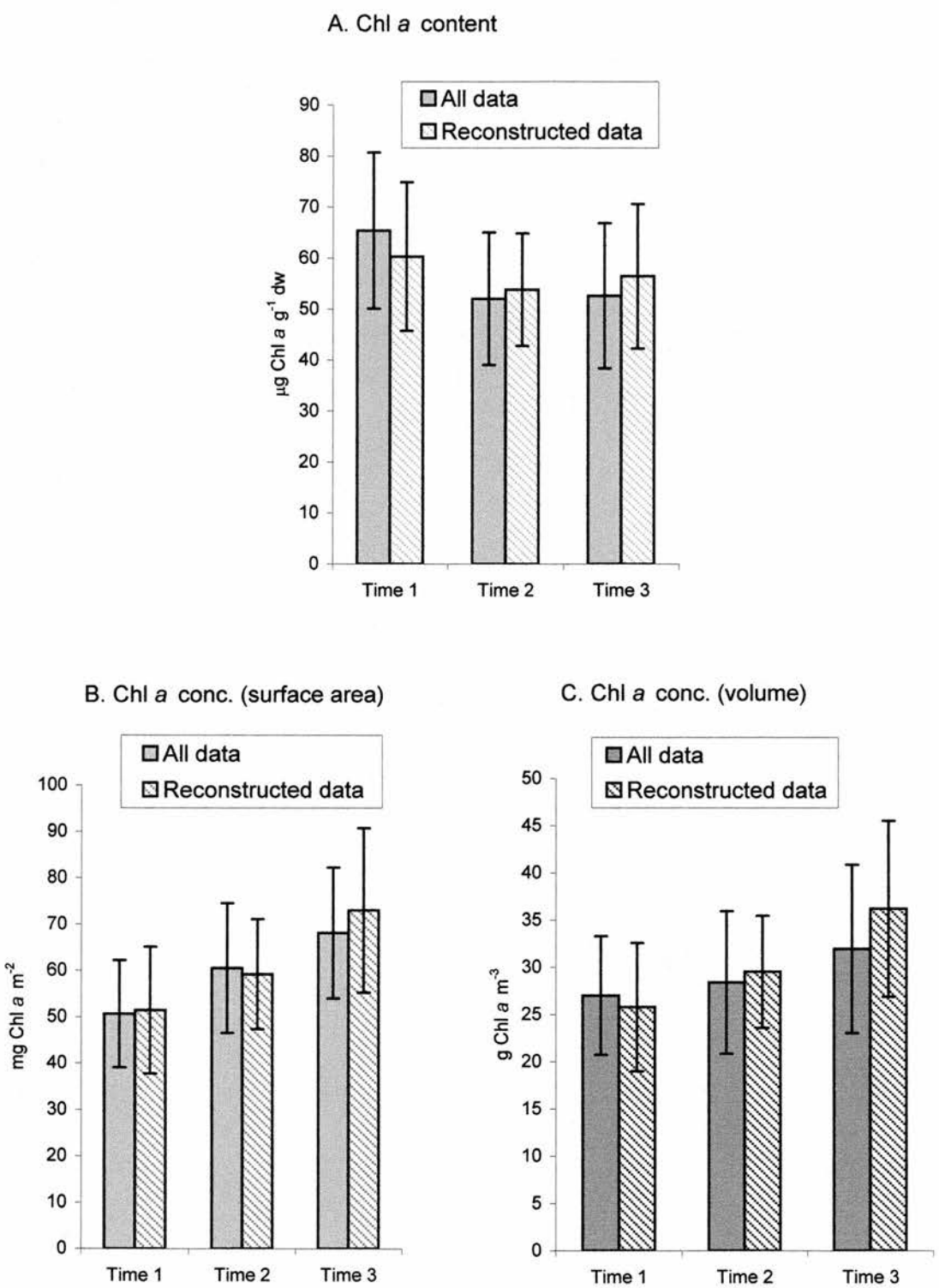

Figure 6.8. Chl *a* in approximately the surface 2 mm (from contact cores). A comparison of three different units of expression over a tidal emersion period. Time 1 was just after tidal ebb, Time 2 was at low tide and Time 3 was just before tidal flood, during May 2000 (data from temporal study, Chapter 7). Samples were taken over 6 emersion periods and pooled for the set of all data (n = 30, error bars are SD). Samples for reconstructed data set were samples of similar contact core depth (n = 5 or 6). A) Chl *a* content. B) and C) Chl *a* concentration (conc.) of unit area and unit volume, respectively

There was a significant decrease in sediment water content over the emersion period ($F_{1(2, 89)} = 152.61$, $P < 0.001$) (Fig. 6.9A). This coincided with an increase in dry sediment mass per surface area (Fig 6.9B). The sediment was sampled to known depths and thus known volumes; therefore dry density was determined. There was a significant increase in dry density of the sediment bed over the emersion period ($F_{1(2, 89)} = 85.54$, $P < 0.001$) (Fig. 6.9C).

6.3.4.2. Reconstructed data of similar core depth

Sediment dry density of the reconstructed data also significantly increased over time ($F_{1(2, 15)} = 25.66$, $P = < 0.001$; Fig 6.9C). Chl *a* content and concentration from samples of similar depth (reconstructed data set) showed the same pattern as the other data (set of all data, Fig. 6.8A, B, C). That is, there was a decrease over time in Chl *a* content, and an increase over time in Chl *a* concentration, however these patterns were not significant in the reconstructed data set (Chl *a* content, $F_{1(2, 15)} = 2.97$, $P = > 0.05$; Chl *a* concentration, mg Chl *a* m^{-2}, $F_{1(2, 15)} = 0.30$, $P = > 0.5$ and g Chl *a* m^{-3}, $F_{1(2, 15)} = 2.64$, $P = > 0.1$).

6.4. Discussion

This study confirms that Chl *a* decreases exponentially with sediment depth in cohesive sediments inhabited by microphytobenthos. Chl *a* is present at depth (PIB), which can interfere with the measurement of PAB (Kelly *et al.*, 2001). The present investigation showed that the interference of PIB in measurements of PAB is exacerbated by temporal changes in sediment density. Sediment density can also change over a microscale in the surface sediments (Taylor, 1998), with time (as in this study) and between locations of different grain size.

6.4.1. Chl a determined from different processing methods and different core depths

Significant differences were found between the top micro-section of sediment and deeper cores when Chl *a* was expressed as content in sediment. Significant differences in Chl *a* content were also found when mixed sections sampling of 2 mm were compared with summed sections of Chl *a* content. These differences were not as pronounced when Chl *a* was expressed as a concentration in sediment. The top layer of surface sediment (the photic zone) can be much less dense than deeper layers (Taylor and Paterson 1998), and expressing Chl *a* as a content (or indeed any biomarker) will essentially exclude any variation caused by changes in the density of

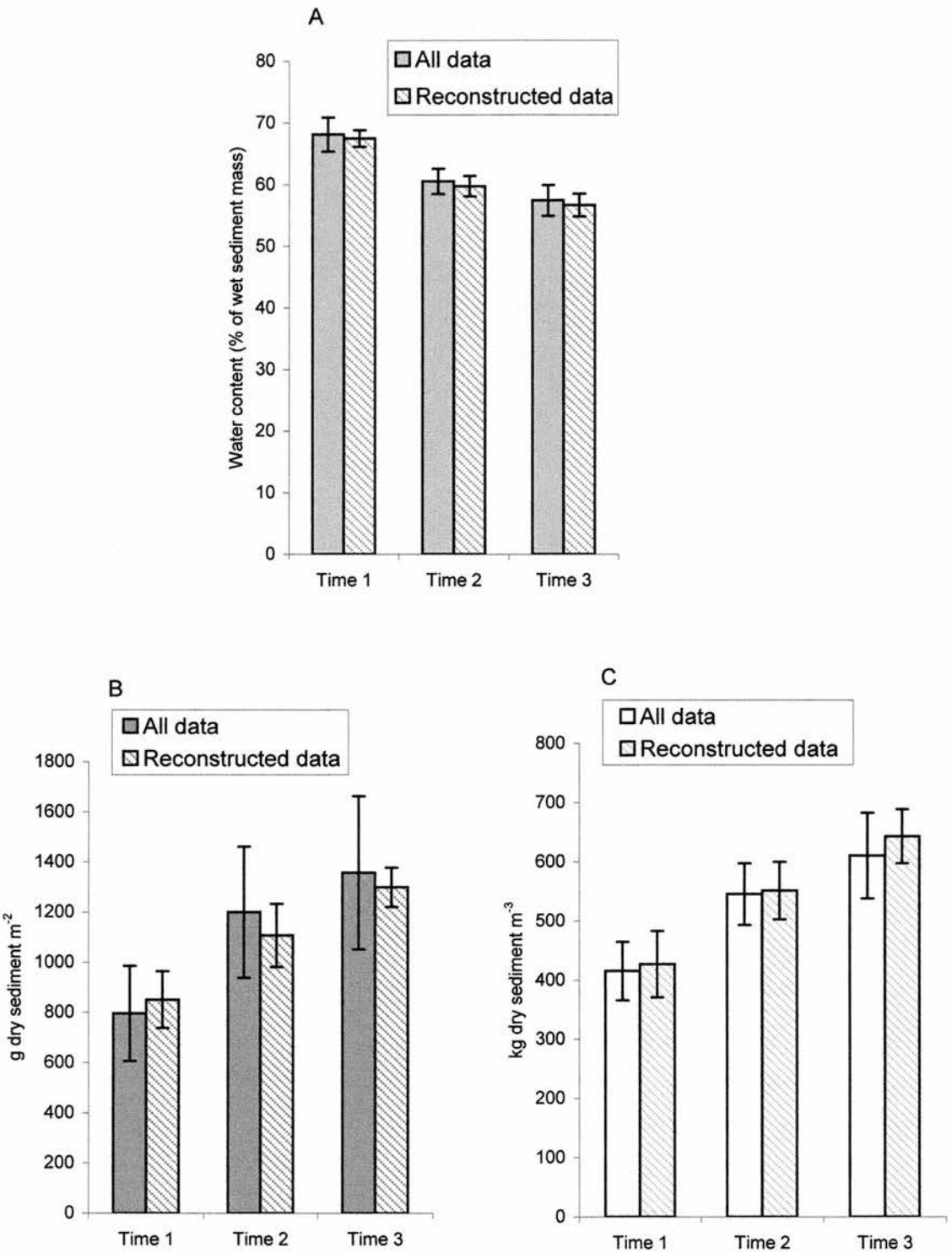

Figure 6.9. Physical data of contact cores over a tidal emersion period. Time 1 is just after tidal ebb, Time 2 is at low tide and Time 3 is just before tidal flood, during May 2000 (data from temporal study, Chapter 7). Samples were taken over 6 emersion periods and pooled for set of all data (n = 30, error bars are SD). Samples for reconstructed data set were samples of similar contact core depth (n = 5 or 6). A) Sediment water content. B) Mass of sediment per area. C) Sediment dry density

the sediment. When deeper layers, and thus denser layers, are included in the sample, average density increases, which, in turn, masks the low density in the thin surface layer. Thus a deeper sample core will have, on average, denser sediment.

6.4.2. The relationship of Chl *a in different core depths*

There was a good correlation between Chl *a* concentrations in deep cores (2, 3 and 5 mm) and Chl *a* in 0.2 mm. Although these samples were collected over seasonal periods, they were collected at the same time during the tidal exposure (low tide) and from the same location, and may have had similar densities. However, samples collected on a shorter temporal scale (within an exposure period), or in different locations, may show a different relationship between core depths, because of greater variability in sediment density. Never the less, this study showed that, for similar samples, a rough estimation of Chl *a* in 0.2 mm might be determined from Chl *a* in deeper cores. This may be useful as determination of Chl *a* in 0.2 mm, which is more representative of the biomass in the photic zone than deeper cores.

Chl *a* in 0.2 mm of surface sediment as a percentage of that in 2 mm deep cores showed a logarithmic increase with increasing biomass (Fig 6.6) and although the relationship was significant, data were scattered. At low biomass (< 25 mg Chl *a* m^{-2} in 0.2 mm depth), any surface enrichment (of Chl *a*) is a relatively small proportion of the Chl *a* in the whole 2 mm core. An increase in surface enrichment, in this case, will have a significant effect and the increase in proportion (of Chl *a* in 0.2:Chl *a* in 2 mm) will be steep. At higher biomass (> 30 mg Chl *a* m^{-2} in 0.2 mm depth) the surface enrichment is a much greater proportion of the Chl *a* in the total 2 mm core depth. Thus, any surface enrichment will have a small effect on the total Chl *a* in the whole 2 mm core. An increase in surface enrichment, in this case, will have a a weak effect and the increase in proportion (of Chl *a* in 0.2:Chl *a* in 2 mm) will be shallow. Chl *a* in 0.2 mm of surface sediment as a percentage of that in 3 or 5 mm deep cores showed a linear increase with biomass (Fig 6.6). Further studies, including samples at higher biomass than this study would be necessary to confidently reveal any relationships. It may, however, be demonstrated (from these data) that a larger proportion of Chl *a* in the 3 or 5 mm deep cores was from PIB, when compared to the PIB proportions in 2 mm. A more pronounced surface enrichment in 3 and 5 mm cores, than found in this study, may be necessary before the relationship becomes shallower. Further studies into the relationship of Chl *a* in 0.2 mm with deeper cores

and their sediment density would be necessary before any confident correction factors of PAB can be calculated from samples containing PAB + PIB.

6.4.3. Temporal changes in Chl *a*

During the temporal investigation of sediment phyto-biomass during this study, there was a significant increase of Chl *a* concentration (mg Chl *a* m^{-2}) with time during an exposure period. Conversely, there was a decrease of Chl *a* content (μg Chl *a* g^{-1} dw) with time. The increase in Chl *a* concentration (or decrease in Chl *a* content) was coupled with an increase in the sediment dry density and a decrease in water content of the sediment. During the whole exposure period (~ 7hr) the sediment dry density increased by nearly 50%. Sampling surface area to a set depth, and thus volume, of sediment will thus include any effects of sediment consolidation. Therefore the decrease in Chl *a* per unit dry sediment mass of sediment could be due to incorporation of Chl *a* from deeper sediments. This would dilute any surface sediment enriched with Chl *a*. Conversely the increase in Chl *a* found per volume (or per surface area) could be purely due to consolidation of the surface sediments, incorporating deeper Chl *a* into the sample. This increase in Chl *a* concentration would largely be due to PIB and hence would result in underestimates in measurements of, for example, primary productivity per unit biomass (Kelly *et al.*, 2001).

Theoretically, if there were no change in standing stock (due to migration) in the surface 2 mm of sediment, then consolidation alone could incorporate more Chl *a* in a set depth of sediment (and thus volume) by the end of the emersion period. Because Chl *a* in sediments is associated with the particulate material (i.e. the sediment and any other particulate matter, e.g. cells) not the water. The extra dry sediment (particulate matter) present in the same volume of sediment is significantly higher at the end of the emersion period than at the beginning. For example, based on a theoretical calculation of a sample containing a Chl *a* concentration of 57 mg m^{-2} in a 2 mm deep sample at the start of the emersion period (when sediment dry density would be minimal). By the end of the emersion period (sediment dry density is higher) an extra 561g m^{-2} (real value; see Fig. 6.9B) of dry sediment could be present in the same sample depth (i.e. volume). This would result in an increase of 19 mg m^{-2} of Chl *a* in the same sample volume of sediment (Chl content of 34 μg g^{-1} dw present in the extra sediment). Thus, over the emersion period Chl *a* concentration would

increase from 57 to 76 mg Chl *a* m^{-2} from consolidation alone. In contrast, with a Chl *a* content of 65 μg g^{-1} dw at the beginning of the emersion period. Extra sediment (561 g m^{-2}) present by the end of the emersion period (Chl *a* content of 34 μg g^{-1} dw) would dilute the surface enriched Chl *a* per mass of dry sediment. This would result in a decrease from 65 to 50 μg Chl *a* g^{-1} dw over the emersion period solely due to sediment compaction. This theoretical increase per unit area or decrease per unit mass in Chl *a* determination was similar to the changes found in Chl *a* shown in this study (Fig. 6.8A, B). Thus, when Chl *a* is expressed as a concentration, the background Chl *a* has an additive effect. Whereas when Chl *a* is expressed as a content, incorporation of sediment of low Chl *a* content has a dilution effect (Fig. 6.10).

6.4.4. Sediment density in the photic zone

The sediment dry density and water content of the photic zone may not follow similar patterns to that of deep cores (2-5 mm). The temporal change in sediment dry density of fine sections (0.2 mm) of sediment was measured, but gave inconclusive results with no particular pattern in sediment dry density (not shown). This was probably due to error in obtaining accurate surface slices because of uneven sediment topography. However, the sediment dry density of the surface 0.6 mm of sediment was measured in a previous study, and was found to increase 130 % during the exposure period (175 to over 400 kg m^{-3}; Taylor 1998; from the Eden Estuary in April, 1996). The increase in sediment dry density in the surface 0.6 mm shown in this previous study was much higher than the 47 % increase found in 2 mm of sediment in this study. Another study, however, showed no clear pattern in water content over an exposure time, from which we may infer no increase in sediment dry density (Christie *et al.*, 2001). Therefore the problems of comparing biomarker determination from different densities may vary over spatial or temporal scales.

It is unclear whether the photic zone would increase in sediment dry density during an exposure period, as it does in deeper cores (this study). Diatoms exude carbohydrate (during movement to the surface during emersion), which is highly hydrated. The motile nature of diatoms will also aerate the surface; the photic zone may therefore become less dense over the emersion period. This should be investigated in future work.

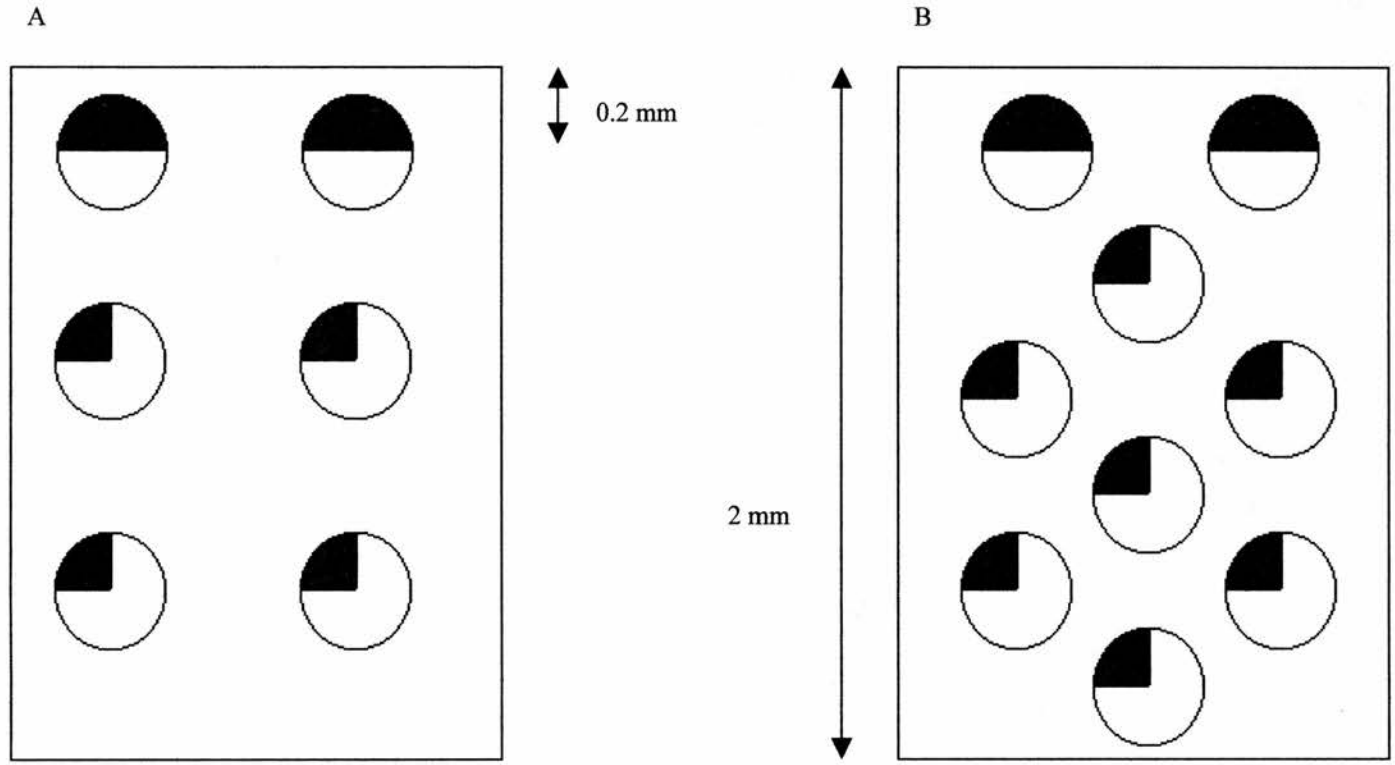

A. Sediment units = 6
Chlorophyll units = 8
Chl *a* units per volume or surface area = 8
Chl *a* units per unit sediment = 1.3

B. Sediment units = 9
Chlorophyll units = 11
Chl *a* units per volume or surface area = 11
Chl *a* units per unit sediment = 1.2

Figure 6.10. Schematic drawing of unit volumes of sediment (rectangles). The circles represent sediment units and each ¼ shaded portion represents a biomass unit (in the form of Chl *a*). The surface (~ 0.2 mm) of the sediment contains a greater proportion of Chl *a* than the deeper sediment. A. High water content sediment at the beginning of the emersion period. B. Lower water content sediment at the end of the emersion period with 50% increase in sediment units, with an increase in the associated Chl *a* units. This will result in a dilution of the surface layer and a decline in Chl *a* unit density per sample volume

6.4.5. General

A common approach in biology is to express biomass as a concentration (per surface area or volume). Generally, areal measurements are more representative of processes (in terms of productive biomass) at the surface of the sediment. Expressing biomass per unit mass of sediment on the other hand has also been widely used in studies of the abiotic factors or physical dynamics of estuaries (Flemming and Delafontaine, 2000). These authors point out that comparing biotic variables as a measure of standing stock per unit content in sediment (unit mass per mass) between different sediment types with different physical properties (e.g. grain size, dry mass densities and water contents) can lead to spurious results. A change in environment can also be accompanied by physical changes (Flemming and Delafontaine, 2000), for instance de-watering over an exposure period or as a function of tidal zone. This was evident from this study where Chl *a* content showed opposite patterns to Chl *a* concentration, over an emersion period and when comparing Chl *a* in different core depths. Acknowledging these fundamental rules of physics, expressing biomass as a content is highly dependent on the density of the sample. A sample containing a high water content or a high proportion of microphytobenthos will be very low in density in comparison to a sample with lower water content or containing fewer cells (the latter will be mostly sediment). Surface sediments containing microphytobenthos are low in density due to the movement of cells making the sediment matrix porous (Paterson, 1995). Microphytobenthos also exude highly hydrated carbohydrates (during movement), adding to the surface sediment water content (Taylor and Paterson, 1998).

It could be suggested that sampling only the photic zone would be a more representative measurement of the active biomass. However, determining photic depth is difficult and time consuming, the most accurate method presently is the use of fibre optic light microsensors (Lassen *et al.*, 1992; Paterson *et al.*, 1998). Microprobe measurements of the light field within the surface layers is a relatively new technique and few studies have been published which show any spatial or temporal variation in the photic zone.

6.5. Summary

This, and other studies (Flemming and Delafontaine, 2000; Kelly *et al.*, 2001) have highlighted important aspects of determination of active microphytobenthos

biomass; and that different patterns can be found depending on how the sediment was sampled and how the results are expressed. There are also implications when comparing Chl *a* content or concentration from samples of different density, i.e. over temporal or spatial scales. This study demonstrated that:

- Chl *a* contents of sediment (mass per mass) determined from fine resolution sampling (summed to comparative depths) cannot be compared with coarse resolution sampling. Chl *a* concentrations (mass per volume or surface area), on the other hand, are similar between these coring techniques.
- Temporal and spatial variations in water content and sediment density have serious affects on comparing Chl *a* over these scales, both as Chl *a* content and concentration.
- The expression of Chl *a* either as a content or a concentration both have implications when inferring standing stock of productive biomass.
    - When Chl *a* was expressed as a concentration, background Chl *a* (or PIB) coupled with increasing sediment density and has an additive effect on resulting Chl *a*.
    - When Chl *a* was expressed as a content, background Chl *a* (or PIB) coupled with increasing sediment density has a diluting effect on resulting Chl *a*.

6.6. Conclusion

This study showed that dry density of the sediment bed significantly affected the measurement of both Chl *a* content and concentration (and indeed the measurement of any biomarker) in opposite directions. This may lead to unjustifiable conclusions and spurious interpretation of the data. Sampling only the surface photic zone of the sediment and expressing Chl *a* as a concentration is probably the most representative way of expressing Chl *a* quantity as a measure of the standing stock of biomass or PAB.

This research highlights the complex nature of sediment dynamics and how they might influence biological measurements. To safeguard against unrepresentative measurements in the changes of biomass over temporal and spatial scales the following steps should be taken. The water content or dry density of the sediment should be determined and;

a) if there are significant variations in these parameters over the scales measured, a correction factor should be applied. This may include the determination of PIB.

b) if there are no differences in these parameters then patterns in biomass can be confidently demonstrated.

Fluorescence measurements of the surface sediment may be a more representative measure of PAB, as the beam measures less than the photic depth (Chapter 4). It has been reported that most of the fluorescence (detectable by a PAM fluorometer) emanates from a sediment depth of 0.15 mm (Kromkamp *et al.,* 1998), however many factors may affect the yield of fluorescence and are discussed in Chapter 4, 5 and 7. Other remote sensing techniques (e.g. spectral reflectance) have recently been explored as an alternative measure of sediment biomass than the quantity of Chl *a*. This may lead to a better representation of the active standing stock of biomass of microphytobenthos in the photic zone, although as yet the results are inconclusive (Paterson *et al.*, 1998; BIOPTIS final report).

Chapter 7

7. TEMPORAL STUDIES OF MICROPHYTOBENTHOS USING FLUORESCENCE AND PIGMENT ANALYSIS

7.1. Introduction

Assemblages of benthic diatoms are known to migrate into the sediment during periods of tidal immersion (Round and Palmer, 1966), however some assemblages may stay at the surface if the flooding water is clear (Perkins, 1960). Diatoms may also migrate down into the sediment in response to stressful conditions; e.g. enhanced UVBR (Underwood *et al.*, 1999).

Studies of diatom migration have used several methods to trace diatom movement; visual assessment of surface coloration (Perkins, 1960); cell counts to Chl *a* distribution; and remote sensing techniques (see below for references). Cells have been collected for counts using either lens tissue to trap the algal cells as they surface (Eaton and Moss, 1966), counted from 1 mm sections (Hopkins, 1963, Joint *et al.*, 1982) or counted whilst on the sediment surface using low-temperature scanning electron microscopy (Janssen *et al.*, 1999). The vertical distribution of Chl *a* has been studied within the top 5 mm of sediment surface at 1 mm depth intervals (Pinckney *et al.*, 1994) and in the top 2 mm at 0.2 mm intervals (Taylor, 1998; Wiltshire, 2000; Kelly *et al.*, 2001). Remote sensing techniques have recently been employed to show a qualitative change in cells at the sediment surface. These studies have measured spectral reflectance (SR) of pigments (Paterson *et al.*, 1998; Kromkamp *et al.*, 1998) or fluorescence of Chl *a* at the sediment surface (Serôdio *et al.*, 1997; Serôdio and Catarino, 2000; Barranguet and Kromkamp, 2000; Chapter 4). These latter studies have not yet included enough replication for statistical evaluation of any changes.

Most authors agree that there is an increase in cells, or Chl *a* at the very surface on muddy sediments soon after tidal ebbing when low tide occurs during daylight hours (Palmer and Round, 1967; Happey-Wood and Jones, 1988; Janssen *et al.*, 1999; Serôdio and Catarino, 2000), although the rate of increase can vary. Pinckney *et al.* (1994) also found Chl *a* within the top 1 mm of surface sediment during tidal exposure at night, as well as day tidal exposure, on an estuary in South Carolina, USA. These authors also found when high tide was at midday, microalgae migrated to the surface 1 mm of sediment in the early morning and stayed there for the remaining daylight hours. In both sandy and muddy sediments (in Massachusetts, USA and North Wales,

UK, respectively) a rapid increase of cells occurred at the surface in the first hour, followed by plateau of cell numbers (Palmer and Round, 1967; Happey-Wood and Jones, 1988). In cohesive, intertidal sediments of the River Avon and in muddy sediments in North Wales, at least 2 hours of tidal emersion was needed for all cells to migrate to the surface at dawn in some situations (Round and Palmer, 1966; Happey-Wood and Jones, 1988). It has also been documented that that there were more rapid rates of population increases when the previous day had shorter exposure times to light compared with previous longer light exposure times (Happey-Wood and Jones, 1988).

The rate of increase of the accumulation of cells at the sediment surface can differ, but it is as yet unclear whether this is due to location, environmental effects or species composition. Kromkamp *et al.* (1998) using SR on cohesive sediments (The Netherlands) found 50% of the change occurs within the first hour (of a 6 h period). Paterson *et al.* (1998), also using spectral reflectance on cohesive sediments, but in the U.K., found a faster rate of increase; 50% of the change occurred within the first 18 min (of a 5 h 30 min period), this was then followed by a slower increase. Serôdio *et al.* (1997), using fluorescence on undisturbed cohesive sediments on a Portuguese estuary, found 50% of the increase occurred within 2 hours of tidal ebb. The peak of cells or Chl *a* at the surface varies from the middle of the tidal exposure to towards, or at the end of the tidal emersion period. Pinckney *et al.* (1994) show a peak of Chl *a* at the surface at the time of low tide, whereas Serôdio and Catarino (2000) show a peak at low tide or towards the end of the emersion period.

Many studies also showed a decrease in cell numbers or Chl *a* just prior to tidal flooding, although some studies show no decrease as the tide floods (see below). Palmer and Round (1967) found a decrease in cells at the surface in last 30-60 min before tidal flooding. Round and Palmer (1966) found that some species migrate away from the surface earlier than others do, and some have bimodal rhythms within one emersion period. Serôdio *et al.* (1997) showed a slight decrease in biomass at the surface after 5 hr 30 min. Janssen *et al.* (1999) showed cell densities, decreased or stayed constant prior to tidal flooding, when emersion was in the morning. They also found that in some situations when tidal emersion occurred in the afternoon, cell densities were still increasing at tidal flooding. Perkins (1960) noted no visual decrease when the tide covered the biofilm. Paterson *et al.* (1998) from Humber estuary sediments, UK, and Kromkamp *et al.* (1998) using SR, show no decrease within 5 hr 20 min or 5 hr of measurements respectively.

In addition to studies dealing with entire assemblages, varying responses in the migratory behaviour of different species has been documented. When low tide was at either end of the daylight period, the migratory rhythm of a diatom species, *Hantzschia* stayed unimodal; i.e. migration shifts from the 2nd exposure to the first exposure on consecutive days (Palmer and Round, 1967). However, the migratory rhythms of *Pleurosigma* were bimodal on days when exposure was at either end of day; i.e. migration to the surface occurred during both emersion periods (Happey-Wood and Jones, 1988).

The migratory rhythms of diatoms may be affected by several factors. Round and Palmer (1966) studied migratory behaviour under different treatments in the laboratory on undisturbed cores, and found that diatoms did not migrate in the dark, either under natural night time emersion periods or during the day under forced darkness. Contrary results were found using fluorescence, which showed cores kept in the dark had sharp peaks of fluorescence at low tide (in the middle of the emersion period), only when exposure coincided with daytime (Serôdio *et al.,* 1997). Cell counts, collected using lens tissue, showed that migration continued under constant light conditions (Round and Palmer, 1966). These authors also found that low temperatures (2°C) suppressed migration, probably due to low temperatures altering the speed of motility (Hopkins, 1963). The effects which suppressed migration (dark and cold) were found to be transient, as once normal light or temperatures were re-introduced the migratory rhythms returned even after 63 h of darkness or 4 d of cold temperatures (Round and Palmer, 1966). These authors also found that different intensities of light (112, 75, 35 foot candles approximately equivalent to 25, 17, 8 μmol m^{-2} s^{-1} (Walker, 1987)) had little effect on the migratory rhythms of diatoms (Round and Palmer, 1966).

Rhythmic responses other than accumulation of cells at the sediment surface also occur in benthic diatoms. The speed and distance travelled (on glass under a microscope) of *P. angulatum* also followed a tidal rhythm, both increasing during emersion periods (Happey-Wood and Jones, 1988). Productivity also follows a tidal rhythm, but this has been attributed to the migratory behaviour of the microphytobenthos, and good correlations between the biomass at the surface and productivity have been shown (Pinckney and Zingmark 1991; Pinckney *et al.,* 1994). The hourly variability in productive biomass, associated with the vertical migratory rhythms of motile microalgae, has been quantified by non-destructively measuring the

dark-level chlorophyll *a* fluorescence (*Fo*) emitted from undisturbed microphytobenthic samples (Serôdio *et al.*, 1998; Serôdio and Catarino 2000; Chapter 4). *Fo* was found to be a good predictor of community-level photosynthesis parameters; α (light utilisation efficiency) and P_{max} (maximum photosynthesis) under the range of conditions found *in situ* (Serôdio and Catarino 2000). These authors estimated the hourly production rates from hourly time series of *in situ* observations of *Fo* and irradiance.

Pigment quantification from photosynthetic organisms can give an indication of the physiological status of the light harvesting and photoprotection processes. In diatoms, Chl *c* and fucoxanthin are the main light harvesting pigments other than Chl *a*, and an increase in their concentration may indicate a decrease in available light. Diadinoxanthin, diatoxanthin and β - carotene are the main photoprotective pigments in diatoms. Diadinoxanthin de-epoxidates and is converted to diatoxanthin in the light, and diatoxanthin is converted back to diadinoxanthin in low light or darkness (Olaizola and Yamomoto, 1994). This inter-conversion of pigments is known as the diadinoxanthin cycle and is similar to the xanthophyll cycle in green algae and higher plants. As a protective mechanism, diatoxanthin may transfer absorbed energy to Chl *a* with lower efficiency than diadinoxanthin, (Falkowski and Raven, 1997, Robinson *et al.*, 1997). β - carotene is also known to dissipate excess energy away from the reaction centres, to avoid photo-damage (Falkowski and Raven, 1997). Therefore an increase in the concentration of these photoprotective pigments may indicate that cells have experienced excessive irradiance. Any changes in the quantity of pigments can be measured absolutely as a concentration, normalised to cell count or by calculating the ratio of pigment to the main light harvesting pigment Chl *a*.

Minimum fluorescence (Fo^{15}) was correlated with Chl *a* biomass of microphytobenthos on the sediment surface *in situ* (Chapter 4) and in the laboratory by previous workers (Serôdio *et al.*, 1998; Barranguet and Kromkamp, 2000). The technique described in Chapter 4, measured Fo^{15} simultaneously with maximum photochemical efficiency at PSII (*Fv/Fm*) as a check that fluorescence had reached its minimum (i.e. unaffected by photosynthetic processes). A high *Fv/Fm* is a good indicator of relaxed (oxidised) primary electron acceptors at PSII (Genty *et al.*, 1989) and low values indicate stress, which can affect the value of Fo^{15} (Büchel & Wilhelm,

1993). Stress can be caused by excessive photons causing dynamic or chronic photoinhibition, nutrient limitation, desiccation or toxins.

The aims of this study were to monitor *in situ* diatom migratory behaviour on the Eden Estuary hourly (during emersion periods) and daily periods (over six days as the emersion period became later on in the day). The variation of microphytobenthic biomass was also estimated on a spatial scale. Pigments were measured from the surface layer to ascertain any changes in Chl *a* and light harvesting or photo-protective pigments in response to time or physical factors. The changes in algal biomass and ecophysiology were measured at the surface of exactly the same small patch of diatoms, using a non-destructive technique (Fo^{15}). Microphytobenthic stress (*Fv/Fm*) and relative electron transport rate, which has shown to be useful in the determination of photosynthetic parameters (Kromkamp *et al.*, 1998), were also monitored.

7.2. Materials and Methods

7.2.1. Study A; May 2000

An area of sediment surface (10 x 10 m) was monitored both destructively and non- destructively over a period of 6 consecutive days on the Eden Estuary in May 2000. Sampling began on each day as soon as the tide ebbed from the site and ended just prior to immersion, only one emersion period per day was sampled. The site was selected at low tide, on the day prior to the experiment to ascertain areas of visible diatom population.

The tide ebbed in the morning of first day of the experiment and low tide was just after mid day (Day 1; Tuesday 9.5.00). The tidal ebb and flood was over an hour later each day. On the last day (Day 6; Sunday 14.5.00) of study, the tide ebbed in the late afternoon and low tide was during the evening (see Table 7.1 for the exact times). The early tidal emersion was sampled on Day 5 for comparative reasons.

7.2.1.1. Physical measurements

Measurements of irradiance, temperature and tidal water turbidity were made throughout the experimental period. Ambient incident irradiance was measured every 30 minutes using a cosine corrected radiometer (LI-COR LI 189), and irradiance was expressed as photosynthetic photon flux density (PPFD) in μmol m^{-2} s^{-1}. The dose of irradiance per emersion period was determined to asses the additive effect of light, and

Table 7.1. Tide times and weather at migration study site. BST = GMT + 1h

Day	Date	Low tide (from Admiralty Charts) BST	Tidal ebb at site BST	Tidal flood at site BST	Emersion period BST	Weather
1	Tuesday 9 May 2000	13:37	09:55	16:40	06:45	Sunny, hot
2	Wednesday 10 May 2000	14:44	10:57	17:55	06:58	Windy, cloudy but brightened at 13:30.
3	Thursday 11 May 2000	16:08	11:55	19:20	07:25	Windy Sunny spells
4	Friday 12 May 2000	17:29	13:20	20:39	07:19	Breezy, Hazy sun
5	Saturday 13 May 2000	05:51	02:30	08:40	06:10	Clear, sunny (after dawn!) Gentle breeze
6	Sunday 14 May 2000	19:37	15:45	22:25	06:40	Hazy sun, warm, gentle breeze

was calculated as the sum of the average irradiance every hour taking into account the dark adaption period (i.e. 15 minutes every hour). Temperature of the surface 5 mm of sediment was logged every 10 minutes using a Grant probe and datalogger. Turbidity of tidal water (pre and post emersion) was measured by sampling the water. The water was then analysed in the laboratory using a Nephelometer. Nephelometer units (NTU) were previously calibrated to the weight of dry Eden sediment per volume of seawater (mg dry sed l^{-1}). The calibration between NTU and sediment concentration was linear and the calibration equation used to determine the sediment concentration of the tidal water was;

$$\text{Sediment (mg } l^{-1}) = 2.8 * \text{NTU} + 13.8$$

7.2.1.2. Fluorescence measurements

Non-destructive measurements were taken using a portable Hansatech fluorescence monitoring system (FMS2). Algal biomass at the sediment surface was estimated using Fo^{15} measurements (Chapter 4). A measure of algal stress was determined using maximal photochemical efficiency at PSII (*Fv/Fm*) (Genty *et al.,* 1989). Fluorescence measurements of Fo^{15} and *Fv/Fm* were made at 4 mm from the sediment surface using an inverted opaque funnel fitted over the probe tip (Fig. 2.18). These two sets of measurements (Fo^{15} and *Fv/Fm*) were made on exactly the same 15 patches of sediment each hour during an emersion period, for six consecutive days. Recordings were taken hourly from time zero, which was about 20 minutes after the tidal ebb, through to time 6 (Days 1, 2 and 5) or time 7 (Days 3, 4 and 6) which was just prior to tidal flood. Each undisturbed patch (numbered 1 to 15) measured an area of approximately 120 mm^2 (see Fig. 7.1A, non-destructive site; each patch was measured at the end of each arrow; Fig. 7.1B). This non-destructive area was marked with 2 permanent upright canes. A 100 cm long cane was placed on the sediment surface between the uprights during each sampling period. This horizontal cane was marked at 10 cm intervals as a template. These 2 rows of measurements were 17 cm apart and the entire non-destructive sampling area was 0.18 m^2 (Fig. 7.1B). Each patch was dark adapted using an opaque inverted dish which was quickly replaced by the probe tip, with fitted funnel, prior to measurement. Relative electron transport rates (rETR) were determined using the formula $\Delta F/Fm'$ x PPFD (Kromkamp *et al.*, 1998), and were estimated from random patches under natural ambient light and filtered ambient light

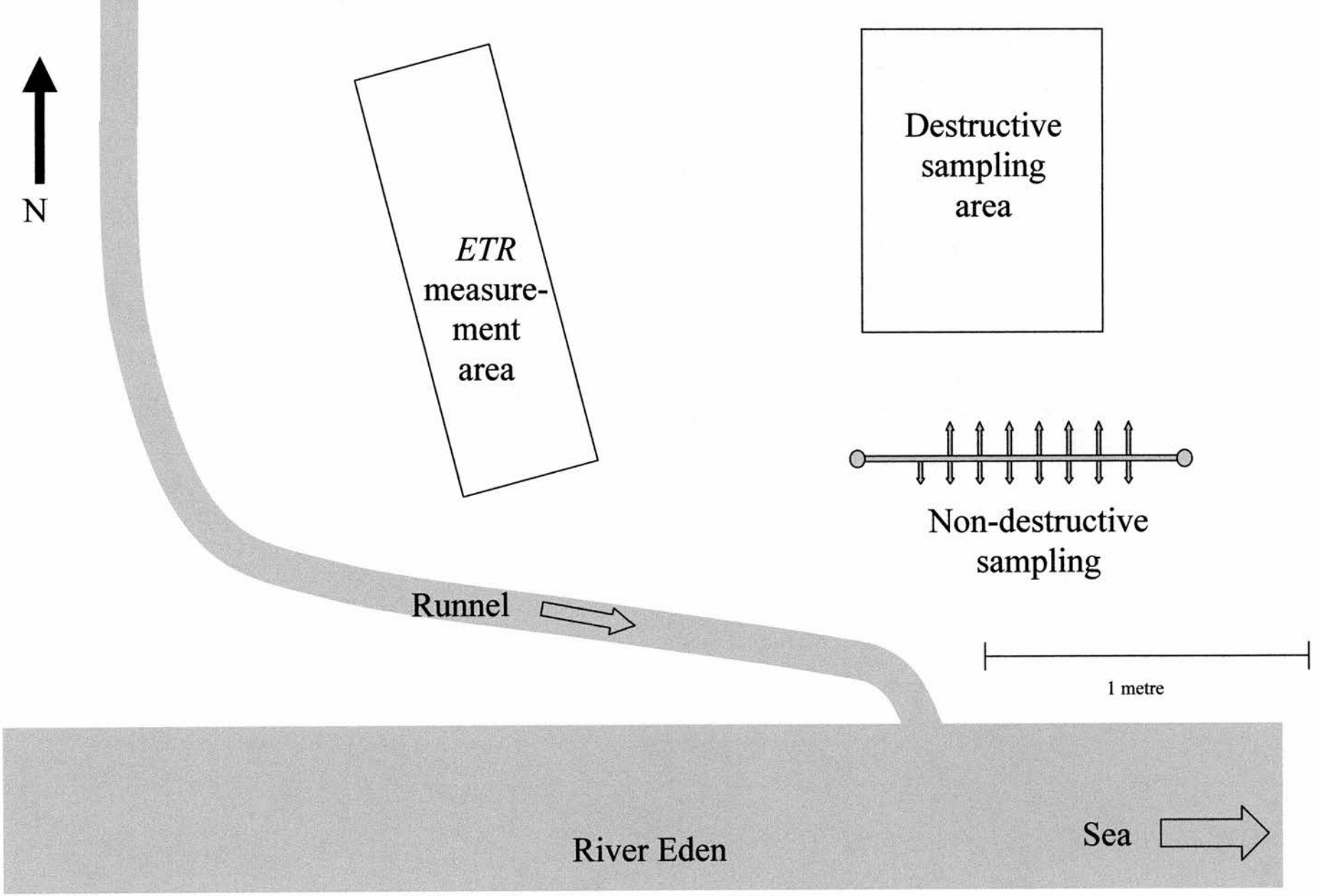

Figure 7.1. A) Temporal study site, situated in the low shore zone, Eden north shore, May 2000

B

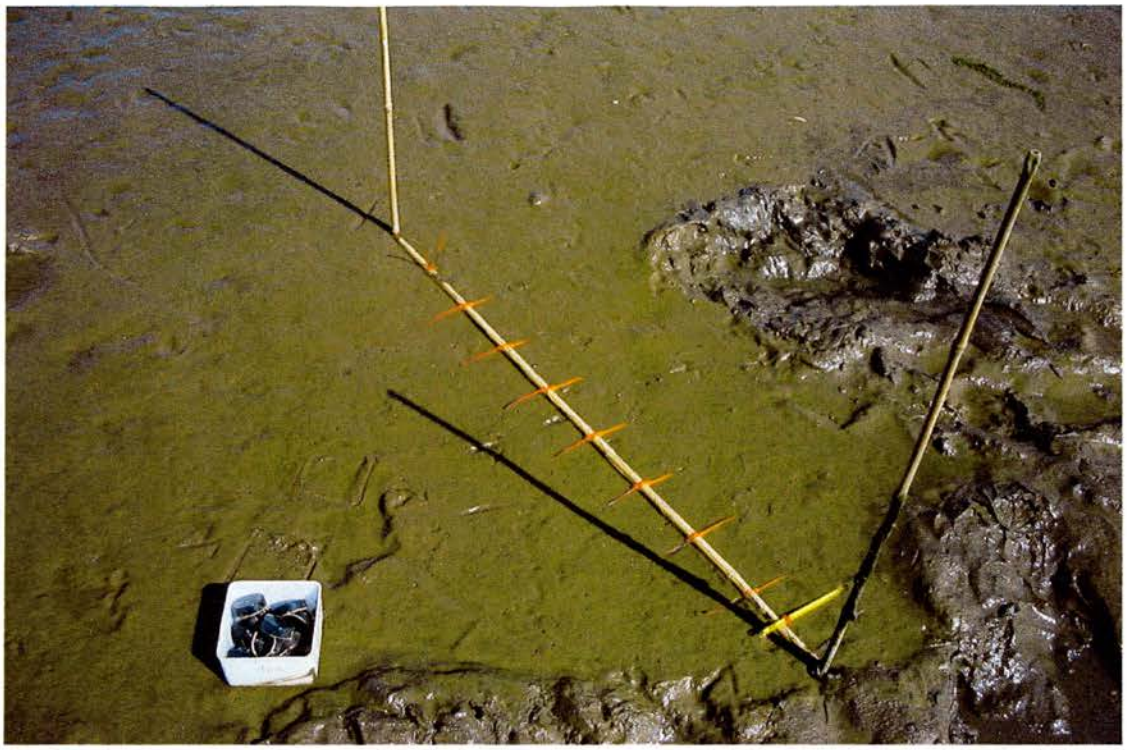

C

Figure 7.1 B and C. Photographs of areas of sediment used for dark adapting microphytobenthos *in situ*. B) Non-destructive Fo^{15} measuring area. The two upright canes are 1 m apart. The horizontal cane has markers attached, which point to the each of the 15 patches for repeated temporal measures. C) Destructive Chl *a* measuring area. Pegs were randomly placed at the beginning of each day and 5 contact cores were taken at 3 intervals throughout the tidal emersion period

(Fig. 7.1A; ETR area). Measurements under filtered light were performed by shading adjacent patches of sediment with 4 different neutral density filters (28, 36, 48, 66% reduction of natural irradiance) to give a range of 5 PPFD levels including natural irradiance. Each patch (chosen randomly) was adapted to each filter for a period of 3-5 min. Approximately two replicates at each irradiance level were made every hour. Measurements for rETR were made with the fluorometer probe tip at an angle to the sediment, and PAR sensor, both held in the angled probe holder (Chapter 3). PPFD was plotted against rETR to produce photosynthesis versus irradiance (*P-E)* curves. *P-E* curves were fitted after Walsby (1997), and *P-E* parameters were determined from these curves.

An *Fv/Fm* value was recorded for each Fo^{15} measurement made, however, only *Fv/Fm* values of higher biomass ($Fo^{15} > 150$) were considered as reliable (see Chapter 3) and used in analysis. The $\Delta F/Fm'$ was recorded every hour on separate patches, and only $\Delta F/Fm'$ values with corresponding steady state fluorescence values (F) > 100 values were considered as reliable (as many of the outliers had low F values, also see Chapter 3) and used in analysis.

7.2.1.3. Pigment analysis

Five random surface sediment samples were taken at 3 intervals (approximately 10 cm apart) using the contact corer during the emersion period (beginning/mid/end) for pigment analysis and water content determination (Fig. 7.1A, destructive sampling area; Fig. 7.1C). The Chl *a* concentration of the sediment and ratios of other pigments to Chl *a* were ascertained from sediment extracts analysed on the HPLC (Chapter 2). Prior to contact cores being taken, fluorescence measurements (Fo^{15} and *Fv/Fm*) were made on the patch of sediment to be sampled, to check that the non-destructive fluorescence (see above) measurements were similar.

Lens tissue and samples for Low Temperature Scanning Electron Microscopy (LTSEM) for diatom species analysis were also collected every hour (these results were analysed separately by M. Consalvey and are not shown here).

7.2.2. Study B; August 1997

A pigment study at finer resolution was also completed on Eden samples collected previously from an area used in the Study A site (low shore, close to Paper Mill transect), during an emersion period on the 23 August 1997. Three Cryolander

replicates were taken at three times during an emersion period; as the tide ebbed, at low tide and just before the tide flooded. This emersion period was similar to the tidal pattern of Day 1 in Study A, when low tide was at 12:30 hrs (tidal ebb at 09:46). Each Cryolander was sliced to a depth of 1 mm at varying intervals of 0 – 0.2 mm, 0.2 – 0.4 mm and 0.4 – 1 mm. The turbidity of the ebbing water was also measured on this date.

7.2.3. Statistical analysis

Unless otherwise specified data was normally distributed and homoscedastic, thus ANOVA and GLM were used, with Tukeys pairwise comparisons for *post hoc* analysis. Non-parametric tests were used on non-normally distributed data and are described in the text. Regression analysis (line of least squares) was completed on normally distributed data.

7.3. Results

7.3.1. Physical variables

7.3.1.1. Irradiance

The ambient incident irradiance during the emersion periods over the six days was generally variable, but usually quite high, since cloud cover was limited (Fig. 7.2A). The emersion periods on Day 4, 5 and 6 were almost cloud free, Day 1 was initially cloudy for about an hour just before the time of low tide. Day 2 emersion period was initially cloudy and became sunnier after 2 hrs 30 min. The irradiance on Day 3 was very changeable (Fig. 7.2A). The dose of irradiance per emersion period (ep) generally decreased over the 6 days with a PPFD of 439 mmol m^{-2} ep^{-1} on Day 1, decreasing to 99 mmol m^{-2} ep^{-1} on Day 6 (Fig. 7.2B). Day 5 however had a PPFD of 65 mmol m^{-2} ep^{-1} due to the emersion period starting early morning, with low tide only 30 min after dawn.

7.3.1.2. Temperature

The surface sediment temperatures generally followed the same pattern as incident irradiance, apart from the emersion period on Day 5 which gradually dipped by ~4°C (to 9°C) at the time of low tide, which coincided with dawn (Fig. 7.3A). The emersion period on Day 1 had the highest temperatures recorded during this study (22.5 °C) and had the warmest average sediment temperature of 19°C. The temperature on Day 1 was

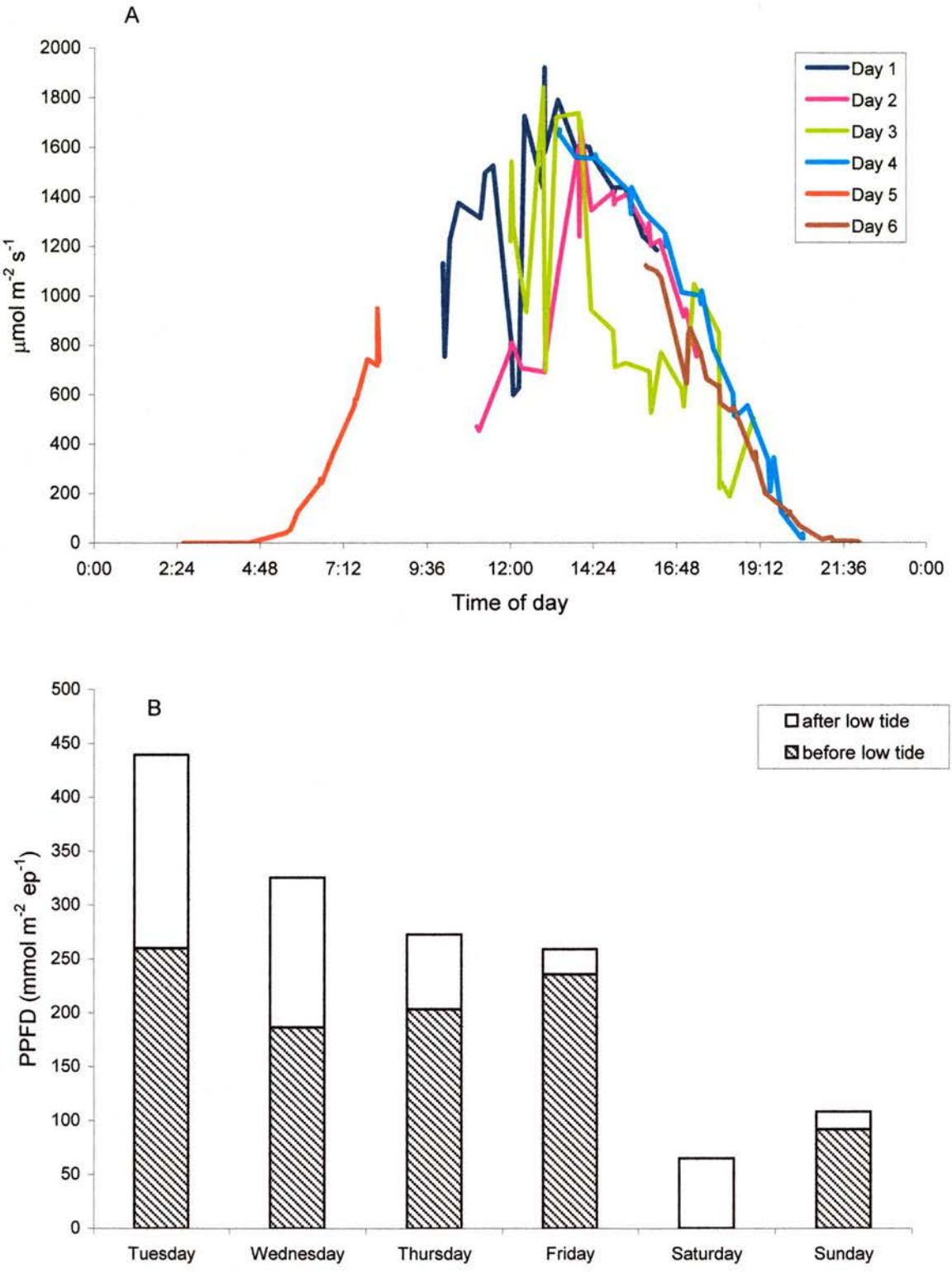

Figure 7.2. The incident irradiance on the sediment surface during 6 emersion periods, May 2000. A) The irradiance, logged every half hour, during each emersion period. B) The dose of irradiance during each emersion period

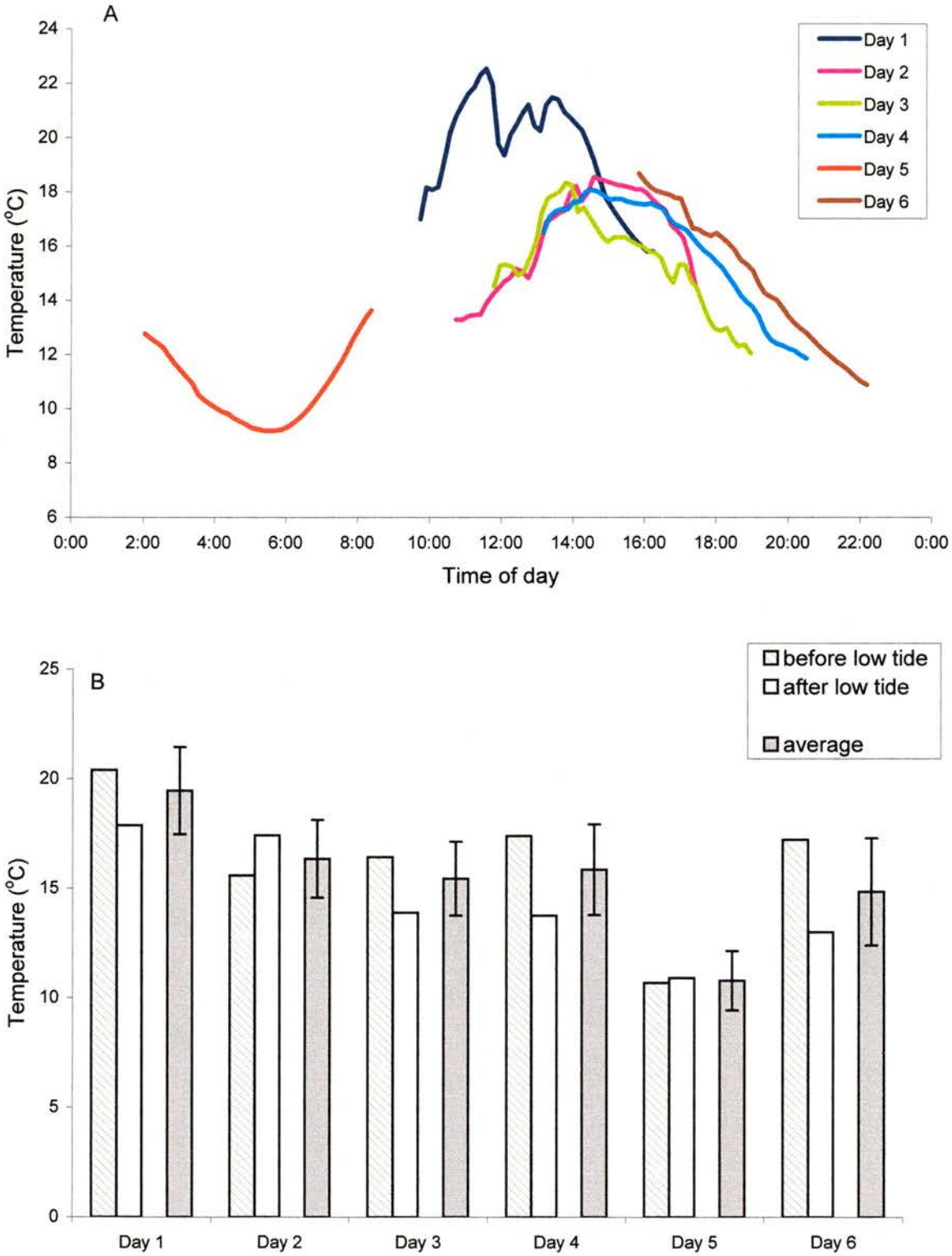

Figure 7.3. The temperature of the sediment surface during 6 emersion periods, May 2000. A) The temperature, logged every 10 min, of the surface sediment throughout each emersion period . B) The average temperatures of the surface sediment during each emersion period (average of 39 to 45 readings per period, +/- SD)

significantly higher than all the other days ($F_{1(5, 242)} = 84.2$, $P < 0.001$ followed by *post hoc* analysis ($P = 0.05$)) (Fig. 7.3A and B). Day 5, predictably, was the coolest emersion period, with and average temperature of 11°C and was significantly lower than all the other days (same ANOVA statistics as above).

7.3.1.3. Water content

There was a significant decrease in water content of the surface 2-3 mm of sediment between the start of the emersion period compared with the mid or end ($F_{2(2, 5, 10)} = 73$, $P < 0.001$) (Fig. 7.4). *Post hoc* analysis revealed all pairs were significantly different (start vs. mid and start vs. end ($P < 0.001$), mid vs. end ($P = 0.017$). Water content of the surface sediment varied from 70 % as the tide ebbed to 55 % just before flooding. There was no difference in sediment water content between days ($F_{2(2, 5, 10)} = 0.69$, $P > 0.5$).

7.3.1.4. Tidal water turbidity

The turbidity of the tidal water varied significantly over the six emersion periods sampled ($F_{2(5, 1, 35)} = 10.3$, $P < 0.001$). High turbidity of the tidal water was found on the ebbing tide on Day 2 and both the ebbing and flooding tide of Day 3, with values in the region of 400 mg dry sediment l^{-1} (Fig. 7.5). Tidal water turbidity was lowest on the ebbing tides on Day 1 and 2 (below 40 mg dry sediment l^{-1}).

During the study in August, 1997, the turbidity of the ebbing water was low; 23 mg sediment l^{-1}.

7.3.2. Minimum Fluorescence

There was a general increase in Fo^{15} at the sediment surface throughout the emersion period on most days (Figs 7.6A-F). The increase in Fo^{15} was very variable between the 15 patches (treated as replicates), each patch also varied greatly between days (Figs 7.6A-F). The area being sampled was visually very patchy and thus variation in measurements was expected. Both the average Fo^{15} of the 15 patches and single patch dynamics will be discussed in more detail below.

7.3.2.1. Biofilm Dynamics

Biofilm dynamics was inferred by averaging the 15 patches. The lowest average value of Fo^{15} was 17 which was before sunrise on the morning of Day 5, and the highest average value of Fo^{15} was 412 on Day 3, some 2 hours before tidal flood (Fig.

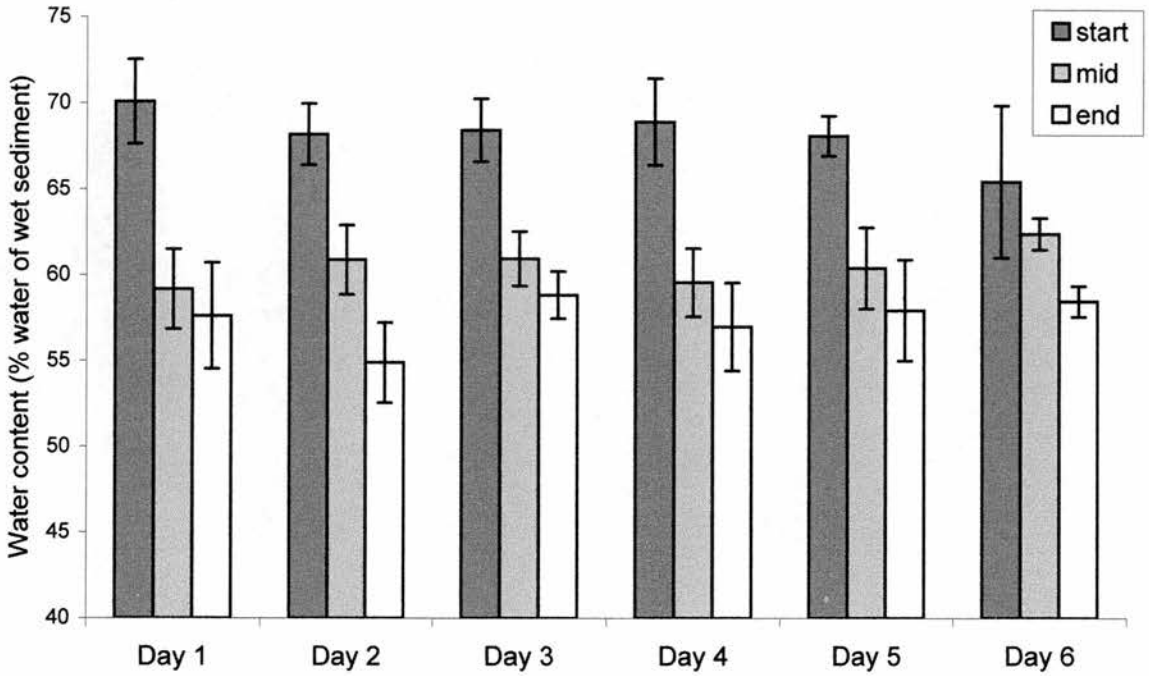

Figure 7.4. Water content of surface sediment during 6 emersion period, May 2000 (n = 5 +/-SD)

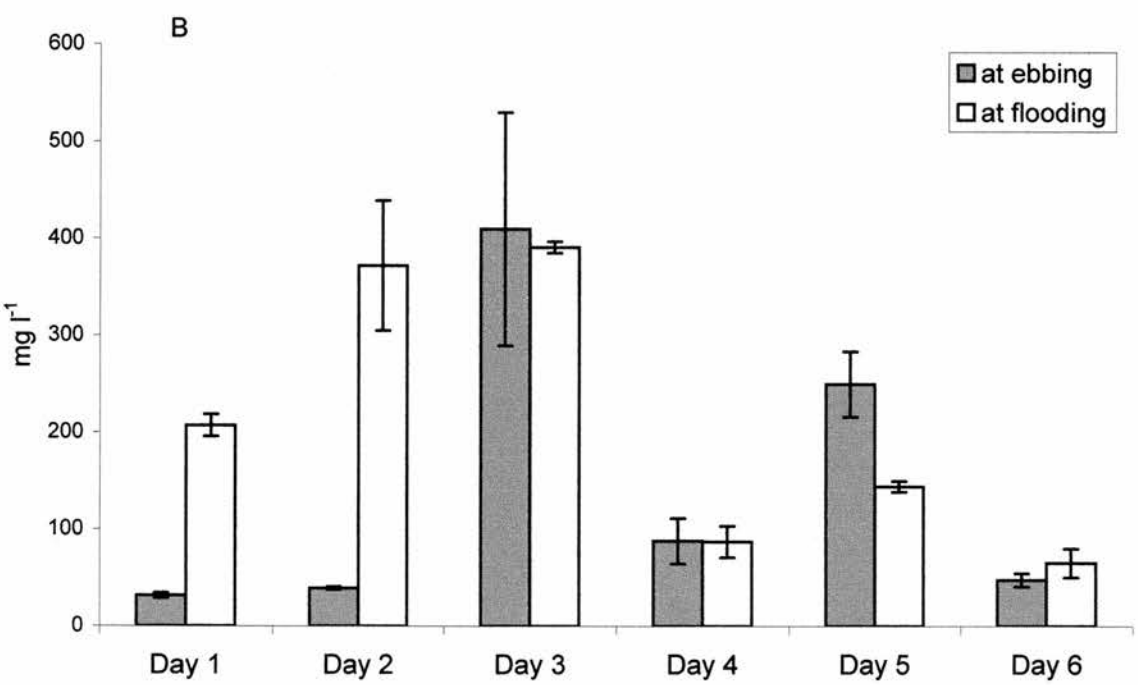

Figure 7.5. Turbidity of tidal water at the beginning and the end of 6 emersion periods, May 2000 (n = 5 +/-SD)

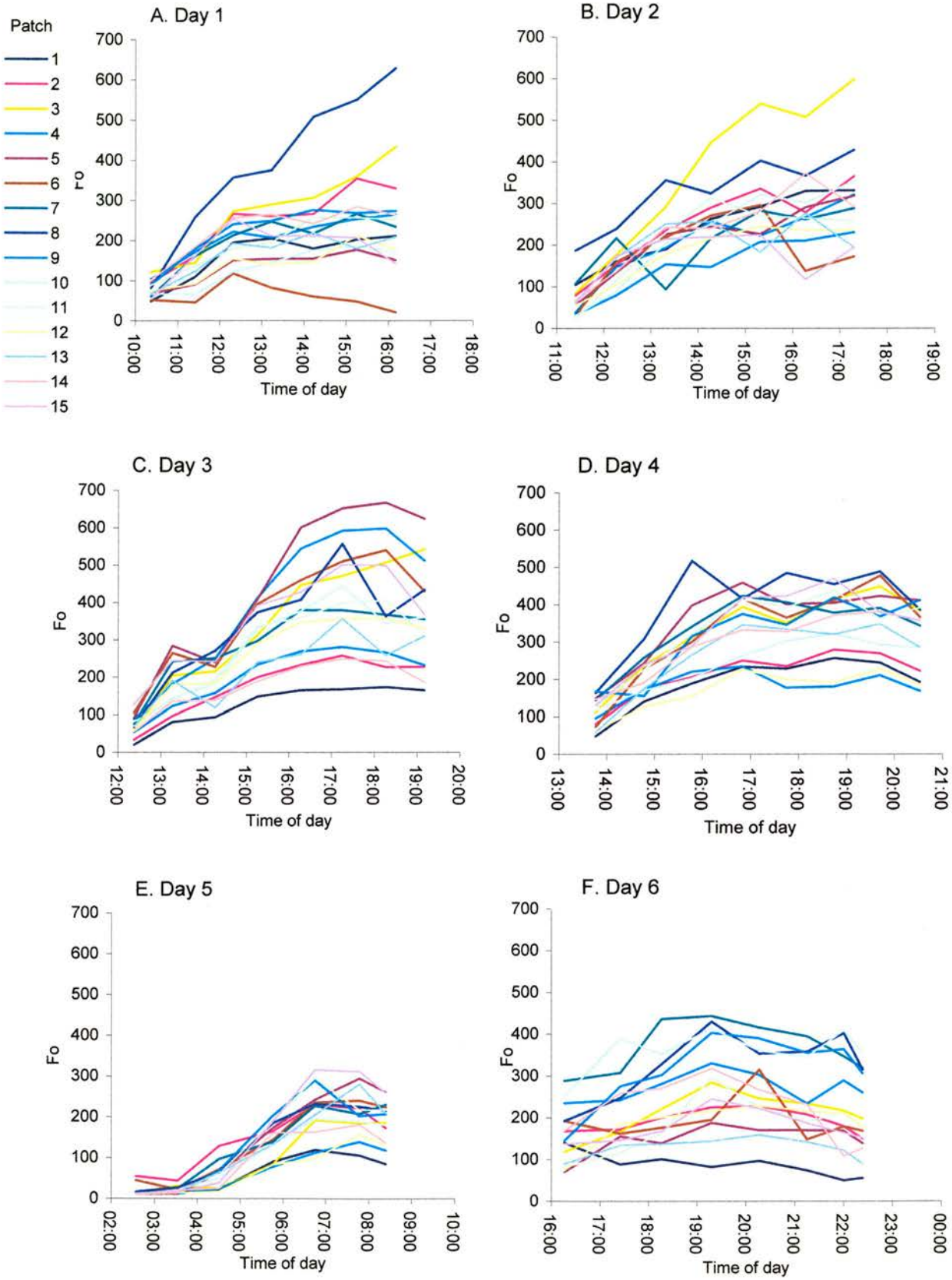

Figure 7.6. Changes in Fo'^{15} during each emersion period

7.7). The lowest and highest single patch readings of Fo^{15} ranged from 9 (Fig. 7.6E) to 667 (Fig. 7.6C). The largest increase over a whole emersion period was on Day 3 with an Fo^{15} value of 341 and the smallest increase was on Day 6 with a value of 124 (Fig. 7.7). There were significant differences between patches, between days and between times during emersion period ($F_{3(15, 5, 6, 629)} = 11.3, 81.2, 125.4$ respectively, $P < 0.001$ for all factors). Differences between patches will be discussed in a following section (7.3.2.2, single patch biomass dynamics). Differences between days will be addressed on a more specific basis (e.g. comparisons between all Fo^{15} values at tidal ebb or peak Fo^{15}; see following sections; 7.3.2.1a-d). Differences in Fo^{15} values between times were significant (see above) and when all data was pooled, time 0 had significantly lower Fo^{15} values than all other times (*post hoc* analysis; $P < 0.001$), times 1 and 2 were also significantly lower than all other times (*post hoc* analysis; both $P < 0.001$). Days were analysed separately and showed significant differences in Fo^{15} with time on all days (Table 7.2). *Post hoc* analysis showing which times were different in Fo^{15} are also shown in Table 7.2.

7.3.2.1.a. Fo^{15} at tidal ebb

The first set of Fo^{15} measurements (taken as soon as the tide ebbed) for each day was significantly different between days ($F_{1(5, 89)} = 43.0$, $P < 0.001$) and varied from 17 before dawn on Day 5 to 157 on Day 6 when the first measurements were late afternoon (Fig. 7.8). The first set of Fo^{15} measurements on Days 1, 2, and 3 were 79, 68 and 70 respectively and were not significantly different from each other (*post hoc* analysis; $P > 0.05$). The first set of Fo^{15} measurements on Day 4 was 112 and was not significantly different than the first set of measurements on Days 1 or 6 ($P > 0.05$). All other combinations were significantly different ($P < 0.05$), most notably; the first Fo^{15} measurements on Day 5 were significantly lower than all other days and the first Fo^{15} measurements on Day 6 were significantly higher than all days (except Day 4) (Fig. 7.8).

7.3.2.1.b. Peak Fo^{15}

The Fo^{15} values peaked (determined as the first highest average Fo^{15} measurement) on Days 1, 3 and 4 in the 6th hour, Day 2 peaked during the time 6 and Days 5 and 6 peaked at time 4 and 3 respectively (Fig. 7.10A and B). The peak in Fo^{15} values were significantly different between days ($F_{1(5, 89)} = 7.06$, $P < 0.001$). *Post hoc*

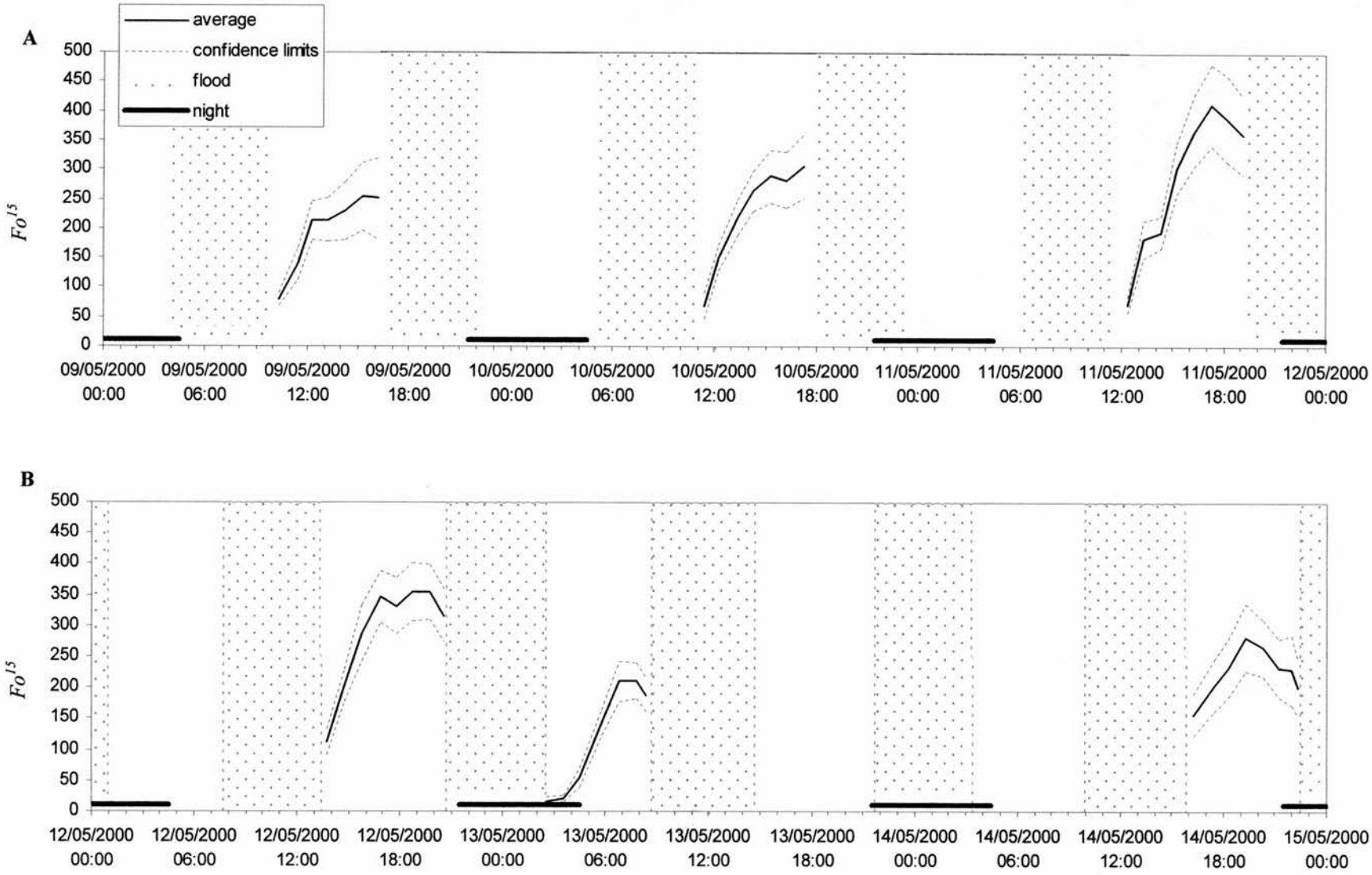

Figure 7.7. The average Fo^{15} (with confidence limits) over the six sampling days in May 2000, in relation tidal and diurnal cycles. The first 3 days (A) and the last 3 days (B) of the sampling period

Table 7.2. ANOVA of Fo^{15} values between times of each separate day.

	Day 1	**Day 2**	**Day 3**	**Day 4**	**Day 5**	**Day 6**
numerator, denominator	6, 104	6, 104	7, 119	7, 119	6, 104	7, 119
F	10.9	19.9	20.4	17.8	111.4	2.7
P	< 0.001	< 0.001	< 0.001	< 0.001	< 0.001	< 0.02
Times which were significantly different at P < 0.05	0 and 2 0 and 3 0 and 4 0 and 5 0 and 6 1 and 4 1 and 5 1 and 6	0 and 2 0 and 3 0 and 4 0 and 5 0 and 6 1 and 3 1 and 4 1 and 5 1 and 6 2 and 6	0 and 3 0 and 4 0 and 5 0 and 6 0 and 7 1 and 3 1 and 4 1 and 5 1 and 6 1 and 7 2 and 4 2 and 5 2 and 6 2 and 7	0 and all subsequ-ent times 1 and 3 1 and 4 1 and 5 1 and 6 1 and 7	0 and 2 0 and 3 0 and 4 0 and 5 0 and 6 1 and all subsequ-ent times 2 and all subsequ-ent times 3 and 4 3 and 5	0 and 3 0 and 4

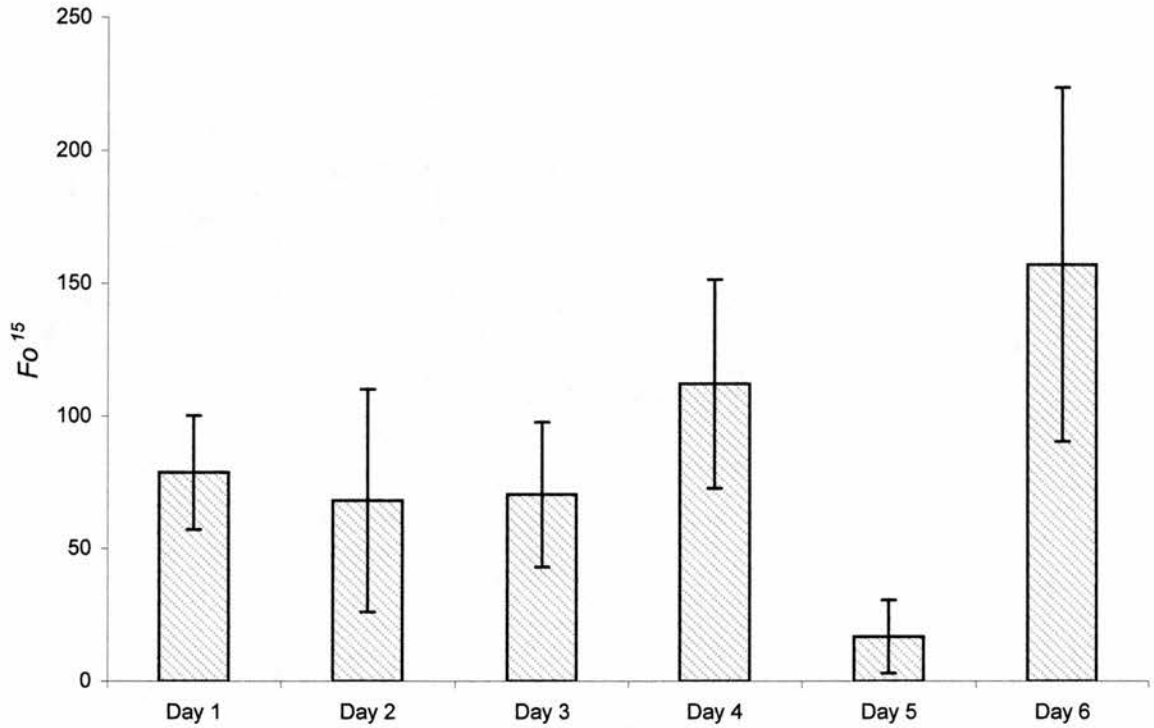

Figure 7.8. The first average *Fo* ^{15} readings, just after the tidal ebb during 6 emersion periods, May 2000 (n = 15 +/-SD)

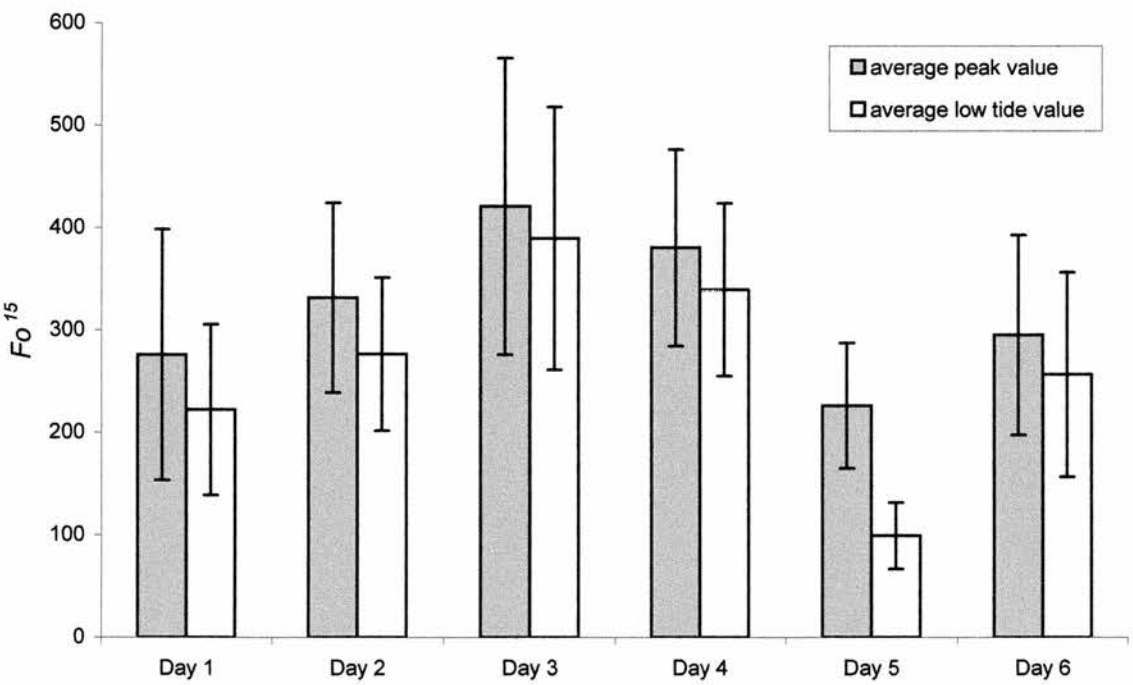

Figure 7.9. The highest average *Fo* ^{15} and the low tide average *Fo* ^{15} readings during 6 emersion periods, May 2000 (n = 15 +/-SD)

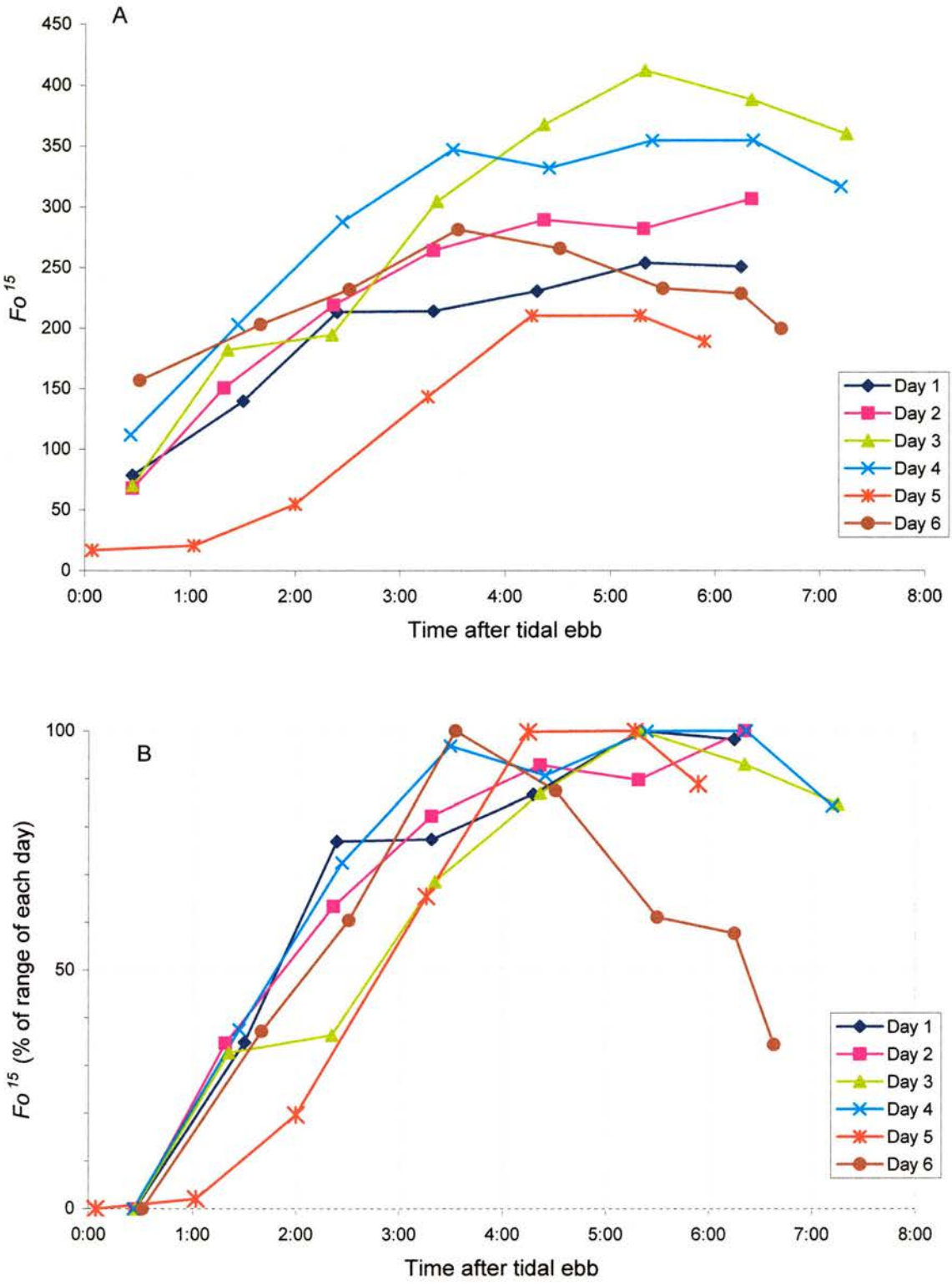

Figure 7.10. Changes in Fo^{15} after tidal ebb during each emersion period, May 2000. A) The change in Fo^{15} after tidal ebb on all days . B) The percentage change in Fo^{15} of range for each day after tidal ebb

analysis ($P < 0.05$) revealed significant differences between the lowest peak Fo'^{15} values on Day 5 with the highest peak values on Days 2, 3 and 4. The highest peak Fo'^{15} values on Days 3 and 4 were also significantly higher than the peaks on Day 1 and 5.

As the peak in Fo'^{15} did not occur until after low tide on most days, the Fo'^{15} values at low tide (as a measure of biomass, see Chapter 4) was compared to the highest (peak) Fo'^{15} value during the emersion period (Fig. 7.9). Low tide Fo'^{15} values were significantly lower than peak values ($F_{2(1, 5, 179)} = 15.6$ $P < 0.001$). *Post hoc* analysis, however, revealed the only significant difference between low tide and peak values was on Day 5 ($P < 0.05$, all other days $P \geq 0.9$).

7.3.2.1.c. Fo'^{15} at the end of the emersion period

There was no significant difference from the peak Fo'^{15} measurements and all subsequent measurements on all days (*post hoc* analysis; $P > 0.05$). This shows that although Days 3 to 6 showed decreases in Fo'^{15} near the end of the tidal emersion, they were not significant decreases.

7.3.2.1.d. The rate of increase in Fo'^{15}

Excluding readings on Days 5 and 6, which were affected by dawn and dusk, the average rate of increase in Fo'^{15} measurements at the surface were 92 per hour for the first hour of measurement (between time 0 and 1), followed by 61 and 54 for the next two hours (Fig. 7.11A). The rate of increase of Fo'^{15} then decreased to approx. 22 in the 4th and 5th hour, there was no increase in the 6th hour, and a decrease of 39 in the 7th hour (Fig. 7.11A). On Day 5, when the tide ebbed before dawn, there was no significant increase in Fo'^{15} until the 2nd hour after tidal ebb, when it was beginning to get light ($F_{1(6, 98)} = 61$, $P < 0.001$, followed by *post hoc* analysis determined significance at the level of $P < 0.05$) (Fig. 7.11B). The largest hourly increase in Fo'^{15} was 124 in the first hour on Day 3 and the steepest decline in Fo'^{15} was 75 in the 7th hour on Day 6 (Fig. 7.11B). As a more comparative assessment of the rate of increase on each day, Fo'^{15} was expressed as a percentage of the range of each day (Fig. 7.10B). The rate of increase, expressed as a percentage of the daily range, within the first 3-4 h was remarkably similar between days. Although Fo'^{15} on different days peaked over a period spanning 3 h, 90% of the increase on all days occurred within a period of an hour and a half of each other (between 3h 10 min to 4 h 40 min after tidal ebb). Also,

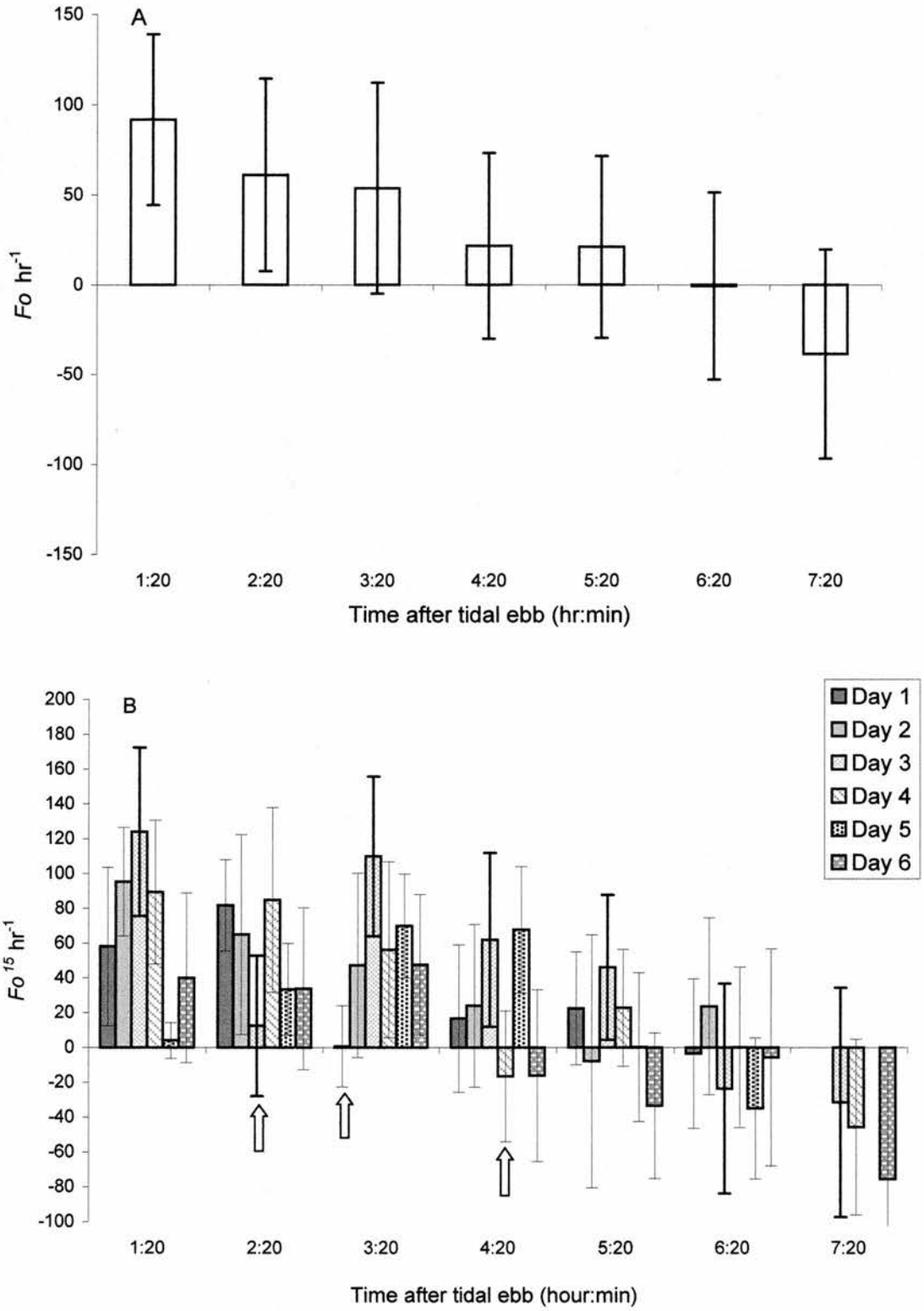

Figure 7.11. The hourly change in Fo^{15} during each emersion period, during 6 emersion periods, May 2000. A) The average hourly change in Fo^{15} on Day 1 to 4 pooled (n = 60 +/-SD). B) The hourly change in Fo^{15} on each separate day (n = 15 +/-SD). Block arrows indicate low rates of increase during a period of normally high rates

50 % of the daily increase in Fo^{15} occurred within 65 min of each other (between 1 h 45 min to 2 h 50 min after tidal ebb) (Fig. 7.10B).

7.3.2.2. Single Patch Biomass Dynamics

A patch of sediment which showed a high or low increase in Fo^{15} on one particular day did not necessarily show a similar increase on consecutive days (compare patches between days in Figs 7.6A-F). The variation of the highest peak in Fo^{15} during an emersion period was used as an indication of how each patch varied in photosynthesising biomass on a day to day basis (between-day patch dynamics). Single patches differed enormously in peak Fo^{15} between days (Fig. 7.12A). The patch with the lowest variation in peak Fo^{15} between days was patch 2 with a coefficient of variation (CV) of 20% and the most variable patch (6) had a CV of 60% between days (Fig. 7.12A). Two thirds of the patches were less variable between days in peak Fo^{15}; having lower CV (between 20-36%; Fig. 7.12B). The peak Fo^{15} (mean of 15 replicates) varied between days with a CV of 23%.

Variability (CV) between patches at any one moment in time ranged between 24% to 82%, 31% on average (across all days and sampling times). Variation between patches was at its lowest around the time of low tide (Fig. 7.13). Most of the CV between the replicate patches were below 40%.

7.3.3. Microphytobenthos stress

Only reliable *Fv/Fm* measurements were used in analysis (those corresponding to Fo^{15} values > 150), thus many of the early emersion period measurements could not be used (and are indicated as no data in Table 7.3). The single highest reliable *Fv/Fm* value recorded for study period was 0.793 on the morning of Day 5 at 05:46, the average highest reliable reading (0.776) was also measured at this time.

There was low variation in *Fv/Fm* values between patches (Fig. 7.14A); with an average CV of 4% (ranging from 1.3 to 13.5%). There was a general average decrease of *Fv/Fm* over the emersion period on Days 1, 2 and 5, and a general increase of *Fv/Fm* over the emersion period on Days 4 and 6 (Fig. 7.14B). Day 3 had variable *Fv/Fm* values. Many of the increases on Days 1, 2 and 5 and decreases on Days 4 and 6 were statistically significant (see Table 7.3). There was slight increase (not significant) in *Fv/Fm* on Day 1 during the 5th hour and a significant increase on Day 3 during the 3rd hour, which lasted until the 6th hour (see Table 7.3). Day 6 was the only

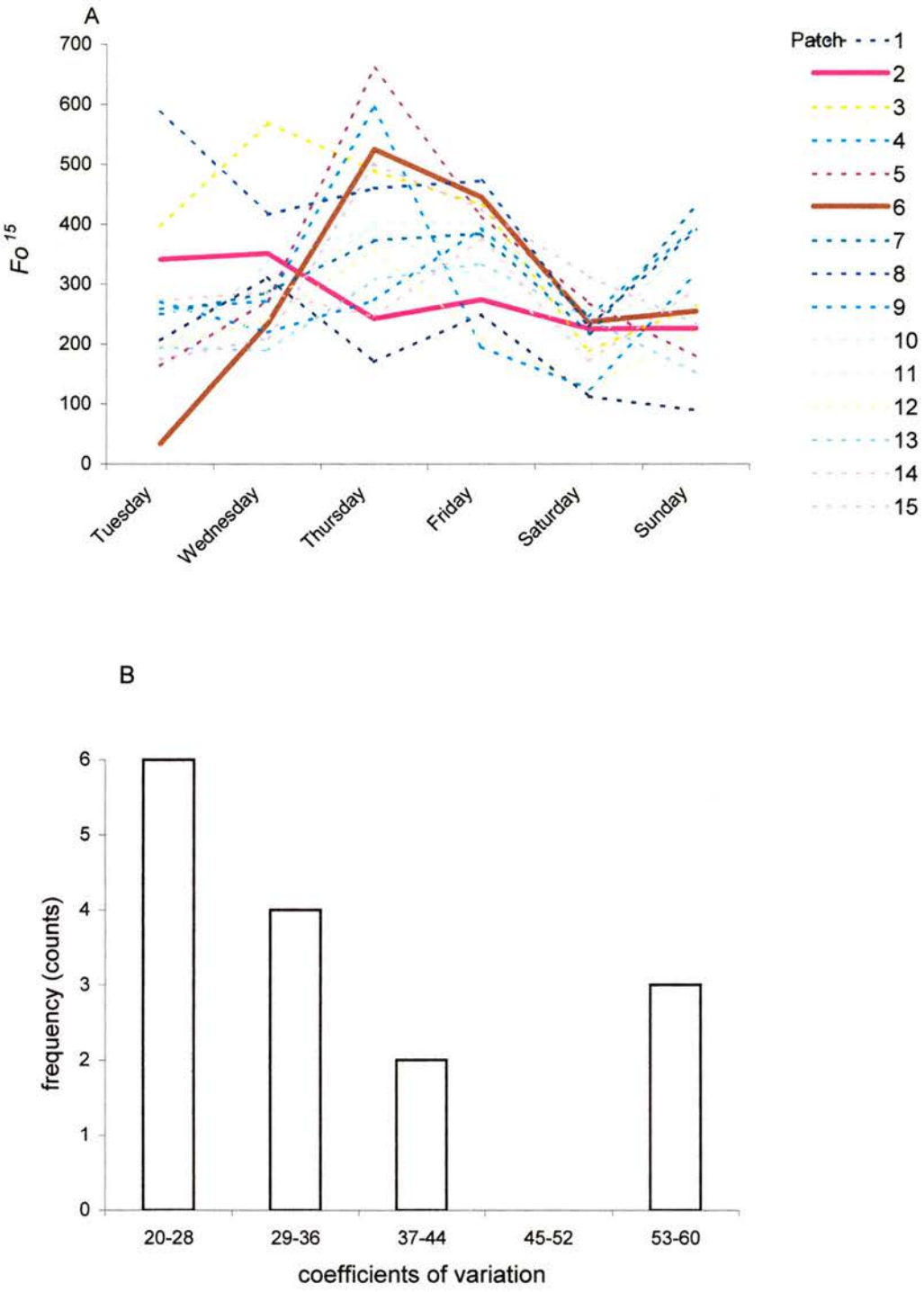

Figure 7.12. Variation in peak Fo^{15} during 6 emersion periods, May 2000. A) The change in peak Fo^{15} over sampling days (bold lines indicate highest and lowest CV between the six days). B) Distribution of the CV peak Fo^{15} of each patch between days

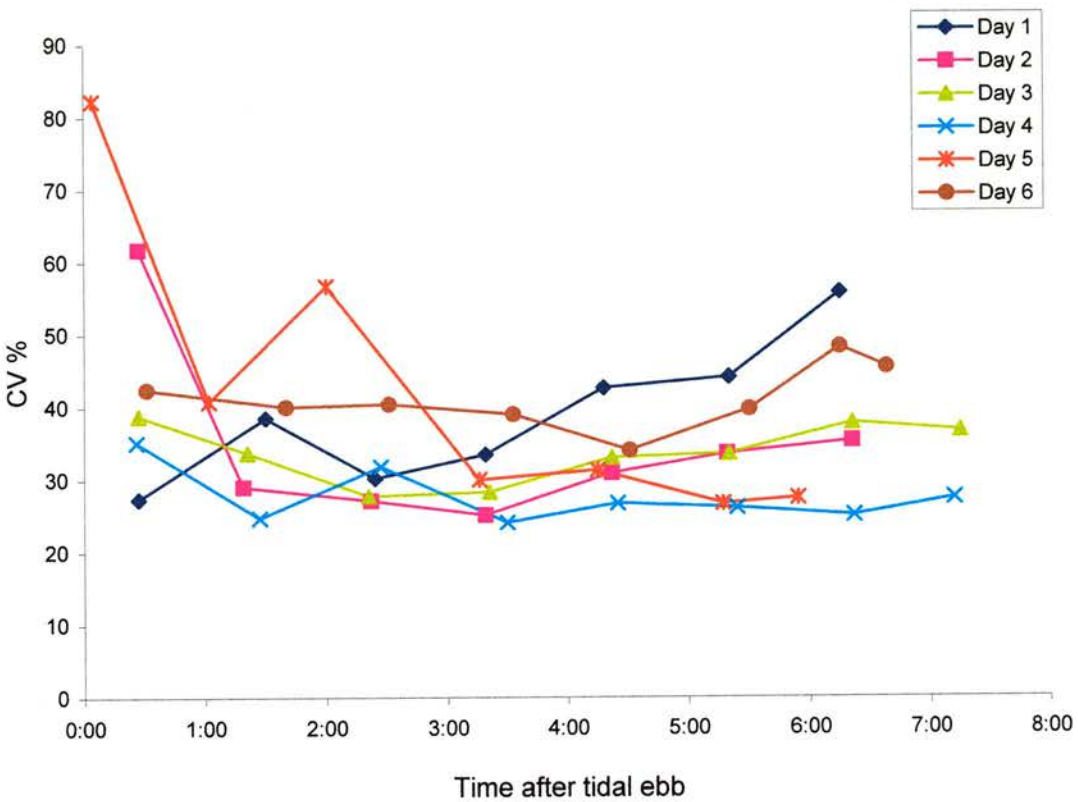

Figure 7.13. Coefficients of variation of Fo^{15} between 15 replicate patches

Table 7.3. ANOVA of *Fv/Fm* values between times of each separate day. (nd = no data; because of unreliably low Fo^{15} measurements)

	Day 1	**Day 2**	**Day 3**	**Day 4**	**Day 5**	**Day 6**
numerator, denominator	5, 66	5, 72	6, 88	6, 97	3, 39	7, 85
F	8.7	13.4	15.2	14.0	47.1	28.5
P	< 0.001	< 0.001	< 0.001	< 0.001	< 0.001	< 0.001
Times which were significantly different at P < 0.05	Time 0 =nd	Time 0 = nd	Time 0 = nd	Time 0 (only 2 reps)	Time 0 = nd	0 and 3 0 and 4 0 and 5 0 and 6 0 and 7
	1 and 6	1 and 3 1 and 4 1 and 5 1 and 6	1 and 2 1 and 3 1 and 4 1 and 5 1 and 7	1 and 5 1 and 6 1 and 7	Time 1 = nd	1 and 3 1 and 4 1 and 5 1 and 6 1 and 7
	2 and 4 2 and 5 2 and 6	2 and 4 2 and 5 2 and 6	2 and 3 2 and 4 2 and 5 2 and 6	2 and 5 2 and 6 2 and 7	Time 2 = nd	2 and 3 2 and 4 2 and 5 2 and 6 2 and 7
	3 and 6	3 and 5 3 and 6	3 and 7	3 and 5 3 and 6 3 and 7	3 and 4 3 and 5 3 and 6	3 and 6 3 and 7
			4 and 7	4 and 6 4 and 7	4 and 5 4 and 6	
			6 and 7			

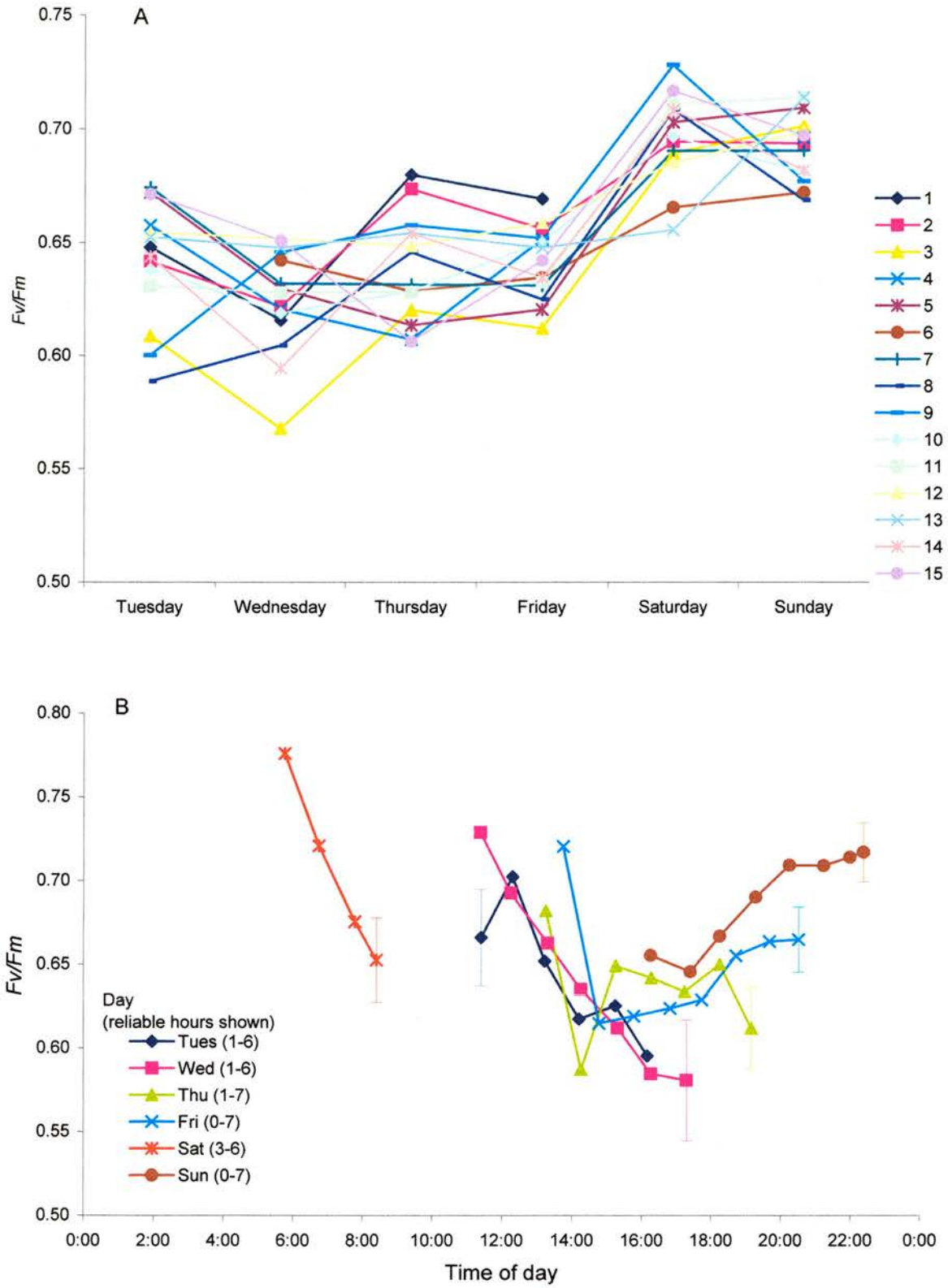

Figure 7.14. *Fv/Fm* values during 6 emersion periods, May 2000. A) The average daily *Fv/Fm* of each patch of sediment. B) The average *Fv/Fm* values during each emersion period (n varies (see Table 7.3), for clarity only the first or last SD error bar is shown for each day)

day in which the first measurements of *Fv/Fm* were lower than at the end of the emersion period. The average *Fv/Fm* per day was significantly higher on Days 5 and 6 than on all other days (times pooled; $F_{1(5, 480)} = 38.23$, $P < 0.001$; *post hoc* analysis at the $P < 0.001$ level) (Fig. 7.14A). Day 4 also had significantly higher *Fv/Fm* values than Day 2 ($P < 0.04$).

7.3.4. Electron transport rate

Relative electron transport rate (rETR) was plotted against irradiance to produce *P-E* curves, where *P* in this case was rETR. Variability in rETR was much greater at saturating light levels than at limiting levels (Fig. 7.15). $\Delta F/Fm'$ (a determinant of rETR) values were also more variable at higher irradiance levels, but also show variation at lower irradiance levels (Fig. 7.16).

The rETR data was grouped in 3 different ways to ascertain any changes in *P-E* parameters; 1) grouped by day (Fig. 7.17); 2) grouped by period of day (3 hour sections, Fig. 7.18B); and 3) grouped by period after tidal ebb (2 hours sections, Fig. 7.18B). The *P-E* parameters determined from curve fitting (Walsby 1997) were the light utilisation efficiency (α), light saturation intensity (E_k) and maximum relative electron transport rate (ETR_{max}) (described in Chapter 1). Analysis of α was also obtained from linear regressions (as well as from curve fitting) on data which had an acceptable range of low irradiance rETR values (< 300 μmol m^{-2} s^{-1}) thus ANOVA and *post hoc* analysis could be performed on the slopes. α calculated from curve fitting or calculated from linear regressions were slightly different, although the trend in the data was the same between methods. α was not significantly different between Days 4, 5 and 6 ($F_{1(2, 62)} = 2.04$, $P > 0.5$; Fig. 7.19A). α could not be determined reliably from Days 1, 2 and 3, as there were insufficient low PPFD values. There was a decrease in α with progressing time of day between the first 3 hours of daylight (to 8:30) and the last 6 hours (although this was not significant; $F_{1(2, 74)} = 1.08$, $P > 0.5$; Fig. 7.19B). α could not be determined reliably from periods around midday, as there were insufficient low PPFD values. There was a significant decrease in α with increasing exposure time/emersion period ($F_{1(3, 99)} = 4.52$, $P < 0.02$) (Figs 7.19A to C); *post hoc* analysis revealed significant difference between the period 0-2 hrs and the period 4-6 hrs after tidal ebb ($P < 0.05$; Fig. 7.19C). ETR_{max} and E_k did show

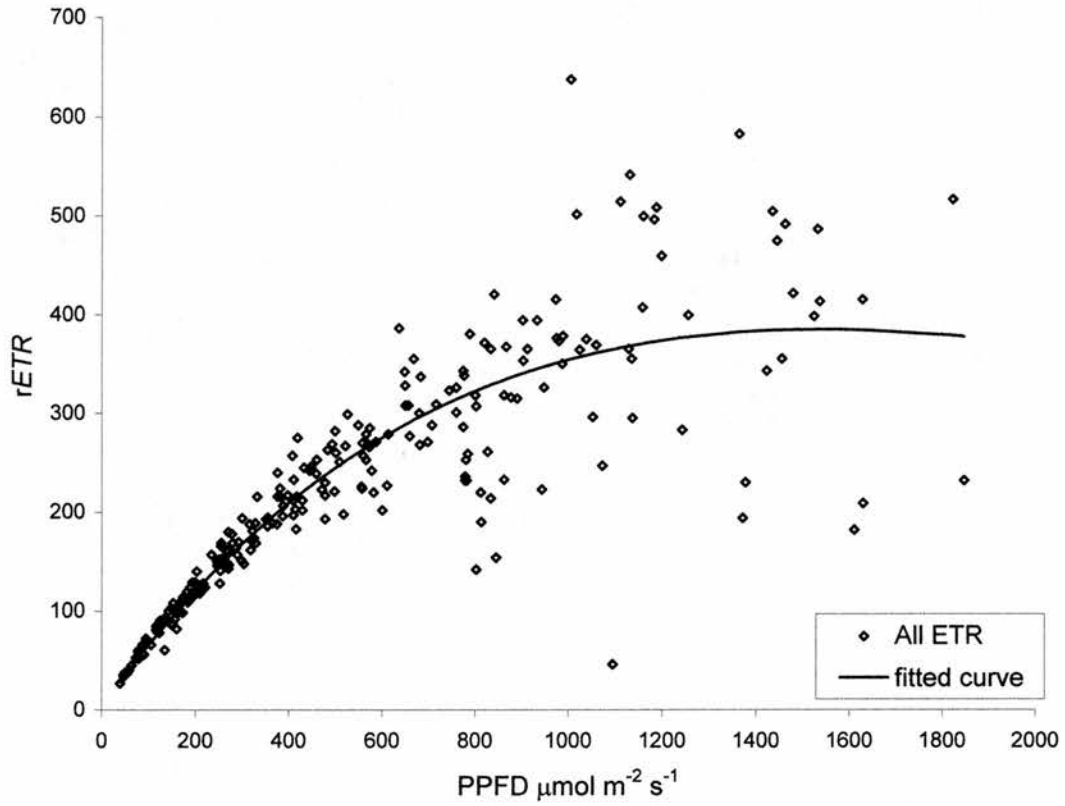

Figure 7.15. Relative electron transport rates from all emersion periods versus irrradiance (ETR-*E* curve) of microphytobenthos from migration study, May 2000

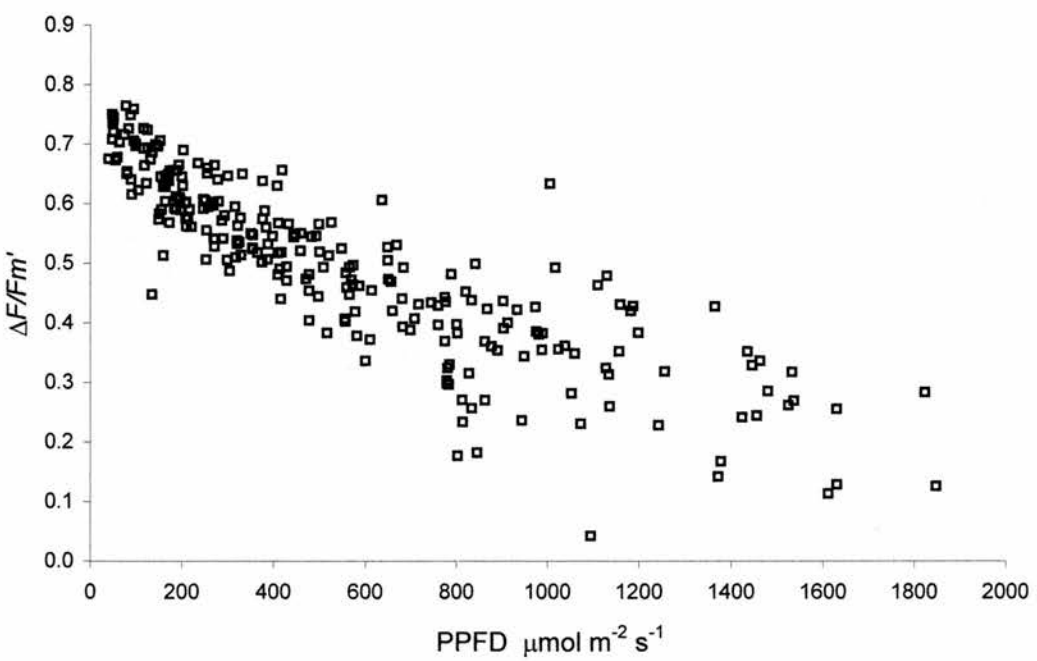

Figure 7.16. $\Delta F/Fm'$ values from all emersion periods versus irrradiance of microphytobenthos from migration study, May 2000

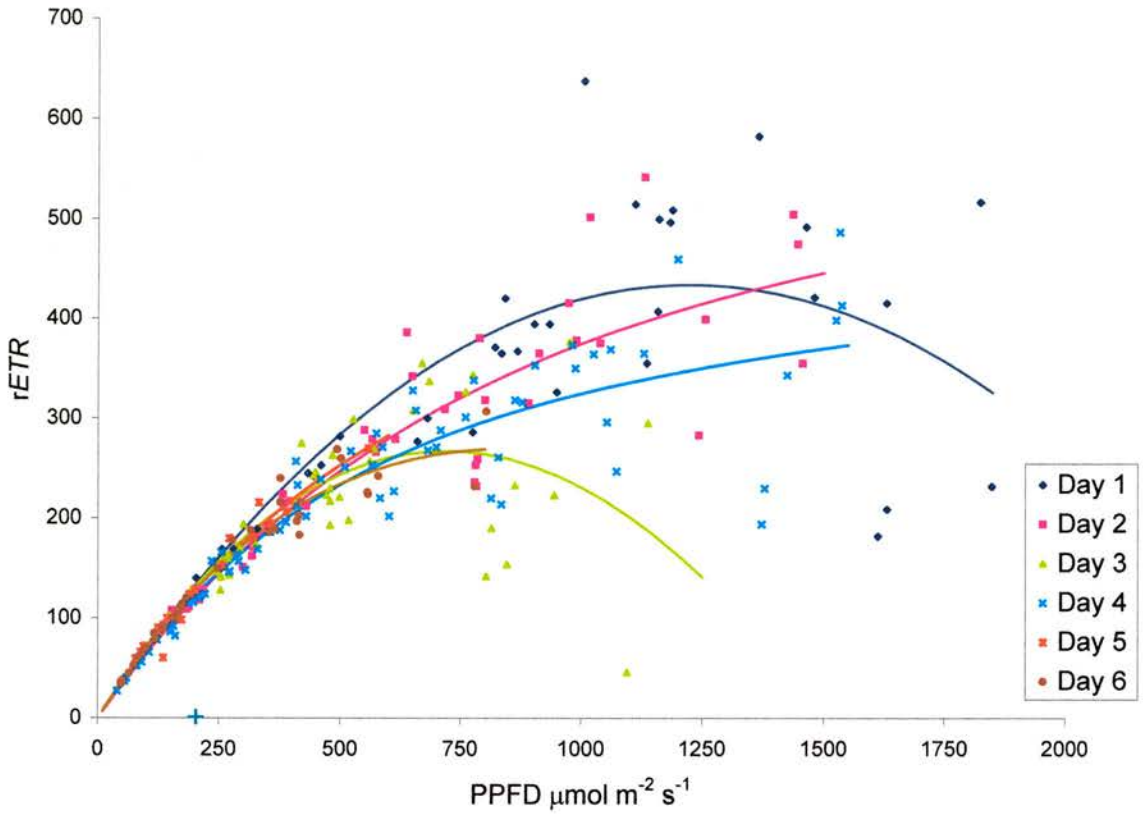

Figure 7.17. Relative electron transport rates versus irrradiance (ETR-*E* curve) of microphytobenthos from each day during the migration study, May 2000

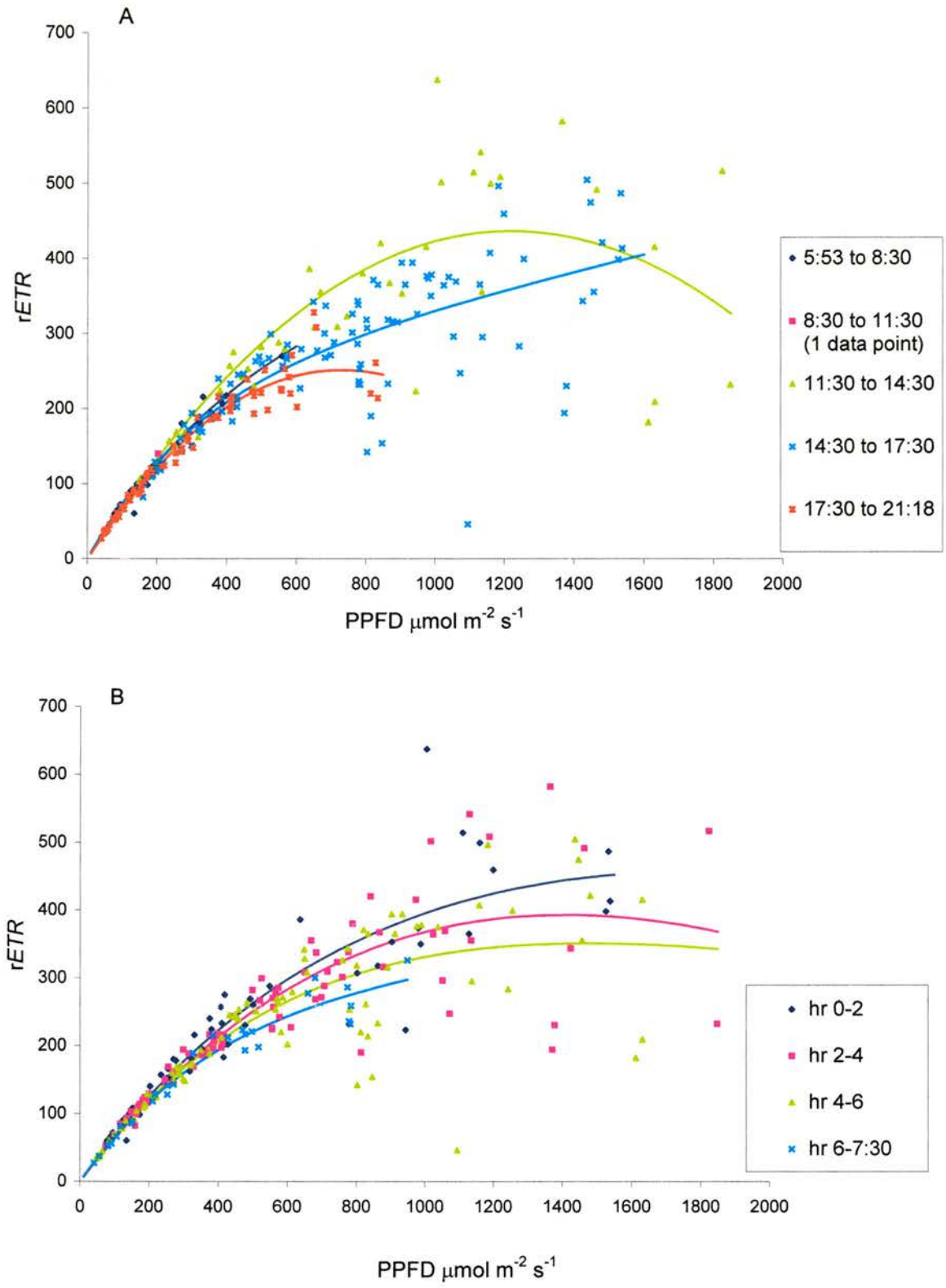

Figure 7.18. Relative electron transport rates versus irrradiance (ETR-*E* curve) of microphytobenthos during 6 emersion periods, May 2000. A) Data grouped by periods during the day. B) Data grouped by periods during emersion

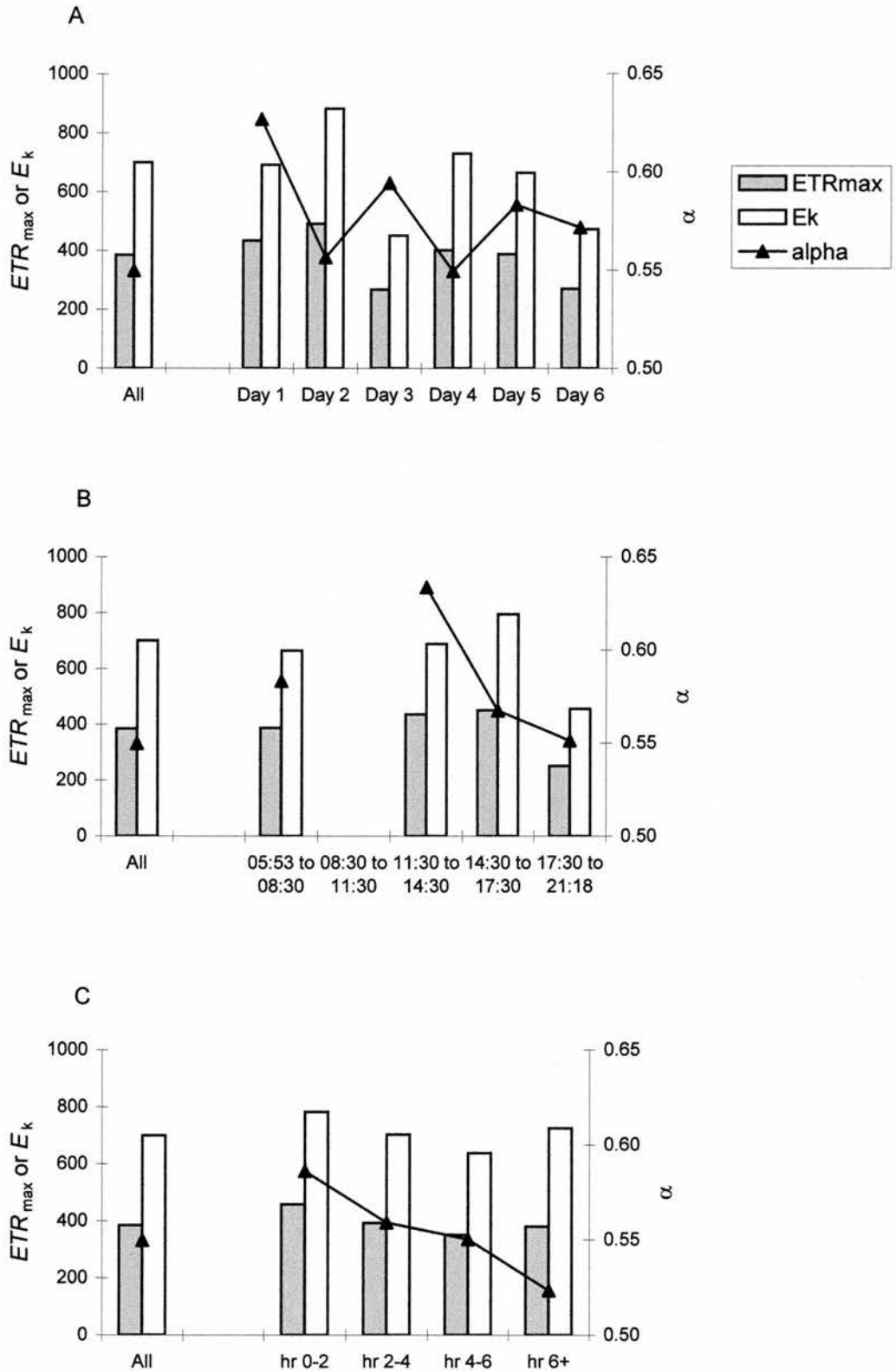

Figures 7.19. Relative electron transport rates versus irrradiance curve parameters of microphytobenthos during 6 emersion periods, May 2000. A) Parameters grouped by day. B) Parameters grouped by periods during day. C) Parameters grouped by periods during emersion

differences, but the large variability in ETR_{max} impeded any significant distinctions being determined (Figs 7.19A to C).

The average E_k for all the data was 700 μmol m^{-2} s^{-1} and determined the point at which irradiance becomes saturating for photosynthesis. Between the hours of 8:00 and 18:00, ambient irradiance was saturating for photosynthesis, except for the first hour on Day 2 and a period of 90 min on Day 3 around low tide, where irradiance levels were between 400 and 700.

7.3.5. Pigments

7.3.5.1. Study A; May 2000

Chlorophyll a (Chl *a*) was sampled three times during the tidal emersion period; start, mid and end, over the 6 consecutive days. Sampling at the start of the emersion period was equivalent to time 0, just after tidal ebb, mid was equivalent to time 4, at low tide and the end of the emersion period was equivalent to time 7, just before tidal flood. Chl *a* concentration in 2 mm of surface sediment differed significantly between times during the emersion period and between days ($F_{2(2,\ 5,\ 89)} = 20.8$ for between times, $F = 7.0$ for between days, $P < 0.001$ for both, Figs 7.20A and B). There was a significant increase over time in Chl *a* concentration over the emersion periods (*post hoc* analysis, all times were significantly different, $P < 0.02$, Figs 7.20A and B). Only on Day 5 did the Chl *a* decrease by the end of the emersion period (Fig. 7.20A).

The Chl *a* concentration between days (all times pooled) showed no recognisable pattern (Fig. 7.20B). Day 5 had the highest Chl *a* concentration (69 mg Chl *a* m^{-2}) and Day 1 had the lowest Chl *a* concentration (49 mg Chl *a* m^{-2}). *Post hoc* analysis ($P < 0.05$) showed Chl *a* concentrations on the day with the lowest values (Day 1) were significantly lower than the three days with the highest values (Days 2, 4 and 5). Day 6 also showed significantly lower Chl *a* concentrations than Day 5 (Fig. 7.20B).

Pigments were also analysed from the contact cores and were expressed as the ratio of the peak area to that of Chl *a*. Some data was unbalanced but data was normally distributed, except for the fucoxanthin data. The fucoxanthin data could not be transformed to a normal distribution therefore Kruskall Wallis analysis of differences of the medians was used for the analysis of changes in this pigment.

There were significant differences in ratios of Chl *c*:Chl *a* between days but no differences between times during emersion periods ($F_{2(5,\ 2,\ 58)} = 14.98$, $P < 0.001$

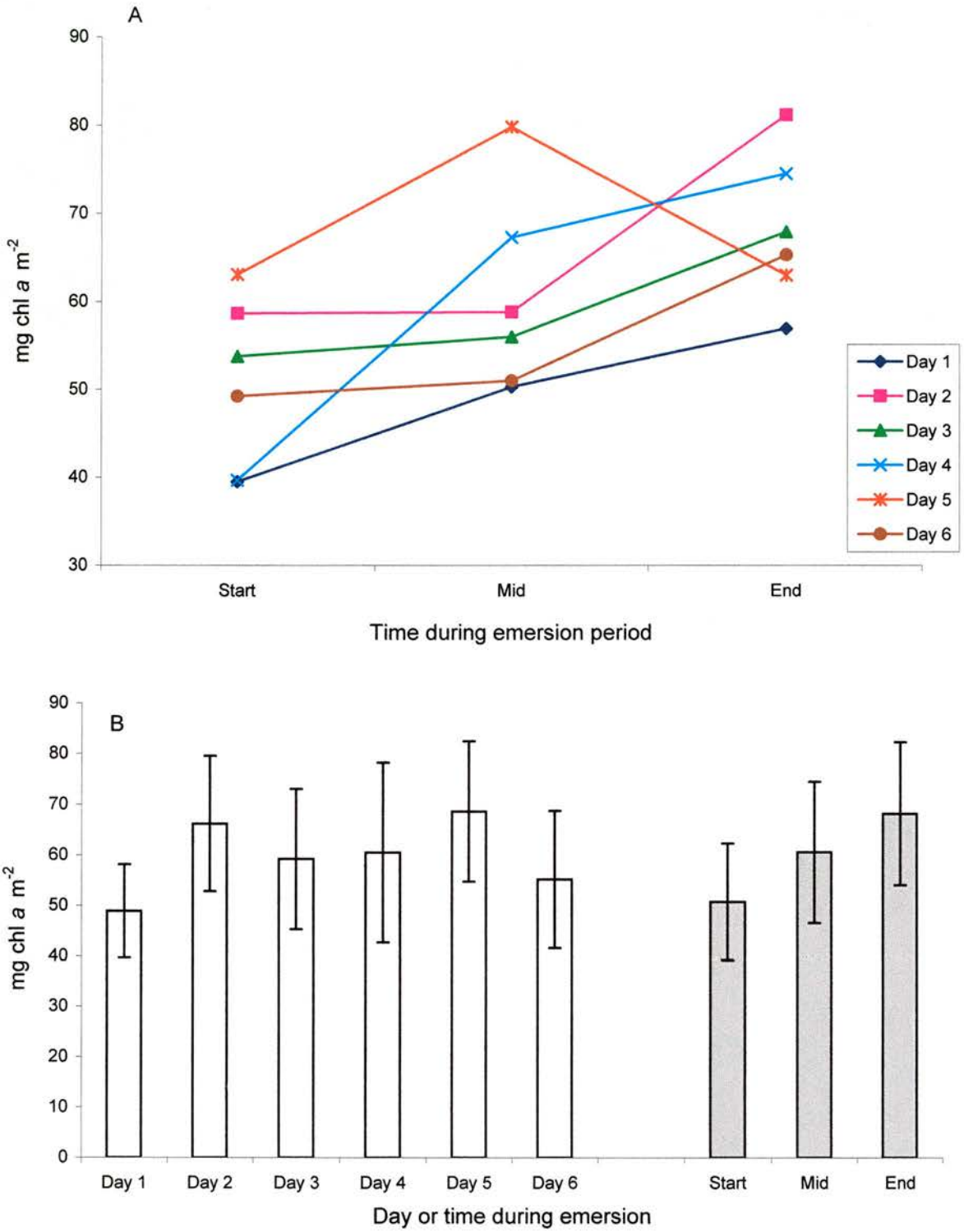

Figure 7.20. The Chl *a* content in the surface 2 mm of sediment during tidal emersion, May 2000. A) Chl *a* content during each day at three different times during the emersion period. B) The average Chl *a* content during each day (pooled emersion times) and three different times during the emersion period (pooled days)

between days, $F = 0.8$, $P > 0.2$ between times) (Figs 7.21A, 7.22A, 7.23A). This analysis showed that the highest ratio, on Day 2, was significantly different than the lowest ratio on Day 6. *Post hoc* analysis was not performed, as the data was unbalanced (due to poor HPLC integration on some samples). There were relatively lower ratios of Chl *c*:Chl *a* on Days 3 and 6, and higher ratios on Days 2 and 5 (Fig. 7.22A).

There were significant differences in the ratio of fucoxanthin:Chl *a* between days, with pooled times during emersion periods ($H_{(5)} = 44.0$, $P < 0.001$), and no difference between times during emersion periods, when days were pooled ($H_{(2)} = 1.14$, $P > 0.5$) (Figs 7.21B, 7.22B, 7.23B). This shows that the highest ratio, on Day 3 was significantly different than the lowest ratio on Day 5. *Post hoc* analysis was not performed, but there were relatively lower ratios of fucoxanthin:Chl *a* on Days 2 and 5, and higher ratios on Days 3 and 6 (Fig. 7.22B).

There were significant differences in ratios of diadinoxanthin:Chl *a* between days and between times during emersion periods ($F_{2(5, 2, 89)} = 14.9$, $P < 0.001$ between days; $F = 5.4$, $P < 0.01$ between times) (Figs 7.21C, 7.22C, 7.23C). *Post hoc* analysis was performed, which showed there were significantly higher ratios of diadinoxanthin:Chl *a* on Days 2 and 5 than all other days, and lower ratios on Days 6 and 1 than Days 2 and 5 (Fig. 7.22C). *Post hoc* analysis also revealed over all days that there were significantly lower ratios of diadinoxanthin:Chl *a* at the start of the emersion period than at low tide (Fig. 7.23C). More specifically, studying each day separately, this increase occurred on all days except Day 5 (Fig. 7.21C)

There were no significant differences in ratios of diatoxanthin:Chl *a* between days but there were significant differences between times during emersion periods ($F_{2(5, 2, 88)} = 2.0$, $P > 0.05$ between days; $F = 6.5$, $P < 0.005$ between times) (Figs 7.21D, 7.22D, 7.23D). *Post hoc* analysis revealed there were significantly lower ratios of diatoxanthin:Chl *a* at the start of the emersion period than at the time of low tide or at the end of the emersion period (Fig. 7.23D).

β - carotene, lutein and phaeopigments were also present in the contact cores, however they were below the level of reliable detection on some days. There were no discernible patterns in the distribution of minor pigments over the emersion period or between days when these pigments were at detectable concentrations.

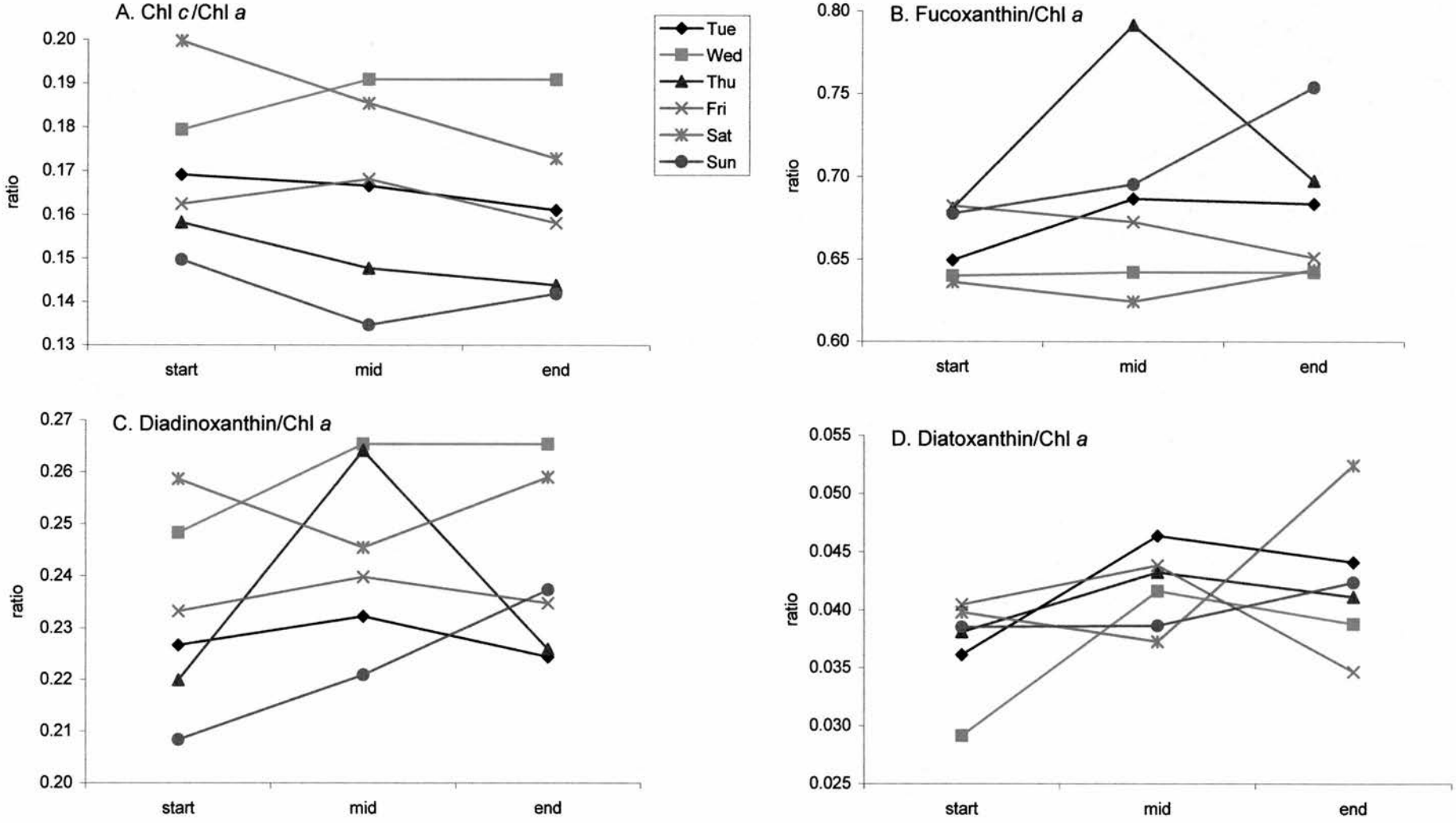

Figures 7.21. Pigment ratios to Chl *a* in the surface 2 mm of sediment each day, and at 3 times during 6 emersion periods, May 2000

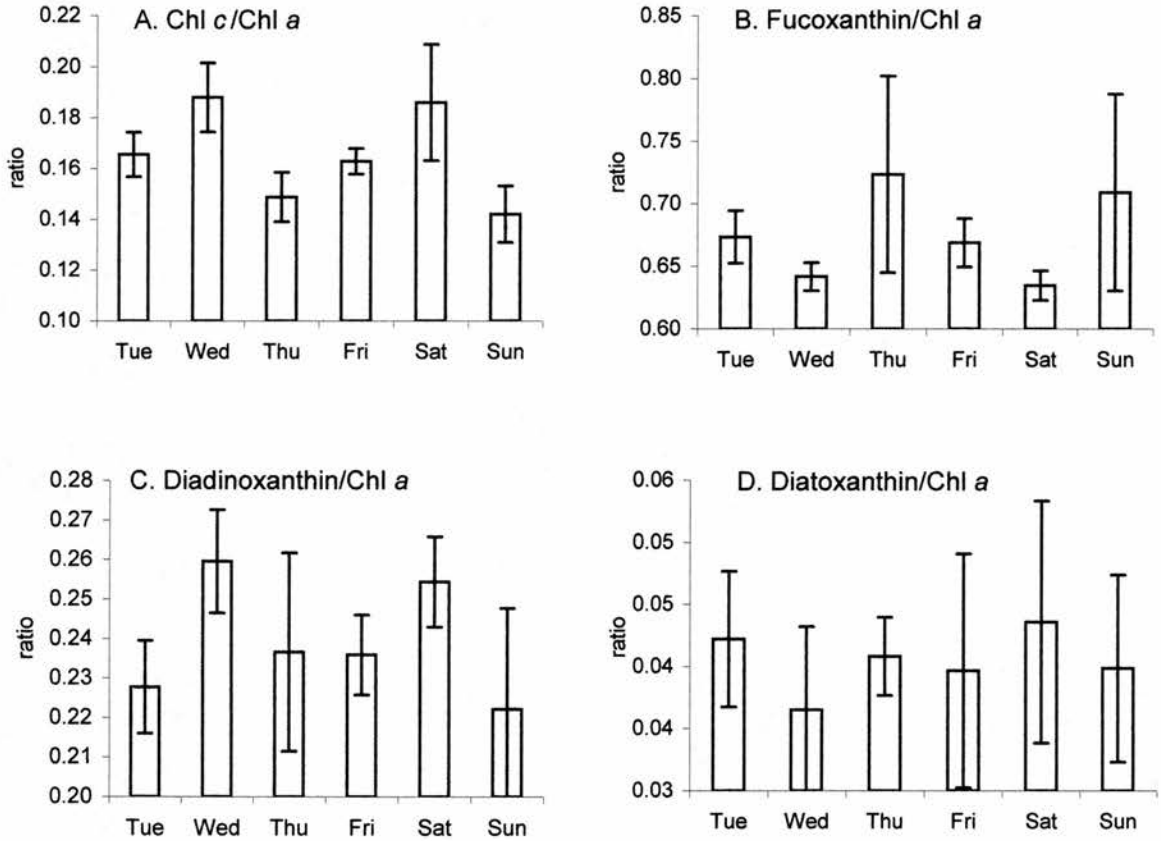

Figure 7.22. Pigment ratios to Chl *a* in the surface 2mm of the sediment each day on each day (pooled emersion times), May 2000

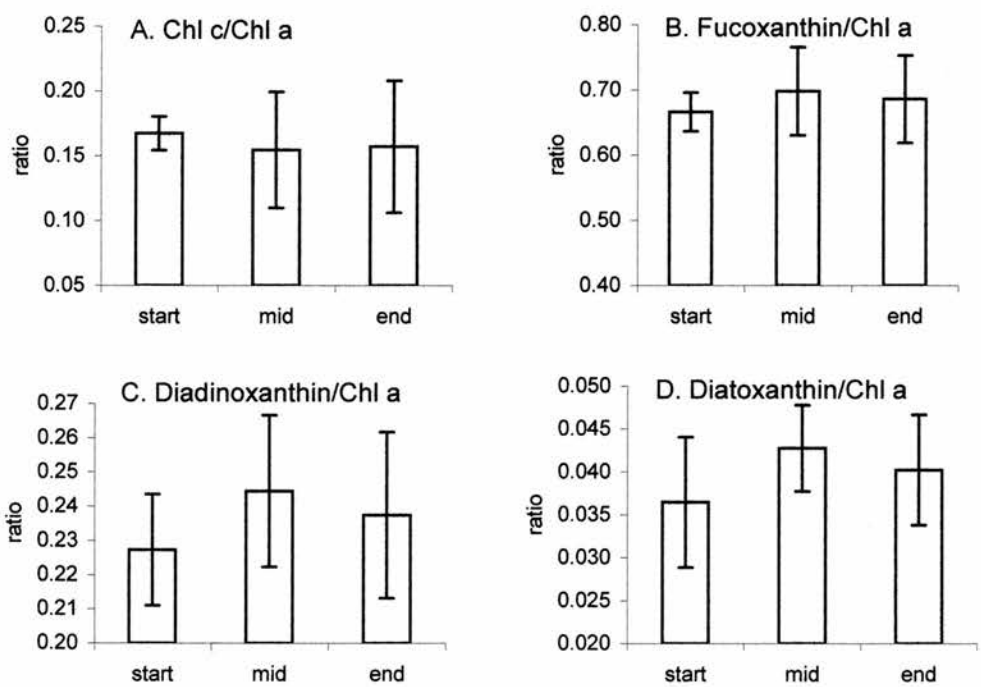

Figure 7.23. Pigment ratios to Chl *a* in the surface 2mm of sediment at 3 times during 6 tidal emersion periods (pooled days), May 2000

7.3.5.2. Study B; August 1998

In August 1998, only pigment analysis was performed (i.e. no fluorescence measurements were made). Samples were collected using the Cryolander for the determination of fine vertical resolution of pigments. Chl *a* concentration within the surface 0.2 mm did not change significantly over the emersion period ($F_{1(2, 8)} = 0.6$, $P > 0.5$) (Fig. 7.24A).

Chl *c* was not extracted from these samples, as acetone was used as an extractant (see Chapter 3). The ratio of fucoxanthin:Chl *a* within the surface 0.2 mm, increased throughout the emersion period, although this was not significant ($F_{1(2, 8)} = 1.3$, $P > 0.1$) (Fig. 7.24B). However, diadinoxanthin and diatoxanthin (ratios to Chl *a*) changed significantly in the surface 0.2 mm, after the first sampling time (Fig. 7.24C). The ratio of diadinoxanthin:Chl *a* significantly increased between tidal ebb and low tide ($F_{1(2, 8)} = 12.4$, $P < 0.01$). The ratio of diatoxanthin:Chl *a* on the other hand decreased between tidal ebb and low tide ($F_{1(2, 8)} = 24.8$, $P < 0.001$) (Fig. 7.24C). The ratio of β-carotene:Chl *a*, within the surface 0.2 mm, did not change throughout the emersion period ($F_{1(2, 8)} = 0.2$, $P > 0.5$) (Fig. 7.24D).

7.4. Discussion

7.4.1. Changes in Fo^{15}

An increase in Fo^{15} at the sediment surface has been previously shown to correlate with an increase in Chl *a* (Chapter 4). Thus, the change Fo^{15} traced during this study could indicate a change in the Chl *a* the sediment surface and may well be a useful fast measuring technique for the determination of the migratory patterns of microphytobenthos.

However fluorescence from diatom cells is affected in opposite ways by photochemistry and non-photochemical quenching. The influence these two processes have on the value of Fo^{15} may to an extent cancel each other out, leading to a relatively stable value of Fo^{15}. However, the balance between these processes is unclear, and may be highly influenced by acclimation status (Demers *et al.*, 1991). During photochemistry, the primary electron acceptor in PSII (Q_A) is reduced and fluorescence increases. In the dark, when there is no photochemistry, Q_A is oxidised and fluorescence is at its minimum. An increase of Fo^{15} can therefore be due to incomplete oxidisation of Q_A because of inadequate dark adaption. A high value of *Fv/Fm* is

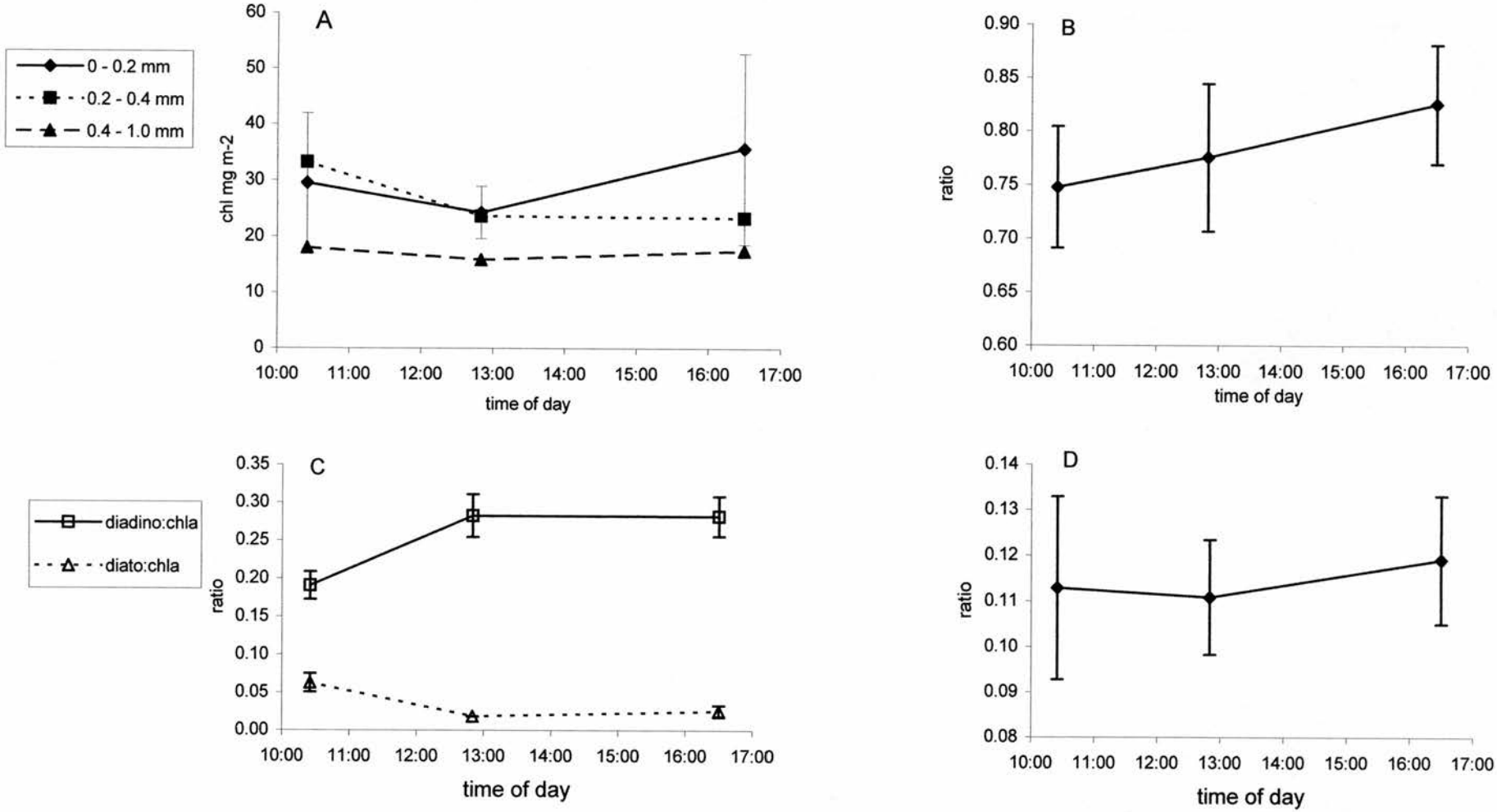

Figures 7.24. Chlorophyll *a* content and pigment ratios to Chl *a* in fine scale sections of the surface sediment during tidal emersion August 1997. A) Chl a over time in 3 subsequent layers at 3 times during the emersion period (n= 3 error bars are shown only on surface data). B) The atio of fucoxanthin/Chl *a*. C) The ratio of diadinoxanthin cycle pigments to Chl *a*. D) The ratio of β-carotene to Chl *a*. C-D are pigment ratios in the surface 0.2 mm of sediment, at 3 times within the emersion period. diadino = diadinoxanthin; diato = diatoxanthin

known to be a good measure of fully oxidised Q_A (Genty *et al.*, 1989). Therefore if *Fv/Fm* is shown to decrease with an increase in Fo^{15}, incomplete oxidisation of Q_A may well be a mechanism for an increased Fo^{15}. The effect this has on Fo^{15} however appears minor when compared with the natural variability in Fo^{15} values at similar *Fv/Fm* values. In this experiment *Fv/Fm* was determined simultaneously with every Fo^{15} measurement and thus the state of Q_A was assessed throughout the experiment. *Fv/Fm* rarely dropped below 0.6. Values of *Fv/Fm* were within the range measured in the previous study where Fo^{15} correlated with Chl *a* biomass (Chapter 4). Fo^{15} did sometimes increase, coupled with a decrease in *Fv/Fm* (on Days 1, 2 and 5), however Fo^{15} also increased with increasing *Fv/Fm* on Days 4 and 6.

A decrease in Fo^{15} can be due to non-photochemical quenching (NPQ), such as heat or xanthophyll cycling. On Day 1, the rate of increase in Fo^{15} was small in the 3rd h of emersion compared to other days. Day 3 also had a relatively small rate of increase in Fo^{15} in the 2nd h (Fig. 7.11B). These relatively small increases in Fo^{15} coincided with a period of high irradiance, following a period of fluctuating light conditions (Fig.7.2A). *Fv/Fm* also dropped significantly for this period (Fig. 7.14B). A steep decrease in *Fv/Fm* would indicate light stress, and thus NPQ may be surpressing a period of normally high Fo^{15} increase. But it is unclear whether a drop in Fo^{15} was due to diatoms migrating away from the surface, to avoid excessive irradiance. Further experiments could be performed to compare migrating and non-migrating biofilms under different light conditions, to clarify this response. Direct measurements of NPQ (using calculations with *Fm'* and *Fm* parameters, Schrieber *et al.*, 1986) would be difficult to make in a migrating biofilm; as calculations incorporating measurements 15 min apart (before and after dark adaption), may be affected by moving biomass. Measurement of xanthophyll cycle pigments on a finer temporal scale than this study may resolve the extent that NPQ might have on microphytobenthos *in situ*. Thus there is strong evidence that the increase in Fo^{15} was due to primarily to migration of diatom cells to the surface of the sediment.

7.4.2. Patterns found in Fo^{15}

The first Fo^{15} measurements before dawn on Day 5, were the lowest recorded for the whole study period, indicating that very few cells were present at the surface. All other days had higher Fo^{15} values, which implies that although the tide was covering them, some biomass was present at the surface. There were no differences in the first

Fo^{15} readings on days when the tidal water was clear (Days 1 and 2), to a day when the tidal water was turbid (Day 3) at ebb. The tidal ebb was similar on these 3 days; and happened during mid to late morning. This is interesting as it shows that even when light reaches the sediment surface before emersion, there was no difference in surface biomass than when water is turbid, when light to the sediment surface was effectively hindered. The first Fo^{15} value on Day 4 however, was higher than all previous days and the first Fo^{15} value on Day 6 was also higher than all previous days (Fig. 7.8). This could be attributed to the fact that on these days (Days 5 and 7) there was a short period of emersion in the early morning, and a covering of relatively clear tidal water before the later emersion. Thus, more biomass was at the surface on days when ebbing was late in the day. The first *Fv/Fm* on Day 6 (time zero) was also low in comparison to both the first readings on other days and in comparison to measurements made later on Day 6. This would indicate that the microphytobenthos were stressed whilst the tide was covering the sediment surface before ebb. The stress is likely to be due to light, as CO_2 or nutrient stress are unlikely during immersion of estuarine water rich in CO_2 and nutrients (Underwood and Kromkamp, 1999).

On Day 5, no biomass was present at the sediment surface before dawn, and Day 6 showed a decrease (not significant) in biomass by tidal flood, which was after dusk. This shows that microphytobenthos have a strong diurnal rhythm. Some biomass was present on the sediment surface after turbid tidal cover during the day (Day 3). This could suggest that the diurnal rhythm is stronger than the tidal rhythm. It is puzzling that only a proportion of the biomass stays at the surface during immersion, even when not illuminated. It may be that only certain species are present at the sediment surface during daylight immersion. Further laboratory experiments manipulating light and tidal coverage, or visualisation of immersed samples using low temperature electron microscopy could elucidate the mechanism of this response. A significant quantity of biomass was present at the sediment surface at the time of tidal flood on all days. This could have implications of cell re-suspension, especially during day-time immersion. Further studies could examine the presence and movement of biomass during immersion periods.

This study showed the rate of increase in Fo^{15}, once it had begun to get light after ebb (on Day 5) was no different than the rate of increase on other days when tidal ebb was during daylight hours (Fig. 7.11B). This study (Day 5) also found that diatoms began migrating to the surface before light levels were of measurable quantity (< 1

$\mu mol\ m^{-2}\ s^{-1}$). This is contrary to previous findings, which showed a slow emergence of diatom cells in the early morning (Round and Palmer, 1966).

7.4.3. Fo^{15} as a measure of biomass

The optimum time for measurement of microphytobenthic biomass using remote techniques would be when the majority of cells were at the surface. This study showed a plateau or peak in Fo^{15} occurred toward the end of tidal emersion. It was previously shown that cells continue to migrate to the surface at or after low tide (Pinckney *et al.*, 1994; Serôdio and Catarino, 2000) or plateau after an hour of tidal emersion (Round and Palmer 1966; Happy-Wood and Jones, 1988). This peak or plateau was shown to either stay constant or decrease just prior to tidal flooding (Round and Palmer, 1966; Palmer and Round, 1967; Janssen *et al.*, 1999; Serodio and Catarino, 2000). Thus, it was previously concluded that low tide was the optimum time to measure surface fluorescence (Fo^{15}) as a measure of biomass at the surface (Chapter 4). A comparison was made between Fo^{15} values at low tide and the peak to determine which would give the highest reading. On the days when the emersion period occurred during daylight hours, there was no significant difference between peak values and values at low tide. Measuring biomass at low tide is rather restrictive; therefore an optimum period of measurement was calculated from the data measured in this study. This optimum period of measuring Fo^{15}, as an indicator of biomass, was inferred as the period of the tidal emersion which shows no significant decrease from the peak Fo^{15} value. When tidal ebb occurs before dawn (Day 5, in this study) all the biomass does not have time to reach the very surface. This was inferred as Day 5 had similar Chl *a* concentrations to other days, but significantly lower peak Fo^{15} than other days. On days when emersion was during daylight hours (Day 1 to 4) there was no significant difference in Fo^{15} from peak measurement to all subsequent measurements. Generally there were no significant differences in Fo^{15} after time 2. Thus, there is no significant increase in Fo^{15} after the 3rd hour of emersion, and Fo^{15} after that time will be representative of the surface biomass.

This study showed 50% of the increase in Chl *a* (determined using Fo^{15}) to the surface occurred within 1h 45 min to 2h 50 min of tidal ebb. This was comparable to a Portuguese study where 50% of the Chl *a* (determined from *Fo*) increase was found in the first 2 h after tidal emersion (Serôdio *et al.*, 1997). Two other studies using remote sensing techniques as indicators of the surface Chl *a* showed that 50% of the Chl *a*

increase at the surface occurred in the first 18 min (Paterson *et al.*, 1998) or the first hour (Kromkamp *et al.*, 1998) after tidal ebb.

7.4.4. Spatial distribution

Microphytobenthos are renowned for having patchy distributions, on a variety of scales, in muddy estuaries, and numerous repetitions are needed to get representative values (MacIntyre *et al.*, 1996). This study, using non-destructive techniques, enabled greater replication on a spatial and temporal scale than has been previously made. Variation between the peak Fo^{15} (as a measure of biomass) had an average CV of 36% with 15 replicates. However when the CV were analysed at decreasing replication within the specified area of 0.18 m^2 (evenly spaced within the area), no difference in CV was found. That is, there was no difference between CV of 3, 5, 10 or 15 replicates. This indicated that 3 replicates would have been sufficient to determine the change in Fo^{15} over time. CV were also analysed at increasing spatial scales (with set lags at 10cm). This also showed no difference between CV between 3, 5, 10 or 15 replicates at sampling area. Thus indicating that 3 replicates 10 cm apart (~0.006 m^2) would have been sufficient to determine the change in Fo^{15} over time. CV were also analysed at increasing lags (10, 20 and 30 cm). This also showed no difference between CV between 3 replicates at increasing lag scale. The average CV at different replication and scale ranged between 30 and 40%. These analyses show that the spatial distribution of patches is below the smallest scale measured (10 cm lag). Also, the lack of increased CV at low replication (n = 3) indicates that the patch size is likely to be lower than the area of measurement (1.2 cm^2). The horizontal distribution of microphytobenthos has been statistically investigated with patches ranging from < 4 to 113 cm^2 (Blanchard, 1990). Previous studies suggest a minimum of 5 replicates (12.6 cm^2 each) were needed to reduce the CV to 45% in a 2500 cm^2 area (MacIntyre *et al.*, 1996). The samples in this previous study were relatively large core areas compared to our measuring area (1256 mm^2 versus 120 mm^2 respectively). Thus patch size and number of replicates needed for a representative measure of biomass may be different in different locations.

7.4.5. Electron transport rate

Previous authors have found rETR to be useful in the determination of photosynthetic parameters after the construction of ETR-*E* curves (analogous to *P-I* or *P-E* curves; Kromkamp *et al.*, 1998).

Temperature is known to affect maximum photosynthesis (P_{max}, Blanchard *et al.*, 1996, 1997) and growth rate (Admiraal, 1977a, Davidson, 1991), with an increase in both, up to an optimum temperature of 25°C (for P_{max}). Maximum rETR (ETR_{max}) in this study was highly variable and thus comparisons were unable to be made with temperature. Biomass, either directly as Chl *a* concentration or peak Fo', showed no increase on warmer days, but this is not surprising in a natural situation which includes grazers, which could also be feeding faster at higher temperatures (Retrabaun *et al.*, 1996; Berkanbusch and Rowden, 1999).

Relative electron transport rate measurements in this study showed a great deal of variability at the higher irradiance levels, thus few conclusions could be made; similar conclusions were found in Chapter 3. A previous study showed ETR-*E* curve determination from cores in the laboratory showed much less variation in rETR at the higher irradiance levels than field based measurements (Chapter 3, Fig. 3.10). Other studies, using the PAM2000, also show less variability in rETR measurements than field based measurements from intact surface sediment microphytobenthos (Kromkamp *et al.,* 1998, fig. 5). The effective efficiency of photochemistry at PSII ($\Delta F/Fm'$): a determinant of rETR, is highly influenced by light history, where high levels or long periods of irradiance can induce dynamic or chronic photoinhibition. Photoinhibition is a mechanism which decreases efficiency of electron transport, to avoid damage to PSII reaction centres. Therefore photoinhibited cells will have a decreased efficiency of both photochemistry at PSII and electron transport; these parameters will thus be lower than those found in unstressed cells. Thus ETR-*E* curves constructed from *in situ* measurements may incorporate any conditions of stress, and variability in rETR will be larger than those found under laboratory conditions. The variability found at high irradiance levels in rETR could also be due to the fact that spatially different diatom patches were being measured. Different diatom patches may be composed of different species, which may in turn vary in species composition with time. It has been shown that species composition at the sediment surface can change dramatically over periods of minutes, and certain species within a biofilm may be at

the surface during different times of the day or prefer different irradiance levels (Perkins *et al.,* submitted). It has also been documented that different species (in the same biofilm) can show different responses of effective efficiency of photochemistry at PSII ($\Delta F/Fm'$) and thus rETR (Perkins pers com). Thus species with different $\Delta F/Fm'$ responses may be responsible for the variation found in rETR at high irradiance levels. Both light history and species composition may thus affect rETR measurements and may have implications when comparing spatial or temporal measurements. Species composition was sampled throughout this experiment and will be shown elsewhere (M. Consalvey). However, this variation found in rETR *in situ* of microphytobenthic biofilms may be part of the natural dynamics of the system. However these measurements may not then be particularly useful for ETR-*E* curve determination. Absolute measurements of ETR may show less variation than rETR, as they incorporate measurements of mean specific absorption coefficients (a*) of the algae (Hartig *et al.*, 1998). At present, a* are measured in the laboratory from suspended cells, separated from the sediment (using spectrophotometry). However, removing cells from the sediment under laboratory conditions will, by definition, affect the a*. Changes in a* can occur in very short time spans in response to different light conditions. At present, a* measurements are impossible to do *in situ*. Further studies incorporating replication on exactly the same patch of algae under natural light conditions or the effect of light history on rETR under controlled conditions may clarify the mechanism behind this variation.

7.4.6. Pigment analysis

Fine sectioning of the sediment surface has previously been used as an attempt to reveal the migration of microphytobenthos to the sediment surface (Paterson *et al.*, 1997 PRO-MAT report). This was unsuccessful and the fine sectioning in this study was also unable to show microphytobenthos moving to the surface. No difference in Chl *a*, in the surface 0.2 mm, over the emersion period was found. Contact coring, however, showed an increase in Chl *a* concentration within the surface 2-3 mm over time within the tidal emersion period. This could be attributed to migration of microphytobenthos into this layer. However water content decreased as Chl *a* concentration increased, thus the increase found is probably due to sediment compaction (Chapter 6).

Fine sectioning of the sediment surface (0.2 mm) showed a significant change in diadinoxanthin cycle pigments with time during the emersion period. Diadinoxanthin is the pigment that is most abundant in cells in the dark (Olaizola and Yamomoto, 1994). When exposed to irradiance, diadinoxanthin de- epoxidates to diatoxanthin, thus diadinoxanthin decreases and diatoxanthin increases in the light (Demers *et al.*, 1991; Olaizola and Yamomoto, 1994). As the tide ebbed, the majority of the microphytobenthos would have been in the dark (in deeper sediment layers or under turbid water), thus diadinoxanthin would be expected to be at its highest, decreasing with exposure to irradiance. However diadinoxanthin, in both in 0.2 mm and 2 mm of the sediment surface, increased with emersion time. Conversely, diatoxanthin would be expected to increase with exposure, where in fact it decreased with time during the tidal emersion. Tidal ebb water was quite clear (in Study B) and the microphytobenthos may have already been in the sediment photic zone whilst the tide was in. However, diatoms accumulate to a greater degree in the photic zone when the tide is out. In 0.2 mm surface sections the increase in diadinoxanthin was paired with a decrease in diatoxanthin, indicating diadinoxanthin cycling. However the increase in diadinoxanthin with time in the deeper sediment sections was not paired with a decrease in diatoxanthin. This could be due to pigments below the photic zone (> 1 mm deep) diluting any photic zone pigment changes (Kelly *et al.*, 2001). Increased diatoxanthin, which is known to transfer absorbed energy at lower efficiencies than diadinoxanthin, at tidal ebb may indicate stress. At tidal ebb the sediment surface was exposed to approximately 10 min of irradiance (unknown levels) prior to sampling, thus light stress may have caused energy dissipation at a time when cells were unprepared for ETR due to an inherent tidal rhythm. As well as its photoprotective properties, diadinoxanthin is also thought to be a precursor of the light harvesting pigment fucoxanthin (Lohr and Wilhelm 1999; Bjørnland and Liaaen-Jensen, 1989). An increase in diadinoxanthin with time (without a decrease in diatoxanthin) may thus be an indication of biosynthesis of diadinoxanthin as a precursor to fucoxanthin. Further studies on a finer temporal resolution (at fine vertical resolution) are needed to verify this result with paired measurements of the ambient irradiance and comparisons made with samples taken in the dark.

7.4.7. Limitations

High light conditions may decrease surface Fo'^{15} measurements in two ways. Biomass at the surface may decrease as an escape response to damaging light levels by migrating deeper into the sediment, or because of NPQ processes. The influence of either of these mechanisms on fluorescence were not separated here, and further studies using biofilms unable to migrate may give an indication of the extent either may affect Fo'^{15}.

Measurements of Fo'^{15} and Chl *a* of high biomass, dense biofilms may result in an asymptotic relationship between Fo'^{15} and Chl *a*. Thus, the migratory behaviour may be masked beyond a particular surface density of cells. The biofilms measured in this study were not particularly thick and had Chl *a* concentrations (maximum of 80 mg Chl *a* m^{-2}) below those found in a previous study where Fo'^{15} and Chl *a* had a linear relationship up to 160 mg Chl *a* m^{-2}. Some intertidal flats have Chl *a* concentrations much higher than those found in the Eden Estuary, e.g. The Ems Dollard has Chl *a* concentrations up to 400 mg m^{-2} (Colijn & de Jonge, 1984) and Texel has concentrations up to 800 mg m^{-2} (Paterson *et al.*, 1994).

Nutrient deficiency of phytoplankton has been shown to increase the fluorescence to Chl *a* ratio (Kiefer, 1973a). Therefore systems which encounter nutrient limitation may show increases in Fo'^{15} due to nutrient deficiency as well as accumulation of cells to the surface. Nutrient deficiency is rarely reported for microphytobenthos in cohesive sediment estuarine environments, as there is generally thought to be sufficient (or excessive) nutrient loading in these systems (Underwood and Kromkamp, 1999).

7.5. Further studies

A comparison a migrating and non-migrating biofilm under different light conditions may clarify whether, under excessive irradiance, a drop in Fo'^{15} is be due to diatoms migrating away from the surface, or due to NPQ.

Visualisation of immersed samples using LTSEM could elucidate the species composition of the proportion of cells which are at the surface during daylight tidal exposure.

This study showed opposite diadinoxanthin cycle pigment changes to those found in diatoms in other habitats (Demers *et al.*, 1991). Further experiments using HPLC pigment analysis from fine sections of surface sediments could be implemented, to follow diadinoxanthin cycle pigment quantities during:

- a shorter temporal scale during emersion periods than this study, to verify changes found in this study
- emersion periods where tidal ebb occurs in the dark, to examine diadinoxanthin cycle pigments during complete darkness. This study, using contact cores, showed no difference in diadinoxanthin cycle pigments when tidal ebb was during the night (Day 5) than when tidal ebb was during the day (all other days).

Further studies might explore the strength of the cues that induce migration. This could be implemented by measuring Fo^{15} at the sediment surface of:

- microphytobenthos artificially darkened during daytime exposure periods
- microphytobenthos artificially covered in water during daytime exposure periods
- microphytobenthos artificially illuminated during the night

7.6. Summary and conclusions

This study shows that fluorescence can trace microphytobenthos migration to the sediment surface. Measurements of Fo^{15} at the sediment surface followed similar patterns to those found in previous studies using other techniques (e.g. cell counts, LTSEM and spectral reflectance).

The main conclusions found in this study:

1. The patterns found in Fo^{15} at the sediment surface showed:
   a) An increase at the surface after tidal ebb
   b) The rate of increase was unaffected by time of tidal ebb (which ranged from early morning to late afternoon) or light dose (which ranged between 92 to 260 mmol m^{-2} in the 3h to 3h 30 min period before low tide)
   c) A peak towards the end of the tidal exposure period
   d) Although not significant, decreases were only found at the end of the tidal exposure periods on Days 3 to 6
2. Measurements of biomass using Fo^{15} at the sediment surface can be made on days which dawn or dusk does not occur during the emersion period. Fo^{15} measurements can be made any time after the 3rd hour of exposure for representative measurements of the surface biomass, without the migratory

behaviour of microphytobenthos affecting the results. However care must be taken if ambient light conditions are constantly high or fluctuating.

3. Measurements of rETR showed highly variable results in the field and thus may not be useful in determining ETR-*E* curve parameters, although further studies are necessary.

4. Chl *a* concentration of the sediment increased over time, but it has been shown this could be wholly due to sediment compaction (Chapter 6). Therefore Chl *a* measurements may be misleading for inferences of cell movement over periods which also change in sediment density.

5. Pigment analyses of fine sections of sediment show interesting, but puzzling diadinoxanthin cycling changes (increasing diadinoxanthin and decreasing diatoxanthin with increasing tidal, and thus light, exposure), and is the opposite of that which would be expected.

Chapter 8

8. GENERAL DISCUSSION

8.1. The measurement of microphytobenthic biomass in sediments

8.1.1. Microscale measurements of biomass

Microphytobenthos play a major role in the primary productivity of cohesive depositional intertidal systems (Pinckney and Zingmark, 1991; Pinckney *et al.*, 1994; MaIntyre and Cullen, 1996; Middleburg *et al.*, 2000). Accordingly, the measurement of microphytobenthic biomass and the vertical distribution of biomass within the sediment, is an important aspect of understanding the ecology of cohesive sediment systems. Cohesive sediments have only a very thin photic region in which the microphytobenthos can photosynthesise (Serôdio *et al.*, 1997; Kromkamp *et al.*, 1998) and cells are able to migrate into the photic zone, from deeper sediments, during tidal emersion (Palmer and Round, 1967). The photic zone in cohesive sediments has been measured to a depth as shallow as 0.27 mm (Serôdio *et al.*, 1997) or deeper to 0.6 or 1.8 mm (Kromkamp *et al.*, 1998; Paterson *et al.*, 1998, respectively). The measurement of biomass in the photic region of sediments is thus essential for the determination of the biomass responsible for primary productivity. A fine sectioning technique, has recently become available, to section sediment samples to a 0.2 mm resolution (Chapter 4, 6; Wiltshire, 2001; Kelly *et al.*, 2001).

In microphytobenthic rich sediments, Chl *a* exponentially decreases with increasing sediment depth, at a section resolution of 0.2 mm to a depth of up to 5 mm (Chapter 6). This strong gradient in Chl *a* in the surface layers results from the response of cells to the strong light gradient at the same microscale. The Chl *a* found below the photic zone was generally thought to have a relatively minor contribution to the total content in coarser core sampling (to 2 or 5 mm depth), although the studies in Chapter 6 and those of Kelly *et al.* (2001) prove that there are exceptions.

Until very recently microphytobenthic biomass, using the proxy Chl *a*, has been determined from relatively coarse cores (1, 2 or 5 mm). A depth of sampling, for example to 2 mm, cannot detect the fine scale vertical resolution of biomass or the migratory movements of the cells within the sediment (Kelly *et al.*, 2001). This may be confirmed by determining the depth to which motile diatoms can move within the given time period of emersion. Diatoms are known to move at an average rate of 0.19

μm s^{-1} (Hay *et al.*, 1993). Assuming this speed to be representative of the rate of movement for the community and constant throughout the sediment depth, then burrowing depths of diatoms can be approximated. If 90% of the community has reached the surface between 190 and 280 minutes after tidal ebb (Chapter 7), then they cannot have migrated from more than a depth 2.1 to 3.2 mm. Consequently, measurement of the Chl *a* within 2 mm will measure biomass at most stages of migration. Fine sectioning has not yet been able to resolve an enrichment of Chl *a* over the emersion period in the top 0.2 mm (PROMAT report; Chapter 7). This may be due to the irregular surface topography of the sediment, which affects the amount of sediment, in volume or mass, in the top slice. Thus the variation due to uneven surface topography masked any changes in Chl *a* due to migration. This thesis has shown however, that microphytobenthic biomass distribution can be followed by non-invasive fluorescence techniques.

8.1.2. Coarse scale measurements of biomass

Chl *a* is relatively labile, although a significant quantity has been found at depth in cohesive sediments (Chapter 6; Kelly *et al.*, 2001). Thus coarse core sediment sampling (varying from 1 to 5 mm sediment depth) incorporates photosynthetically inactive biomass (PIB); e.g. Chl *a* which is below the photic zone, in combination with photosynthetically active biomass (PAB).

Under certain conditions, the measurement of Chl *a* in the top 2 mm of sediments may be an unrepresentative measure of the standing stock of PAB (Chapter 6). It was demonstrated, from 2 mm deep cores, that an increase in Chl *a* concentration (mg m^{-2}) over an emersion period could be wholly due to sediment compaction (Chapter 6). Sediment compaction was found to incorporate a significant quantity of PIB into the same volume of sample over the emersion period. This led to the danger of spurious inferences of the changes in PAB over an emersion period (Chapter 6 and 7).

Increased sediment density was shown to have an opposite affect on Chl *a* content and Chl *a* concentration (Chapter 6). From these studies it was concluded that measurement of Chl *a* within the sediment (either as a content or concentration) may not be showing representative patterns in biomass when sediment densities varied across the same scales. Accordingly, correction of Chl *a* measurements, to sediment density, should be employed in future studies. This may be accomplished by

determining the dry mass density of the sediment samples, and if necessary determining the amount of Chl *a* present at depth.

The distribution of sediment density over temporal and fine vertical scales has rarely been studied (Taylor and Paterson, 1998) and should be explored in future work. Fine scale vertical distribution of both Chl *a* and sediment density could then be incorporated into sediment system productivity models to increase their accuracy.

8.1.3. Remote sensing

Significant correlations were found from microphytobenthos *in situ* between Chl *a* concentration and the minimum fluorescence parameter after 15 minutes of dark adaption, Fo^{15} (Chapter 4). The relationship was strongest in diatom dominated samples and became stronger when the depth (0.2 mm) of sediment sampled for Chl *a* measurements became closer to the depth of Fo^{15} detection (Chapter 4). A stronger relationship between Chl *a* and spectral reflection was also found when Chl *a* from shallower sediment cores was determined (Paterson *et al.*, 1998). It was also shown that different algae show selective responses when measured with fluorometers of different wavelength excitation beams (Chapter 5; Forster *et al.*, in prep). The yield of fluorescence emission was found to be dependant on the excitation wavelength for different types of algae, and a single wavelength measuring beam will give selective results from a mixed algae assemblage (Chapter 5). However, this could prove to be extremely useful in the measurement of the biomass contribution and responses of specific taxa, within a mixed algae sample. This could be facilitated by using fluorometers which have a suite of different wavelength excitation beams (e.g. Walz Phyto-PAM; Schreiber, 2000).

The measurement, at the sediment surface, of signals from phyto-pigments can be easily and rapidly taken and separated from those of the sediment and will thus facilitate non-destructive temporal studies. These remote sensing techniques include spectral reflectance (Kromkamp *et al.*, 1998; Paterson *et al.*, 1998) and Chl *a* fluorescence (Chapter 4, 5, 7; Serôdio *et al.*, 1997) but are not without pitfalls. Variation was found in the relationship between Chl *a* and Fo^{15}, which were unidentified in this *in situ* study, but maybe introduced from several sources. The inaccuracy of Chl *a* concentration determination because of varying sediment densities could be a possible source of variation. Thus, correlating remote sensing with inaccurately determined biomass in sediments (because of the physical properties

of sediment) would lead to disparity from the independent variable (Chl *a*). It may thus be wise to ascertain the relationship between remote sensing and Chl *a* biomass in sediments, without the interference of sediment density, and then introduce factors which might influence remote sensing (thus isolating the source of variation).

Signals radiating from biomass can be reflected or absorbed by sediment and neighbouring cells, and thus the density of either the sediment or cells may affect the strength of signal. The processes (photochemical and non-photochemical) involved in photosynthesis affect emission of fluorescence from algae, but this may be overcome by a period of dark adaption to relax photosynthetic processes (Chapter 4). Incomplete dark adaption may however affect the relationship between Chl *a* and Fo^{15} as in the case of incomplete oxidation of the primary electron acceptor at PSII, or incomplete reversal of non-photochemical quenching (NPQ). Other factors which may also affect the relationship between these two parameters are nutrient deficiency, pigment composition and the presence of other fluorescing material. Never-the-less, strong relationships have been found between Chl *a* and Fo^{15}, *in situ* (Chapter 4) on undisturbed cores (Barranguet and Kromkamp, 2000) and from sediment/diatom slurries (Serôdio *et al.*, 1997).

An advantage of using fluorescence over spectral reflectance would be the opportunity to measure the physiology of the microphytobenthos in tandem with biomass. Light adapted measurements using fluorescence can, in some circumstances, give an estimate of productivity (electron transport rate; ETR; Kromkamp *et al.*, 1998), and dark adapted measurements can give an indication of the stress status of the algae (Genty *et al.*, 1989). Spectral reflectance measures of biomass on the other hand may be less affected by potential stresses than fluorescence measurements (e.g. light, nutrients, desiccation and toxins).

8.1.3.1. Migratory rhythms of microphytobenthos

This study included the first non-destructive quantitative temporal study of microphytobenthos distribution at the sediment surface, inferred from Fo^{15} measurements (Chapter 7). Microphytobenthos were found to accumulate at the sediment surface during the emersion period, but, surprisingly were found to remain at the surface just prior to tidal flood (Chapter 7; Janssen *et al.*, 1999). A proportion of the microphytobenthic community was also found to be present at the surface of the sediment when tidal ebb occurred during daylight hours (Chapter 7).

Microphytobenthos were found at the sediment surface, to a greater degree at tidal ebb when the tidal ebb was later in the day, even when no light reached the sediment surface during tidal coverage because the water was turbid (Chapter 7). This showed that, unless migration occurred at a rate too rapid to measure, significant quantities of cells were present at tidal ebb or flood during the day, and may have implications of re-suspension of cells during daylight immersion. Biomass was always lower at tidal ebb than tidal flood; thus cells, once immersed, must migrate away from the surface, be removed or grazed. Future studies might examine migratory patterns during day-time immersion.

The rate of increase of microphytobenthos to the surface was remarkably similar between days of varying time of low tide (Chapter 7). This rate of increase was comparable to microphytobenthos on a Portuguese estuary (Serôdio *et al.*, 1997), but slower than the rate of increase shown in other studies (Paterson *et al.*, 1998; Kromkamp *et al.*, 1998). The horizontal movement of microphytobenthic cells was not considered in this study and may have a significant influence on temporal remote sensing studies (Chapter 7). For example, a patch of microphytobenthos of low biomass may show a greater rate of increase in biomass, due to horizontal migration from surrounding high biomass areas. Conversely, a high biomass patch of microphytobenthos may show a greater decrease in rate of biomass if cells move horizontally into the surrounding area. However the extent of replication in this study ($n = 15$) should take into account any affects such as these (Chapter 7).

Remote sensing of the sediment surface has recently shown to be an extremely useful tool in the repeated temporal measurements of the biomass of the same sample of microphytobenthos (Chapter 7; Paterson *et al.*, 1998, Kromkamp *et al.*, 1998). Microphytobenthos migrate to the sediment surface during the tidal emersion and prior to remote sensing techniques, had been monitored qualitatively or quantitatively using destructive techniques (Palmer and Round, 1967; Happey-Wood and Jones, 1988; Pinkney *et al.*, 1994; Janssen *et al.*, 1999). Qualitative studies of the vertical resolution of cells within the sediment have shown the accumulation of cells at the surface during tidal emersion (Tolhurst, 1999). The measure of Chl *a* accumulation in 1 mm deep sediment cores has been used, but is poorly matched to the vertical resolution of cell movement (Pinkney *et al.*, 1994). Counts of cells at the sediment surface have been used to quantitatively assess migratory rhythms (Palmer and Round, 1967; Happey-Wood and Jones, 1988). Previous quantitative studies have all

used destructive techniques; hence samples were unable to be paired on temporal scale. The measurement of the accumulation of microphytobenthos at the sediment surface, using fluorescence analysis, has thus shown (statistically) many of the aspects of microphytobenthos migratory behaviour (Chapter 7).

Active escape mechanisms are unusual in photosynthetic organisms, and further studies might compare the photosynthetic responses of these migratory cells to non-migratory species (e.g. epipsammic species). Further studies could also explore the photochemical and non-photochemical responses of migrating microphytobenthos in comparison to microphytobenthos prevented from migrating (e.g. on filter papers). This may elucidate whether migration is the main, the only, or a minor, photoprotective mechanism of these algae. Whole assemblage studies may however give different responses than more specific studies (e.g. that of the workers in Essex using a high resolution imaging of Chl *a* fluorescence from single cells). Recent work has shown 2 species within the same biofilm showed different photoprotective mechanisms, one which migrated and the other which decreased its thylakoid membrane surface area, in response to increased irradiance (Perkins *et al.*, in prep).

8.1.3.2. Spatial distribution

During estuary-wide studies of spatial distribution of surface biomass (using Fo^{15}), patches of diatoms may be smaller than the area of measurement (in this case 1.2 cm), or may be completely randomly dispersed (Chapter 5 and 7). The coefficient of variation (CV) between replicate Fo^{15} measurements, made at scales from 2.5 cm to 500 m, ranged from 5 to 150 % (Chapter 5). Another spatial study, within a diatom dominated area, showed a CV between 30-40% at scales varying from 10 cm to 30 cm (Chapter 7). These and other studies (Blanchard, 1990; MacIntyre *et al.*, 1996)) show that diatom patches can be highly variable in size and dispersion. Microscopic examination (LTSEM) of the sediment surface has shown isolated single cells within an area, clusters of cells or total coverage of the surface with cells (Tolhurst, 1999; M. Consalvey and I. R. Davidson pers. comm.), showing that diatoms most probably have a random dispersion.

8.2. Fluorometric measurements of photosynthetic activity

This study included measurements of the relative electron transport rate (rETR) of microphytobenthos, measured using pulse modulated fluorescence.

Previous authors have found rETR to be useful in the determination of photosynthetic parameters (Kromkamp *et al.*, 1998). Highly variable measurements of rETR at high irradiance were found *in situ* (Chapter 3 and 7). This led to the conclusion that, at present, using rETR measurements of spatially different patches of microphytobenthos *in situ* has not been useful for the modelling of photosynthesis-irradiance (*ETR-E*) curves. Spatially discrete patches of microphytobenthos may be experiencing localised variation in conditions or may contain a different community assemblage. These discrete patches could thus have potentially different ETR responses. High-resolution imaging of Chl *a* fluorescence has shown that under different light conditions, a species community shift was induced in the photic zone (Perkins *et al.*, in press). Further studies could explore paired ETR measurements under stepped irradiance, with spatial replicates. This would be easily deployable with a single fluorometer and the hardware developed in Chapter 3. Several stationary angled probe holders could be placed on selected microphytobenthic patches and alternately covered with different density filters. If a species shift were induced under varying irradiances using natural light conditions, ETR measurements would be measuring the natural dynamics of the system as a response of the whole community.

8.3. Pigments

This study found significant patterns in the occurrence of photoprotective pigments measured in the photic zone (top 0.2 mm) over a tidal cycle, compared to insignificant patterns in pigments from sediment contact coring (top 2 mm) (Chapter 7). The quantification of diadinoxanthin cycle pigments in relation to that of Chl *a*, from fine sediment surface sections (0.2 mm) showed interesting but unexpected results (Chapter 7). Diadinoxanthin increased over a tidal emersion period instead of an anticipated decrease (Demers *et al.*, 1991). A decrease in diadinoxanthin was expected as the light dose increased over the emersion period. The increase found (in Chapter 7) of diadinoxanthin was matched with a decrease in its de-epoxidated form diatoxanthin. An increase in diatoxanthin (with a stoichiometric decrease in diadinoxanthin) is an indication of absorbed energy dissipation (Demers *et al.*, 1991; Olaizola and Yamamoto, 1994). Absorbed energy dissipation is a mechanism which occurs when irradiance absorbed is in excess of that needed for photosynthesis. This does not only happen in high light conditions, but also under photosynthetically stressful conditions (e.g. low temperatures, toxins, nutrient or CO_2 limitation). These

stresses were not measured in this study (Chapter 7; August 1997), but were unlikely. Nutrient stress or CO_2 limitation, at tidal ebb, were unlikely as estuarine water is known to be rich in CO_2 and nutrients (Underwood and Kromkamp, 1999). Temperatures during the summer period (northern temperate) were also unlikely to be at stressful levels and toxins are unlikely to be different over hourly scales. This increased absorbed energy dissipation at tidal ebb could be because;

a) some irradiance was reaching the cells, which were unprepared for photosynthesis (due to inherent tidal rhythms), and thus the absorbed energy was dissipated via diadinoxanthin cycling

b) NPQ may not be fully reversed in total darkness and may need some electron transfer further along the chain, to alleviate a build up of electrons (Perkins pers. comm.), although this has not been documented for algal cultures (Demers *et al.*, 1991)

Further studies should verify these findings, to incorporate measurements in the dark and on a finer temporal scale within the tidal emersion. These further studies could be coupled with maximum efficiency at PSII (*Fv/Fm*) readings, which could elucidate the patterns in NPQ under natural conditions.

It has been well-documented that microalgae community composition found in estuarine habitats can be identified using their pigment fingerprints (Cariou-Le Gall and Blanchard, 1995; Barranguet *et al.*, 1997; Brotas and Plante-Cuny, 1998). However, the quantification of pigments to infer physiological information of microphytobenthos in these habitats is as yet unpublished. Information on the photacclimated status can be determined from minor pigment quantification and the intracellular Chl *a* concentrations. It is not surprising that physiological status, inferred from minor pigment determination has not yet been explored, as the depth of sampling has only recently matched the resolution of the photic depth.

Minor pigment determination from cells in the photic zone (0.2 mm micro-section), may demonstrate the acclimation status of microphytobenthos. Further pigment studies of cells in the photic zone may verify the theory that cells microcycle as a protective mechanism under illumination during the emersion period. Microcycling is the movement of cells within the surface micrometers of sediment to optimise their position within the light gradient (Kromkamp *et al.*, 1998; Underwood and Kromkamp, 1999). If cells in the photic zone exhibited acclimation to low light (showing low photoprotective pigment concentration (Robinson *et al.*, 1997)) under

high light conditions (e.g. on a sunny day) this would show evidence of microcycling. However, some species in these habitats migrate and others do not, and different species within the same biofilm can show very different NPQ responses (Perkins *et al.*, in prep).

8.4. Summary

1) The main aim of this study was to ascertain the relationship between Fo^{15} and Chl *a*, under natural field conditions. A strong relationship was found between these parameters in diatom-dominated samples (Chapter 4), some scatter was evident and the source of was not identified, but could be from;
    - inaccurate Chl *a* determination
    - nutrient deficiency
    - free Chl *a* (not bound to proteins)
    - not fully dark adapted samples (therefore still influenced by photochemical or non-photochemical processes)
    - signal re-absorption at high biomass
2) The relationship between Fo^{15} and Chl *a*, became stronger with finer depth of sample for Chl *a* determination (Chapter 4). The relationship between these two parameters broke down across large scales (Chapter 5). The source of variation in this case was determined as;
    - mixed algal types
    - samples of differing grain size
    - inaccurate probe height
    - too deep a coring depth for Chl *a*
3) Temporal studies of microphytobenthos were made using the fluorescence parameter Fo^{15}, which discovered aspects of the migratory patterns of these algae not previously measured, namely;
    - the rate of increase of cells to the surface was unaffected by time (during the day) of tidal ebb, when 6 consecutive days were compared
    - the rate of increase of cells to the surface was unaffected by light dose
    - a significant increase of cells to the surface up to the 3rd hour following tidal ebb

Temporal studies of microphytobenthos also statistically verified that;

- no significant migration of cells away from the surface at the end of the tidal emersion
- the peak in cells to the surface occurred towards the end of the emersion period

4) The variability in sediment density influences Chl *a* content and concentration determination, in opposite ways and, if present, should be corrected for in future studies. This becomes more severe as vertical resolution increases.
5) Microphytobenthos patch size and dispersion (assessed using fluorescence) varied to such a degree as to show no structure, i.e. randomly distributed cells/patches.
6) Measurements of rETR of microphytobenthos *in situ* proved to be highly variable and further studies are needed to ascertain the source of the variability.
7) The determination of pigment fingerprints from the photic zone showed significant patterns of change in photoprotective pigments. This study showed unexpected results of increasing diadinoxanthin with increasing illumination; therefore further studies are needed to verify these findings.

8.5. Conclusion

Fluorescence has been shown to be a valuable tool in the tracing of microphytobenthic biomass, but is limited to resolving biomass from the top portion of the photic zone. The photophysiology of microphytobenthic patches is varied and may be due to disparity at a cellular level. Thus fluorescence is a highly useful technique in these systems, but must be used with a good understanding of the ecology and physiology of microphytobenthos.

Appendix

PROTOCOL FOR THE USE OF THE HPLC

1. Consumables

90% Dimethylformamide (for extraction)
Acetone (for gradient)
Methanol (for gradient)
Tetrabutyl ammonium acetate (buffer for gradient)
Ammonium acetate (buffer for gradient)
Propanol (for gradient)
Chlorophyll *a* standard
Minor pigment standards (optional)

Eppendorfs
Syringes
Syringe-filters
Vials for auto-sampler carousel

25 x 3 mm, 5 µm Nucleosil C18 NL5 Column (Capital HPLC Ltd.) approx. £164 each.
C8 guard columns or pre-column inserts (WAT035880, Waters).
Ferrules and screws (if multi-column users).

2. System

Waters HPLC System with Perkin Elmer Pump (see Fig. 2.14). Ran by computer with Millennium software, also processes and stores results.

2.1. Pump (quaternary)

Up to 4 solvents per gradient.
10 gradient protocols can be stored.

2.2. Autosampler

Cools to 5°C.
Takes up to 100 samples (for 40 min per sample, usual batch number 30 samples in 24 hours)
Common chemical additions to each injection (eg water to aid peak distinction)can be pre-programmed.

2.3. Rheodyne

For single injections. Not used when batches run using auto-sampler.

2.4. Column oven

Holds up to 4 columns.
Warms so constant temperature (and therefore viscosity) of solvents can be facilitated.

2.5. PDA

Measures absorbance at set wavelengths (e.g. 350 to 700 for phyto-pigments) over time.

2.6. Computer

Sample and running details need to be entered. All printed out with PDA results.
Needs frequent backing up.
N.B. Resolution of spectra will affect the ease of pigment identity, but increase storage.

3. Protocol

Add extractant to samples, 24 hours in advance.
Filter extracted samples and keep cool and dark.
Switch on all components separately; pump (check plugged into timer), auto-sampler, column oven (at back), oven thermostat, PDA and computer.

3.1. Pump

Make solvents, each sample needs approx. 15 ml of solvent A, 20 ml of solvent B and 5 ml of solvent C per sample run.
Select method.
De-gas solvents with He.
Purge pump with all solvents to be used (5-10ml of each).

3.2. Column oven

Check correct column attached to inflow from rheodyne and outflow to PDA. If leaks occur after running solvent, replace ferrule and screw on said attachment joints.

3.3. Pump

Press start (F8 starts line 0 of method).
Wait for 5mins for solvent to purge system.

3.4. Auto-sampler

Set cooler to on (second configuration page).

3.5. Rheodyne

Used for manual injection (not used for repetitive analysis).
When using auto-sampler, keep in load position.

3.6. Column oven thermostat

Set to 25°C.

3.7. Photodiode array (PDA)

Check both lamps are on (at front) and not flashing. If lamp flashes, wait for solvent to flush through (may have to switch off and on again).

3.8. Computer

Go to > Millenium > Login > Run samples > setup (instruments, bottom of page).
Monitor (the baseline, bottom of page).
Enter sample names and other particulars, important things to remember are; run time (40 mins) and solvent volume (70 µl), as well as correct vial number for each sample.
Remember standards with every batch.

3.9. Autosampler

Program for sample set including auto-addition. 70 µl for each injection and 30 µl auto addition (step function). Remember to imput correct run time. Only 18 lots of 30 µl per autoaddition vial.
Put samples into carousel (filtered) and (auto addition) water vials in specified positions.

Continue only when baseline is constant.

3.10. Computer

Press stop (red), baseline monitor.
Press go (green) and enter name for sample set.

3.11. Autosampler

Press auto start

3.12. Timer

Calculate run time (40 min per sample, include 5 min rinse and pre-injection between samples) plus condition column (40 min), set timer to switch pump off at the end of the run.

References

REFERENCES

Admiraal, W. 1977a. Influence of light and temperature on growth rate of estuarine benthic diatoms in culture. Marine Biology, 39: 1-9.

Admiraal, W. 1977b. Tolerance of estuarine benthic diatoms to high concentrations of ammonia, nitrite ion, nitrate ion and orthophosphate. Marine Biology, 43: 307-315.

Admiraal, W. 1977c. Influence of various concentrations of orthophosphate on the division rate of an estuarine benthic diatom, *Navicula arenaria*, in culture. Marine Biology, 42: 1-8.

Admiraal, W. and Peletier, H. 1980. Influence of seasonal variations of temperature and light on the growth rate of cultures and natural populations of intertidal diatoms. Marine Ecology Progress Series, 2: 35-43.

Admiraal, W. 1984. The ecology of estuarine sediment-inhabiting diatoms. Progress in Phycological Research, 3: 269-322.

Admiraal, W., Peletier, H. and Brouwer, T. 1984. The seasonal succession patterns of diatom species on an intertidal mudflat - an experimental-analysis. Oikos, 42: 30-40.

Amos, C. L., Brylinsky, M., Sutherland, T. F., O'Brian, D., Lee, S. and Cramp, A. 1998. The stability of a mudflat in the Humber Estuary, South Yorkshire, UK. In: Sedimentary Processes in the Intertidal Zone. K. S. Black, D. M. Paterson and A. Cramp (Eds.) London, Geological Society, London, Special Publications. 139: 25-43.

Anderson, F. E. and Black, L. F. 1980. A method for sampling fine-grained surface sediments in intertidal areas. Journal of Sedimentary Petrology, 50: 637-638.

Anning, T., MacIntyre, H. L., Pratt, S. M., Sammes, P. J., Gibb, S. and Geider, R. J. 2000. Photoacclimation in the marine diatom *Skeletonema costatum*. Limnology and Oceanography, 45: 1807-1817.

Arsalane, W., B., R. and Duval, J. C. 1994. Influence of the pool size of the xanthophyll cycle on the effects of light stress in a diatom - competition between photoprotection and photoinhibition. Photochemistry and Photobiology, 60: 237-243.

Asmus, R., Jensen, M. H., Murphy, D. and Doerffer, R. 1998. Primary production of microphytobenthos, phytoplankton and the annual yield if macrophytic biomass in the sylt-Romo Wadden Sea. In: Ökosystem Wattenmeer. C. Gätje and K. Reise (Eds.) Heidelberg, Springer-Verlag Berlin: 367-391.

Barranguet, C., Herman, P. M. J. and Sinke, J. J. 1997. Microphytobenthos biomass and community composition studied by pigment biomarkers: importance and fate in the carbon cycle of a tidal flat. Journal of Sea Research, 38: 59-70.

Barranguet, C. 1997. The role of microphytobenthic primary production in a Mediterranean mussel culture area. Estuarine, Coastal and Shelf Science, 44: 753-765.

Barranguet, C., Kromkamp, J. and Peene, J. 1998. Factors controlling primary production and photosynthetic characteristics of intertidal microphytobenthos. Marine Ecology Progress Series, 173: 117-126.

Barranguet, C. and Kromkamp, J. 2000. Estimating primary production rates from photosynthetic electron transport in estuarine microphytobenthos. Marine Ecology Progress Series, 204: 39-52.

Berkenbusch, K. and Rowden, A. A. 1999. Factors influencing sediment turnover by the burrowing ghost shrimp *Callianassa filholi* (Decapoda : Thalassinidea). Journal of Experimental Marine Biology and Ecology, 238: 283-292.

BIOPTIS final report. 2001. Assessing the biological and physical dynamics of intertidal sediment ecosystems: A remote sensing approach. Gatty Marine Laboratory, University of St. Andrews. MAS3-CT97-0158.

Bjørnland, T. and Liaaen-Jensen, S. 1989. Distribution patterns of carotenoids in relation to chromophyte phlogeny and systematics. In: The Chromophyte Algae: problems and perspectives. J. C. Green, B. S. C. Leadbeater and W. L. Diver (Eds.) Oxford, Clarendon Press. Special Volume 38: 37-60.

Blanchard, G. F. 1990. Overlapping microscale dispersion patterns of meiofauna and microphytobenthos. Marine Ecology Progress Series, 68: 101-111.

Blanchard, G. F. and Cariou-Le Gall, V. 1994. Photosynthetic characteristics if

microphytobenthos in Marennes-Oleron Bay, France: Preliminary results. Journal of Experimental Marine Biology and Ecology, 182: 1-14.

Blanchard, G. and Guarini, J.-M. 1996. Studying the role of mud temperature on the hourly variation of the photosynthetic capacity of microphytobenthos in intertidal areas. C.R. Acad. Sci. Paris, Sciences dela vie/Life sciences, 319: 1153-8.

Blanchard, G. F., Guarini, J.-M., Richard, P., Gros, P. and Mornet, F. 1996. Quantifying the short-term temperature effect on light-saturated photosynthesis of intertidal microphytobenthos . Marine Ecology Progress Series, 134: 309-323.

Blanchard, G. F., Guarini, J.-M., Gros, P. and Richard, P. 1997. Seasonal effect on the relationship between the photosynthetic capacity of intertidal micrphytobenthos and temperature. Journal of Phycology, 33: 723-728.

Brotas, V. and Serôdio, J. 1997. A mathematical model for the vertical distribution of chlorophyll *a* in estuarine intertidal sediments. Netherlands Journal of Aquatic Ecology, 29: 315-321.

Brotas, V. and Plante-Cuny, M. R. 1998. Spatial and temporal patterns of microphytobenthic taxa of estuarine tidal flats in the Tagus Estuary (Portugal) using pigment analysis by HPLC. Marine Ecology Progress Series, 171: 43-57.

Brown, D. H., Gibby, C. E. and Hickman, M. 1972. Photosynthetic rhythms in epipelic algal populations. British Phycological Journal, 7: 37-44.

Bryant, D. A. 1986. The cyanobacterial photosynthetic apparatus: Comparison to those of higher plants and photosynthetic bacteria. In: Photosynthetic picoplankton. T. Platt and W. K. W. Li (Eds.).

Büchel, C. and Wilhelm, C. 1993. In vivo analysis of slow chlorophyll fluorescence induction kinetics in algae: progress, problems and perspectives. Photochemistry and Photobiology, 58: 137-148.

Cariou-Le Gall, V. and Blanchard, G. F. 1995. Monthly HPLC measurements of pigment concentration from an intertidal muddy sediment of Marennes-Oleron Bay, France. Marine Ecology Progress Series, 121: 171-179.

Christie, M. C., Dyer, K. R., Blanchard, G., Cramp, A., Mitchener, H. J. and Paterson, D. M. 2000. Temporal and spatial distributions of moisture and organic contents across a macro-tidal mudflat. Continental Shelf Research, 20: 1219-1241.

Clelland, B. 1994. A catchment study of the River Eden, Fife. Tay River Purification Board. Technical Report, TRPB 1/94.

Colijn, F. 1978. Primary productivity measurements in the Ems-Dollard estuary during 1975 and 1976. Publications and reports of the project 'Biological Research in the Em-Dollard estuary'.

Colijn, F. and Dijkema, K. S. 1981. Species composition of benthic diatoms and distribution of chlorophyll *a* on an intertidal flat in the Dutch Wadden Sea. Marine Ecology Progress Series, 4: 9-21.

Colijn, F. and de Jonge, V. D. 1984. Primary production of microphytobenthos in the Ems-Dollard Estuary. Marine Ecology Progress Series, 14: 185-196.

Crooks, S. and Turner, R. K. 1999. Integrated coastal management: sustaining estuarine natural resources. In: Advances in Ecological Research: Estuaries. D. B. Nedwell and D. G. Raffaelli (Eds.) Acedemic Press. 29: 241-289.

Daniel, G. F., Chamberlain, A. H. L. and Jones, E. B. G. 1987. Cytochemical and electron microscopical observations on the adhesive materials of marine fouling diatoms. British Phycological Journal, 22: 101-118.

Davidson, I. R. 1991. Environmental effects on algal photosynthesis: temperature. Journal of Phycology, 27: 2-8.

Davidson, N. C. and Buck, A. L. 1997. An inventory of UK estuaries. Volume 1. Introduction and methodology. Joint Nature Conservation Commitee. Volume 1 of 7.

Decho, A. W. 1990. Microbial expolymer secretions in ocean environments: their role(s) in food webs and marine processes. Oceanographical Marine Biological Annual Review, 28: 73-153.

Demers, S., Roy, S., Gagon, R. and Vignault, C. 1991. Rapid light induced changes in

cell fluorescence and in xanthophyll-cycle pigments of *Alexandrium excavatum* (Dinophyceae) and *Thalassiosira pseudonana* (Bacillariophyceae): a photo-protection mechanism. Marine Ecology Progress Series, 76: 185-193.

Demmig-Adams, B. and Adams III, W. W. 1992. Photoprotection and other responses of plants to high light stress. Annual Review of Plant Physiology and Plant Molecular Biology, 43: 599-626.

Dijkema, K. S. 1975. Verkennend onderzoek naar de invloed van abiotische faktoren op de benthische diatomeen in de oostelijke Waddensee. Publications and reports of the project 'Biological Research in the Em-Dollard estuary'.

Eaton, J. and Moss, B. 1966. The estimation of numbers and pigment content in epipelic algal populations. Limnology and Oceanography, 11: 584-595.

Edgar, L. A. and Pickett-Heaps, J. D. 1984. Diatom locomotion. Progress in Phycological Research, 3: 269-322.

Emiliani, C. 1993. Extinction and viruses. Biosystems, 31: 155-159.

Falkowski, P. G. and Kiefer, D. A. 1985. Chlorophyll *a* fluorescence in phytoplankton: relationship to photosynthesis and biomass. Journal of Plankton Research, 7: 715-731.

Falkowski, P. G. and LaRoche, J. 1991. Acclimation to spectral irradiance in algae. Journal of Phycology, 27: 8-14.

Falkowski, P. G. and Kolber, Z. 1995. Variations in chlorophyll fluorescence yields in phytoplankton in the world oceans. Australian Journal of Plant Physiology, 22: 341-355.

Falkowski, P. G. and Raven, J. A. 1997. Aquatic photosynthesis. In: Aquatic Photosynthesis. Blackwell Science, London. (375).

Flameling, I. A. and Kromkamp, J. 1998. Light dependence of quantum yields for PSII charge separation and oxygen evolution in eucaryotic algae. Limnology and Oceanography, 43: 284-297.

Flemming, B. W. and Delafontaine, M. T. 2000. Mass physical properties of muddy intertidal sediments: some applications, misapplications and non-applications.

Continental Shelf Research, 20: 1179-1197.

Forster, R. M., Kromkamp J. C., Honeywill, C. (in prep.; also in BIOPTIS final report) Comparison of commercially-available modulated chlorophyll fluorimeters for laboratory and field-based estimates of chlorophyll biomass and photosynthetic electron transport in microphytobenthos.

Fowler, J. and Cohen, L. 1990. Practical Statistics for Field Biology. In: Practical Statistics for Field Biology. John Wiley and Sons Ltd, Chichester. (227).

Garcia-Pichel, F., Mechling, M. and Castenholz, R. W. 1994. Diel Migrations of Microorganisms within a Benthic, Hypersaline Mat Community. Applied and Environmental Microbiology, 60: 1500-1511.

Geel, C., Versluis, W. and Snel, J. F. H. 1997. Estimation of oxygen evolution by marine phytoplankton from measurement of the efficiency of Photosystem II electron flow. Photosynthesis Research, 51: 61-70.

Genty, B., Briantais, J.-M. and Baker, N. R. 1989. The relationship between the quantum yield of photosynthetic electron transport and quenching of chlorophyll fluorescence. Biochimica and Biophysica Acta, 990: 87-92.

George, C. R. 1995. Variation in the erosion threshold of natural intertidal sediments. Ph.D. Thesis; Bristol. 262

Gieskes, W. W. C. and Kraay, G. W. 1975. The phytoplankton spring bloom in Dutch coastal waters of the North Sea. Netherlands Journal of Sea Research, 9: 166-196.

Govindjee 1995. 63 years since Kautsky - Chlorophyll *a* fluorescence. Australian Journal of Plant Physiology, 22: 131-160.

Greene, R. M., Kolber, Z. S., Swift, D. G., Tindale, N. W. and Falkowski, P. G. 1994. Physiological limitation of phytoplankton photosynthesis in the Eastern Equatorial Pacific determined from variability in the quantum yield of fluorescence. Limnology and Oceanography, 39: 1061-1074.

Guarini, J.-M., Blanchard, G. F., Bacher, C., Gros, P., Riera, P., Richard, P., Gouleau, D.,

Galois, R., Prou, J. and Sauriau, P.-G. 1998. Dynamics of spatial patterns of microphytobenthic biomass: inferences from a geostatistical analysis of two comprehensive surveys in Marennes-Oléron Bay (France). Marine Ecology Progress Series, 166: 131-141.

Happey-Wood, C. M. and Jones, P. 1988. Rhythms of vertical migration and motility in intertidal benthic diatoms with particular reference to *Pleurosigma angulatum.* Diatom Research, 3: 83-93.

Harrison, S. J. and Phizacklea, A. P. 1985. Seasonal changes in heat flux and heat storage in the intertidal mudflats of the Forth Estuary, Scotland. Journal of Climate, 5: 473-485.

Hartig, P., Wolfstein, K., Lippemeier, S. and Colijn, F. 1998. Photosynthetic activity of natural microphytobenthos populations measured by fluorescence (PAM) and ^{14}C-tracer methods: a comparison. Marine Ecology Progress Series, 166: 53-62.

Hay, S. I., Maitland, T. C. and Paterson, D. M. 1993. The speed of diatom migration through natural and artificial substrata. Diatom Research, 8: 371-384.

Hillebrand, H. and Sommer, U. 1997. Response of epilithic microphytobenthos of the Western Baltic Sea to *in situ* experiments with nutrient enrichment. Marine Ecology-progress series, 160: 35-46.

Hofstraat, J. W., Peeters, J. C. H., Snel, J. F. H. and Geel, C. 1994. Simple determination of photosynthetic efficiency and photoinhibition of *Dunaliella tertiolecta* by saturating pulse fluorescence measurements. Marine Ecology progress series, 103: 187-196.

Holfeld, H. 1998. Fungal infections of the phytoplankton: seasonality, minimal host density, and specificity in a mesotrophic lake. New Phytologist, 138: 507-517.

Hopkins, J. T. 1963. A study of the diatoms of the Ouse estuary, Sussex. I. The movement of the mud-flat diatoms in response to some chemical and physical changes. Journal of the Marine Biological Association, UK, 43: 653-663.

Janssen, M., Hust, M., Rhiel, E. and Krumbein, W. E. 1999. Vertical migration behaviour of diatom assemblages of Wadden Sea sediments (Dangast, Germany): a study using cryo-scanning electron microscopy. International Microbiology, 2: 103-110.

Jeffrey, S. W., Mantoura, R. F. C. and Bjornland, T. 1997. Data for the identification of 47 key phytoplankton pigments. In: Phytoplankton pigments in oceanography. S. W. Jeffrey, R. F. C. Mantoura and S. W. Wright (Eds.) Paris, UNESCO. 449-559.

Joint, I. R., Gee, J. M. and Warwick, R. M. 1982. Determination of fine-scale vertical distribution of microbes and meiofauna in an intertidal sediment. Marine Biology, 72: 157-164.

Kautsky, H. and Hirsch, A. 1931. Neue Vesuche zur Kohlensaureassimilation. Naturwissenschaften, 964.

Kelly, M. G. and Whitton, B. A. 1995. The Trophic Diatom Index: a new index for monitoring eutrophication in rivers. Journal of Applied Phycology, 7: 433-444.

Kelly, J. A., Honeywill, C. and Paterson, D. M. 2001. Microscale analysis of chorophyll *a* in cohesive, intertidal sediments: the implications of microphytobenthos distribution. Journal of the Marine Biological Association, UK, 81: 151-162.

Kiefer, D. A. 1973a. Chlorophyll *a* fluorescence in marine centric diatoms: responses of chloroplasts to light and nutrient stress. Marine Biology, 23: 39-46.

Kiefer, D. A. 1973b. Fluorescence properties of natural phytoplankton populations. Marine Biology, 22: 263-269.

King, S. and Lester, J. 1995. The value of salt marsh as a sea defence. Marine Pollution Bulletin, 30: 180-189.

Kolber, Z. S., Prasil, O. and Falkowski, P. G. 1998. Measurements of variable chlorophyll fluorescence using fast repetition rate techniques: defining methodology and experimental protocols. Biochimica et Biophysica Acta-Bioenergetics, 1367: 88-106.

Korb, R. E., Saville, P. J., Johnston, A. M. and Raven, J. A. 1997. Sources of inorganic carbon for photosynthesis by three species of marine diatom. Journal of Phycology, 33: 433-440.

Krause, G. H. and Weis, E. 1991. Chlorophyll fluorescence and photosynthesis: The Basics. Annual Review of Plant Physiology and Plant Molecular Biology, 42: 313-49.

Kromkamp, J., Barranguet, C. and Peene, J. 1998. Determination of microphytobenthos PSII quantum efficiency and photosynthetic activity by means of variable chlorophyll fluorescence. Marine Ecology Progress Series, 162: 45-55.

Kuhn, S. F. 1997. Infection of *Coscinodiscus* spp. by the parasitoid nanoflagellate Pirsonia diadema .1. Behavioural studies on the infection process. Journal of Plankton Research, 19: 791-804.

Kühl, M., Lassen, C. and Jørgensen, B. B. 1994. Optical properties of microbial mats: light measurement with fibre-optic microprobes. In: Microbial Mats. L. J. Stal and P. Caumette (Eds.) Berlin, Springer-Verlag. 35: 149-166.

Lalli, C. M., Parsons, Y. and Parsons, T. R. 1984. Manual of chemical and biological methods for seawater analysis. In: Manual of chemical and biological methods for seawater analysis. Pergamon Press.

Lassen, C., Ploug, H. and Jørgensen, B. B. 1992. A fibre-optic scalar irradiance microsensor: application for spectral light measurements in sediments. FEMS Microbiology Ecology, 86: 247-254.

Lewis, M. R. and Smith, J. C. 1983. A small volume, short -incubation-time method for measurement of photosynthesis as a function of incident irradiance. Marine Ecology Progress Series, 13: 99-102.

Lohr, M. and Wilhelm, C. 1999. Algae displaying the diadinoxanthin cycle also possess the violaxanthin cycle. Proceedings of the National Acadamy of Sciences of the United States of America, 8784-9.

Lorenzen, C. J. 1966. A method for the continuous measurement of *in vivo* chlorophyll concentration. Deep-Sea Research, 13: 223-227.

MacIntyre, H. L. and Cullen, J. J. 1996. Primary production by suspended and benthic microalgae in a turbid estuary: time-scale of variability in San Antonio Bay, Texas. Marine Ecology Progress Series, 145: 245-269.

MacIntyre, H. L., Geider, R. J. and Miller, D. C. 1996. Microphytobenthos: The Ecological Role of the "Secret Garden" of Unvegetated, Shallow-Water Marine Habitats.

I. Distribution, Abundance and Primary Production. Estuaries, 19: 186-201.

Mathieson, S. and Atkins, S. M. 1995. A review of nutrient enrichment in the estuaries of Scotland: implications for the natural heritage. Netherlands Journal of Aquatic Ecology, 29: 437-448.

Mathieson, S. and Atkins, S. M. 1995. A review of nutrient enrichment in the estuaries of Scotland: implications for the natural heritage. Netherlands Journal of Aquatic Ecology, 29: 437-448.

Middelburg, J. J., Barranguet, C., Boschker, H. T. S., Herman, P. M. J., Moens, T. and Heip, C. H. R. 2000. The fate of intertidal microphytobenthos carbon: An in situ ^{13}C-labeling study. Limnology and Oceanography, 45: 1224-1234.

Miles, A. 1994. The influence of selected heavy metals on estuarine microphytobenthos. Ph.D. Thesis; Bristol.

Millie, D. F., Paerl, H. W. and Hurley, J. P. 1993. Microalgal pigment assessments using high-performance liquid chromatography: a synopsis of organismal and ecological applicatons. Canadian Journal of Aquatic Science, 50: 2513-2527.

Olaizola, M. and Yamamoto, H. Y. 1994. Short-term response of the diadinoxanthin cycle and fluorescence yield to high irradiance in *Chaetoceros-muelleri* (Bacillariophyceae). Journal of Phycology, 30: 606-612.

Oppenheim, D. R. 1991. Seasonal changes in epipelic diatoms along an intertidal shore, Berrow flats, Somerset. Journal of Marine Biology Association. U.K., 71: 579-596.

Palmer, J. D. and Round, F. E. 1965. Persistent, vertical-migration rhythms in benthic microflora. I. The effect of light and temperature on the rhythmic behaviour of *Euglena obtusa.* Journal of marine biological association. U.K., 45: 567-582.

Palmer, J. D. and Round, F. E. 1967. Persistent, vertical-migration rhythms in benthic microflora. VI. The tidal and diurnal nature of the rhythm in the diatom *Hantzschia virgata..* Biological Bulletin, 132: 44-55.

Paterson, D. M. 1986. The migratory behaviour of diatom assemblages in a laboratory

tidal micro-ecosystem examined by low temperature scanning electron microscopy. Diatom Research, 1: 227-239.

Paterson, D. M., Yallop, M. and George, C. 1994. Spatial variability in sediment erodability on the island of Texel. In: Biostabilization of Sediments. W. E. Krumbein, D. M. Paterson and L. J. Stal (Eds.) Oldenburg, Verlag/Vertrieb. 107-120.

Paterson, D. M. 1995. Biogenic structure of early sediment fabric visualized by low-temperature scanning electron microscopy. Journal of the Geological Society, London, 152: 131-140.

Paterson, D. M. 1997. Biological mediation of sediment erodability: ecology and physical dynamics. 4th Nearshore and Estuarine Cohesive sediment Transport Conference, Wallingford, John Wiley & Sons. 215-229.

Paterson, D. M., Wiltshire, K. H., Miles, A., Blackburn, J., Davidson, I., Yates, M. G., McGrorty, S. and Eastwood, J. E. A. 1998. Microbiological mediation of spectral reflectance from intertidal cohesive sediments. Limnology and Oceanography, 43: 1207-1221.

Paterson, D. M., Tolhurst, T. J., Kelly, J. A., Honeywill, C., de Deckere, E. M. G. T., Huet, V., Shayler, S. A., Black, K. S., de Brouwer, J. and Davidson, I. 2000. Variations in sediment properties, Skeffling mudflat, Humber Estuary, UK. Continental Shelf Research, 20: 1373-1396.

Peletier, H. 1996. Long-term changes in intertidal estuarine diatom assemblages related to reduced input of organic waste. Marine Ecology Progress Series, 137: 265-271.

Perkins, E. J. 1960. The diurnal rhythm of the littoral diatoms of the River Eden estuary, Fife. Journal of Ecology, 48: 725-8.

Peterson, C. G., Dudley, T. L., Hoagland, K. D. and Johnson, L. M. 1993. Infection, growth, and community-level consequences of a diatom pathogen in a sonoran desert stream. Journal of Phycology, 29: 442-452.

Pinckney, J. and Sandulli, R. 1990. Spatial autocorrelation analysis of meiofaunal and microalgal populations on an intertidal sandflat: Scale linkage between consumers and

resources. Estuarine Coastal and Shelf Science, 30: 341-353.

Pinckney, J. and Zingmark, R. G. 1991. Effects of tidal stage and sun angles on intertidal benthic microalgal productivity. Marine Ecology Progress Series, 76: 81-89.

Pinckney, J. and Zingmark, R. G. 1993c. Biomass and production of benthic microalgal communities in estuarine habitats. Estuaries, 16: 887-897.

Pinckney, J., Piceno, Y. and Lovell, C. R. 1994. Short-term changes in the vertical distribution of benthic microalgal biomass in intertidal muddy sediments. Diatom Research, 9: 143-153.

Pistocchi, R., Guerrini, F., Balboni, V. and Boni, L. 1997. Copper toxicity and carbohydrate production in the microalgae *Cylindrotheca fusiformis* and *Gymnodinium* sp. European Journal of Phycology, 32: 125-132.

Porra, R. J., Thompson, W. A. and Kriedemann, P. E. 1989. Determination of accurate extinction coefficients and simultaneous-equations for assaying chlorophyll-a and chlorophyll-b extracted with 4 different solvents - verification of the concentration of chlorophyll standards by atomic-absorption spectroscopy. Biochimica et Biophysica Acta, 975: 384-394.

PRO-MAT final report 1997. Primary productivity and microbially activated transport of elements (C, P, Fe) in tide-influenced deposits. Gatty Marine Laboratory, University of St. Andrews. EV5V-CT94-0411.

Retraubun, A. S. W., Dawson, M. and Evans, S. M. 1996. Spatial and temporal factors affecting sediment turnover by the lugworm *Arenicola marina*. Journal of Experimental Marine Biology and Ecology, 201: 23-35.

Revsbech, N. P. and Jørgensen, B. B. 1981. Primary production of microalgae in sediments measured by oxygen microprofile, $H^{14}CO^{3-}$ fixation, and oxygen exchange methods. Limnology and Oceanography, 26: 717-730.

Revsbech, N. P. and Jørgensen, B. B. 1983. Photosynthesis of benthic microflora measures with high spatial relofution by the oxygen microprofile method. Limnology and

Oceanography, 28: 749-756.

Robinson, D. H., Kolber, Z. and Sullivan, C. W. 1997. Photophysiology and photoacclimation in surface sea ice algae from McMurdo Sound, Antarctica. Marine Ecology Progress Series, 147: 243-256.

Robinson, D. H., Kolber, Z. and Sullivan, C. W. 1997. Photophysiology and photoacclimation in surface sea ice algae from McMurdo Sound, Antarctica. Marine Ecology Progress Series, 147: 243-256.

Rotatore, C. and Colman, B. 1992. Active uptake of CO_2 by the diatom *Navicula pelliculosa.* Journal of Experimental Botany, 43: 571-576.

Round, F. E. and Palmer, J. D. 1966. Persistent, vertical-migration rhythms in benthic microflora. Journal of Marine Biological Association U.K., 46: 191-214.

Round, F. E. 1971. Benthic marine diatoms. Oceanographic Marine Biological Annual Review, 9: 83-139.

Round, F. E. 1981. The ecology of algae. In: The ecology of algae. Cambridge University press, Cambridge. (653).

Ruban, A. V. and Horton, P. 1995. Regulation of nonphotochemical quenching of chlorophyll fluorescence in plants. Australian Journal of Plant Physiology, 22: 221-230.

Sakshaug, E., Bricaud, A., Dandonneau, Y., Falkowski, P. G., Kiefer, D. A., Legendre, L., Morel, A., Parslow, J. and Takahashi, M. 1997. Parameters of photosynthesis: definitions, theory and interpretation of results. Journal of Plankton Research, 19: 1637-1670.

Schreiber, U., Schliwa, W. and Bilger, U. 1986. Continuous recording of photochemical and non-photochemical chlorophyll fluorescence quenching with a new type of modulation fluorimeter. Photosynthesis Research, 10: 51-62.

Schreiber, U. 2000. Chlorophyll fluorescence: new instruments for special applications. Walz product information leaflet.

Schweikert, M. and Schnepf, E. 1996. Pseudaphelidium drebesii, gen et spec nov (*incerta*

sedis), a parasite of the marine centric diatom *Thalassiosira punctigera*. Archiv fur Protistenkunde, 147: 11-17.

Schweikert, M. and Schnepf, E. 1997. Light and electron microscopical observations on *Pirsonia punctigerae* spec nov, a nanoflagellate feeding on the marine centric diatom *Thalassiosira punctigera*. European Journal of Protistology, 33: 168-177.

Seppälä, J. and Balode, M. 1998. The use of spectral fluorescence methods to detect changes in the phytoplankton community. Hydrobiologia, 363: 207-217.

Serôdio, J., Da Silva, J. M. and Catarino, F. 1997. Non destructive tracing of migratory rhythms of intertidal benthic microalgae using *in vivo* chlorophyll *a* fluorescence. Journal of Phycology, 33: 542-553.

Serôdio, J. and Catarino, F. 2000. Modelling the primary productivity of intertidal microphytobenthos: time scales of variability and effects of migratory rhythms. Marine Ecology Progress Series, 192: 13-30.

Smith, D., Hughes, R. G. and Cox, E. 1996. Predation of epipelic diatoms by the amphipod *Corophium volutator* and the polychaete *Nereis diversicolor*. Marine Ecology progress series, 145: 53-61.

Snoejis, P. 1994. Distribution of epiphytic diatom species composition, diversity and biomass on different macroalgal hosts along seasonal and salinity gradients in the Baltic Sea. Diatom Research, 9: 189-211.

Stewart, P. M. 1995. Use of algae in aquatic pollution assessment. Natural Areas Journal, 15: 234-239.

Sukenik, A., Bennet, J., Morain-Bertrand, A. and Falowski, P. G. 1990. Adaption of the photosynthetic apparatus to irradiance in *Dunaliella tertiolecta*. Plant Physiology, 92: 891-898.

Sullivan, M. J. 1978. Diatom community structure: taxonomic and statistical analyses of a Mississippi salt marsh. Journal of Phycology, 14: 468-475.

Sullivan, M. J. and Moncreiff, C. A. 1990. Edaphic algae are an important component of

salt-marsh food webs: evidence from multiple stable isotope analysis. Marine Ecology Progress series, 62: 149-159.

Taylor, F. J. 1976. A fungal parasite in the marine diatom *Coscinodiscus oculus-iridis*. Batanica Marina, 19: 61-62.

Taylor, I. S. 1998. Fine-scale distribution of carbohydrate on intertidal sediments in relation to diatom biomass and sediment properties. Ph.D. Thesis; University of St Andrews. 211.

Taylor, I. S. and Paterson, D. M. 1998. Microspatial variation in carbohydrate concentrations with depth in the upper millimeters of intertidal cohesive sediments. Esturine, Costal and Shelf Science, 46: 359-370.

Tillmann, U., Hesse, K. J. and Tillmann, A. 1999. Large-scale parasitic infection of diatoms in the Northfrisian Wadden Sea. Journal of Sea Research, 42: 255-261.

Ting, C. S. and Owens, T. G. 1992. Limitations of the pulse-modulated technique for measuring the fluorescence characteristics of algae. Plant Physiology, 100: 367-373.

Ting, C. S. and Owens, T. G. 1993. Photochemical and nonphotochemical fluorescence quenching processes in the diatom *Phaeodactylum tricornutum*. Plant Physiology, 10`: 1323-1330.

Ting, C. S. and Owens, T. G. 1994. The effects of excess irradiance on photosynthesis in the marine diatom *Phaeodactylum tricornutum*. Plant Physiology, 106: 763-770.

Tolhurst, T. J. 1999. Microbial mediation of intertidal sediment stability. Ph.D. Thesis; University of St Andrews. 163.

Underwood, G. J. and Paterson, D. M. 1993. Recovery of intertidal benthic diatoms after biocide treatment and associated sediment dynamics. Journal of the Marine Biological Association of the United Kingdom, 73: 25-45.

Underwood, G. J. 1994. Seasonal and spatial variation in epipelic diatom assemblages in the Severn Estuary. Diatom Research, 9: 451-472.

Underwood, G. J. C., Paterson, D. M. and R.J., P. 1995. The measurements of microbial

carbohydrate exopolymers from intertidal sediments. Limnology and Oceanography, 40:

Underwood, G. J. C., Phillips, J. and Saunders, K. 1998. Distribution of estuarine benthic diatom species along salinity and nutrient gradients. European Journal of Phycology, 33: 173-183.

Underwood, G. J. C. and Kromkamp, J. 1999. Primary production by phytoplankton and microphytobenthos in estuaries. In: Advances in Ecological Research: Estuaries. D. B. Nedwell and D. G. Raffaelli (Eds.) Acedemic Press. 29: 93-153.

Vyhnálek, V., Fišar, Z., Fišarová, A. and Komárková, J. 1993. *In vivo* fluorescence of chlorophyll *a*: estimation of phytoplankton biomass and activity in Římov Reservoir (Czech Republic). Water Science and Technology, 28: 29-33.

Walker, D. 1987. The use of the oxygen electrode and fluorescence probes in simple measurements of photosynthesis. In: The use of the oxygen electrode and fluorescence probes in simple measurements of photosynthesis. Packard Publishing Ltd., Sheffield.

Walsby, A. E. 1997. Numerical integration of phytoplankton photosynthesis through time and depth in a water column. New Phytologist, 136: 189-209.

Willemöes, M. and Monas, E. 1991. Relationship between growth irradiance and the xanthophyll cycle pool in the diatom *Nitzschia palea*. Physiologia Plantarum, 83: 449-456.

Wiltshire, K. H. and Schroeder, F. 1994. Pigment patterns in suspended matter from the Elbe Estuary, Northern Germany. Netherlands Journal of Aquatic Ecology, 28: 255-265.

Wiltshire, K. H., Blackburn, J. and Paterson, D. M. 1997. The Cryolander: a new method for fine scale *in situ* sampling of intertidal surface sediments. Journal of Sedimentary Research, 67: 977-981.

Wiltshire, K. H., Tolhurst, T., Paterson, D. M., Davidson, I. and Gust, G. 1998. Pigment fingerprints as markers of erosion and changes in cohesive sediment surface properties in simulated and natural erosion events. In: Sedimentary Processes in the Intertidal Zone. K. S. Black, D. M. Paterson and A. Cramp (Eds.) London, Geological Society. 139: 99-114.

Wiltshire, K. H. 2000. Algae and associated pigments of intertidal sediments, new observations and methods. Limnologica, 30: 205-214.

Wright, S. W. and Jeffrey, S. W. 1997. High resolution HPLC system for chlorophylls and carotenoids of marine phytoplankton. In: Phytoplankton pigments in oceanography. S. W. Jeffrey, R. F. C. Mantoura and S. W. Wright (Eds.) Paris, UNESCO. 327-341.

Wright, S. W., Jeffrey, S. W. and Mantoura, R. F. C. 1997. Evaluation of methods and solvents for pigment extraction. In: Phytoplankton pigments in oceanography. S. W. Jeffrey, R. F. C. Mantoura and S. W. Wright (Eds.) Paris, UNESCO. 261-282.

Xu, D. Q. and Wu, S. 1996. Three phases of dark-recovery course from photoinhibition resolved by the chlorophyll fluorescence analysis in soybean leaves under field conditions. Photosynthetica, 32: 417-423.

Yallop, M. and Paterson, D. M. 1994. Survey of Severn Estuary. In: Biostabilization of Sediments. W. E. Krumbein, D. M. Paterson and L. J. Stal (Eds.) Oldenburg, Verlag/Vertrieb. 107-120.

Yallop, M. L., Winder, B. D., Paterson, D. M. and Stal, L. J. 1994. Comparative structure, primary production and biogenic stabilization of cohesive and non-cohesive marine sediments inhabited by microphytobenthos. Estuarine Coastal and Shelf Science, 39: 565-582.

Yentsch, C. S. and Yentsch, C. M. 1979. Fluorescence spectral signatures: The characterisation of phytoplankton populations by the use of excitation and emission spectra. Journal of Marine Research, 37: 471-483.